

A COMPLEX-SYSTEMS APPROACH TO SIMULATING  
THE SEA URCHIN ECOLOGY

By

Graham Andrew Morehead

BA, Boston University, 1995

A THESIS

Submitted in Partial Fulfillment of the  
Requirements for the Degree of  
Master of Science  
(in Computer Science)

The Graduate School

The University of Maine

May 2014

Advisory Committee:

Roy Turner, Associate Professor of Computer Science, Director of Maine Software Agents/AI Laboratory, School of Computing and Information Science, Advisor

James Wilson, Prof. of Marine Sciences and Economics, School of Marine Sciences

Larry Latour, Chair of the Department of New Media, Associate Professor Department of Computing and Information Science

## THESIS ACCEPTANCE STATEMENT

On behalf of the Graduate Committee for Graham Andrew Morehead I affirm that this manuscript is the final and accepted thesis. Signatures of all committee members are on file with the Graduate School at the University of Maine, 42 Stodder Hall, Orono, Maine.

---

Roy Turner, Associate Professor of Computer Science

4/18/14

## LIBRARY RIGHTS STATEMENT

In presenting this thesis in partial fulfillment of the requirements for an advanced degree at The University of Maine, I agree that the Library shall make it freely available for inspection. I further agree that permission for "fair use" copying of this thesis for scholarly purposes may be granted by the Librarian. It is understood that any copying or publication of this thesis for financial gain shall not be allowed without my written permission.

---

Signature

Date

A COMPLEX-SYSTEMS APPROACH TO SIMULATING  
THE SEA URCHIN ECOLOGY

By

Graham Andrew Morehead

Thesis Advisor: Roy Turner, Associate Professor of Computer Science

A THESIS

Submitted in Partial Fulfillment of the  
Requirements for the Degree of  
Master of Science  
(in Computer Science)

May 2014

Stocks of the native sea urchin (*Strongylocentrotus droebachiensis*) dropped dramatically during the peak of the urchin fishery in the early 1990's and have not recovered. The current regulatory regime is based on analytic population models and two monolithic zones. Analytic models are insufficiently complex to capture many features that cause demise or survival of an urchin population. Scale, or granularity size, is too coarse. In contrast, a complex-systems-based model is able to capture these features. Presented here is a fine-scale simulation of a sea urchin fishery in the Gulf of Maine which behaves like a complex system, i.e. exhibits patchiness and nonlinear dynamics. Also presented is an alternative harvesting scheme which fosters sustainability. The model presented here is merely a hypothesis. Its predictions may not be verifiable until it either (1) becomes a part of a larger project, or (2) is paired with fine-scale data.

## ACKNOWLEDGEMENTS

I am grateful to the following people for making this thesis possible. They have supplied me with indispensable information and data, and much needed advice. I could not have completed this without them.

*(Alphabetically by name)*

Amy Johnson  
Bob Steneck  
Brian McGill  
Caitlin Cleaver  
Christian Wilson  
Clare Bates Congdon  
Jack Hill  
James Acheson  
James Wilson  
Jui-Han Chang  
Lawrence Latour  
Larry Whitsel  
Lucas Kaim  
Margaret Hunter  
Peter Hayes  
Robert Russell  
Robert Vadas  
Roy Turner  
Ted Ames  
Teresa Johnson  
Tim Waring  
Yong Chen

## TABLE OF CONTENTS

ACKNOWLEDGEMENTS . . . . .	iii
LIST OF TABLES . . . . .	x
LIST OF FIGURES . . . . .	xi
1 INTRODUCTION . . . . .	1
1.1 The Urchin Fishery and Its Problems . . . . .	1
1.2 The Focus of this Thesis . . . . .	2
1.3 Software Design and Engineering . . . . .	4
1.4 Appropriateness of a Complex Systems Model . . . . .	5
1.5 Numerosity Not Sufficient . . . . .	6
2 BACKGROUND . . . . .	8
2.1 Problems With the Urchin Fishery . . . . .	8
2.1.1 A Tale of Two States . . . . .	8
2.1.2 A Scale Mismatch . . . . .	9
2.1.3 Incentives . . . . .	10
2.2 The Fine-Scale Problem . . . . .	13
2.3 The Classical Population Model . . . . .	17
2.3.1 A Discrete and Sometimes Chaotic Predictor . . . . .	18
2.3.2 Slow Movement Makes Spatial Distribution Important . . . . .	19
2.4 Models Currently Used in Maine . . . . .	21
2.5 The Complex System Model . . . . .	23
2.6 Elements of the Urchin Ecological System . . . . .	27

2.7	A System of Subsystems . . . . .	30
2.8	Summary . . . . .	31
<b>3</b>	<b>REPRESENTATION OF AN URCHIN ECOLOGY . . . . .</b>	<b>33</b>
3.1	Basic Description . . . . .	33
3.2	Representation of Time . . . . .	34
3.3	Representation of Topology . . . . .	35
3.4	Representation of Kelp . . . . .	35
3.5	Representation of Urchins . . . . .	37
3.6	Kelp Dynamics . . . . .	38
	3.6.1 Kelp Growth and Reproduction . . . . .	38
	3.6.2 Effects of Kelp on the Environment . . . . .	41
3.7	Urchin Dynamics . . . . .	42
	3.7.1 Urchin Movement . . . . .	42
	3.7.2 Administrative Challenges . . . . .	44
	3.7.3 Unexplained Urchin Aggregations . . . . .	45
	3.7.4 Urchin Mortality . . . . .	46
	3.7.5 Urchin Herbivory . . . . .	47
	3.7.6 Effect on Gonad Index . . . . .	47
	3.7.7 Urchin Growth . . . . .	49
	3.7.8 Discretization of Urchin Growth . . . . .	51
3.8	Urchin Reproduction . . . . .	53
	3.8.1 Harvesting Methods . . . . .	55
	3.8.2 Population Health . . . . .	57

4	STRUCTURE OF THE MODEL . . . . .	<b>60</b>
4.1	Object-Oriented Mesh Network . . . . .	60
4.2	Bathymetries . . . . .	62
4.2.1	Depth Assignment . . . . .	62
4.2.2	Acquiring GIS Data . . . . .	64
4.3	The Seaweed Object . . . . .	66
4.4	The Urchins Object . . . . .	68
4.5	Flow Control . . . . .	69
4.5.1	World <i>tick</i> Method . . . . .	70
4.5.2	Layer <i>tick</i> Method . . . . .	70
4.5.3	Cell <i>compute</i> Method . . . . .	71
4.5.4	Cell <i>tick</i> Method . . . . .	71
5	VISUALIZATION . . . . .	<b>74</b>
5.1	Overview . . . . .	74
5.1.1	Colors . . . . .	75
5.1.2	Structure . . . . .	75
5.1.3	Flow Control . . . . .	77
5.2	Description of the Visuals . . . . .	78
5.2.1	Considerations for Visual Communication . . . . .	78
5.2.2	Depth Color . . . . .	80
5.2.3	Biomass Color . . . . .	83
5.3	Objects Used in Visualization . . . . .	85
5.3.1	The Map Object . . . . .	85
5.3.2	The Frame Object . . . . .	86
5.3.3	The Sector Object . . . . .	87

6	RESULTS . . . . .	88
6.1	Simulation Setup . . . . .	88
6.2	Expectations . . . . .	89
6.2.1	The No-harvesting Condition . . . . .	89
6.2.2	The Standard-harvesting Condition . . . . .	89
6.2.3	The Circular-harvesting Condition . . . . .	89
6.3	Sample Triptych: Eastern Bay, day 2190 . . . . .	90
6.3.1	Graphs of the Metrics . . . . .	92
6.4	Big Nash . . . . .	94
6.4.1	Metrics <i>topDensity</i> and <i>topGI</i> . . . . .	96
6.5	Black Ledge . . . . .	102
6.5.1	Metrics <i>topDensity</i> and <i>topGI</i> . . . . .	103
6.6	Eastern Bay . . . . .	109
6.6.1	Metrics <i>topDensity</i> and <i>topGI</i> . . . . .	110
6.7	Flint Island . . . . .	116
6.7.1	Metrics <i>topDensity</i> and <i>topGI</i> . . . . .	117
6.8	Great Wass . . . . .	123
6.8.1	Metrics <i>topDensity</i> and <i>topGI</i> . . . . .	124
6.9	Petit Manan . . . . .	130
6.9.1	Metrics <i>topDensity</i> and <i>topGI</i> . . . . .	130
6.10	Seal Cove . . . . .	136
6.10.1	Metrics <i>topDensity</i> and <i>topGI</i> . . . . .	136
6.11	Shabbit Island . . . . .	142
6.11.1	Metrics <i>topDensity</i> and <i>topGI</i> . . . . .	143
6.12	Conclusion . . . . .	149

7	SENSITIVITY ANALYSIS . . . . .	<b>150</b>
7.1	Input Parameters . . . . .	150
7.2	Output Variables . . . . .	151
7.3	Perturbation then Simulation . . . . .	152
7.4	Sensitivity: Parameter Delta vs. Output Delta . . . . .	154
7.4.1	Distance in Parameter / Output Space . . . . .	154
7.5	Correlation . . . . .	164
7.6	Conclusion . . . . .	165
8	DISCUSSION . . . . .	<b>166</b>
8.1	Implications for Regulation . . . . .	167
8.2	Implications for Cooperative Action . . . . .	168
8.2.1	A Model Fishery . . . . .	168
8.2.2	A Different Urchin Regulatory Scheme . . . . .	170
9	FUTURE WORK . . . . .	<b>174</b>
9.1	Multiple Simultaneous Simulations . . . . .	174
9.2	Agent Integration . . . . .	174
9.2.1	Application Programmer Interface (API) . . . . .	175
9.2.2	WorldSim . . . . .	175
9.3	Mid-levels in the K-ary Tree . . . . .	176
9.4	An Accurate Distance Measure . . . . .	177
9.5	Arbitrary Site Selection . . . . .	179
9.6	Modular Form . . . . .	179
	REFERENCES . . . . .	<b>181</b>
	APPENDIX A : GLOSSARY . . . . .	<b>190</b>

APPENDIX B : PARAMETERS . . . . .	<b>193</b>
APPENDIX C : PSEUDOCODE . . . . .	<b>208</b>
APPENDIX D : BATHYMETRIES . . . . .	<b>222</b>
BIOGRAPHY OF THE AUTHOR . . . . .	<b>231</b>

## LIST OF TABLES

Table 1	Correlations Between Inputs and Outputs . . . . .	164
Table 2	Values & ranges for parameters in the model. . . . .	193

## LIST OF FIGURES

Figure 1	Payoff Matrix showing husbandry payoffs . . . . .	12
Figure 2	Eastern Bay with circular harvesting . . . . .	57
Figure 3	World Object . . . . .	61
Figure 4	Layer Object . . . . .	61
Figure 5	The Cell Object . . . . .	61
Figure 6	The Display Object . . . . .	62
Figure 7	Map Object . . . . .	76
Figure 8	glut (OpenGL) . . . . .	76
Figure 9	Database Object . . . . .	76
Figure 10	The Frame Object . . . . .	77
Figure 11	The Sector Object . . . . .	77
Figure 12	Sample snapshot trio for Eastern Bay, day 2,190 . . . . .	91
Figure 13	Big Nash: <i>topDensity</i> . . . . .	96
Figure 14	Big Nash: <i>topGI</i> . . . . .	97
Figure 15	Big Nash: Snapshots . . . . .	98
Figure 16	Black Ledge: <i>topDensity</i> . . . . .	103
Figure 17	Black Ledge: <i>topGI</i> . . . . .	104
Figure 18	Black Ledge: Snapshots . . . . .	105
Figure 19	Eastern Bay: <i>topDensity</i> . . . . .	110
Figure 20	Eastern Bay: <i>topGI</i> . . . . .	111
Figure 21	Eastern Bay: Snapshots . . . . .	112
Figure 22	Flint Island: <i>topDensity</i> . . . . .	117
Figure 23	Flint Island: <i>topGI</i> . . . . .	118

Figure 24	Flint Island: Snapshots . . . . .	119
Figure 25	Great Wass: <i>topDensity</i> . . . . .	124
Figure 26	Great Wass: <i>topGI</i> . . . . .	125
Figure 27	Great Wass: Snapshots . . . . .	126
Figure 28	Petit Manan: <i>topDensity</i> . . . . .	130
Figure 29	Petit Manan: <i>topGI</i> . . . . .	131
Figure 30	Petit Manan: Snapshots . . . . .	132
Figure 31	Seal Cove: <i>topDensity</i> . . . . .	136
Figure 32	Seal Cove: <i>topGI</i> . . . . .	137
Figure 33	Seal Cove: Snapshots . . . . .	138
Figure 34	Shabbit Island: <i>topDensity</i> . . . . .	143
Figure 35	Shabbit Island: <i>topGI</i> . . . . .	144
Figure 36	Shabbit Island: Snapshots . . . . .	145
Figure 37	Big Nash: Parameter Delta vs. Output Delta . . . . .	156
Figure 38	Black Ledge: Parameter Delta vs. Output Delta . . . . .	157
Figure 39	Eastern Bay: Parameter Delta vs. Output Delta . . . . .	158
Figure 40	Flint Island: Parameter Delta vs. Output Delta . . . . .	159
Figure 41	Great Wass: Parameter Delta vs. Output Delta . . . . .	160
Figure 42	Petit Manan: Parameter Delta vs. Output Delta . . . . .	161
Figure 43	Seal Cove: Parameter Delta vs. Output Delta . . . . .	162
Figure 44	Shabbit Island: Parameter Delta vs. Output Delta . . . . .	163
Figure 45	Pseudocode: Urchin Movement . . . . .	208
Figure 46	Pseudocode: Target Selection . . . . .	209
Figure 47	Pseudocode: Urchin Growth . . . . .	210
Figure 48	The Depth Interpolation Algorithm . . . . .	211
Figure 49	The Point Selection Algorithm . . . . .	211

Figure 50	World <i>tick</i> Method . . . . .	212
Figure 51	Layer <i>tick</i> Method . . . . .	212
Figure 52	Animals <i>compute</i> Method . . . . .	213
Figure 53	Plants <i>tick</i> Method . . . . .	213
Figure 54	Animals <i>tick</i> Method . . . . .	214
Figure 55	Urchins <i>mortality</i> Method . . . . .	215
Figure 56	Harvesting Event . . . . .	216
Figure 57	Urchins <i>recruit</i> Method . . . . .	217
Figure 58	Cell <i>update</i> Method . . . . .	217
Figure 59	Visualizer Overview . . . . .	218
Figure 60	Map Object's <i>display</i> Method . . . . .	218
Figure 61	<i>Sector</i> Object Usage for the 4-quadrant Display . . . . .	219
Figure 62	The Sector <i>setPoint</i> Method . . . . .	219
Figure 63	The Frame <i>drawRectangle</i> Method . . . . .	220
Figure 64	The <i>WorldSim</i> Object . . . . .	221
Figure 65	The Agent's <i>tick</i> Method . . . . .	221
Figure 66	Petit Manan: bathymetry . . . . .	223
Figure 67	Seal Cove: bathymetry . . . . .	224
Figure 68	Black Ledge: bathymetry . . . . .	225
Figure 69	Big Nash: bathymetry . . . . .	226
Figure 70	Shabbit Island: bathymetry . . . . .	227
Figure 71	Flint Island: bathymetry . . . . .	228
Figure 72	Great Wass: bathymetry . . . . .	229
Figure 73	Eastern Bay: bathymetry . . . . .	230

# 1. INTRODUCTION

## 1.1 THE URCHIN FISHERY AND ITS PROBLEMS

*Strongylocentrotus droebachiensis*<sup>1</sup> is the sea urchin native to the Gulf of Maine. During the open season, fishermen harvest the urchins in Maine and ship them daily on flights to Japan, where they are considered a delicacy [Taylor, 2004]. Each urchin fishing boat may have as few as two people: one to captain the boat and one diver. Wearing drysuits in the middle of winter, these divers operate in waters no deeper than 15 meters, filling tote bags as fast as can be done while paying some attention to quality and size [Cleaver (pers. com.), 2012]. Some urchins are caught by draggers, but in Maine most are caught by divers [Taylor, 2004]. Only divers were considered in this research.

The sea urchin fisheries in the Gulf of Maine experienced a classic boom and bust cycle beginning in the mid 1980's [Sullivan, 1995]. The regulations governing this fishery became stronger over the years, but the urchins have continued to decline [Chen and Hunter, 2003]. It is difficult for regulators to operate at a speed comparable to a developing fishery. The biology takes time to assess, and there is typically a delay in any management action [Perry et al., 2002]. It is thought by some that current regulations are inadequate because they operate at the wrong scale [Wilson (pers. com.), 2012]. They operate at the scale of two monolithic regions that cover the entire coast of Maine [State Legislature, Maine, 2012]. The management of a fishery can benefit from analysis at the fine scale (tens of meters) [Wilson et al., 2007]. Under certain circumstances, environmental variability and resource patchiness become significant at the fine scale.

Previous to any exploitation of Maine's sea urchin population, sea urchins were numerous enough to be considered pests, called "sea vermin" by some [Miller, 1985]. In the early 1980's, urchin stocks were much larger than they currently are. They were also larger than they had been historically. These larger numbers were likely a direct

---

<sup>1</sup> Variant spelling: *droebachiensis*

result of less pressure coming from their predators [Scheibling and Hamm, 1991]: lobsters, crabs, fish, and wolf fish (AKA wolf eels) which were all in decline. Where larger urchins are concerned, the wolf fish is the most prominent predator [McNaught, 1999]. Lobstermen at the time expressed significant frustration. They pressured those managing the lobster fishery to seek some method of pest control to limit the urchin stocks [Sheibling (pers. com.), 2011]. A solution came from the Japanese market.

The Japanese market for sea urchin roe has been the main driver behind a number of urchin fisheries over the last several decades. The Japanese urchin harvest was the largest in the world until 1984. Their own stocks were diminishing after having been harvested heavily for decades. Since that time, the Japanese have been importing more tonnage each year. By the mid-1990's, the US fisheries were the largest supplier of urchin roe to the Japanese market, bringing in more than \$150M per year [Sonu, 1995].

The Japanese urchin fishery exhibited the classic rise and fall of what is termed a "gold-rush" fishery [Hancock, 1979]. This same process has been seen in various other urchin fisheries around the world [Perry et al., 2002]. The Gulf of Maine urchin fishery has been affected in this same way [Chen and Hunter, 2003]. If a new regulatory regime cannot be found, a full recovery is unlikely for Maine's urchin stocks.

## 1.2 THE FOCUS OF THIS THESIS

In this thesis we highlight spatial scale as an important factor for understanding the collapse of the urchin fishery.

Consider the spatial scale of fishing regulations. Urchin fishermen in the Gulf of Maine are not restricted to small regions. There are no exclusive regions. Where regulations are concerned, the urchin fishery is treated as two large homogeneous entities called *zones* [State Legislature, Maine, 2012].

The monolithic nature of these zones implies that spatial distribution is unimportant. However, it is commonly known among scientists and fishermen that urchins are not uniformly distributed across the two zones of regulation. Urchins cluster themselves into "urchin barrens," [Vadas (pers. com.), 2012, Steneck (pers. com.), 2012, Smith (pers. com.), 2010]. For this thesis, the author investigated the claim that the sustainability of urchin populations is sensitive to local conditions, i.e. that fine-scale effects (at tens of meters) on the fishery are indeed significant. Effects at this scale are currently ignored by the state's regulatory scheme.

Presented here is a tool for investigating the problem of falling urchin stocks and potential solutions. Design decisions were informed by the field of *complex systems* (to be described later in detail). The tool took the form of a biophysical simulator. The design of the simulator came from numerous discussions, over the course of a year and a half, with researchers associated directly and peripherally with the University of Maine School of Marine Sciences. The author hypothesized that a simulator developed in this way would provide currently unavailable insight into the state and dynamics of the urchin ecology. If the model proves to have explanatory power, it might also generate new ideas for management strategies.

Evaluating this hypothesis required a substantial computer science research project. This work implements a model of the urchin ecology as envisioned by James Wilson with input from other researchers acknowledged earlier. The final product is a simulator that can be used to test hypotheses related to the urchin ecology. More empirical knowledge may improve the model's underlying parameters in the future, but even without accurate values, similar models have already made valuable contributions to the field of habitat-based management [Lauzon-Guay, 2009, 37].

The model presented here is merely a hypothesis. For any given set of conditions it is able to make numerous highly-detailed predictions. These predictions may not be verifiable until it either (1) becomes a part of a larger project, or (2) is paired with fine-scale data. Large scale data is available, but there are no applicable fine-scale datasets. Scale is of supreme importance in this concern because of the important

of granularity size when harvesting. The chosen granularity in fishing patterns will either augment or lower the sustainability of a fishing site.

### 1.3 SOFTWARE DESIGN AND ENGINEERING

The bulk of the work for this thesis was a project in software design and implementation. The result is a working computer simulation.

The goals and parameters of the project were initially undefined. They were determined through discussions with economists, ecologists, anthropologists, biologists, fishermen, and marine policy researchers. The multidisciplinary nature of this project required an iterative process. Discussion was followed by changes to the simulation, then interviews, and then more discussion. Many such cycles were completed.

The author synthesized details from these sources into a structure consistent with the aims and theoretical basis behind the National Science Foundation-funded project, "Fine-Scale Dynamics of Human Adaptation in Coupled Natural and Social Systems: An Integrated Computational Approach Applied to Three Fisheries," directed by professor James Wilson. This effort was supported by the entire group, and some researchers not officially in the group (see Acknowledgements).

Since its original implementation, the codebase has undergone 26 significant revisions. The current version of the code comprises approximately 7,000 lines of Python, leaning heavily on Python's facile syntax for programming under the object-oriented paradigm. Python was chosen because of its relative ease of maintenance and alteration. The author believed that most algorithms run significantly faster in C++ (depending on the compiler), but deemed computation time as being less prohibitive than limits on man-hours spent coding.

In its current implementation, hundreds of complete runs of the simulation can be performed in a matter of hours using one of the computer clusters on the University of Maine campus.

The fine-scale elements of the model (e.g. urchins and seaweed), were modeled discretely in terms of their respective state and dynamics. The mathematics behind these dynamics included differential equations, random variables (Statistics), and the conversion of some continuous functions to the discrete space of the model. Challenges were confronted related to feature selection, complexity, computational efficiency, and parallelization. In later sections, the model's configuration and operation are described in detail.

#### 1.4 APPROPRIATENESS OF A COMPLEX SYSTEMS MODEL

The author believes that the state and dynamics of the sea urchin ecology presents a problem which can be better understood as a "complex system". A complex system is a system of numerous elements, interacting with each other according to prescribed rules (more complete definition provided later). This hypothesis was tested by designing and implementing a computer model of the urchin ecology consistent with this perspective. The behavior of this model was judged by experts for its ability to qualitatively capture known behavior of urchin populations in the Gulf of Maine.

Later chapters will explain why a coarse-scale classical model, e.g. the logistic map, cannot capture localized conditions such as urchin barrens. Later chapters will also show why localized conditions can be highly correlated with either the survival or demise of a given urchin population. This question of demise or survival is the core issue to be addressed by the overall research project. Ostensibly, sustainability is also the core issue addressed by state fishing regulations. Appropriate models are those which can explain why some populations survive while others do not. The author believes that current regulation is founded on an inappropriate model.

A complex-systems model could theoretically include a separate entity for every individual urchin and operate at an arbitrarily small scale, such as the size of an urchin. As such, it could capture features such as urchin barrens or kelp beds, which are much larger than an urchin. It wouldn't share the weaknesses of the classical model, but its computational requirements would be onerous.

A complex-systems model which operates at a slightly larger scale could save computation time, but still capture important features such as urchin barrens. We believe that a complex-systems model of the urchin ecology, at a scale of tens of meters, can capture the important features of the urchin ecology discussed in this thesis without prohibitive computational requirements.

Following chapters of this thesis will describe the implementation of this complex-systems model in detail. The model will show sensitivity to local conditions and will exhibit phenomena which have been described by fishermen and biologists. The main phenomenon of interest here is the state-flip from urchin-barren to kelp-bed. These two states (urchin-barren and kelp-bed) are the two stable states we see in the Gulf of Maine [Lauzon-Guay, 2009]. It is important to understand the transition from one state to the other.

The model could also be described as an agent-based model (ABM). ABM's are used to model various types of systems, some of which easily reach and maintain equilibrium. A complex-systems model could be considered a special case of an ABM, where the model is populated inhomogeneously and is sensitive to minute changes in the environment. In contrast to much of economic theory, such a system maintains "far-from-equilibrium" dynamics [Nishiura, 1999], i.e. it does not behave like a system nearing equilibrium. This is important because many equations used historically to study systems were based on the premise that said system approaches equilibrium. Substructures within a complex system (e.g. urchin barrens) may form and appear to maintain equilibrium, but the system overall does not. Typically, these subsystems continually vary in both location and size, exhibit a constant flux of materials and/or energy across their borders, and may disappear rapidly and non-linearly.

## 1.5 NUMEROSITY NOT SUFFICIENT

Efforts in the past to model the dynamics of the urchin population have all ignored the structures that exist within urchin populations. This is to say that no officially utilized urchin population models consider the spatial distributions of urchins with

respect to each other and to kelp. Despite the modern statistical methods employed to determine urchin stocks in the Gulf of Maine, official methods point to stock numerosity<sup>2</sup> as the salient feature of an urchin population. The author contends that a simple number of urchins, no matter how accurate, is less predictive of future viability than the substructures which make up an urchin ecology.

Consider an ant hill having a million ants. It is a complex structure with many tunnels and ants dedicated to various tasks. At each instant ants are choosing tasks based on the manifold historical data encoded as pheromone trails within these tunnels. The complex relationships between the ants and their structure are necessary for survival. It is not realistic to equate an ant hill with a similarly-sized hole in the ground containing one million ants. The author contends that this analogy holds for urchin populations in the Gulf of Maine. Numerosity-based population models implicitly treat urchins monolithically, i.e. as a pile of ants in a hole. Instead, structures and substructures should be incorporated into future discussions of urchin stock assessment.

---

<sup>2</sup>A single scalar representing the number of individuals in a population

## 2. BACKGROUND

### 2.1 PROBLEMS WITH THE URCHIN FISHERY

Despite increasingly restrictive urchin regulations [State Legislature, Maine, 2012], urchin stocks have not recovered [Maine DMR, 2004a, Chen and Hunter, 2003]. The absolute number of urchins removed each year is not in itself excessive. The crux of the problem lies in where urchins are harvested and how many are left behind per unit area. The density of a remaining population is a determining factor in the viability of any particular group [Vadas (pers. com.), 2012].

#### 2.1.1 A TALE OF TWO STATES

At the scale of a few meters, a given benthic environment can often be qualitatively described as either "urchin barren," (a relatively shallow patch having many urchins and a very low level of seaweed) or "kelp bed," (a kelp-dominated zone). Any given sublittoral area in the Gulf of Maine, at depths shallower than 60 feet, will gravitate toward one of these two stable states [Lauzon-Guay, 2009, Breen and Mann, 1976].

The amount of herbivory versus the amount of kelp determines the future state of a location [Vadas and Elner, 1992, Taylor, 2004]. In the urchin-barren state, a site is maintained by urchins engaged in continuous herbivory. If too many larger (legal-sized) urchins are removed from a given site, the remaining urchins are unable to maintain sufficient herbivory. The seaweed grows tall and thick, inviting an influx of predators which favor dense kelp and eat these smaller urchins [Taylor, 2004].

Urchins find difficulty moving and surviving in thick kelp, so a kelp site will have a tendency to remain in this state. Under certain conditions any given site can flip from one state to the other. Ice and storms are considered able to remove kelp from a patch allowing urchins to move in [Vadas (pers. com.), 2012, Steneck (pers. com.), 2012], but state-flips have so far only been observed going from barren to kelp

[Vadas (pers. com.), 2012, Steneck (pers. com.), 2012]. The Gulf of Maine is losing its urchin habitats. The flip from urchin barren to kelp bed is the central phenomenon of concern in this thesis.

At issue here is whether urchin habitats exist in a steady-state equilibrium. Steady and near-steady-state models exhibit only linear dynamics. They are characterized by having some property with a partial derivative of zero with respect to time, or at least being described by a system of linear equations [Allesina and Bondavalli, 2003]. If an urchin habitat can be faithfully modeled this way, a complex-system model isn't necessary. If, however, urchin barrens exhibit *nonlinear dynamics* (e.g. system-flips), then a complex-system model would be an appropriate tool.

### 2.1.2 A SCALE MISMATCH

There is a mismatch between the state of urchin populations and the rules we set to govern the urchin fishery. The mismatch is manifested through incentives and through scale. Fishermen are incentivized, for obvious reasons, to seek out locations with a high density of urchins. Urchins cluster together in regions of high density to maintain the urchin barren. At lower densities urchin herbivory is not sufficient to maintain an urchin barren. The fishermen are incentivized to harvest exactly where the urchin populations can be most affected.

Current regulations are expressed in terms of the number of fishing licenses, the number of zones (two), and upper and lower size limits [State Legislature, Maine, 2012]. Most of the focus is on the number of urchins being caught. Apart from the two fishing zones, there is no regulatory attention to where each urchin comes from or its relationship to surrounding urchins. The current regulatory scheme in Maine operates at the scale of a hundreds of miles [Maine DMR, 2004b]. It is not sensitive to fine-scale conditions (on the order of 10 to 30 m). *S. droebachiensis* operates at this smaller scale. If fine-scale conditions are crucial to the urchin ecology, as hypothesized by [Wilson et al., 1996], then current regulations are ill-equipped to address the problem.

On more than one occasion, regulators and scientists have expressed that only one thing is necessary – to maintain urchin landings that are smaller (by number) than urchin recruitment in the same year [Fogarty, 1995, Wilson (pers. com.), 2012]. This statement is true for a steady-state system, but it does not describe urchins for at least two reasons. First, a new urchin is not an equivalent replacement for a mature one. Herbivory rates grow linearly with urchin volume (approximately) [Vadas (pers. com.), 2012]. A juvenile urchin eats much less than the mature one. It cannot contribute the amount of herbivory needed to maintain an urchin barren. Two small urchins cannot replace an urchin equal to the sum of their diameters. Additionally, smaller urchins have a smaller probability of reaching maturity [McNaught, 1999, Vadas and Steneck, 1995].

Second, the above sentiment is ignorant of local conditions. The survival of a given urchin is tightly tied to its local environment. Urchins live most successfully at the edge between an urchin barren and a kelp-dominated region [Scheibling et al., 1999]. The barren is necessary for them. Although they eat the kelp, they find it difficult to exist in a kelp-dominated area. The kelp also harbors urchin predators. If a region that was an urchin habitat switched to a kelp-dominated habitat, the urchins that are still there would have a smaller chance of survival and a higher chance of predation. New urchins will no longer be successful when they settle at such a site because of their especially vulnerable state [Vadas (pers. com.), 2012, Steneck (pers. com.), 2012].

### 2.1.3 INCENTIVES

Confounding the problems described above, current regulations and conditions in Maine create an incentive to remove all legal-sized urchins when found, potentially causing a state-flip. Consider the problem of finding urchins from the perspective of a fisherman. Finding them requires significant time and effort. Once found, there is an obvious financial incentive to take every legal-sized urchin found. When a fisherman happens upon an aggregation of urchins, there is no discernible incentive to leave

some of them in place. It is true that mature urchins with a low Gonad Index (GI)<sup>3</sup>, if left in place, could become healthier and thus a more valuable product, but the next fisherman to come along would likely take them first [Vadas (pers. com.), 2012]. The probability is not negligible that another fisherman will find them before the first fisherman has a chance to return.

A better approach would be somehow cognizant of fine-scale conditions and/or fisherman incentives. Better regulation would "focus on the system structure, not a population number" [Wilson et al., 1996].

Fisherman incentives spring from the universal goal to harvest as many urchins with a high Gonad Index (GI) as possible. Over the years divers have become better at guessing which urchins have high or low GI. Those which have been eating consistently for some time tend to have higher GI. Some divers also point to a negative correlation between spine length and GI [Cleaver (pers. com.), 2012, Vadas (pers. com.), 2012].

Urchin density is also a factor in urchin health. An extremely dense urchin population may be comprised entirely of starving urchins [Vadas (pers. com.), 2012]. In such situations a fisherman may thin the herd and return at a later date. Not having to share the food source, the remaining urchins should have a higher GI on the second visit. Husbandry is not without risk, however. Other divers pose a constant potential risk. At any given site each diver must choose which urchins to take. If that diver has reason to think that some urchins have a mediocre GI, he or she may choose to leave those urchins in place. However, the next diver to come along might take them. The GI may have increased by then, or that diver may care less about GI. Importantly, a decrease in the number of good fishing sites would increase the probability that another diver will harvest that site before he or she has a chance to return.

Consider the incentives from the perspective of a fisherman (diver). Given an environment where few good fishing sites exist, let  $A$  be the first to find a fishing site having urchins of mediocre quality. After finding these mediocre urchins,  $A$  can leave them in place to allow for further grazing and roe growth, or  $A$  can harvest them

---

<sup>3</sup>GI is a value, typically between 5 and 25, representing the percentage of urchin biomass comprised by the gonads.

in their current suboptimal state. If left in place, some other fisherman might find and harvest them. From the perspective of fisherman A, where outcomes can be described relatively as "Poor," "Good," and "Best," the payoff matrix in **Figure 1** shows actions open to A and their associated outcomes.

		Harvested by another	Site left alone
Diver	Leaves some	Poor	Best
	Takes all	Good	Good

**Figure 1:** Payoff Matrix showing husbandry payoffs. Fisherman A arrived first at a site with urchins of mediocre Gonad Index (GI). A can either harvest all urchins, or leave some to grow (husbandry), taking the risk that another fisherman will harvest them first. Payoffs are relative: Poor, Good, Best.

The "Best" payoff comes for Fisherman A in the top right quadrant, when he or she leaves those urchins having suboptimal GI, and then harvests them after they have had sufficient grazing time. This outcome is contingent on the site not being found by any other diver. If the site is found, A would have been better off taking all the suboptimal urchins on the first visit. As the number of suitable sites decreases, and fisherman gain knowledge of these sites, the probability increases that the site will be found. As the perception of this probability increases, fishermen become more likely to take all the legal-sized urchins on the first visit.

One may consider whether urchin fishermen may be convinced to practice some form of husbandry or maintain some level of urchin density at each location. Current levels of trust between fishermen are low. Urchin fishermen rarely talk with each other. They attempt to watch each other and maintain some idea of where others are making catches, but site information is a closely guarded secret. Information on the location of thriving urchin populations is considered tantamount to an income stream [Smith (pers. com.), 2010]. The implementation of exclusive zones in Maine could change the payoff matrix for each fisherman, thus incentivizing hus-

bandry, but there are many impediments to such a change, such as resistance by current license holders and lack of clear evidence that it has worked in other situations [Wilson (pers. com.), 2012].

Just such a strategy was implemented in Nova Scotia. Urchin fisherman pay for the right to fish in an exclusive zone [Miller and Nolan, 2000, Miller, 2008]. After some early setbacks where fishermen didn't respect the new boundaries, it seemed that fishermen began to practice some level of husbandry over their exclusive zones. Despite the new plan, however, percentage roe yield did not significantly increase [Miller and Nolan, 2000]. Soon thereafter several zones in NS were decimated by the effects of an amoeba, *Paramoeba invadens* [Miller and Nolan, 2000]. The water in Halifax becomes slightly warmer in the summer than temperatures along the Maine coast. In the slightly warmer water this amoeba can survive. *P. invadens* can quickly infect and kill all urchins in a bay [Jones, 1985]. Halifax urchin fishermen who cultivated robust urchin populations had a high probability of sudden die-offs. The incentive was in the end no different in Nova Scotia than it is in Maine: harvest all urchins that can be found; leave none. Impending climate change could mean that Maine will soon contend with this same amoeba. We are protected by a matter of two or three degrees C.

## 2.2 THE FINE-SCALE PROBLEM

In the 1990's, James Wilson identified spatial scale and local conditions as salient features of human-natural coupled systems [Wilson et al., 1996]. The fine-scale effects of these factors often create complex systems because of interspecies interactions [Wilson, 2002] (predators and kelp in this case). Resource patchiness can increase a fisherman's search cost [Wilson, 1990], and the size of these patches can incentivize or deincestivize cooperation [Wilson, 1990, pg.24]. The size of urchin patches are often small enough to be completely harvested by a single boat.

Even so, these effects are often overlooked [Wilson (pers. com.), 2012], especially by regulators [State Legislature, Maine, 2012, Taylor, 2004], and have even been patently

denied [Barinaga, 1995, Fogarty, 1995]. In the intervening years Wilson's conjectures have gained acceptance. Supporting them is a main objective of this thesis.

First, Wilson highlights the fact that fine-scale distribution inhomogeneity matters to fishermen. Traditional theory assumes that fish are distributed randomly because it is mathematically convenient. This is a poor assumption which merely assumes away the complexities behind finding fish [Wilson, 1990, pg.12].

Not only do fine-scale distribution patterns affect fisherman behavior, information at this level is among the most valuable. Wilson defines two kinds of information: coarse and fine-grained. Fine-grained information is idiosyncratic and ephemeral. It relates to the immediate location and movements of animals and fish. Coarse-grained information is more stable. These two types are treated differently because the fine-grained determines the probability of success or failure, especially in times of scarcity [Wilson, 1990, pg.14].

Fishermen are very focused on finding and exploiting "patches," i.e. areas of high density. They each have a strong incentive to distort, withhold, and deceive for strategic advantage. Anybody who withholds information and deceives stands to gain an individual advantage [Wilson, 1990, pg.20].

This knowledge even affects how they work together. The exact location of a fine-scale resource in a patchy, changing environment, is an obvious key to competitive success. Fishers acquire this knowledge individual search. This search is costly. Knowledge can also be gained by communication, but this can't always be depended on. Still, the principal determinants of the social relationships between fishermen are the patterns of information availability in their arena [Wilson et al., 2007, pg.15217].

Wilson realized that simple fishing limits will not help when a species is a component in a complex system, i.e. a system of subsystems. As long as the effect of fishing is slower than the ability of a system to rebuild itself, the system will be maintained. However, if subsystems within it are impaired or destroyed, the system overall will start to collapse in a similar way to how a person's entire health diminishes when one substructure (e.g. the liver) is severely impaired. Overfishing is a major disturbance

to a system that may or may not be able to adapt. Restoration of such a system can't be done by simple reductions. A real solution requires attention to the health of any destroyed subsystems [Wilson et al., 1996, pg.431].

Simple fishing limits do not work on sparse, clustered species because of the economics of fishing. Even moderate levels of fishing lead to long-term failure in slow-response species because fishing efforts are unproportionally aimed at the best locations. The spatial economics of fishing create distinct patterns of removal [Wilson et al., 1996, pg.432]. The economics of fishing dictate that fishermen exploit at the densest locations. Fishing by intelligent humans is highly effective at attacking the strongest subsystems. Fishing that would seem moderate for the system as a whole is likely to be disastrous for individual subsystems. The most desirable subsystem is typically targeted and destroyed first. The economics of fishing dictate that the second-best is then targeted. Over time, moderate levels of fishing will erode the entire system. Reductions in effort will only slow this process, not prevent it. The problem is that remaining effort is concentrated on those subsystems which are most nearly restored [Wilson et al., 1996, pg.435].

Even chaotic systems can be reliably modeled because they do have order. They are characterized by clear cause-and-effect relationships. They follow laws like any other system. Those laws only indicate what will happen in the next moment. Long-term outputs are difficult to intuit because they are nonlinear. Their final output is also highly sensitive to initial conditions. Fish populations are chaotic systems. Accurate predictions of fish stocks is a practical impossibility [Wilson and Acheson, 1996, pg.584].

There is a deep mismatch between governance and what we now understand about ecological complexity. Our governing institutions have a very particular and inappropriate scientific conception of the ocean that assumes much more control over natural processes than we actually have. Scientific uncertainty in this complex system even more of a problem because (1) we assume we are dealing with an analog of a simple physical system, and (2) the individual incentives that result from this fiction are not aligned with social goals of sustainability [Wilson, 2002, pg.327].

We cannot consider the urchins in isolation from other species. The fate of an urchin population is linked to factors other than numerosity<sup>4</sup> and birthrate. Single-species theory follows the belief that the future size of individual stocks is strongly related to spawning stock biomass. This biomass is in turn strongly determined by fishing levels. Many scientists are firmly convinced that the sustainability of each population depends on the maintenance of an adequate number of the species without consideration of other factors [Wilson, 2002, pg.329].

Analytical equations are unable to model complex systems due to their nonlinearity. Such systems have pervasive nonlinear, causal relationships. Outcomes are affected by a large number of factors, each with a different strength. The result is a decline in predictability [Wilson, 2002, pg.334].

Topology has a strong effect on a population's dynamics, especially at the fine scale. Kelp and urchin-barren patches arise in similar but novel patterns at different sites because of environmental heterogeneity. A host of factors may cause these patches including bottom-type, coastal topography, currents, and wind. These patterns tend to concentrate biological activity. The flows of plant and animal life between small patches roll up into the patterns that define behavior at larger scales [Wilson, 2002, pg.344].

If we understand and model fine-scale effects, perhaps we will understand their aggregate impact on a given population's viability. Interaction within subsystems contains important information about systemic perturbations. This information can be used as feedback by which to understand the system's behavior and the kinds of strategies which lead to positive outcomes. When feedback is lost at a fine scale it can often be captured in a more aggregate form at a coarser scale [Wilson, 2002, pg.344].

Some scales are far too coarse, however. We do not have the luxury of regulating urchin fishing only at the large scale (e.g. two zones covering the entire coast of Maine). Learning to recognize patterns is a problem of capturing system behavior and changes at a multitude of scales. For scientific purposes it is often sufficient to

---

<sup>4</sup>A single scalar representing the number of individuals in a population

isolate a particular scale of interest, while holding everything higher in the hierarchy constant. In such a scenario, variations in the lower level subsystems are treated as noise. The urchin fishery, however, does not have the luxury of attending only to higher scales [Wilson, 2002, pg.345].

Fine-scale effects are too important to ignore. They matter both to humans and to animal populations. They must be included in any model of a *S. droebachiensis* in order to have a predictive or explanatory power of population dynamics. Such models can indeed be built because the low-level dynamics (e.g. urchin-kelp interactions) are well understood. Marine-management in Maine will continue to have problems as long as it trusts models which ignore fine-scale effects.

### 2.3 THE CLASSICAL POPULATION MODEL

Historically, populations have been modeled in aggregate because no other option was feasible. The classical, or *logistic*, population equation is one of the most studied and utilized population models (See Eqn.1). Its simplicity makes it an appealing model for policy makers to use. Under such a model, each of Maine's two fishing zones could be treated as a single set of urchins. Such a model is agnostic to local conditions. The goal of sustainability is pursued merely by aiming for a catch rate that is lower than the recruitment rate.

Consider another animal resource in Maine: deer. Their hunting season (for firearms) is about a month [Maine IFW, 2013], and the regulated zone covers most of the state of Maine [Lavigne, 1997, pg.60]. These numbers are comparable to those for urchins. The entire coast of Maine is split into only two regulated zones. In Zone 1 the season consists of 15 days. In Zone 2 it has a length of 36 days [Maine DMR, 2012]. In terms of days and square kilometers, these two differ, but they are within an order of magnitude of each other. Deer provide an interesting example for comparison. In contrast to urchins, deer will be used below as a case where classical population models should be applied.

### 2.3.1 A DISCRETE AND SOMETIMES CHAOTIC PREDICTOR

Classical animal management focuses on predicting population numbers. Under this perspective the number of individuals from a given species is taken as the overwhelmingly important feature for judging the state of a fishery. Estimates of current numbers along with short-term and long-term predictions provide the inputs to classical management [Fogarty, 1995, Hilborn and Gunderson, 1996]. Prediction is typically done using some variation of the logistic population model.

The logistic population model follows this recursive relation (in the discrete time case) [Verhulst, 1838]:

$$N_{t+1} = N_t + rN_t \left(1 - \frac{N_t}{K}\right) \quad (1)$$

*Where :*

$N_t$  = population at time  $t$

$r$  = growth rate

$K$  = carrying capacity

Pierre-François Verhulst was inspired to formulate the above equation after reading Malthus' influential essay, "An Essay on the Principle of Population" [Verhulst, 1838]. When the population is much lower than the carrying capacity, it increases in proportion to current numbers. For some values of  $r$  and  $K$ , the rate slows down asymptotically until the carrying capacity is reached. Such is the behavior of a non-chaotic population. However, this model also allows chaotic behavior. When the value of  $r$  is greater than 3.57, under certain conditions, the population varies chaotically. The chaos comes from a bifurcation of solutions to the differential form of the equation [May, 1976].

When this function is plotted, the rightmost portion of the graph shows the bifurcation of the curve. After the first bifurcation points, the population in the next timestep is no longer proportional to the current one. The graph bifurcates repeatedly, fractally, until the population has so many possible states that its dynamics are considered chaotic. The smallest perturbation in the value of  $N_t$  could make the difference between a large value for  $N_{t+1}$ , or  $N_{t+1} = 0$  [May, 1976]. The real problem with chaotic populations is that many of the solutions to such an equation reach zero. Once a population reaches zero, it remains at zero, barring immigration. Many populations are modeled this way.

The analysis of when this population function becomes either stable or chaotic is apropos to the management of deer populations. Deer population management is described here for the purpose of contrasting it with urchin population dynamics. This contrast will illustrate the need for a different kind of model to manage urchins.

This line of study has been confirmed throughout the years and provides a suitable model for deer populations in Maine [Lavigne, 1997]. According to regulators, the carrying capacity of white-tailed deer in Maine is:  $K = 1.85$  million deer ( $63 \text{ deer}/\text{mi}^2$ ) [Lavigne, 1997, pg.62], but the maximum growth rate  $r$  is a function of environmental conditions and food availability [Lavigne, 1997, pg.21-]. Deer evolved in the presence of predators. They do not maintain stable populations without predation. Their birth rates diminish asymptotically as they approach  $K$ , so absolute numbers is not the problem. They become unhealthy because  $K$  represents an extreme. As the population nears  $K$  the nutritional intake of the average deer becomes so low that bucks lose the capacity to grow antlers, indicating extremely poor health [Lavigne, 1997, pg.21-].

### 2.3.2 SLOW MOVEMENT MAKES SPATIAL DISTRIBUTION IMPORTANT

Regulators of deer hunting do not face the same scale problem as the one faced by urchin regulators because deer have high mobility. The timescale under consideration is a single hunting season. The spatial scale under consideration is almost the entire

state of Maine [Lavigne, 1997, pg.60]. Regulators are aware that one important factor is the ability of deer to disperse throughout the regulated zone [Lavigne, 1997, pg.28]. Since deer are capable of significant dispersion throughout the regulated space within the regulated time-period (before the following hunting season), this model works at the appropriate scale for both *time and space*. The same is not true for Maine's green sea urchin.

Consider the distribution of deer across the state of Maine on day one of deer hunting season. Consider the distribution on day 20. Deer move fast enough that the distribution on day one is not highly correlated with the distribution on day 20 (relative to the case for urchins). On almost the same scale (one of Maine's two urchin fishing zones), the distribution of urchins on day one of any month is very highly correlated with their distribution on day 20. This fact follows logically from each species' speed of movement. The logistic population model works well for deer because they can disperse significantly throughout the relevant zone during the managed timescale. Spatial distribution on day one of deer-hunting season is not important in their case. The same is not true for urchins. Spatial distribution can be ignored for deer regulations, but not for the urchins.

The goal of resource management is long-term sustainability. Catch limits based on a logistic population should work if the scale is correct. In theory, one could devise catch limits that operated at the appropriate scale for sea urchins. It would be small enough that urchins could disperse evenly throughout the regulated zone within the regulated time. Either the spatial zone would be exceedingly small, or the timeperiod extremely long. The first one is too difficult and the second wouldn't allow sufficient opportunity for monitoring or course correction. Urchins have a maximum speed of 3 m/hr [Vadas (pers. com.), 2012], and do not move in straight lines. Their movements are similar to a random walk [Dumont et al., 2004], effectively shrinking their rate of dispersal over large areas. It is unrealistic to expect a top-down regulatory scheme to operate at such a fine spatial scale, and we certainly need the ability to reassess at least once a year. Another solution must be found.

## 2.4 MODELS CURRENTLY USED IN MAINE

All regulatory schemes operate in loose accordance with some model. Most have some form of the logistic equation as a model, even if implicitly. For the Maine urchin fishery, the classical logistic function is used, but not in its simple form. Carrying capacity and birth/death rates are both modeled on their own. A set of terms is used that includes sophisticated calculations to account for catchability and error in current stock assessments [Chen and Hunter, 2003].

Of concern here is that these regulations implicitly function according to a model that is not able to capture the very effects that cause urchin populations to collapse. The Maine DMR is aware that spatial scale effects are not currently represented in their models:

[T]he models do not take into account several of the important factors uncovered by research. For example, studies have shown that as urchin numbers decline the habitat tends to shift toward more extensive kelp beds, which are unfavorable to young urchins. The model also does not include the possible increase in urchin death rates due to outbreaks of predators such as the Jonah crab [Taylor, 2004, pg.26]

Any model that applies monolithically to a large urchin regulatory zone will not be sensitive to fine-scale conditions. Fine-scale conditions lead to viability or extirpation of entire urchin populations.

Policy-makers in Maine employ models for two main functions: (1) Stock assesment, and (2) Stock projection. The Maine Department of Marine Resources (DMR) currently uses sophisticated models for each, estimating the parameters for both from two different observational models: catch per unit effort (CPUE), and a relative-abundance index  $I$ . CPUE is estimated using data from the commerical fishery.  $I$  is estimated from diver surveys [Chen et al., 2000].

Stock assessment is a challenge because of the small number of datapoints being used to estimate numbers for such a large area – the entire coastline of Maine. It is in essence a likelihood function. What is the likelihood of a given stock assessment given the observations? We can choose the estimate that maximizes this function. This estimate is our stock assessment.

Likelihood functions are formulated using some distribution. It is standard to use the normal distribution, but because of its thin tail, the estimate will be very sensitive to outlier datapoints. Distributions with thicker tails have been investigated, but better results have been found with non-normal thin-tail distributions which have been altered to reduce sensitivity to outliers [Chen et al., 2000].

For stock assessment, the Maine DMR currently favors a likelihood function based on the t-distribution. By varying the degrees of freedom its tail-thickness can be adjusted as needed, but more importantly, this distribution was compared to both the normal and mixture distributions. It produces a more stable likelihood function in the presence of outliers [Chen et al., 2000].

Stock projection is the act of predicting future stocks given what we know about a fishery. For projecting urchin stocks, the Maine DMR currently favors a length-structured population-dynamics model [Chen (pers. com.), 2012], similar the one described by Breen et al., and used to project the 1999 abalone assessment in Wellington, New Zealand [Breen et al., 2000].

This projection model is built upon a number of pieces, beginning with a discretization of animal size. Having a set of equally spaced bins representing animal size, the von Bertalanffy growth function (VBGF) is used to estimate a growth probability vector [Chen et al., 2003]. This vector contains a separate probability associated with each bin that represents the probability that an animal in that bin will advance to the successive bin during a given timestep. Operation of the model begins with some given distribution across the size bins. During each timestep, the number of animals that advance from one bin to the next is determined stochastically in a manner

consistent with the growth probability vector. Also included in the projection model are recruitment rates and death rates associated with each size bin [Chen et al., 2003].

The parameters of the assessment and projection models are estimated to maximize the likelihood of the two observational models, CPUE and  $I$ . Despite the sophistication of these models, neither incorporates fine-scale inhomogeneity. But as we have argued, fine-scale effects are necessary in the case of *S. droebachiensis*.

## 2.5 THE COMPLEX SYSTEM MODEL

The burgeoning field of complex systems provides many new tools for scientific research. This section describes research showing that the complex system model provides explanatory power for organisms that are more complex than urchins. By describing its use in a more complicated scenario (e.g. ants), we argue that this model is therefore powerful enough to describe a sea urchin ecology.

As a field of study, complexity is not new, but it still lacks a widely-accepted mathematical foundation. In her book, *Complexity*, Melanie Mitchell describes an exchange between some young scientists and prominent faculty at the Santa Fe Institute, the preeminent institution for the study of complex systems. These faculty members, among whom were a number of well known scientists, were seated in a panel and had just opened the floor to questions. The first question was, "How do you define complexity?" They all laughed, then they each gave a different answer, and then they argued [Mitchell, 2009].

It is not easy to precisely define the term "complex system". Most definitions for a complex system are along these lines:

**complex system** : a set of active elements or "agents", interacting locally with other agents, according to prescribed rules, whose aggregate behavior exhibits the emergence of interesting regularities and depends on feedback between agents<sup>5</sup>

---

<sup>5</sup>Author's definition

The vague word *interesting* is most of the problem. Most complex systems researchers do their work within a given context. Context can often inform the process of defining "interesting."

To researchers in this field, the concept of a "complex system" is considered to be more than just a notion or a loose collection of ideas. Re-imagining concepts such as "emergence" and "feedback," a *complex system* is a paradigm [Amaral and Uzzi, 2007], opening new avenues of research (e.g. "Science of cities") and new classes of solutions to well-studied problems (e.g. non-equilibrium economic models)[Santa-Fe-Inst., 2012].

One canonical example of a complex system is an ant colony. Ant colonies have been studied for decades. Their behavior provides insight into complexity in general and shows the strength of this paradigm over other biological models. If the complex system model can satisfactorily explain ant behavior, then it should be able to explain urchin/kelp interaction, which is certainly a simpler case.

The ant colony is a robust system. A large number of ants can be removed without killing off the colony. Despite the limiting characteristics of each ant, they are able to efficiently solve complex problems [Uhrmacher and Weyns, 2009, pg.13]. They use a set of pheromones to form the basis of their communication system, a set of continuous functions which contain foraging-related meaning for any same-species ant [Wilson, 1962]. Ants choose the shorter of two paths and the better of two food sources not only in terms of magnitude, but long versus short-term productivity [Jackson and Ratnieks, 2006]. Despite the fact that each individual female is identical, an appropriate number of them will choose to forage while others are digging, caring for young, protecting the colony, etc. [Jackson and Ratnieks, 2006]. Older colonies behave differently toward other colonies [Sturgis and Gordon, 2012] despite the fact that ants themselves have no capacity for learning [Dornhaus, 2008].

The urchin ecology (including seaweed and location-specific features) can also be seen as a system. Urchin foraging is dependent on topology and cooperation. Urchins in deeper zones are safe from harvesting, but are often starving. If steep enough, these urchins may move up an inclination to a food source within a reasonable time. The

moving urchins depend on other urchins to be consistently eating at the target location. Herbivory disseminates chemical signals. Urchins can sense these signals [Lauzon-Guay, 2009]. Some biologists believe that urchins can only move randomly [Dumont et al., 2004], while others believe that urchins are able to follow these gradients to the source [Vadas (pers. com.), 2012]. Urchins have been observed moving toward active feedlines, and at other times starving just a few feet from a food source they were not able to sense because of a lack of herbivory [Norris, 2012]. Urchins in the wild do not solve this problem through simple random movement. In the absence of scent signal, urchins have been known to stay put for months [Vadas (pers. com.), 2012].

Under a classical model of an ant colony, where salient features might include population number, food stores, and the size of their underground structure, one cannot predict when a given colony might avoid war, or when topological oddities may interfere with foraging. Under a complex systems model the salient features may include the composite configuration of the pheromone trails, topological details, and the tasks to which each ant is currently engaged. Such a model at the very least incorporates details such as pheromone trails and topology.

A complex-systems model of the sea urchin ecology would include the state of its urchins (with size and GI as salient features), the topology, and the distribution of food and predators across that topology. As with ants, the actions that urchins select have consequences for their health and survival. Since these actions depend on topology and chemical gradients generated by other agents, urchin behavior cannot be predicted without the inclusion of such factors. Such a model becomes extremely important when a modeled population is close to collapse.

The model developed by [Kawamura et al., 1999], is an example of what Epstein calls a *generative* model<sup>6</sup> [Epstein, 1999]. This is the kind of model developed in this thesis research. It is not the first generative model of an urchin ecology [Lauzon-Guay, 2009]. The model described here was designed to emulate the simple interactions we are able to observe between agents in the system being modeled. Its explanatory power

---

<sup>6</sup>A model which employs bottom-up processes to allow larger structures or phenomena to emerge.

comes from the regularities that emerge. The desired outcome of this project is a dynamic model having fine-scale interactions programmed to be consistent with the literature, and macroscopic regularities deemed plausible by experts in the field. These regularities emerge without having been explicitly programmed.

One alternative would be to model the urchin population as a single entity, with no sensitivity to the state of individuals. Such a model would likely produce different results. Even if it were able to exhibit the emergent behavior expected by biologists, it would not contain the information necessary for decomposing a large-scale effect into the constituent acts that caused it. This decomposition is essential to being able to explain large-scale effects.

Consider two urchin populations  $A$  and  $B$  which are identical in all ways except a small difference in topology or distribution. Interviews with scientists and fishermen indicate that such differences may cause  $A$  to collapse and  $B$  to thrive. A monolithic model is unable to disambiguate  $A$  from  $B$  if they are of similar size and macroscopic quality. As a direct result, it would be unable to reliably model a distinct result for  $A$  and  $B$ .

The complex-system model is widely accepted amongst researchers of cooperative insects [Kawamura et al., 1999, Miller and Page, 2009, Pham et al., 2006]. It has proven itself capable of describing at least that amount of complexity and providing some much-needed explanatory power. A literature review did not reveal evidence that urchin groups are as complex as those of social insects, such as ants. It is therefore safe to assume that a complex model is capable of describing urchin behavior. Using ant-related research as a point of argument, a generative complex-systems model was chosen for simulating the sea urchin ecology. This model will be described in further detail below.

## 2.6 ELEMENTS OF THE URCHIN ECOLOGICAL SYSTEM

Any model of the ecology of *S. droebachiensis* should include the animals themselves, their physical environment, and any other organism with which they maintain significant interaction. Urchins interact with each other, their food, and their predators. These interactions are mediated by relatively well-understood mechanisms. A literature review indicated that these mechanisms, even if largely stochastic, are reasonably-well documented.

A complex system model of the urchin ecology can be considered at any spatial scale necessary. A complex-systems model at the scale of a square centimeter could potentially capture all important features of the urchin ecology, but such a model is computationally cumbersome. A scale of 1,000 square km is too coarse (discussed). What is the optimum scale? How coarse can this model be while still capturing the most important dynamics of the ecology? Similarly to statistical ordination [Manly, 2005, ch.12], one objective of a complex system model is to present the simplest version possible of a system while still maintaining a faithful representation of its most important phenomena.

Consider the elements of this system in greater detail. Kelp, a plant, is immobile except during its pelagic spore stage. After settlement it grows at different rates and to different densities with some relationship to depth [Brawley (pers. com.), 2011]. Urchins float in the water during their larval stage. They disperse ubiquitously throughout the Gulf of Maine [Strathmann, 1978] and remain suspended in the water until settlement upon some substrate. From there they move slowly, grow, consume kelp, are consumed by predators, and some die of natural causes [Vadas (pers. com.), 2012]. The predators are the least understood elements of this system. We have some indirect knowledge of predation levels and which urchins are affected, but little is known about the proportion of overall urchin predation accounted for by each type of predator (lobster, fish, crab, etc.) [Vadas (pers. com.), 2012].

Urchin dynamics can be classified into the following categories: eating, growing, moving, reproducing, dying (of natural causes), and predation. The state of an urchin, as

it pertains to the prediction of future dynamics, can be sufficiently represented by its diameter and Gonad Index (GI) [Vadas (pers. com.), 2012]. A high GI (e.g. 25) is maintained by consistent feeding at a quality food source. The only exception being that GI goes to near zero after a spawning event.

The diameter is a reasonable but imperfect measure of age [Chen et al., 2003]. In the presence of food, urchins will grow at a relatively predictable rate. An urchin which is not eating, however, does not grow. During such starvation periods, urchins survive by slowly consuming their gonads. This activity can continue in some cases for an entire year [Vadas (pers. com.), 2012]. Since a healthy urchin has no need to consume his or her gonads, GI can be used as a proxy measure of urchin health (With the exception of the period following a spawning event).

Urchins reproduce sexually, but are broadcast spawners. Their spat is fertilized in the open water [Taylor, 2004]. During spawning events the males broadcast sperm and the females broadcast eggs. In appearance the spawning event looks like a thin continuous puffing of smoke coming from the top of the urchin. Urchins typically have one spawning event per year. New recruits settle during May and June [Taylor, 2004].

Suspended in the water, larval urchins can travel for many miles carried on ocean currents [Gaylord et al., 2004]. They become distributed throughout the Gulf of Maine. They become ubiquitous in the system. Their density is not known to be tied to local population abundance [Strathmann, 1978]. Once an individual urchin settles on the ocean floor, it becomes a purely benthic animal, moving only along the floor using its tube feet. Once mature, it can move at a top speed of three meters per hour [Vadas (pers. com.), 2012]. In the benthic state the urchin becomes sensitive to local conditions.

When available, *S. droebachiensis* may consume a number of different kelp species, but typically focuses on one. In the laboratory, urchins have been observed eating *Saccharina longicuris*, *Saccharina latissima*, *Agarum fimbriatum*, *Agarum cribosum*, *Nereocystis luetkeana*, *Costaria costata*, *Laminaria groenlandica*, *Monostroma fuscum*, but

they show a high preference for *S. longicuris* [Vadas, 1977, Kling, 2006].<sup>7</sup> Growth rates of these kelps may be estimated using depth, latitude, temperature, time of year, and the nutritional content of the water [Vadas et al., 2004, Mathieson, 1976]. The pertinent actions performed by kelp in this ecology include growing, reproducing, and being consumed by the urchins. *Being consumed* is not normally considered an action taken by seaweed. This is merely a simple way to view this phenomenon from a programmer’s perspective.

Direct physical contact is required for most interaction between *S. droebachiensis* and kelp, but it is also believed that they can follow a scent toward kelp [Vadas (pers. com.), 2012]. The urchin has no brain in the usual sense of the word, and no cephalization, but there are nerves throughout its body. There are sensory neurons, ganglia, and motor neurons in each spine of an adult sea urchin. This neural system differs in obvious ways from that of vertebrates, but the connections between these appendages and radial nerves provide control and coordination [Sea Urchin Genome Sequencing Consortium, 2006]. Much urchin movement appears random, but researchers [Vadas (pers. com.), 2012] and fishermen [Norris, 2012] have observed urchins move directionally toward a food source. The urchins can move from a deep zone to the edge of the shallow zone where kelp thrives [Vadas (pers. com.), 2012, Norris, 2012]. They are also able to find detritus (broken pieces of kelp that have drifted), and have been known to fill lobster traps [Miller, 1985].

Urchin predation comes from at least three non-human sources in the north Atlantic: fish, lobsters, and crabs [Taylor, 2004, Vadas (pers. com.), 2012]. Historically, the wolf fish, AKA wolf eel (*Anarrhichthys ocellatus* Ayres, 1855) [FishBase, 2012] was a primary predator of urchins along with various fish [McNaught, 1999, pg.8], such as american plaice, cod, cunner, haddock, longhorn sculpin, ocean pout, and winter flounder [Vadas and Steneck, 1995]. Wolf fish stocks in the Gulf of Maine are now functionally extirpated, and Cod stocks are very low. These absences were evident before the inception of the urchin fishery in 1986, and are a potential cause of the excessive urchin stocks of the early 1980’s [Scheibling and Hamm, 1991, Steneck, 1997].

---

<sup>7</sup> *S. longicuris* was formerly known as *Laminaria longicuris* (Bachelot de la Pylaie), and *S. latissima* was formerly known as *Laminaria saccharina* [AlgaeBase, 2012]

Current non-human predation of urchins occurs almost entirely to urchins smaller than 50 mm [Vadas (pers. com.), 2012].

Marine biologists have some level of understanding of the elements involved in the ecology described above. Urchins and kelp patches can be described as elements in this system. Urchin reproduction, predation and natural mortality can be modeled with random variables. This ecology can be described as a system of numerous elements, interacting with each other according to prescribed rules. The aggregate phenomenon of interest is the eventual survival or demise of urchin stocks in the Gulf of Maine. It is clear that a century of overfishing has dramatically affected our coastal food web [Jackson et al., 2001].

## 2.7 A SYSTEM OF SUBSYSTEMS

The impetus for this project comes from an important but failing fishery. Fishing limits have become lower over the last decade, and the fishing season has become shorter, but urchin stocks are not rebounding [Maine DMR, 2004a]. The problem isn't that too many urchins are being removed from the Gulf of Maine. The problem is where they are harvested. A level of fishing that is moderate for the system is capable of destroying any subsystem unfortunate enough to bear its full weight.

The Gulf of Maine is a system of subsystems. The subsystems that exist in the shallower regions of the Gulf of Maine (i.e. less than 60 ft depth), manifest two stable states: (1) Kelp-dominated, and (2) Urchin-barren. Sustainability of urchin stocks is dependent on the maintenance of urchin barrens.

A lack of understanding of subsystem dynamics can lead to a misinterpretation of the meaning behind stock estimates. Overfishing may not appear at first to damage the system. The damage becomes obvious once a certain threshold is passed. Passing this threshold carries the implication that the problem is now much more difficult to resolve. Resolution will come through the maintenance of system structure, not through a fishing limit determined from stock assessment and prediction. The cur-

rently used *constant fraction quota* [Wilson et al., 1996] (a fishing limit equal to a set fraction of the current population estimate) will not be sufficient.

Current regulations ignore the importance of subsystems. They are set at the large scale [State Legislature, Maine, 2012]. At the large scale, it may appear that divers have not removed an excessive number of urchins. The urchin landings for a given year are small when compared to the estimated total urchin stock within the given fishing zone. At the fine scale, however, another diagnosis is apparent. About 1,520t ( $t=metric\ tons$ ) were landed from Zone 1 in 2001 [Maine DMR, 2004a]. Estimates of total urchin stock for Zone 1 in 2001 run from 37,860t [Hunter et al., 2010, pg.40] to 45,870t [Grabowski et al., 2005, pg.19]. Urchins were harvested from relatively dense aggregations. Those aggregations had been maintaining urchin barrens. After losing significant capacity for herbivory, many of these aggregations have now flipped to the kelp-dominated state [Norris, 2012, Vadas (pers. com.), 2012].

Since consumption capacity varies linearly with mass [Vadas (pers. com.), 2012], more massive urchins are responsible for most of the herbivory in any urchin barren. Fishing over the last few decades has decimated stocks of larger urchins. More specifically, the numbers of "super-legal" urchins (above the upper-size-limit of 76 mm [State Legislature, Maine, 2012]), are currently very low. It is not clear that they were ever high. [Hunter et al., 2010]. Most of the herbivory is performed, therefore, by urchins of legal size. If an insufficient number of larger urchins are left at a site, they will no longer be able to eat as fast as the seaweed can grow. They are unable to keep the kelp at bay, so to speak [Vadas (pers. com.), 2012, Steneck (pers. com.), 2012]. The site begins to flip to the kelp-dominated state.

## 2.8 SUMMARY

In an almost indirect way, urchin fishermen are causing the demise of urchin aggregations one-by-one. Their actions cause a reduction in herbivory. This reduction is the most common reason for the site-flip to occur (from urchin-barren to kelp-dominated). The kelp-dominated state is highly unfavorable to urchins, and especially to smaller

urchins. This is because the predators of smaller urchins have an affinity to dense kelp. Once a site flips to the kelp state, the probability of flipping back to the urchin-barren state is extremely low.

Predators are few for urchins larger than 50 mm, and in Maine we find no evidence of *P. invadens*, which is due to slightly colder temperatures in summer [Miller and Nolan, 2000, pg.11]. Therefore, this loss of larger urchins is typically anthropogenic – the result of harvesting events. Fishermen are the main predator of larger urchins in Maine. Even though their actions are consistent with the laws meant to protect these populations, the smaller urchins they leave behind do not have a reasonable chance for viability.

There are a number of strategies which may be employed in an effort to ebb the tide of overfishing. The outcome of most strategies cannot be determined without years of testing. The current population estimates and associated trends make it very difficult to attempt multi-year experiments with little more than hope. A reliable simulation could explore the effectiveness of each idea. The model described in the next section functions as just such a simulator.

### 3. REPRESENTATION OF AN URCHIN ECOLOGY

Having described the salient aspects of the urchin ecology in the previous section, this section describes how that ecology is represented in the simulation. Some biological material is repeated for the sake of clarity. For the sake of specificity, some of the algorithms described in this section are further detailed in Appendix C: *Pseudocode*.

#### 3.1 BASIC DESCRIPTION

The author designed and implemented a discrete-time cellular automata model of the sea urchin ecology. The model was implemented as a simulator written in Python leaning heavily on the object-oriented paradigm. A *World* object contains a set of *Cell* objects. Each cell is populated with urchins and seaweed. Each cell evolves in parallel. Their activity is functionally simultaneous, but not actually simultaneous due to the fact that each site is being simulated on a single serial processor. The dynamics of each cell were derived from the literature.

After consulting scientists and fishermen, eight fishing sites in the Gulf of Maine were selected for modeling. Each site is an actual location in the Gulf of Maine for which topological data (bathymetry) was available. Each site's bathymetry was mapped onto its own grid having cells approximately 20 meters square. The model simulates each cell in the grid as a cellular automaton having internal objects performing the functions of sea urchins and kelp.

The urchins in each cell are organized into discrete size bins. Size discretization has been a practice of previous research [Chen et al., 2003] and is a common technique among modelers [Lauzon-Guay, 2009]. The urchins consume, grow, and die as a function of size. Each cell contains kelp which is represented by percentage of coverage and percentage of maximum height. Interaction rules for the urchins and the seaweed were designed to be consistent with the observations of both fishermen and marine biologists who have studied urchins in situ and in the laboratory. These interaction

rules depend on urchin mass, seaweed mass, depth, detritus, and chemical gradients in the water.

In the remainder of this thesis the design and results of the model will be discussed. First, the representation of each element is discussed. Second, the interaction and functions performed by these elements are described. These descriptions also include approximations which were necessary for computational simplicity and efficiency.

### 3.2 REPRESENTATION OF TIME

Time is discrete in the model. The current state of the model depends only on the immediately previous step. It is in this sense Markovian. Functioning in parallel, the state of any given cell at time  $t$  depends only on the state of that cell and its immediate neighbors at time  $t - 1$ .

Urchins move sufficiently slowly that a timestep of 24 hours was deemed appropriate by the author. This resolution maintains the necessary resolution to observe significant daily urchin migration from cell to cell. A 24-hour timestep has the added benefit of making the effects of tide upon the model negligible.

Each timestep in the simulation presents an opportunity for interaction between the urchins and the kelp. The rates of all time-dependent processes (e.g. growth) are keyed to the length of the timestep. During each time step, each cell performs a set of internal processes. Each cell also interacts with adjacent cells. This interaction consists of the movement of urchins and the flow of seaweed scent and detritus. The internal processes of a cell include the growth of seaweed and urchins (details in following sections).

### 3.3 REPRESENTATION OF TOPOLOGY

The earth is not a sphere, but it is simpler to model it as if it were. At the small scale of a few kilometers the resulting distance errors are not significant. All selected fishing sites are square regions less than ten kilometers on a side. Similarly, the bathymetry of the Gulf of Maine which was used for this project does not perfectly reflect reality, but it is more than sufficient for the purposes of this thesis. However, future considerations required planning for the larger scale.

The code for this simulation is intended for larger simulations that might span significant portions of the Gulf. Using the spherical model, distance measurements which span large sections of the Gulf of Maine can be significantly inaccurate. The author performed a test in which the distance between two points, each at either end of Maine's coastline, was first calculated using the spherical model. This value was then compared to highly accurate modern methods. The two distance measures differed by more than 100 km [Kaim (pers. com.), 2011]. Such measurements will become worse as more latitude and longitude lines are crossed [Kaim (pers. com.), 2011].

The codebase developed for this model is part of a larger project managed by James Wilson. At the scale of the model described here, the discrepancy between spherical and accurate models is negligible. However, interaction with the larger project required an answer to this problem. Fishermen were to be modeled moving between the simulated sites. At the scale of the entire Gulf of Maine, these discrepancies become significant.

### 3.4 REPRESENTATION OF KELP

We sought a simple way to represent kelp in the model. Many species of seaweed occur in Maine. Each species has a different productivity and provides a different level of nutrition to urchins [Vadas and Elner, 1992, Vadas et al., 2004]. We decided to model these species as a single virtual species having average productivity and providing average nutrition to the urchins. Biologists which were connected with this

project indicated that this approximation was reasonable [Vadas (pers. com.), 2012, Steneck (pers. com.), 2012].

It was clear from discussions with the biologists that there was no need to model individual plants. Early discussions and previous research [Lauzon-Guay, 2009] indicated that a single quantity, *biomass*, might be sufficient. At first, then, seaweed was represented by a single floating point number associated with each cell.

After several versions it became clear that a single value was not sufficient. Consider two locations with identical biomass. One of them, site *A*, has very few plants, but all are at their maximum height. The other, site *B*, is 100% covered, but with recent settlements that are all very short. There is a potential for these two sites to exhibit significantly different productivities (in terms of biomass), and different levels of predation. Early versions of the model did not disambiguate between two such locations. The aggregate dynamics of kelp in the model appeared unreasonable.

Coverage and height were chosen as a way to split biomass into two variables. Coverage is a floating point number that represents how much of a cell is currently covered by the seaweed. Height is another floating point that represents the average height of plants in that cell. Biomass is then a computed quantity: coverage  $\times$  height. The density of kelp is outlined in the appendices. Maximum coverage depends on cell size, and maximum height depends on photic energy (and therefore depth). Later sections provide greater detail. Area is measured in  $m^2$  and height in  $m$ .

Discussions with biologists indicated that there is a difference between the rate at which biomass is added to existing plants and the rate at which new plants settle. The importance of this separation can be seen between sites that have the same biomass, but different productivity because one is productive through growth and the other through settlement. Estimates of means and reasonable ranges of these rates, along with source references, are detailed in the appendices.

In the model, kelp height and kelp coverage are not visible to the simulated urchins. Kelp biomass is the parameter of interest for kelp-urchin interactions. Kelp biomass is also the main parameter of interest for many empirical results. All kelp-related

parameters were estimated to ensure that the modeled seaweed biomass was consistent with these results (details in the appendices). The dynamics of *S. longicruris* were used as the basis for this kelp along with some data from other species, when available. *S. longicruris* is the species most favored by *S. droebachiensis* [Vadas et al., 1980].

Every cell in the model of depth greater than zero has some nonzero amount of kelp, represented via height and coverage. Its density diminishes on average as depth increases in order to be consistent with the relationship between kelp incidence and photic energy.

### 3.5 REPRESENTATION OF URCHINS

Each cell has a set of urchins. There are two important quantities to be tracked for each individual urchin: size and gonad index (GI). For the sake of computational efficiency, urchin size is represented by discrete size bins, and GI is a cell-level attribute.

The use of size bins allows all urchins within a cell to be represented by a single list of integers, where each integer refers to the number of urchins in each corresponding size bin. The size associated with each bin is set at the beginning of the simulation and is identical for all cells. All urchins within a given bin are treated as if their size is exactly the mean size of urchins of that bin.

GI is a function of food availability. Since food availability is consistent throughout a cell, an approximation made by the model is to attribute the same GI to all urchins within a given cell. This simplification is not inconsistent with the reports that urchins feeding near each other typically have similar GI [Vadas (pers. com.), 2012, Norris, 2012].

## 3.6 KELP DYNAMICS

Kelp performs two actions during each timestep: *growth* and *settlement*. Growth, measured in  $m$ , is the simple increase in height of existing plants. It is at its maximum in the shallowest regions. Settlement, measured in  $m^2$ , is the increase of coverage of a cell through the presence of new plants becoming affixed to some spot on the cell.

### 3.6.1 KELP GROWTH AND REPRODUCTION

Some complicated models of kelp growth have been used in other models, such as Ricker's recurrence relation [Turchin, 2003]. However, a simpler function was sought to model kelp dynamics in this model. Estimates of biomass productivity in the literature indicate that a given location will have a constant rate of growth per unit area [Vadas et al., 2004, Vadas et al., 04c]. This constant rate can then be modulated by time of year and depth, where time of year implicitly takes into account changes in the presence of nutrients in the water [Vadas and Steneck, 1988, Vadas et al., 2004].

Kelp growth is modeled in terms of vertical height and horizontal-plane coverage. Growth in height represents the augmentation of extant plants, while growth in coverage represents the settlement of new ones. Using height and coverage, assuming a constant kilograms per unit volume, biomass becomes a computed value. The main input parameters of concern are photic energy (a function of depth) and season. Typically, the growth due to settlement is negligible relative to the growth of extant plants. A better model would downgrade the height whenever settlement occurs. This wasn't deemed necessary here because settlement is so low.

The rate of vertical growth per unit area is modeled as a linear function of photic energy flux (relative solar energy per unit area per unit time). In the model, photic energy is greatest at the surface, where it is given the arbitrary value of 1. It diminishes exponentially with depth [Vadas and Steneck, 1988].

Seaweed biomass density decreases as depth increases [Miller, 1984]. Solar-dependent growth implies a negative relationship between biomass density and depth. The exponential function was utilized along with stochasticity to generate an initial seaweed density distribution consistent with observations of kelp density distributions [Vadas and Steneck, 1988], i.e. an exponential distribution was utilized in the function that generated the initial seaweed distribution.

Vertical growth also depends on the nutritional content of the water. Availability of nutrients such as nitrates cause kelp to grow faster during certain seasons than others [Vadas et al., 2004]. Yearly cycles in nutritional content made it possible to use the day of the year as a proxy for nutritional content [Vadas et al., 04c]. Each of the selected sites is sufficiently far from estuaries such that this approximation is acceptable.

The growth rate is first computed taking photic energy into consideration. Next, the effects of nutritional content is manifested as a downgrade to the growth rate. The downgrade is computed using a sinusoidal function on a one-year cycle. Urchin growth rates also vary cyclically. The sinusoidal aspect of kelp growth is out of phase with that of *S. droebachiensis* [Vadas (pers. com.), 2012]. Cobscook Bay has been well-studied in this respect. Peak biomass in Cobscook Bay for some species of algae is between August and September. Frond elongation rates peak between June and July [Vadas et al., 2004]. Rivers, tidal range, and current make the ecosystem in Cobscook Bay different from the rest of Maine [Peacock, 2011, Steneck (pers. com.), 2012]. Growth rates for algae in the rest of Maine are not in phase with Cobscook, but they do each follow a year-long cycle [Vadas (pers. com.), 2012].

Growth in kelp height is bounded on the upper end by a maximum theoretical height computed for each depth. The maximum height is calculated from a maximum theoretical biomass. The maximum biomass is determined by the incident photic energy and the area of the cell.

For instance, the biomass density of *Ascophyllum nodosum* has been observed as high as  $28.94 \frac{\text{kg (wet)}}{\text{m}^2}$  and with a 95% CI in the range 20.78 -37.11 [Vadas et al., 04b].

For *Ulva lactuca* and *Enteromorpha spp.*, the mean biomass has been observed at  $321.1 \frac{g(dry)}{m^2}$ , with a 95% CI range from: 115.8 - 608.4 [Vadas et al., 04c]. Biomass densities of *S. longicuris*, the species most eaten by urchins, have been observed as high as  $500 \frac{g(dry)}{m^2}$  at Mahar Point, and  $1000 \frac{g(dry)}{m^2}$  at Bar Island [Vadas et al., 2004]. Much further south it has been observed at  $47 \frac{kg(wet)}{m^2}$  [Egan and Yarish, 1990] (wet/dry weight ratios for *Laminaria / Saccharina* species can be as low as 5:1 [Tseng, 1987] and as high as 30:1 [Egan and Yarish, 1990]).

Wet weight numbers are used less often [Vadas (pers. com.), 2012], and their conversion is not precise, so only dry numbers were used here. Considering only the dry-weight data, the modeled seaweed is a functional substitute for the limited data we have: the range of  $0.32 - 1.0 \frac{kg(dry)}{m^2}$  for maximum biomass density was considered by the author to be not inconsistent with the above results.

From this we chose a value of  $0.8 \frac{kg(dry)}{m^2}$  for the parameter *maxBiomassDensity*, and a range of 0.32 - 1.0.

The second way for a cell's seaweed biomass to increase is through the settlement of new plants. If a given cell is at maximum coverage, its kelp grows only in height. Any cell that is not totally covered has some nonzero settlement or "re-coverage" rate. This rate represents the probability that some given area of unsettled sea floor will receive the successful settlement of new kelp plants. It is modeled in units of area per unit time. The rate is set for an empty cell. The rate is then diminished with the coverage ratio. The settlement rate will be half of the original rate when that cell reaches half of its maximum coverage. Pre-settlement algae are modeled as being ubiquitous in the water. The algal settlement rate in a given cell is purely a function of the amount of open surface in that cell.

Discussions with biologists indicated that the description above represents a reasonable approximation of kelp growth dynamics [Steneck (pers. com.), 2012] [Vadas (pers. com.), 2012].

### 3.6.2 EFFECTS OF KELP ON THE ENVIRONMENT

Discussions with biologists revealed that the effects of detritus and seaweed scent in the water are not negligible. Urchins have been observed eating a diet entirely composed of detritus [Norris, 2012, Vadas (pers. com.), 2012], and seaweed scent is the best explanation available for the directed movement of urchins [Vadas (pers. com.), 2012].

When urchins move toward food it is not known whether they can sense a scent being released by the kelp being consumed, or if they are smelling products given off by urchins consuming the kelp. In both cases that this sense of smell provides a convincing explanation for urchin aggregations in beneficial feeding areas. It would explain the movement of urchins from deeper zones to the photic zone where kelp is more available [Vadas (pers. com.), 2012]. Others suspect that an urchin can only smell a substance produced at a distance of one or two meters [Steneck (pers. com.), 2012]. At least one diver has observed large numbers of urchins moving together toward a relatively distant group of urchins consuming dense high-quality food. That same diver has observed starving urchins remain where they are, despite the array of food less than five meters away, presumably because no urchins were eating it [Norris, 2012].

In order to strike a balance between the various views encountered by the author, the urchins in this model were not explicitly enabled to sense scents from a given distance. Instead, kelp in the model is imbued with scent-generating capacity in direct relation to biomass. This applies mostly to kelp which is currently being consumed. If no urchins are currently consuming at that location, the scent is still generated but to a much lesser extent.

The amount of kelp-scent in a cell is modeled by a single floating point number. It is generated once during each timestep. It then abates at the start of the next timestep. This is referred to as an attenuation rate. It attenuates as it disperses into the vertical column of water above the cell and undergoes chemical degradation. Scent is also lost to adjacent cells. It diffuses slowly to the adjacent cells and weakens further as it disperses. If the scent is still strong enough after dispersing through several cells,

it can be sensed tens of meters away from where it was generated. This scent inspires gradient-ascent directed movement in simulated urchins that do not already have a food source.

Separately, detritus spreads in a similar way. Detritus was considered an important feature to add to the model due to the high number of anecdotal stories from divers about urchins surviving purely on such detritus. In the model, kelp is imbued with a detritus-generating capacity in direct relation to biomass. This production of detritus does not require urchin activity. It is caused by wave action and other natural processes. This detritus spreads from cell to cell and decomposes (i.e. disappears) slowly. The next section describes how urchins are influenced by the presence of kelp, the scent of kelp, and detritus.

### 3.7 URCHIN DYNAMICS

Urchins do five things during each timestep: eat, move, grow, die, and (potentially) recruit. Much is still unknown about *S. droebachiensis*. For instance, there is no generally accepted average natural lifespan for this species. Knowledge of urchin dynamics comes from experiments performed by marine biologists and from observations made by many divers over the intervening years since the start of Maine's urchin market, (c. 1985). This knowledge was gleaned from the literature when available, and from personal communication otherwise.

#### 3.7.1 URCHIN MOVEMENT

Movement is modeled as the discrete displacement from a given cell to an adjacent cell. Therefore, position can only be measured with the precision of one cell's width.

Since biologists consider urchins of the same size to be equivalent, we save computation time by modeling the dynamics of multiple urchins at each size class as opposed to modeling each urchin individually.

Depending on the circumstances, urchin movement can be either random or directed. In the absence of a food-scent gradient urchins move randomly. Even when urchins move toward a food source their movement has a stochastic element to it. Currents in the water and detritus dispersal add noise to scent signals. The level of randomness of urchin movement is inversely related to the strength of a chemical gradient which an urchin may follow [Vadas (pers. com.), 2012]. These dynamics are captured in the model by making all movement stochastic, but having a tendency to move along scent gradients. This tendency increases with the strength of the signal.

Despite this tendency at times to move toward food sources and away from predators [Vadas (pers. com.), 2012, Steneck (pers. com.), 2012], an urchin's movement typically resembles a random walk, not a straight line [Dumont et al., 2004]. Although urchins have a top speed of 3 meters per hour, they typically move more slowly, about 2 m/hr [Vadas (pers. com.), 2012]. The mathematics behind random walks can predict an average distance traveled after a given amount of time. This distance is significantly less than if the urchin had traveled in a straight line.

For instance, if an urchin travels in a random walk, at a rate of  $2m/hr$ , it's average distance from its starting point will be less than  $2m$  after one hour. Under the approximation that the movements of an individual urchin can be discretized into one hour increments, such that a  $2m$  displacement occurs each hour, after  $n$  hours, the expected value of the length of that urchin's path will be a distance of  $\sqrt{2n}$  meters from origin to final location [Weisstein, 2012]. In other words, during any given day, a moving urchin will travel an average of  $\sqrt{48}$  meters ( $\approx 6.9$  m). If we assume that urchins are homogenously distributed<sup>8</sup> throughout a cell, any of the urchins which are within 6.9 meters of the edge of the cell could move to an adjacent cell (including diagonals) within a single timestep. For a cell of  $20 \times 20m$ , this represents approximately 90% of the cell. Therefore, in cells of this size where all urchins are mobile, an average of not more than 90% of its urchins should move during any given timestep. Typically fewer than that will move. This calculation merely provides an average upper limit against which to check urchin movement. Therefore, movement in the model is a stochastic process that rarely allows 90% to move even in the presence

---

<sup>8</sup>There is no basis here for choosing any distribution other than the uniform.

of a strong scent signal.<sup>9</sup> Since individual urchin speed cannot be measured, it is considered acceptable to have aggregate movement that falls within these limits.

The algorithm that determines urchin movement represents a best attempt to synthesize everything described above. It involves stochastically moving urchins from less favorable cells to more favorable ones. Target selection and movement are done separately. Favorability is determined by food availability, depth, bottom type, and number of urchins present. An overview can be seen in figures 45 and 46.<sup>10</sup>

The model was custom-coded in Python as opposed to utilizing a preexisting agent-modeling package such as MASON. Where random distributions are concerned, Python makes various distributions available for use in its 'random' package. The stochasticity referred to in this section describes the movement of urchins that are presumed to be uniformly distributed across a cell. In this case the uniform distribution was used to generate the necessary pseudorandom numbers. Where indicated in this and other chapters, other sections employ normal, exponential and Poisson distributions for the generation of pseudorandom numbers.

### 3.7.2 ADMINISTRATIVE CHALLENGES

The model requires that each cell functions in parallel, but it was written in such a way that each cell's operation is computed serially. Their operation had to be made functionally parallel despite the fact that the system is inherently serial.

Each timestep affords each cell an opportunity to perform its functions. Without correction of some kind, urchins may end up moving faster than their maximum possible speed. Given cells A and B, A is processed first, then B. Cell B begins with 20 urchins. One hundred urchins move from cell A to cell B, and then 100 urchins move from B to C. At least 80 of those urchins have moved two cells away during a single timestep, which would indicate that some are moving faster than their

---

<sup>9</sup>Exceptions are made for extremely small numbers of urchins. For computational efficiency, very small groups leave none behind

<sup>10</sup>The location of each figure is listed in the Table of Figures.

theoretical maximum speed. To resolve this issue, an "incoming buffer" was added to each cell. Any urchins moving to a target cell are put in that cell's buffer. They are not added to the target cell until the beginning of the next timestep.

A correction was needed for managing GI as well. Since a single value for GI applies to all urchins within a cell, there is a chance that GI mass will be lost or created during a movement event. For example, if urchins move from cell A with high GI to cell B with low GI, they instantly lose some GI mass because they are now attributed with the GI of cell B. To resolve this issue, GI is adjusted in the local and target cells according to the fraction of gonad mass that is leaving the local cell and arriving at the target cell. A test was performed to confirm this solution. Numerous simulations were run with gonad growth set to zero. Summing total gonad mass, each timestep, for the entire fishing site, confirmed that gonad mass was conserved.

### 3.7.3 UNEXPLAINED URCHIN AGGREGATIONS

The typical configuration of urchins on the sea floor is non-random. They aggregate in good feeding areas, called *feed lines*, just at the edge between an urchin barren and a kelp-dominated zone [Scheibling et al., 1999]. These are the healthiest urchins and the only ones worth harvesting [Norris, 2012]. Urchins also aggregate in urchin barrens that are not near kelp. Urchins in barrens may feed on what little seaweed exists there, on kelp detritus, or on diatoms living on the surface of the sea floor [Vadas (pers. com.), 2012, Steneck (pers. com.), 2012].

Urchins are known to aggregate even in deep regions in the absence of any discernible food supply [Vadas (pers. com.), 2012, Steneck (pers. com.), 2012]. Aggregations such as these are difficult to explain biologically, but are widely observed. These aggregations are produced in the model via a slight tendency to aggregate when other signals are absent. This effect only occurs in deep areas that have no food or scent signal. Specifics can be seen in Figure 46 in Appendix C: Pseudocode. On line 06 of Figure 46, the two cells with greatest density are selected, thus favoring ag-

gregations while still allowing for stochasticity. This clause only applies when neither food nor scent is nearby. Such conditions typically occur only in the deeper regions.

#### 3.7.4 URCHIN MORTALITY

Each timestep affords each cell the opportunity to exhibit urchin mortality. In nature there is no good data on how long green sea urchins can live, but some red urchins may live for more than 100 years [Ebert and Southon, 2003]. It is reasonable to assume that any given urchin has some nonzero probability of dying naturally during any given timestep, and that this probability is higher for older urchins. It is also reasonable to assume that this probability is higher for starving urchins. As described earlier, a starving urchin consumes its gonads until such point at which this resource is depleted. These urchins then die [Vadas (pers. com.), 2012]. Urchins in the model die off when their GI goes effectively to zero in a cell that has no food.

Urchins may also die by predation. Since the extirpation of the wolf fish, the effects of predation are, almost exclusively, visited upon the smaller urchins [Vadas (pers. com.), 2012]. The model cuts off the effect of predation once an urchin reaches half of maximum size, about 50 mm in diameter. Urchins which are susceptible to predation experience a specific rate of predation given conditions local to the cell. The predation rate depends directly on the seaweed biomass of the cell.

This predation rate was computed in terms of a stochastic process per unit time. The parameter *predationRatePerMin* is the mean number of urchins eaten *per m<sup>2</sup> per min*.

One investigation looked at small, medium, and large urchins. Tethered to lines, a number of urchins were spread out over an area of about 1000 *m<sup>2</sup>*. Predation of these urchins was closely monitored. This experiment was performed in multiple locations and multiple depths for a cumulative time period of 46 days. Larger urchins were eaten in deeper waters, but were mostly immune closer to shore, where urchins smaller than 40 mm were the most common fare [Vadas and Steneck, 1995]. Rates varied with depth and predator abundance.

Within a 95% confidence interval, the predation rate of small to medium urchins can range from 0.1 to 0.7  $\frac{\text{urchins}}{\text{day} \cdot 1000 \text{ m}^2}$ .

$$0.1 \frac{\text{urchins}}{\text{day} \cdot 1000 \text{ m}^2} \times \frac{\text{day}}{1440 \text{ min}} \approx 7 \times 10^{-8} \frac{\text{urchins}}{\text{m}^2 \cdot \text{min}}$$

$$0.7 \frac{\text{urchins}}{\text{day} \cdot 1000 \text{ m}^2} \approx 4 \times 10^{-7} \frac{\text{urchins}}{\text{m}^2 \cdot \text{min}}$$

From this we chose a value of  $1.5 \times 10^{-7} \frac{\text{urchins}}{\text{m}^2 \text{ min}}$  for the parameter *predationRatePerMin*, and a reasonable range from  $7 \times 10^{-8} - 4 \times 10^{-7}$ .

### 3.7.5 URCHIN HERBIVORY

In the model, urchin herbivory is the main interaction between urchins and kelp. Urchin consumption of kelp reduces the kelp biomass but adds, albeit to a lesser degree, to the urchin biomass. Assuming sufficient food, urchins in the model will eat up to the maximum of their eating capacity for a single timestep.

During certain stages of life, an urchin's capacity to consume per unit time is a function of mass [Vadas (pers. com.), 2012]. An approximation made by the model is to apply this function to all stages of life. The herbivorous capacity of urchins within a cell is a linear function of their collective biomass. Details are in the appendices.

### 3.7.6 EFFECT ON GONAD INDEX

Urchins that have been eating for a sufficient amount of time from a plentiful food source typically have a high GI. The opposite is seen in urchins that have spent sufficient time consuming low quantities or low quality food. [Vadas (pers. com.), 2012, Steneck (pers. com.), 2012, Norris, 2012]. It is widely believed that urchins which are not receiving enough nutrition will slowly consume their own gonads [Vadas (pers. com.), 2012]. Urchins that have been starving for a long time may have

a GI of almost zero. Urchins have been known to survive a whole year without food by consuming themselves in this way [Vadas (pers. com.), 2012]. GI in the model therefore acts as a proxy for general urchin health. This value contains information about the recent nutritional history of local urchins.

In order to maintain or grow its GI, there is some amount of nutrition that urchins must take in per day. This amount is estimated by a linear function of mass. As an approximation, a "health threshold" was set, above which an urchin is presumed to be taking in enough nutrition to maintain or grow its gonads. Urchins in the model that consume at a rate below this threshold will have a slowly diminishing GI. Visual demonstrations and discussions with biologists revealed that this approximation is reasonable [Vadas (pers. com.), 2012]. Demonstrations of the model were performed at multiple stages in development and entailed on-the-fly alterations to not just parameter values but also the underlying logic of the model.

It is known that GI is generally high for urchins found feeding on a copious food source, and low for urchins found at low-food location, but no data exists on how fast an urchin can go from having low GI to high and then back to low. Existing GI data collection only allows for one datapoint per urchin. Such data is garnered from urchins that were opened, or "sacrificed" [Vadas et al., 1980]. Robert Vadas, an expert on *S. droebachiensis*, reported that a medium-sized urchin with high GI can most likely survive without sustenance for up to about a year [Vadas (pers. com.), 2012]. During that time the urchin is living purely by consuming its own gonads. Assuming such urchins begin with a high GI of 25 ( $.25 \times \text{mass}$ ), we can estimate the maximum amount gonad mass that can be lost or gained per min. In the model this parameter is called the *maxGonadChangePerMin*:

$$\text{maxGonadChangePerMin} \times \text{mass} = \frac{.25 \times \text{mass}}{525960 \text{ min}} \approx 4.75 \times 10^{-7} \text{ min}^{-1} \times \text{mass}$$

By adding or subtracting one month (measured in minutes below), and altering the starting GI (in the range 22-26), there are lower and higher bounds which were not inconsistent with our discussion:

$$\text{maxGonadChangePerMin (low)} = \frac{.26}{482760 \text{ min}} \approx 5.39 \times 10^{-7} \text{ min}^{-1}$$

$$\text{maxGonadChangePerMin (high)} = \frac{.22}{569160 \text{ min}} \approx 3.87 \times 10^{-7} \text{ min}^{-1}$$

The term "mass" applies to a single urchin. In the model, this parameter will be a ratio applied to biomass. Gonad change is applied simultaenously to all urchins within a given cell.

From this we chose a value of  $4.75 \times 10^{-7} \text{ min}^{-1}$  for the parameter *maxGonadChangePerMin*, and a range of  $3.87 \times 10^{-7} - 5.39 \times 10^{-7}$ .

### 3.7.7 URCHIN GROWTH

For most stages of life, urchin growth can be reasonably approximated by the Von Bertalanffy Growth Function (VBGF). Many organisms share this property. This function grows asymptotically toward a maximum. Urchins, as measured by diameter, grow more quickly at first [Lauzon-Guay, 2009], eventually approaching a maximum around 100 mm. The VBGF provides the expected size ( $L_t$ ) for an urchin at any time  $t$  using the following [Chen et al., 2003]:

$$L_t = L_\infty (1 - e^{-K(t-t_0)}) \tag{2}$$

Where  $L_\infty$ ,  $K$ , and  $t_0$ . Where:  $t_0$  is the hypothetical age when the urchin had zero size – obviously no urchin ever had a diameter of exactly zero; this is merely one of the values fitted to the urchin’s size curve over time.  $K$ , known as the Brody growth

parameter, augments or diminishes the effect of time.  $L_\infty$  represents the maximum possible size an urchin can grow to.

In the model,  $K$  is in units of  $\frac{1}{time}$ . After researching habitats along the coast of Maine, the observations of Chen et al. yielded values for  $K$  that ranged from  $0.1181 \text{ year}^{-1}$  in the south to  $0.3268 \text{ year}^{-1}$  along the mid-coast. For the model these were converted:

$$0.1181 \frac{1}{yr} \times \frac{1}{525960} \frac{yr}{min} \approx 2.2 \times 10^{-7} min^{-1}$$

$$0.3268 \frac{1}{yr} \approx 6.2 \times 10^{-7} min^{-1}$$

From this we chose a value of  $4.5 \times 10^{-7} min^{-1}$  for  $K$ , and a range of  $2.2 \times 10^{-7} - 6.2 \times 10^{-7}$ .

The observations of Chen et al. yielded values for  $L_\infty$  that ranged from 63.1 mm in the northeast to 95.2 mm in the south. These numbers were not computed by averaging measurements of naturally deceased urchins. Such data is extremely difficult to obtain. These numbers come from fitting the VBGF to size data. Characteristics of the VBGF aside, maximum urchin diameter may be as large as 90 to 100 mm [Vadas (pers. com.), 2012].

We chose a value of 85 mm for  $K$ , and a range of 63.1 - 95.2.

Urchin growth relates directly to the following ratio: *actual* received nutrition to *theoretical maximum* nutrition. This maximum represents the amount which could be absorbed in the presence of superfluous food [Vadas (pers. com.), 2012]. Therefore, the VBGF models urchin growth when urchins are consuming at their maximum capacity. The output of this growth function is attenuated by a proportion consistent with the proportion of actual consumption to maximum possible consumption. Urchins that consume 2/3 of their capacity in a given timestep will only grow at 2/3 the VBGF-determined rate. The amount of nutrition being used to replenish gonadal mass as opposed to diameter growth is not considered here because VBGF function constants were fitted using only diameter and not GI.

Here we are only talking about settled urchins, not larvae. The VBGF doesn't apply well to microscopic urchin young, but can be made to fit well to urchin growth data over the rest of its life. We decided to accept the approximation that the VBGF will be used to model all stages of urchin life.

### 3.7.8 DISCRETIZATION OF URCHIN GROWTH

The VBGF is a continuous function, but the discrete size bins used by the model require the discretization of the VBGF. Modeled urchin growth entails discrete shifts between size bins – not continuous growth. The rest of this section describes a method for ensuring that these discrete bin shifts will approximate the continuous growth rates generated by the VBGF.

Discretization of the VBGF was managed by drawing from random distributions. Integers are drawn from a Poisson distribution with an expected value equal to the output of the continuous VBGF. Poisson was chosen to lessen the incidence of all urchins in a size class being promoted. Such events resemble discrete processes more than continuous ones. The purpose of this step is to generate behavior that over time has greater resemblance to continuous phenomena. The exact process has multiple steps, as described below. It was designed to correct for distortions caused by the discretization of size.

The model's use of discrete size bins makes "promotion" a more appropriate term than "growth". During each timestep, each urchin has some probability of being promoted to the next size bin, in effect growing. The VBGF assigns the fastest growth to the smallest urchins, so urchins in the smallest size bins are those most likely to be promoted. Once an urchin reaches the maximum size it has a zero probability of promotion. During a single timestep of one day, promotions are rare. Over time, however, the average growth rates of urchins in the model approach the output of the VBGF.

Let  $a_u$  be the *hypothetical age* of a single urchin as determined using its size.  $L_t$  comes directly from the VBGF. Then  $a_u$  in equation 3 is isolated to find equation 4.

$$L_t = L_\infty (1 - e^{-Ka_u}) \quad (3)$$

$$a_u = -\frac{1}{K} \ln \left( 1 - \frac{L_t}{L_\infty} \right) \quad (4)$$

The term *hypothetical age* is used because the VBGF is a theoretical curve that assumes constant food availability, implying consistent growth. In actuality, this number represents a lower bound on urchin age. The urchin could have spent a significant amount of time with little to no food, during which time the urchin would not have grown.

Let  $g_a$  be the *absolute growth* (in diameter) of an individual urchin, i.e. the continuously-measured expected growth during a time of length  $h$  (See eq. 5). The absolute growth of a single urchin during a single timestep is a continuous function of the length of the timestep and  $a_u$  :

$$g_a = L_{t+h} - L_t \quad (5)$$

$$= L_\infty (1 - e^{-K(a_u+h)}) - L_\infty (1 - e^{-Ka_u}) \quad (6)$$

$$= L_\infty (e^{-Ka_u} - e^{-K(a_u+h)}) \quad (7)$$

The model attempts to correct for the difference between the continuous value of  $g_a$ , and the growth represented by a discrete promotion from any size bin  $i$  to  $i + 1$ . This correction is made using the ratio of  $g_a$  to the growth represented by a promotion ( $\mu_{i+1} - \mu_i$ ). Let this ratio be called the *relative growth*. We already assume that urchins in a given size bin  $i$  are identical in diameter. The diameter is  $\mu_i$  for urchins in bin  $i$ .

Let  $g_r$  be the *relative growth* of a single urchin. The relative growth of an urchin in bin  $i$  during a single timestep is the following ratio:

$$g_r = \frac{g_a}{\mu_{i+1} - \mu_i} \quad (8)$$

We then have a discrete promotion function that over time will approximate the VBGF. The actual processing of urchin growth for a given cell iterates through all non-empty size bins, starting from the second-largest bin and proceeding downward. The expected number  $N$  of promotions from size bin  $i$  is the number of urchins in that size bin ( $n$ ), multiplied by the relative growth  $g_r$  and the nutrition ratio  $k_n$ :

$$N = n g_r k_n \quad (9)$$

Promotion numbers are drawn from a Poisson distribution having an expected value of  $N$ . The expected growth rate of urchins over time should approach that of a similarly designed system using continuous sizes instead of discrete sizes. Not having built a separate model based on continuous functions, the claim that this system will, over time, approximate the growth behavior of continuous functions is untested. A mathematical proof of this claim may be of interest in future work.

For the sake of computational efficiency, the output of equations (4) through (8) are computed once, before the simulation begins. Computing  $g_r$  is only done once for each size bin. During each growth step, only Equation 9 must be computed, using current values for  $n$  and  $k_n$ .

In Appendix C, the pseudocode in Figure 47 shows how urchin growth is determined.

### 3.8 URCHIN REPRODUCTION

As described in the background section, the settlement rate of larval urchins is not dependent upon the amount of local spawning [Vadas (pers. com.), 2012]. It is a

reasonable approximation to assume that one location is not favored over another, i.e. urchin recruitment is a stochastic process, per unit area, that depends only on season [Vadas (pers. com.), 2012, Steneck (pers. com.), 2012].

New recruits settle during May and June [Vadas (pers. com.), 2012]. In the model, recruitment is the only mechanism by which urchin numbers grow. During May and June every non-land cell has some nonzero probability of receiving new recruits during each timestep. The expected number of urchins recruited into a single cell during a timestep,  $\mu_{rec}$ , is determined by:

$$\mu_{rec} = recruitmentRate \times (\text{cell area})$$

There is some evidence that recruitment rate also depends on environmental properties such as turbulence. Turbulence has an impact on urchin survival at all ages in the model. Other environmental factors do not affect recruitment rate in the model merely because they were not deemed significant enough during the years of discussions that went into the model's design.

In the model, the recruitment rate is measured in urchins per  $m^2$  per minute. This rate is used as the mean for a random variable. It only applies during two months: May and June. During the rest of the year this value is zero.

The rate of successful settlement for *S. droebachiensis* varies greatly from site to site. A reasonable range of values can be determined from data collected at four sites: Damariscove Is., Fisherman Is., Thrumcap Is., and Pemmaquid Pt. W. Astroturf collectors were positioned at each site just before settlement began and left for two months after settlement began. Between 1995 and 1998 settlement rates ranged from 500 to 7500 per  $m^2$  with some sites hovering around 4000 per  $m^2$  [McNaught, 1999, p.21].

Assuming a typical settlement season of about two months, this range can be specified with the desired time units. 4000 per  $m^2$  over two months translates to about 0.046 per  $m^2$  per minute during the settlement season. McNaught reported that these

numbers may be low due to predation. Of concern to the model is a good estimate of the number of urchins reaching median size within the smallest size bin. McNaught's data can therefore be used without any inflation to account for such predation.

From this we chose a value of  $0.04 \frac{\text{urchins}}{\text{m}^2 \text{min}}$  for the parameter *recruitmentRate*, and a range of 0.0057 - 0.086.

The number of recruits that settle in a given cell during a single timestep is drawn from a Poisson distribution having an expected value of  $\mu_{rec}$ . All new urchins are by default in the smallest size bin. As such, they add significantly to the number of urchins but insignificantly to the total biomass.

### 3.8.1 HARVESTING METHODS

Simulations can be performed with and without harvesting. There are two forms of harvesting which can occur within the model. The first is "standard" harvesting. The second occurs in a pattern of concentric circles, and will be referred to as "circular" harvesting. It is theorized that circular harvesting will generate an urchin harvest comparable or better than standard harvesting, but without the serious deleterious effects of standard harvesting.

*Standard* harvesting is intended to model a real-world harvesting event. Its design rests on two assumptions: (1) Divers will attempt to take all legal-sized urchins, (2) Humans are not perfect at any task and therefore leave urchins untouched in a random fashion. The standard harvesting function must be weakened in such a way as to simulate this human imperfection.

A blindspot method is employed to "weaken" the harvesting routine. Just before each harvesting event, a number of cells are randomly chosen. A randomly-sized amorphous area is selected around each of these cells and all are designated as blindspots, i.e. fishermen will not remove any urchins from these cells. Divers miss, or leave behind, all urchins within these cells. Blindspot cells typically represent 10 to 20 per

cent of the site, and they are different for each harvesting event. They have random shapes but are often somewhat circular because of the algorithm by which they are generated. This is considered realistic because topology and other factors contribute to the difficulty of searching every square meter within a modeled region.

*Circular* harvesting is the act of harvesting urchins along concentric circles. It is analogous to standard harvesting where the blindspots are concentric circles in between the harvesting zones. This pattern was chosen because (1) it is easily computed, and (2) every harvested cell is in close proximity to at least one unharvested cell. This proximity affords urchins time to sufficiently redistribute themselves between fishing events. Even if these events happen in quick succession, configuration of overlapping non-concentric circular patterns imply that numerous evenly-distributed small regions are left untouched even after multiple events.

The author contends that any fishing pattern with this feature will yeild a satisfactory number of urchins while not causing an urchin barren to flip to the kelp-dominated state. In many cases, such harvesting is more similar to natural predation, causing higher average gonad index than no harvesting at all. This contention is made from observations of the model under various conditions.

Functioning as a "straw man," or proxy for a theoretical alternative to standard harvesting, circular harvesting highlights the features that a realistic alternative should have. It is understood that such a pattern would be unrealistic in a real-world scenario.

Circular harvesting is put forth as being less devastating to an urchin population than standard harvesting. To strengthen any confirmation which may come in the Results section, circular harvesting is not weakened by random blindspot generation. Under circular harvesting, the fishermen are assumed to be perfect, i.e. they remove 100% of the legal-sized urchins in their target cells. This will add strength to the claim that circular harvesting does not decimate urchin populations.

The circular harvesting pattern is very subtle during a standard visualization of the simulator. In order to easily view the circular pattern, a simulation was run with an unnaturally high density of urchins. See Figure 2 for a screenshot of this visualization.

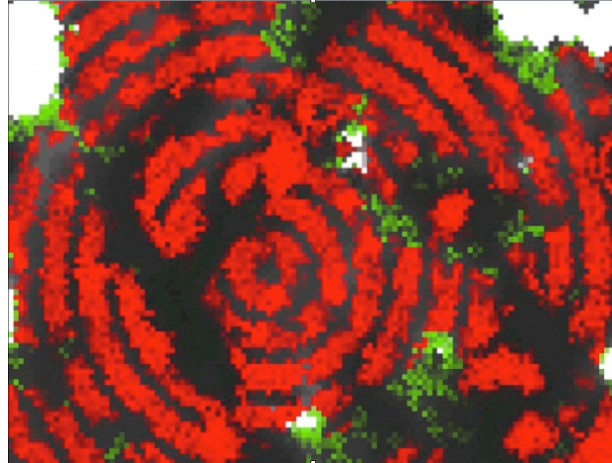


**Figure 2:** Eastern Bay with circular harvesting. White=Land. Darker grey=deeper water. Green=kelp. Red=Urchin biomass. Here Urchin color is amplified to illuminate the circular fishing pattern. The dark circles represent the harvested areas.

### 3.8.2 POPULATION HEALTH

The relative "health," or robustness of the urchin population at a given site is measured using the following two metrics:

**topDensity** : average urchin density (by number) among the top 1% of cells

**topGI** : average gonad index among the top 1% of cells

where "top 1%" refers to cells with the highest numeric density, urchins per  $m^2$ .

Neither metric is sufficient by itself. For instance, if *topDensity* is too high, the urchins will be over the carrying capacity of their local environment, thus causing a low *topGI*.

Even in the presence of a thriving urchin population, most of the cells at a site will not have many urchins. For a given population to be considered "sustainable" it is not required that all cells have urchins. It is only required that some subset of the cells at a given site have sufficient urchin density to maintain a barren. This line of reasoning led to the selection of a metric that measured from the top 1%. This number was chosen heuristically after numerous discussions with biologists and fishermen poring over maps and simulations. It is the result of a common desire to mathematically quantify feedlines and other urchin aggregations.

Density, specifically *topDensity*, is utilized for measuring the quality of a simulated population, and the stability of the simulation itself. Density is taken as a measure of the robustness of a population at a given site because it is related to that population's herbivorous capacity and long-term viability. This same metric is used to measure the stability of the simulation because rapid swings in *topDensity* are more likely to be artifacts of the simulation instead of a realistic portrayal of an urchin ecology. In this case, "stable" refers to a simulation in which key elements (e.g. urchin density) exhibit "typical" dynamics, i.e. their current rates of change are similar to rates at most randomly-selected points in the future. When a simulation begins, *topDensity* is artificially high. This number slowly settles to a number that becomes indistinguishable from future points. At this point the simulation is considered stable. Prior to being stable, the simulation is "burning in," another term used in the literature [Lauzon-Guay, 2009].

Urchin density is an indicator of whether there are enough urchins to maintain herbivory, but not an indicator of the health of those urchins. Many barrens in the 1980's had an excessive number of urchins. The vast majority of those urchins were in a state of starvation. They had enough food to stay alive, but not enough to maintain a high gonad index. Without some level of predation, urchin barrens tend toward overpopulation, and therefore starvation. The second metric, *topGI*, is a measure of the health of the average urchin in the densest cells. If a population of urchins has, on average, a pathologically low GI, it is neither valuable as a fishery, nor innately healthy. A higher GI indicates that the average urchin is healthier, and that there is more urchin roe for the fisherman to sell.

These two metrics, while imperfect, supply a synopsis of overall quality and viability of any given urchin population. The proposed metrics will be used to discuss the state of the simulated populations, and to judge and compare harvesting schemes.

## 4. STRUCTURE OF THE MODEL

The model was implemented as a discrete-time object-oriented simulation written in Python. As the simulation is initiated, a *World* object is created which then self-populates with various other objects with the assistance of a few configuration files. Operation of the simulation continues as long as desired, during which time any required data can be output to a console or a database. A separate process can be used for visualization, showing the sea floor, with a representation of urchins and seaweed upon it.

Let "the simulator" refer to the program operating the virtual sea urchin ecology, along with its ability to operate seaweed and harvesting functions against a given bathymetry and configuration. Let "the simulation" refer to a running instance of the simulator, having some state at each timestep. Let "the visualizer" refer to the program that reads the state of the simulation and displays it graphically.

### 4.1 OBJECT-ORIENTED MESH NETWORK

Each individual simulation simulates a single "fishing site." Sometimes referred to as a "ledge," [Wilson (pers. com.), 2012], it is a representation of a small area of the sea floor of Gulf of Maine, on the order of 4 km<sup>2</sup>. Each fishing site is simulated by a single process (the simulation) that takes bathymetry and configuration files as input.

The simulation begins with a main process. The main process initializes a *Config* object which reads configuration files and prepares all the parameters needed for the various objects in the simulation. Many parameters are normalized for area or time. As various other objects are generated during the simulation, the Config object passes on the desired values for these parameters. Using the Config object for this purpose simplifies the process of configuring objects because it was desirable to have different ways to set parameters, and because setting them in some cases is a two-step process.

The main process then instantiates a *World* object. The World object has everything else that is generated. The World object holds a number of *Layer* objects, each representing the same fishing site, but at different scales. Each Layer object holds a number of *Cell* objects. Each cell object holds at most one Urchins object and one Seaweed object. An overview of several objects can be seen in Figures 3 through 6.

The multiple-layer aspect of this project is described in the section on future work. Only the bottom (finest-scale) layer is utilized in the current simulation. It will be referred to as the "bottom layer."

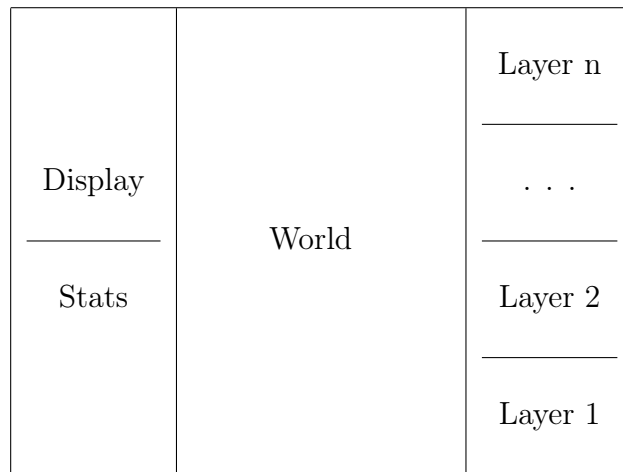


**Figure 3:** Each World object has a Display object, a Stats object, and a list of Layer objects

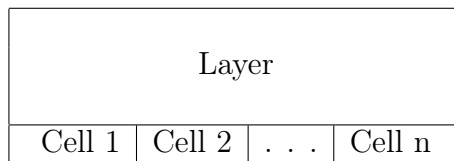


**Figure 4:** Each Layer object has a list of Cell objects

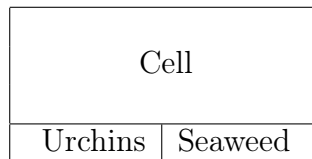


**Figure 5:** Each Cell object has a single Urchins object and a Seaweed object

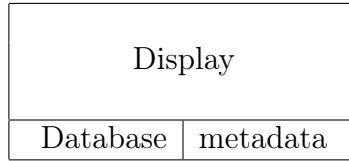


**Figure 6:** The Display Object saves simulation state to a database which is accessed separately by the visualizer. Each *Display* object has a *Database* object, which is used to hide the complexity of database interaction.

The urchins and seaweed are the smallest actors in the simulation, so the cells in the bottom layer are at an appropriate scale for urchin and seaweed dynamics. Early experimentation with different cell sizes (from 1m to 100m) showed that 20 meters on a side represents a relative sweet spot. This size appears to be small enough to exhibit the interesting aggregations and movement patterns of interest to the project [Wilson (pers. com.), 2012] while not requiring excessive computational resources. When using square cells 20 m on a side to simulate an square area 2km on a side, on a standard laptop, a year can be simulated in about 5 minutes.

Once each cell has been initialized and configured, it is linked to nearby cells in a mesh network. By the manner in which they were generated, their configuration forms a square grid. Excepting those along the borders of the site, each cell has another cell immediately to its North, South, East, and West. Bordering cells are linked in both directions by a pointer. These pointers are kept as a list of "neighbors".

The cell is the most important operative element in the simulation. After it has been configured, each cell is populated with urchins and seaweed.

## 4.2 BATHYMETRIES

### 4.2.1 DEPTH ASSIGNMENT

The environment begins with the most basic element: depth. An *input bathymetry* (topological description of the ocean floor) is used to assign a depth to each cell. The GIS community employs a plethora of formats and methodologies for describing

and interacting with bathymetries. This non-trivial aspect of the project consumed considerable time.

Consider the cells in the bottom layer. They form a grid of points, each one equidistant from its nearest neighbors in terms of decimal latitude and longitude. Each requires an associated depth. This model reads GIS point data and uses it to compute a depth for each cell.

Regardless of format, any bathymetry can be converted to a set of coordinates and associated depths, which constitutes a set of point data. GIS practitioners consider this data differently from a "raster" format which attributes depth to rectangular regions of a rectangular mesh. Nuances like these were considered the domain of GIS research and not relevant to our research.

An interpolation algorithm for determining depth was needed because the point data was not aligned with the centers of each cell (the coordinates of the center of each cell is taken as that cell's coordinates). We had selected our sites from maps—not from the GIS datasets. These coordinates did not coincide with the coordinates of published GIS point data, and it is highly unlikely that any GIS data would coincide exactly with all or even some of our points.

Alignment with actual GIS data was sought with considerable effort because of the foundational claim that topology heavily influences urchin outcomes. Intuitively constructed false bathymetric data would introduce greater doubt into any claims made from studying the model.

To align with available datapoints it was important to find an efficient interpolation algorithm. The chosen algorithm iterates over each point of the input bathymetry and uses it to assign depth to a few cells. As described in Appendix C, Figure 48, multiple input points can be averaged iteratively to compute the best possible depth for each cell in the model. Under testing this algorithm worked well with input bathymetries that were both coarser and finer than the model's cell mesh. It also worked on input sets of inhomogenous density.

Given an input point  $p_0$  associated with some bathymetry, the algorithm must first find the closest cell  $q$  to  $p$ . The algorithm described in Appendix C, Figure 49 selects the closest such cell. This cell-selecting algorithm grows linearly with latitudinal or longitudinal resolution. Starting at this closest point, a small neighborhood of radius  $\epsilon$  is then found around the input point  $p_0$ . The depth of cell  $q$  is then assigned a depth equal to the average of all bathymetric points within that  $\epsilon$ . An alternative method was considered in an earlier version where generated points in the model would each search for a point in the bathymetric data, but all algorithms considered for such a process were less efficient than the chosen one.

The next point datum,  $p_1$ , can be more quickly matched to its closest cell by the fact that  $p_1$  is close to  $p_0$ . When the point-selecting algorithm is called on the previous closest cell,  $q_c$ , it likely returns after one recursion. In this manner the bathymetric point data is brought into the existing mesh of cells.

#### 4.2.2 ACQUIRING GIS DATA

Care was taken to find the appropriate bathymetric data. After consulting several sources and experts, the best source appeared to be NOAA's Electronic Navigational Charts (ENC). The only roadblock was that these charts were not easily sourced in a format that was program-readable. One of the available formats was GIS shape files. Specifically, the soundings shape file was used in an attempt to generate a set of point data. This data contained significantly less information than was visible in the online viewer of these charts. The implication was that significant information was contained in the other shape files. ENC for a given zone typically has about 20 shape files, each containing a different type of information. Assistance was sought from GIS experts at this institution numerous times over a period of several months. These experts were asked how to extract depth-related information from the other shape files. These experts did not provide an answer.

Over the course of a year, various datasets and solutions were tried. The preferred solution was a bathymetry generated from the WGS-84 datum,<sup>11</sup> interpolated using professional GIS software to a resolution of 10 m, and represented in decimal latitude and longitude. However, this wasn't possible within a reasonable time.

A quicker, even if suboptimal, solution was required. Synthesizing numerous interviews with fishermen, James Wilson and Caitlin Cleaver selected eight fishing sites in the Gulf of Maine. The coordinates of these sites were specified. Using the on-line ENC viewer, the author captured images of the selected sites. The information in these images, however, was still visual and not machine-readable. For instance, depths were marked at various sounding points with digits rendered using pixels in the image. Other depths were marked on various contour lines. Some indication of the intertidal zone was present e.g. rocks which become visible only at low tide. In order to make this information machine-readable, a drawing program was used to manually apply grey-scale values to each area of the image, sometimes pixel-by-pixel. The grey-scale values were made equal to the depth at each corresponding point.

These grey-scale values were read in programmatically and interpreted as depths. Each pixel in the grey-scale image was treated as a single element of point data. The coordinates corresponding to each pixel were determined from the coordinates of two opposing corners of the original image, marked by hand when the image was acquired from the ENC viewer.

These hand-altered maps became the bathymetries which were used for this project, but the search for a top-quality bathymetry did not stop. More details are described in the section on future work. Some of the work described in this section should have been considered future work, but this determination hadn't been made at the time.

---

<sup>11</sup>plural *datums*

### 4.3 THE SEAWEED OBJECT

As described in a previous chapter, the modeled kelp functions as a substitute for a number of algae local to the Gulf of Maine. It is the only plant modeled so far, but the software is able to incorporate others. With future expansion in mind, the Seaweed object is a subclass of the *Plants* object. Attributes and functions which are generalizable to all plants were kept in the code for the plants. The Seaweed object encodes all attributes and methods specific to our chosen seaweed.

The *Plants* object has the attributes *coverage*, *height*, and *biomass*. The biomass of the *Plants* object is computed from:  $coverage \times height \times density$ , where the density is mass per unit volume. As is explained in the appendices, parameter values were used to keep biomass consistent with empirical data. Seaweed is not shaped like a rectangular volume, but this approximation was deemed acceptable in our discussions.

The *Plants* object has various methods which apply to all plants: *generate* (stochastically create a simulation's original height and coverage), *tick* (manage changes made during a timestep), *grow* (increase height), and *getsEaten* (returns amount of biomass eaten). Various other functions and attributes were also necessary to do effective administration for these functions. Intuitively *getsEaten* would appear to be a function of the animal instead of the plant. Within the construct of the code in this simulation, however, plant consumption as a method of the *Plants* object introduced less complexity.

The *Seaweed* object is a subclass of *Plants*. It has the other attributes and functions necessary to simulate our chosen kelp. The *Seaweed* object has attributes such as *maxBiomassDensity* (max biomass per  $m^2$  possible for the given cell), *timeToMaxBiomass* (time required for seaweed with height zero to reach maximum height), and *probRecoverPerMin* (continuous probability that kelp coverage ratio increases in next timestep). These attributes and functions are in the *Seaweed* object and not the more general *Plants* object because we can envision a future version of the simulation that includes plant species that are not well described by these particular attributes and functions.

Ecosystems in the ocean are patchy [Wilson et al., 2007]. The model attempts to mimic nature as it populates each cell. The patchiness comes from the initial "seeding". The simulation begins with zero seaweed. A number of cells are randomly selected from the bottom layer. Each of these cells is initiated with some nonzero height and coverage of seaweed. The initial height and coverage for each of these cells was drawn from a uniform distribution over a limited positive range. Here the uniform distribution was chosen because no argument was found for using any other distribution. The only objective at this stage is to populate a few cells so that the model appears "natural" after 100 days of simulation. This 100-day settling-in period has been referred to by other researchers as a "burn-in" period [Lauzon-Guay, 2009]. For the sake of stability, the final burn-in period was extended to 365 days. Upon viewing the model, biologists and fishermen agreed that the distributions appeared natural.

Consider a cell that is selected for seeding. After generating seaweed in that cell (by calling *generate*), the same generate function is then called in each empty neighbor, but with a slightly smaller associated probability. Subsequent neighbor cells do the same, calling this function recursively on their unpopulated neighbors. Each recursion has a lower associated probability of generating seaweed. Cells that do not generate seaweed do not call this function on their neighbors, effectively stopping this particular seaweed patch. The result is a randomly-distributed set of clusters populated with seaweed, where each cell has some randomly-generated values for kelp height and coverage.

In this way a patchy random distribution of seaweed is generated for the start of the simulation. This process is preferable over a simple random distribution because the resulting clusters closely resemble the tendency of small regions toward a stable state of kelp-bed or urchin-barren.

#### 4.4 THE URCHINS OBJECT

The focus of this simulation is the sea urchin *Strongylocentrotus droebachiensis*, but the possibility of incorporating other species has been considered from the beginning. The Urchins object is a subclass of *Animals*. As many functions and attributes as possible were kept in the definition of *Animals*. Those which were specific to urchins were put in the *Urchins* code.

The most important attributes of an *Animals* object are *num* (an array of integers, showing how many individuals are in each corresponding size class), *biomass* (the sum of the masses of all the individuals in the object), *mean* (an array of floating points, each representing the mean size of individuals in a given size class). These are generated in the first step.

The most salient functions of the *Animals* object are *generate* (stochastically generate the original *num* array), *tick* (manage action taken during a timestep), *getTargets* (one of several functions used to choose cells for targeted movement), *eat* (returns amount eaten in a timestep), *getProductivity* (a measure of the relative nutrition absorbed during this timestep, from which the output is called the *nutritionRatio*), *grow* (promote some individuals into the next size class), *move* (transfer individuals to another cell), and *cull* (remove some individuals as if they had been harvested).

The Urchins object specifies various attributes which are specific to *S. droebachiensis*, such as: *numClasses* (the number of discrete size classes), *maxTotalNumDensity* (maximum number of urchins allowed in a given  $m^2$ ), *food* (this animal's chosen food type, which is set to 'seaweed' for urchins), *herbivoryRate* (kg of seaweed that one kg of urchin can eat per unit time), *K* (The Brody Growth Parameter), *maxSize* ( $L_\infty$  from the VBGF), *maxGonadChangePerMin* (maximum relative growth/shrinkage of gonadRatio per min), *gonadThreshold* (a *nutritionRatio* value above this value implies an increasing gonad index. This attribute was also called a "health threshold"), *recruitmentRate* (mean number of new urchins  $m^{-2}min^{-1}$ ), *mortalityRatePerMin* (chance of dying of natural causes), *predationRatePerMin* (chance of dying of predation), and *maxPredationPerMin* (maximum urchins eaten  $m^{-2}min^{-1}$ ).

The most salient functions of the Urchins object are: *generateMeans* (generates discrete size classes which are appropriate to the urchin), *generateRelativeGrowths* (for creating a probability table used in generating urchin promotions), *promote* (stochastically promote some subset of urchins from class  $c$  to  $c+1$ ), *mortality* (manage predation and death from natural causes), *recruit* (introduces new young urchins), *getAgeFromSize* (use the VBGF to determine theoretical age from current size), *growthInTime* (use VBGF to determine expected growth during time given age), *isContent* (determines if urchin is content or might prefer to move), *isLegal* (determines if given size class of urchins is legal for harvesting), and *getFavorability\_urchins* (determines how favorable a given cell is to urchin life).

The original distribution must be patchy for urchins as well. In a similar fashion to the generation of the kelp distribution, a number of cells are randomly chosen from the bottom layer. In each of these cells, the *generate* function is called. This function populates the size bins of the given urchins object with numbers from a uniform distribution. The uniform distribution was chosen because field observations can be used to make a case for many different distributions, including the uniform one [Lauzon-Guay, 2009, pg.33] [Miller, 1984, pg.278]. After generating an urchins object, each cell then recursively calls *generate* on its neighbors, but with a slightly lower probability. This probability decreases with each recursion. The final distributions of urchins are patchy and somewhat natural in appearance—like the seaweed. In demonstrations, these distributions are highly clustered on day one, but had a "natural" appearance by the 100-day point [Vadas (pers. com.), 2012]. The "burn-in" period works for both urchins and seaweed.

## 4.5 FLOW CONTROL

This section is meant to show how control flows through the objects during a simulation. Various algorithms are described in pseudocode in the appendices when not already described in a previous section.

In the simulation, control flows from the World object down through the bottom layer to each cell and then to the animals and plants linked to cells in the bottom layer.

#### 4.5.1 WORLD *TICK* METHOD

Once a world is generated and configured, the main process starts a loop that calls `World.tick()`. *tick* is the World's central function that executes each timestep. This function is like the tick of a clock. It starts off with some administration, and then lends control to the bottom *Layer* object by calling its *tick* function. These objects each have their own tick function as well: Cell, Animals, Plants. Once the Layer's tick function has returned, the World's tick function updates the Display object and performs some administration (See Figure 50).

#### 4.5.2 LAYER *TICK* METHOD

The Layer's tick function handles some administration and apportions control to each cell sequentially. It is executed each timestep. Everything that occurs during a timestep in the simulation is initiated by this method. Control flows to each cell more than once during a timestep. The original design gave control to each cell once by calling its tick function. Some steps were added out of necessity (e.g. handling the non-trivial administration of urchin movements), and others were added for computational efficiency (See Figure 51).

For the sake of efficiency, the Layer maintains lists corresponding to subsets of the set of all cells, including *waterCells* (the set of all cells having depth greater than zero), and *activeCells* (the set of all cells that are "active," i.e. they have either animal or plant life).

### 4.5.3 CELL *COMPUTE* METHOD

Each cell has a *compute* method which merely calls the compute method of its Animals object (superclass of Urchins). The plants object does not require this method. It is used to recompute values that may have changed as a result of urchin movement, mortality, or harvesting in the previous step (See Figure 52). This method only needs to be called on active cells – those currently populated with plants or animals.

### 4.5.4 CELL *TICK* METHOD

Each cell has a *tick* function which calls the tick function of both the seaweed and urchins objects. In both cases, the tick function is defined in the superclass (Plants, Animals). The plants version is simpler (See Figures 53 and 54).

If a cell has zero plant biomass after the growth substep it is considered unpopulated (at least by plants). The cell is then slated for removal from the active list. This removal is contingent on it also being devoid of animal life.

The world has a *Stats* object which hides some of the complexity of managing the reporting of aggregate quantities corresponding to each animal and plant. Each layer, cell, plant, and animal has their own pointer to this Stats object. This stats object is updated, in the last step of the plants tick method, with current data on that particular plants object.

The Animals *compute* method is an updating method. It updates some values but doesn't change the actual state of a cell. This method must be called twice during *tick* to maintain consistency. If it isn't called twice, the measurements of the state of the model aren't updated with any changes that occur.

The *mortality* method manages both death by predation and natural causes. It is defined in the urchins object because it is species-specific (See Figure 55).<sup>12</sup>

---

<sup>12</sup>The location of any figure can be found in the Table of Figures.

The Animals *cull* method applies the harvesting event to the cell. The World object determines when a harvesting event occurs. It can be configured to happen regularly or stochastically. In the current embodiment, harvesting occurs at frequency of once per month. This rate was chosen because it is lower than the rate considered by some to be the maximum that a given site might suffer [Wilson (pers. com.), 2012, Vadas (pers. com.), 2012], but still high enough to exert pressure on an urchin population. When harvesting occurs, it lasts a single timestep. The cull method only performs its function during such an event.<sup>13</sup>

The simulator was designed to model post-settlement urchin populations. Recruitment in the model offers no consideration to any differences that may exist between urchins before they settle.<sup>14</sup>

Each cell has a *move* method which merely calls a method of the same name on its Animals object. The Animals *move* method follows the algorithm described in the previous section on urchin movement. After this method has been run on all active cells, moving urchins have been removed from their source cells but have not yet been added to their targets.

Each cell has an *update* method which calls the update method of its animals and plants, and also performs some administration on the cell (See Figure 58). The plants and animals objects each have an *update* method which also perform administration. The animals *tick* method can be further understood by referring to Figure 54).

The reference to *favorability* in Figure 58 concerns the cell's favorability for urchin life. This favorability considers three factors: food content, current urchin density, and depth. Favorability is used both for moving and recruitment (see previous sections on these functions).

The final step of the layer's tick function (See Figure 51), is to activate the cells which just received urchins. This part of the algorithm iterates over all cells with incoming

---

<sup>13</sup>As advised, further description of the cull method was moved out of this section. It can be found in Appendix C.

<sup>14</sup>Further description may be found in Figure 57

urchins currently in their buffers (11). Each cell is added to the active list (12). For the most part these cells will already be on the active list. This step is to ensure a cell is on that list when an urchin is the first to move in. Under most conditions the active list is identical to the "water list," i.e. cells of positive depth. This is because non-land cells very often have some sort of life, either plant or animal.

By default the World's tick function continues to loop indefinitely. Alternatively, this function can be directed to stop after an arbitrary number of days, or even to output numerical data and/or screenshots at given times or intervals.

All aspects of this simulation require significant administration, where "administration" refers to the overhead and myriad details which had to be managed for the simulation function as desired. They have been left out of this description due to their tedious nature. All such details can be found in the code itself, but not the appendices. The code is available upon request.

## 5. VISUALIZATION

### 5.1 OVERVIEW

The objective of the visualizer is to generate a graphical visualization of the state and dynamics of the simulation that can be intuitively understood. The three most important quantities in the model are urchin biomass, seaweed biomass, and depth. These should be easily understood from the visuals.

The important dynamics of the model involve the movement of urchins, the loss of urchins, and the growth and/or decline of seaweed biomass. It is the assertion of the research team that the dynamics are best understood with respect to topology. As the seaweed and urchins in the model move and grow, the underlying topology should be intuitively gathered from the visuals.

The visualizer updates a graphical display with the current state of each cell in the simulation. Each cell is represented by a small rectangle, similar to a large pixel. Each cell is colored red to represent urchins, green to represent seaweed, or grey to indicate depth. Darker red indicates more urchin biomass. Darker green indicates more seaweed biomass, and darker greys indicate deeper water, while lighter greys indicate shallower cells.

Visualization is performed separately from the simulation. The simulator uses its *Display* object to update a *Database* object. That database holds sufficient information to run the visualizer. In a separate thread the visualizer creates a *Map* object that reads from this same database using its own *Database* object.

There are several benefits associated with separating visualization from simulation. Visualization utilizes significant computational resources. When initiated on a separate CPU, or core, it can run on a separate core. Being separate, visualization is not necessary for the function of the simulation. Visualization can be omitted during tests and while running multiple simultaneous instances of the simulator.

The Map object manages all details specific to the simulation, but it doesn't run as the main process. The visualizer uses the OpenGL Utility Toolkit, "glut". glut is optimized to be initiated as a main process. It interacts with the Map object via callbacks.

### 5.1.1 COLORS

Three colors were chosen to communicate the state of the model: red, green, and grey. These colors were selected by the principal investigator. Each color and combination is represented internally by a color vector, i.e.  $(R\ G\ B)^T$ , where  $R$ =red,  $G$ =green,  $B$ =blue, and the superscript  $T$  indicates a column vector. Each of the values for R,G,B is an integer on the range [0, 255].

When a given cell has greater urchin biomass than seaweed biomass, it is colored red. The intensity of the red is a function of urchin biomass. When a cell has greater seaweed mass than urchin, it is colored green. The intensity of the green is a function of seaweed biomass. When the red or green coloring is minimal or absent, the underlying greyscale color can be seen. The darkness of this grey corresponds to the depth of a cell.

### 5.1.2 STRUCTURE

Visualization of the simulation involves the *Map* object, *glut* (OpenGL's utility toolkit), the *Display* object, the *Database* object, and the *Frame* object. See Figures 7 through 10 for a basic outline of their "has-a" relationships.<sup>15</sup> The *Sector* object was utilized more in earlier iterations of the visualizer. In the current embodiment only one Sector object is used.

---

<sup>15</sup>A "has-a" relationship is a conceptual connection between two objects A and B where a person would say that "A has a B", e.g. "A house has a roof."

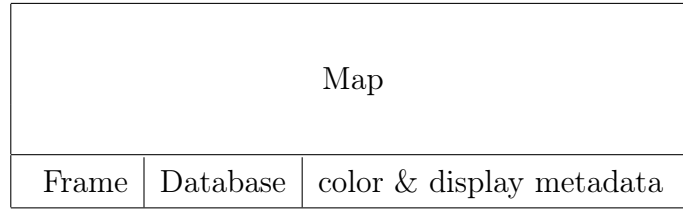


**Figure 7:** The Map object has a *Frame* object, a *Database* object, and some display metadata.

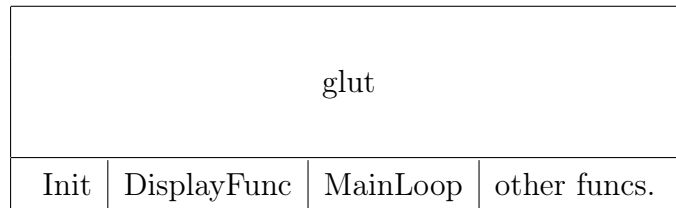


**Figure 8:** glut, the OpenGL utility kit, is initialized with the *glutInit* command. Along with other setup, a callback is set using *glutDisplayFunc*. Once the glut main loop is started, the display function will be called once during each loop.

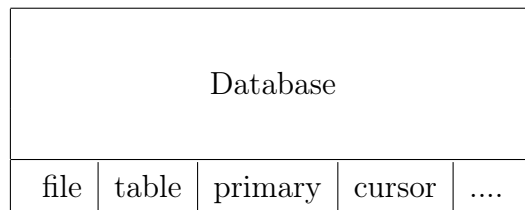


**Figure 9:** The Database object has an associated SQLite3 file. It also has a primary key, cursor object, and other data and methods required for database interaction

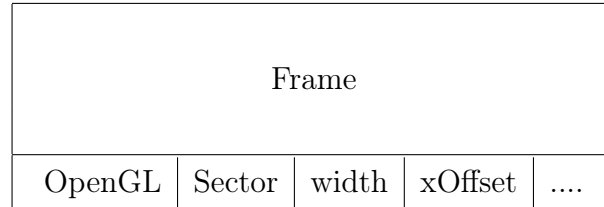


**Figure 10:** The Frame object uses OpenGL for its graphics. It has at least one *Sector* object, and a number of other values (e.g. width, xOffset, rows, cols) used to manage the shapes it draws.

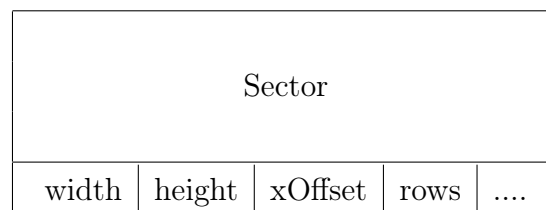


**Figure 11:** The Sector object hides the complexity of converting a cell's X/Y coordinates in the simulation with pixels on the screen.

### 5.1.3 FLOW CONTROL

First, the visualizer initializes a Map object, configures glut, and then initiates the glut main loop. The configuration step includes setting a callback function which glut calls once per loop. The chosen callback function is the *display* method of the Map object. See Figure 59.

The Map object manages details specific to the simulation and visualization. Some of these details are default settings, such as the colors used to indicate urchins, seaweed, and depth.

The Map object also has its own instantiation of the *Database* object. Although separate from the World's Database object, both point to the same SQLite3 database. The Map object only reads from it. The SQLite3 database is specified as input when the Map object is created. It is usually specified using the name of a SQLite3

database file, but can also be pointed to a database existing only in memory. The Map object uses this filename to create its Database object which hides the complexity of interacting with the SQLite3 module.

The Map object also creates a *Frame* object which hides the complexity of interacting with glut. The Map object then interacts with the Frame object by calling its *setSectors* method. This method manages drawing rectangles of certain colors to indicate the state of a corresponding cell.

Once the Map object has been initialized and configured, its only activity will occur when its display method is called by the glut main loop.

## 5.2 DESCRIPTION OF THE VISUALS

### 5.2.1 CONSIDERATIONS FOR VISUAL COMMUNICATION

The objective of the visualizer is to intuitively represent the state of the simulation. A scheme was sought to communicate the state of the model in an intuitive manner. The main elements to be visualized include depth, urchins, and kelp.

Of these main elements, first consider depth. Assuming zero seaweed and zero urchins, depth would be the only visible feature in a visualization. Greyscale was chosen to represent it. A simple linear representation of depth in cell brightness worked satisfactorily.

The two-dimensional nature of the display creates a conflict. It is difficult to represent both urchins and kelp simultaneously in the same cell. Representing these on top of the existing topology also obscures the greyscale color used to indicate depth. Several strategies were considered to address this conflict and multiple tradeoffs were debated. These strategies were devised and tested in an iterative process that lasted most of a year. A three dimensional display allowing rotation was not considered. Such a display could have greater educational value, but model dynamics was deemed more

valuable for the goals of the project than a better visualization. Four years have been dedicated to this effort thus far. During this time period improvements to the visualizer have remained a lower priority than other improvements.

An early version of the visualizer displayed four aspects of the same geographic area simultaneously. The entire visual display was first divided into four quadrants. Each quadrant used a separate color scheme to display the entire simulation. Each quadrant displayed unrelated features. Quadrant 1 held the topology. Quadrant 2 displayed the distribution of urchin biomass on the same area. Quadrant 3 displayed seaweed biomass, and Quadrant 4 showed favorability to urchin life. This display method was deemed suboptimal [Wilson (pers. com.), 2012]. This version satisfactorily communicated the bathymetry, and the distribution of urchins and kelp, but it was difficult for some viewers to mentally put the images together. Pairing these output streams was important to the objectives of the research team.

Another version had a single representation of the simulated area, but each cell was divided into four cell-quadrants, or sub-pixels. This solution was analogous to interweaving the four separate displays from the previous version. Each cell-quadrant displayed a different aspect of that cell's state, such as depth, urchin biomass, and seaweed biomass. In some versions, two cell-quadrants were used to show depth. All applicable information was displayed. The interlaced visual data made it possible to connect urchin distributions with seaweed distributions. However, most viewers also found this display difficult to follow [Wilson (pers. com.), 2012].

The final version has only one display of the simulated area. The topology of the sea floor is displayed by default, with greyscale indicating depth (darker indicates deeper). When any given cell has greater urchin biomass than seaweed biomass, red is used to indicate the intensity of the urchin biomass. In such cases the seaweed biomass is ignored. Alternatively, if seaweed biomass is greater, green is used to indicate the intensity of seaweed biomass and that of urchins is ignored.

By some accounts this scheme is suboptimal. Some viewers may be interested in seeing both the urchin and seaweed density in a given cell. The final version was selected

by the team with all of these issues in mind. While it is clear that improvements can be made, the final design meets the needs delineated by the principal investigator.

When a cell is painted red or green, representing urchins or seaweed, a vector addition is performed between the color vector representing depth and the vector for that cell's urchins or seaweed. When the urchin vector has a small magnitude, the depth can be clearly seen. Otherwise the urchin color dominates. The movement of urchins and constant environmental change allow the depths of different cells to show through at different times. The lower the biomass (urchins plus seaweed) in a cell, the more transparent the associated color becomes, allowing the greyscale to show through. Watching the simulation as a movie allows a viewer to maintain a mental picture of the topology, even as some features become temporarily obscured by the urchin or seaweed biomass.

The final version was chosen because it effectively communicates the state of the model, not because it follows some theory. There may be, however, a theoretical reason for why it works: object permanence. Object permanence is a normal human capacity to understand that objects continue to exist even when they cannot be seen [Piaget, 1977]. The only unchanging element in the simulation is the underlying topology – the set of depths derived from a bathymetry. When viewing a simulation as a movie, it is not difficult to maintain an intuitive grasp of the topology, despite the urchins and seaweed that come and go. The chosen vector addition method for overlaying biomass over topology creates the illusion that low levels of biomass are like transparent color filters. This transparency allows indications of depth to be resolved even when seaweed and/or urchins are present in a cell. This final version has been viewed by members of the research team and various others connected to it. The consensus is that this method works better than any other method tried.

### 5.2.2 DEPTH COLOR

Early on, we decided to represent depth in greyscale, where darker colors represent deeper depths. White was chosen to represent land. Everything darker than white

had a depth greater than zero. The desire was to leave the use of colors available for representing urchins and seaweed.

Colors in the visualization code (even greyscale) are represented by vectors. A given color is grey if the values for each color (R=red, G=green, B=blue) are equivalent. To represent urchins and seaweed, other color vectors are added to the grey vector. Let  $\vec{c}_0$  be the color vector that represents depth.

We needed a function  $f$  to map depths  $D$  in the model onto greyscale values  $G$ :

$$f : D \rightarrow G \tag{10}$$

Where:

$$D = 0, 1, 2, 3, \dots \tag{11}$$

$$G = 0, 1, 2, \dots, 254, 255 \tag{12}$$

At the time the visualizer was being designed we had not yet ruled out any specific region of the Gulf of Maine. The upper bound on  $D$  was, in principle, arbitrarily high.

The author demonstrated different versions of the visualizer to our research team. We judged the performance of each on communication quality. This judgement represents a *communicative* standard. A positive judgement indicated that salience in the model was readily visible, i.e. differences of note in the model were visually notable as well.

It is likely that a review of scientific visualization literature would review more optimal schema. Such schema could be applied in future work if deemed important.

The linear function did not rise to the communicative standard. The brightness output delta between 2 and 4 meters was equivalent to the output delta between 22 and 24 meters. In contrast, the photic difference between a depth of 2 and 4 meters is of greater importance (i.e. more salient), than the difference between 22

and 24 meters. The exponential deterioration of photic energy with depth directly produces a non-linear distribution of kelp, and indirectly affects urchins. Under a linear function, the difference between 2 and 4 meters was not more salient. It was, in fact, indiscernible on some screens. The linear function had the added complication of requiring an a priori upper bound on depth.

After significant thought and experimentation with the group, a function was chosen for  $f$  (See Equation 13). The chosen function communicates the state of the model in a visually intuitive manner.

The color  $\vec{c}_0$  represents a cell's depth. It is determined by Equation 13. Cells with a depth of zero are handled by a conditional branch that sets all land cells to white.

$$\vec{c}_0 = \vec{z}_d + \frac{a_d}{d} \times \vec{c}_d \tag{13}$$

Where the depth  $d$  is specified in meters,  $c_d$  is the color associated with depth (a bright grey),  $z_d$  is a small amount of "background" grey added for aesthetic reasons, and  $a_d$  is an "amplification" coefficient. The amplification coefficient is determined by running tests on a specific display. Its optimum setting depends on the technology in the physical display and ambient lighting conditions.

The human eye is not a precise scientific instrument. There is no deep theoretical basis for this function described in Equation 13. It merely meets the requirements determined by the research group. Namely that it communicates intuitively and requires no a priori depth limit.

For most situations tested so far, these values put into Equation 13 produce a satisfactory result<sup>16</sup> :

$$\vec{c}_0 = \begin{bmatrix} R \\ G \\ B \end{bmatrix} = \begin{bmatrix} 0.1 \\ 0.1 \\ 0.1 \end{bmatrix} + \frac{0.6}{d} \times \begin{bmatrix} 0.9 \\ 0.9 \\ 0.9 \end{bmatrix}$$

---

<sup>16</sup>Where possible, values in the model are computed only once

Where the first  $R, G, B$  vector is included merely to show the meaning behind the components.

As desired, this scheme shows greater difference between distinct depths among the shallows than among the depths. It also provides a scaffold upon which to represent urchins and kelp, as described below.

### 5.2.3 BIOMASS COLOR

A slightly different function is used to compute the color vectors for urchins and seaweed biomass. Where depth is concerned, greater intensity implies less output (i.e. darker). The opposite is true for urchin and seaweed biomass. The same principle was followed as before: find a function from the space of model parameters to color vectors which most faithfully and intuitively communicates the state of the model.

Consider first the case where urchin biomass is greater than kelp biomass. The kelp is visually ignored in such a cell. The final color vector  $\vec{c}$  is computed as a function of the urchin biomass  $b_u$ , an amplification  $a_u$ , a color  $\vec{c}_u$  selected as the base "urchin color", and the depth color vector  $\vec{c}_0$  described earlier (See Eqn.14). The urchin color,  $\vec{c}_u$ , can be thought of as the pure color which is displayed where depth is entirely obscured by urchin biomass. The second term in Eqn.14 is a difference vector extending from  $\vec{c}_u$  (depth obscured) to  $\vec{c}_0$  (depth only). Its magnitude diminishes as urchin the biomass  $b_u$  increases.

$$\vec{c} = \vec{c}_u + \frac{1}{a_u b_u + 1} \times (\vec{c}_0 - \vec{c}_u) \quad (14)$$

When biomass is at a maximum, the second term becomes negligible, leaving only the urchin color  $\vec{c}_u$ . As biomass decreases, the second term becomes more significant, moving the color vector toward the depth-only vector  $\vec{c}_0$ .

Trial-and-error testing revealed that these values and vectors intuitively display urchin biomass on many screens under many lighting conditions:

$$\vec{c} = \begin{bmatrix} 1.0 \\ 0.0 \\ 0.0 \end{bmatrix} + \frac{1}{0.002 \cdot b_u + 1} \times \left( \begin{bmatrix} c_{0,R} \\ c_{0,G} \\ c_{0,B} \end{bmatrix} - \begin{bmatrix} 1.0 \\ 0.0 \\ 0.0 \end{bmatrix} \right) \quad (15)$$

Where the scalars  $c_{0,R}$ ,  $c_{0,G}$ , and  $c_{0,B}$  represent the  $R, G, B$  components of  $\vec{c}_0$ . The "urchin color" used here ( $[1.0 \ 0.0 \ 0.0]^T$ ), is pure red.

In the case where seaweed biomass is greater than that of urchins, the final color is a function of the seaweed biomass  $b_s$ , ignoring the urchin biomass entirely. This function has the same structure as the corresponding one for urchins. The chosen seaweed color  $\vec{c}_s$  and an amplification  $a_s$  are different, of course.

$$\vec{c} = \vec{c}_s + \frac{1}{a_s b_s + 1} \times (\vec{c}_0 - \vec{c}_s)$$

When biomass is at a maximum, the second term becomes negligible, leaving only the seaweed color  $\vec{c}_s$ . As biomass decreases, the second term becomes more significant, moving the color vector toward the depth-only vector  $\vec{c}_0$ .

Trial-and-error testing indicated that, under most conditions, these values and vectors effectively communicate seaweed biomass.

$$\vec{c} = \begin{bmatrix} 0.3 \\ 0.9 \\ 0.0 \end{bmatrix} + \frac{1}{0.1 b_s + 1} \times \left( \begin{bmatrix} c_{0,R} \\ c_{0,G} \\ c_{0,B} \end{bmatrix} - \begin{bmatrix} 0.3 \\ 0.9 \\ 0.0 \end{bmatrix} \right)$$

Taken together, the equations above represent a color selection function that creates the appearance of an underlying topology on top of which varying amounts of seaweed and urchins grow, die, and move.

### 5.3 OBJECTS USED IN VISUALIZATION

The visualizer is also object-oriented. Although not necessary, there appeared to be no reason not to also write the visualizer in Python. The author chose to use a Python connection to OpenGL, a graphics package available on multiple platforms. The only challenge was that main control had to be ceded to OpenGL. The most convenient way to use OpenGL was to allow it to be the main process. The author's code was provided as input to the OpenGL routine as a callback.

#### 5.3.1 THE MAP OBJECT

The visualizer begins by instantiating a *Map* object. The Map object is defined with all the information needed for connecting to the database and displaying the model. This information allows its *display* method to require no input variables.

The visualizer then configures OpenGL and interacts with it using the OpenGL Utility Toolkit (glut). Most importantly, the visualizer specifies *Map.display* as the 'display-Func', or callback function.

After some amount of configuration and administration, the visualizer initiates the glut loop. This loop continues to execute until externally stopped. Once in each loop, glut calls the callback function, `Map.display()`.

The glut loop is optimized and runs faster than the simulator. When the glut loop executes more than once during a single simulation timestep, the visualization has nothing to update. To limit unnecessary cycles, the glut loop is slowed by a momentary pause which occurs in `Map.display`. Depending on the hardware, the pause amount is typically set between .1 and .5 seconds.

The main purpose of `Map.display` is to read the current state of the simulation and output it to the screen in graphical form. The state of the simulation is recorded in

the database, storing all information specific to a given cell in a single row. These rows are retrieved using the Database object's *getRows* method.

Some consideration was given to limiting this action to those cells which have changed since the last timestep. It was found that the "SELECT \*" query underlying the *getRows()* command was optimized and potentially faster than multiple retrievals of individual rows. The visualizer was already able to run much faster than the simulator, so no further optimizations were sought for this particular piece.

Iterating over each row, the *Map.display* method updates each cell's visual representation on the screen. As seen in Figure 60, each row contains information about an individual cell. This information includes depth, the number of urchins, the urchin biomass, the urchin gonad biomass, the favorability to urchin life, and the seaweed biomass. Any of these data are available to the *Map* object. Using some subset of these, the *getColor*s method returns color information. This color information is passed as input to the *Frame*'s *setSectors* method, which updates the OpenGL buffer. Any changes will be visible on the screen after the next glut main loop.

### 5.3.2 THE FRAME OBJECT

The *Frame* object hides the complexity of interacting with glut. Once the *Map* object generates and starts a *Frame* object, the *Map* object only needs to call one method, *frame.setSectors*. This one method does everything required for updating the display and interacting with glut.

Internally, the *Frame* object contains data about the visualization, such as the width and height (in pixels), the size of the margins, and the number of rows and columns of cells. The *Frame* object also contains at least one *Sector* object (described in the following subsection).

The *Frame* object performs the glut configuration using a number of glut functions. The *Frame.start* method (only called once) starts the main glut loop.

### 5.3.3 THE SECTOR OBJECT

The *Sector* object hides the complexity of converting a cell's row and column number to pixels on the screen.

This object was designed to handle the multiple-representation scenario described earlier. Despite the fact that this capability is not currently used (for concerns of visual intuitiveness), this object was not removed from the code. Its description here speaks to the process and the type of design decisions involved with the visualizer. Figure 61 provides a pseudocode description of this code.

See Figure 62 for a description of the *Sector.setPoint* method. Each sector object retains a pointer back to the *Frame* object that initiated it. This pointer is used to call the method *Frame.drawRectangle*.

See Figure 63 for a detailed description of the *drawRectangle* method. In the earlier embodiment this function would be called once for each sector. The current embodiment calls this only once per cell per timestep.

An earlier version of the *drawRectangle* method used the glut option *GL\_POLYGON* instead of *GL\_QUADS*. The *QUADS* option is faster. The *drawRectangle* method was also made faster by submitting all changes from a timestep to the glut buffer before any of them were rendered.

In its current version the visualizer intuitively and efficiently displays a view of the simulation.

## 6. RESULTS

Eight sites in the Gulf of Maine were selected for simulation. Three long simulations were executed for each site. One for each of these conditions: (1) Without harvesting, (2) Standard harvesting, and (3) Circular harvesting.

The coordinates of the eight selected sites were determined by James Wilson and Caitlin Cleaver after consultation with fishermen and biologists. Each site is known to have had a viable urchin population at some point.

Without harvesting, the urchins claimed much of the deeper and mid-level zones while maintaining some presence in the shallowest regions. Under standard harvesting, the mid-level zones flipped to the kelp-dominated state. Deeper zones were left untouched in both cases as divers cannot reach them. Under circular harvesting, urchin populations were greatly reduced in most cases, but not extirpated.

### 6.1 SIMULATION SETUP

Each simulation begins with a random distribution of urchins and seaweed as described in previous chapters. While random, the starting configuration is neither natural-looking nor stable. The natural appearance of an urchin distribution is a subjective measure that developed out of numerous sessions watching the simulator in the presence of marine biologists. The stability of the simulation is measured with respect to *topDensity* .

The first one-to-two years of simulated time are considered a "burn-in" period. Simulated harvesting never occurs before the three year mark to avoid harvesting from an unnaturally dense urchin population. Refer to the longer discussion in the previous chapter on "Population Health."

## 6.2 EXPECTATIONS

Regions in the model are expected to exhibit certain qualitative states (e.g. urchin barren, or kelp bed) under the three harvesting conditions (no harvesting, standard harvesting, circular harvesting). These expectations apply to the average case. Actual outcomes in the model may depend heavily on topology. The hypothesis is that the model described in this thesis will provide explanatory power for various phenomena observed in the urchin fishery, such as state flips from kelp bed to urchin barren and feedlines. 7.2.1 - 7.2.3 describe expectations of model behavior, not blanket assertions.

### 6.2.1 THE NO-HARVESTING CONDITION

The no-harvesting condition is ostensibly the most "natural" condition, but urchins evolved with under more predation than they currently experience. The no-harvesting condition may not be congruent with a sustainable healthy urchin population. It is expected that the urchin habitats under no-harvesting will maintain robust urchin barrens and high numeric density, but will have a low average gonad index due to overpopulation.

### 6.2.2 THE STANDARD-HARVESTING CONDITION

Urchins under the standard-harvesting condition are expected to be depleted within a year or two of monthly harvesting events. In each case the site is expected to flip to the kelp-dominated state and not return to the urchin-barren state. These populations will be lost and not return.

### 6.2.3 THE CIRCULAR-HARVESTING CONDITION

The circular-harvesting condition may have a similar effect as a high level of predation. The author conjectures that urchins may be well-suited to this level of predation.

Their habitats are not expected to flip to the kelp-dominated state. They are expected to maintain small but strong populations with medium to low density, but healthy gonad indices. Such sites are expected to be long-term sustainable and to expand quickly upon cessation of all harvesting.

### 6.3 SAMPLE TRIPTYCH: EASTERN BAY, DAY 2190

All simulations performed for the Results section were executed identically:

1. snapshots of each simulation taken yearly
2. each simulation executed for 15 years of simulated time
3. no harvesting occurs before the 3-year mark
4. no harvesting occurs after the 13-year mark
5. simulations executed under 3 conditions (no harvesting, standard, circular)
6. upon completion of all three, snapshots are compiled into trios
7. snapshots on the same line are contemporaneous to each other
8. column 1 (leftmost) shows the site with no harvesting
9. column 2 shows the site under standard harvesting
10. column 3 shows the site under circular harvesting
11. top snapshot is initial, each successive snapshot is underneath
12. "Day" indicates the number of days simulated so far
13. "Har" indicates the number of legal-sized urchins harvested so far
14. "Den" indicates the value of *topDensity*
15. "GI" indicates the value of *topGI*
16. a single random seed used for all simulations to improve comparisons
17. all harvesting events are once per month
18. all maps are oriented such that north points upward
19. values of both *topDensity* and *topGI* are plotted against time

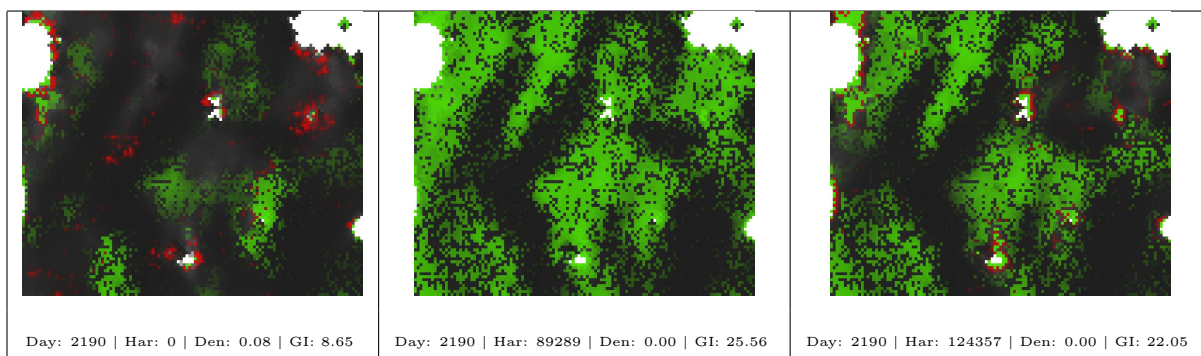


**Figure 12:** Sample snapshot trio for Eastern Bay, day 2,190. These three snapshots are presented in triptych form in order to show the varying state of the model under different conditions but at the same point in time. They capture the state of the model under each of the three modeled conditions: (1) no harvesting, (2) standard harvesting, and (3) circular harvesting.

Let this section serve as a transition and introduction to the next section, which provides the first results. The sample snapshot trio for Eastern Bay (above) is merely a simple example of the content beginning on the following page. Simulations for eight locations are described. So that the reader understands the figures, description is provided first, then graphs and snapshots of actual simulations.

Seen above is a triptych, i.e. three snapshots, each taken on the same day, same location, but under different conditions. In the first panel of the triptych we see an urchin population that has not been harvested. There are many shallow regions with high urchin density, and deeper regions where there is no seaweed. This lack of seaweed is a sign that urchins are present, but not in great enough numbers as to be visible in red. As seen in the data below the panel, these urchins have a low average GI.

The brightness of each color (either red or green) indicates greater biomass. Where dark grey is not easily distinguishable from dim green or red, the biomass is so low as to be insignificant relative to the areas of greater biomass.

The second panel shows the same location under normal harvesting. No urchins are visible. The only reason it is known that a few urchins survive is that the model maintains these numbers which can be output if desired. The GI of these creatures is impressively high, though searching for them and finding them would not be economically feasible.

The third panel shows numerous (more than ten) feedlines, or linear aggregations of urchins. These are visible as thin red lines near the land. As seen in the data below, their GI is quite healthy.

All the results are presented necessarily as triptychs. The comparison of model state at each time is most meaningful in its comparison to states resulting from other conditions. It is for this reason that all three conditions are presented in this way.

### 6.3.1 GRAPHS OF THE METRICS

Before the snapshots of the simulations are presented, graphs showing the evolution of each of these metrics will be presented:

**topDensity** : average urchin density (by number) among the top 1% of cells

**topGI** : average gonad index among the top 1% of cells

where "top 1%" refers to cells with the highest numeric density, urchins per  $m^2$ . Selecting only the densest cells is a heuristic attempt to select the cells of interest to a fisherman. Such cells often comprise a subregion known as a "feedline."

The relative "health," or robustness of the urchin population at a given site is measured by proxy using these two metrics. Neither metric is sufficient by itself. For instance, if *topDensity* is too high, the urchins will be over the carrying capacity of their local environment, thus causing a low *topGI*.

After the charts showing the evolution of each of these metrics over the course of the simulation, snapshots of those same simulations are presented.

## 6.4 BIG NASH

The first simulated location is referred to as "Big Nash." The description below is provided before the visual snapshots so that the snapshots will be more easily understood.

As with all the simulations performed for the Results section, each simulation begins with random populations of seaweed and urchins. Importantly, random but identical distributions are used in each case. This is done using a single integer as the seed for all pseudorandom number generators.

Each site is simulated under three harvesting conditions: 1.No harvesting (column 1), 2.Standard harvesting (column 2), 3.Circular harvesting (column 3). The following pages feature screenshots and some basic data about these simulations at yearly snapshots. There is no snapshot of day 1 because it is merely the initialization of the "burn-in" period and of little scientific value.

All harvesting occurs after day 1,095. The third snapshot trio (third row of snapshots) refers to day 1,095 for all three Big Nash simulations. This is the last point at which all three simulations are in completely equivalent states.

The successive snapshot trio (day 1,460), shows divergence between the three simulations in their values for *Har*, *topDensity*, and *topGI*, though the values for *topDensity* are lower than 0.005 urchins per  $m^2$  and therefore do not register here. Subjectively, at this point there is already a marked difference between column 2 (standard harvesting) and column 3 (circular harvesting). The difference is a visually-obvious decrease in the urchin population under that standard method.

By day 1,825, the urchin population under standard harvesting appears to be extirpated, while the population undergoing circular harvesting appears healthy. *topDensity* is still too low, but the visuals indicate an extant urchin population.

Under both types of harvesting, the value of *topDensity* remains low throughout the end of these simulations. Even so, it can be seen that a stable urchin population remains stable under circular harvesting, but is destroyed under standard harvesting.

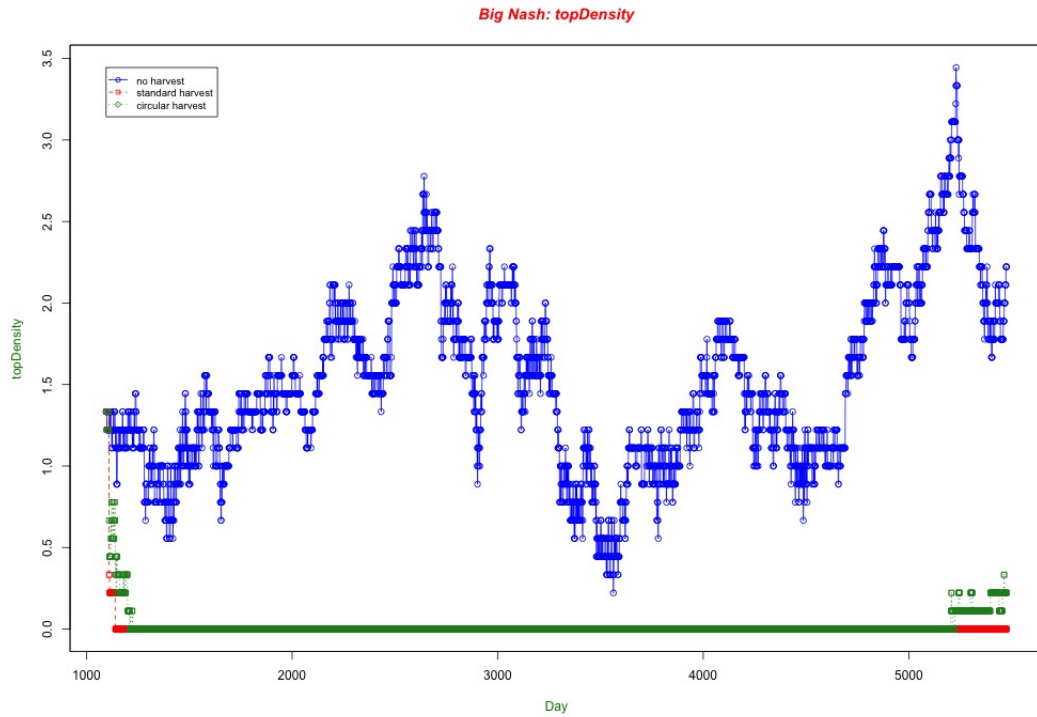
In terms of gonad index, urchins did not do well under either circular harvesting nor no harvesting. Only the standard-harvest urchin population maintained a consistent healthy GI in their densest cells as measured by *topGI*.<sup>17</sup> Most sites were different in that the circular harvesting method resulted in a healthy GI.

Over the course of a decade of monthly harvesting, standard harvesting yielded 45,208 urchins and the site was flipped to the kelp-dominated state. Under circular harvesting, the site yielded 144,679 urchins, a more than 300% increase, with the added benefit that circular harvesting did not flip the site to the kelp-dominated state. The urchin population is both intact and stable as judged over a decade-long period.

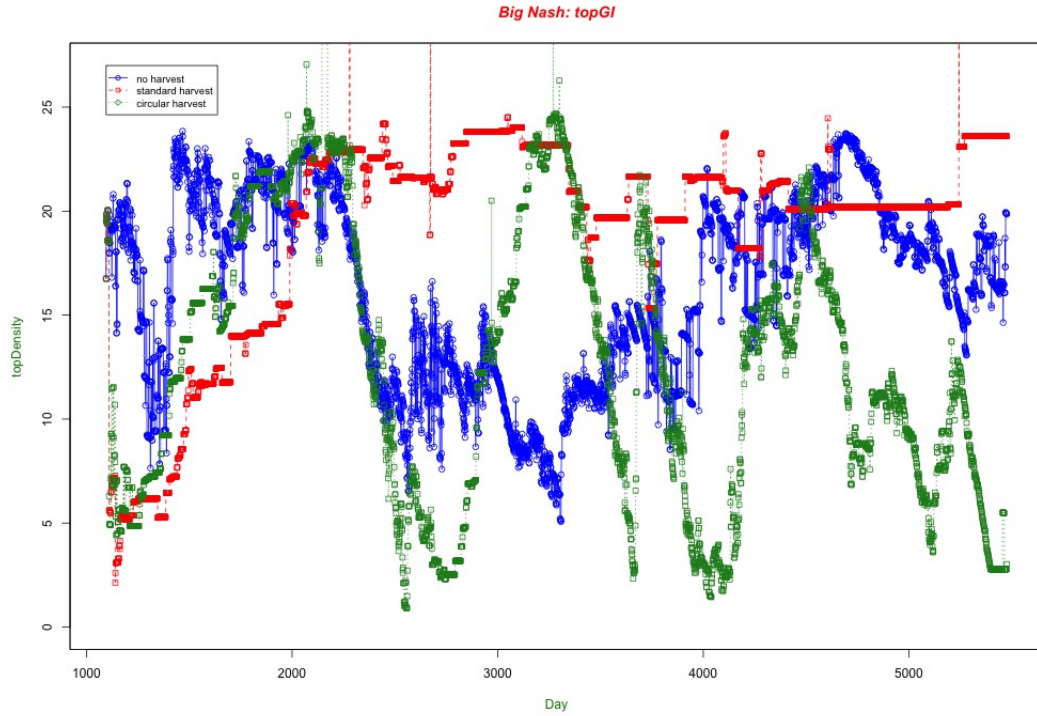
---

<sup>17</sup>A healthy GI is a higher GI. Subjectively some consider a GI above 15 to be healthy.

### 6.4.1 METRICS *TOPDENSITY* AND *TOPGI*

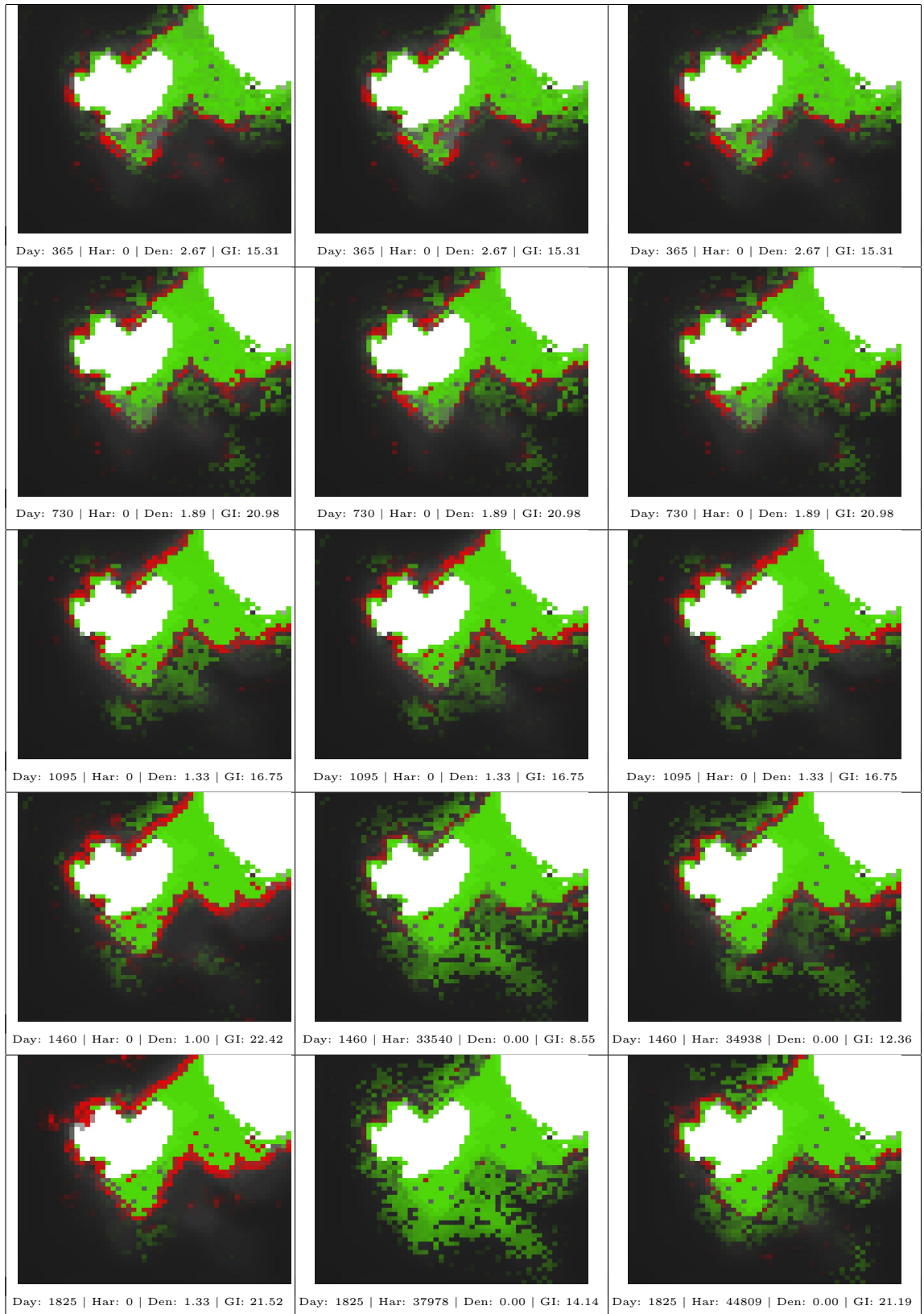


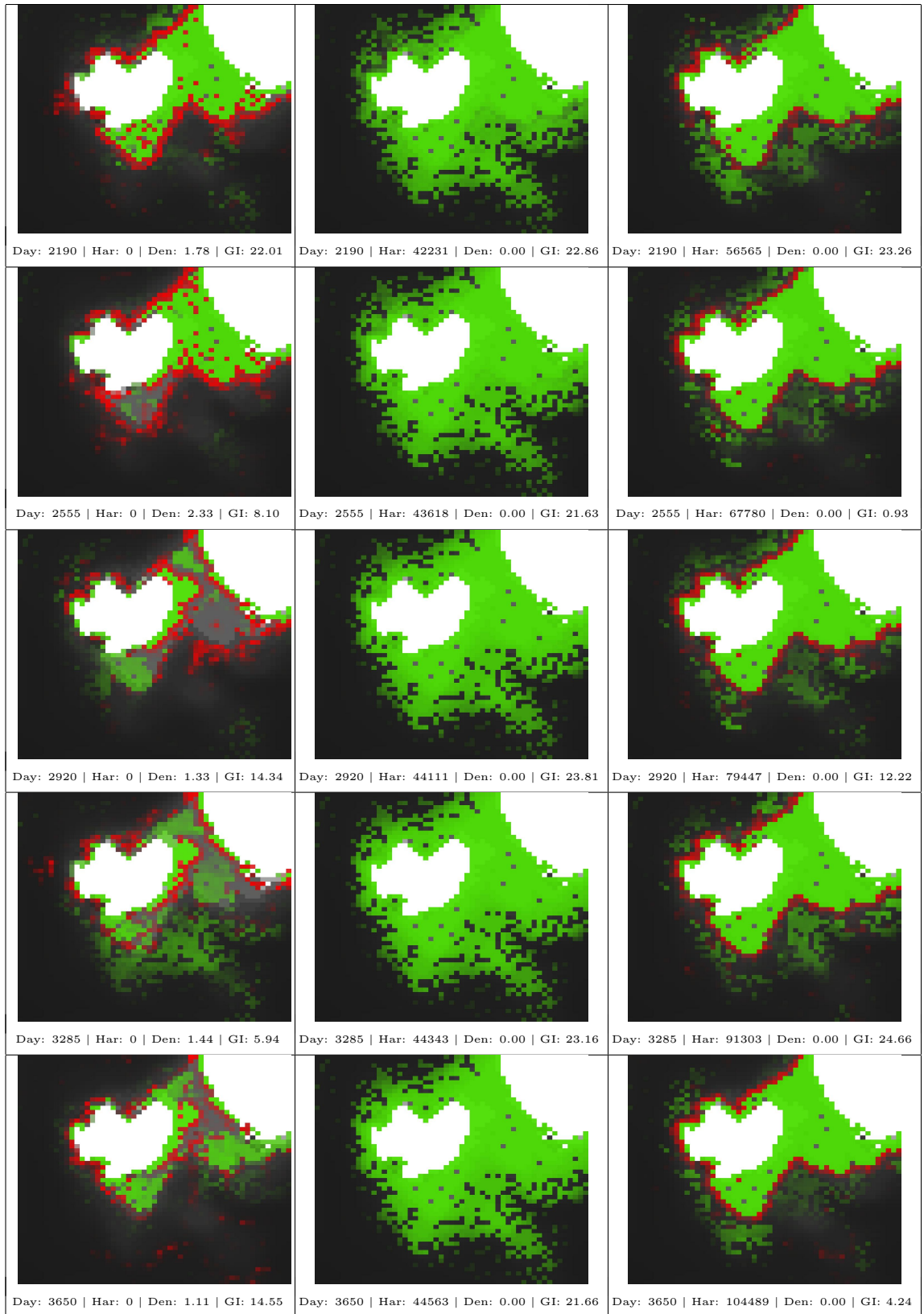
**Figure 13:** Big Nash: *topDensity*. This graph shows the value of *topDensity* over the course of the simulation. In this case it is consistently higher under no harvesting. Under the other two conditions it is negligibly above zero except at the end, after harvesting has ended. At this point the population under the circular harvesting begins to make a comeback. This comeback is more visible in the screenshots.

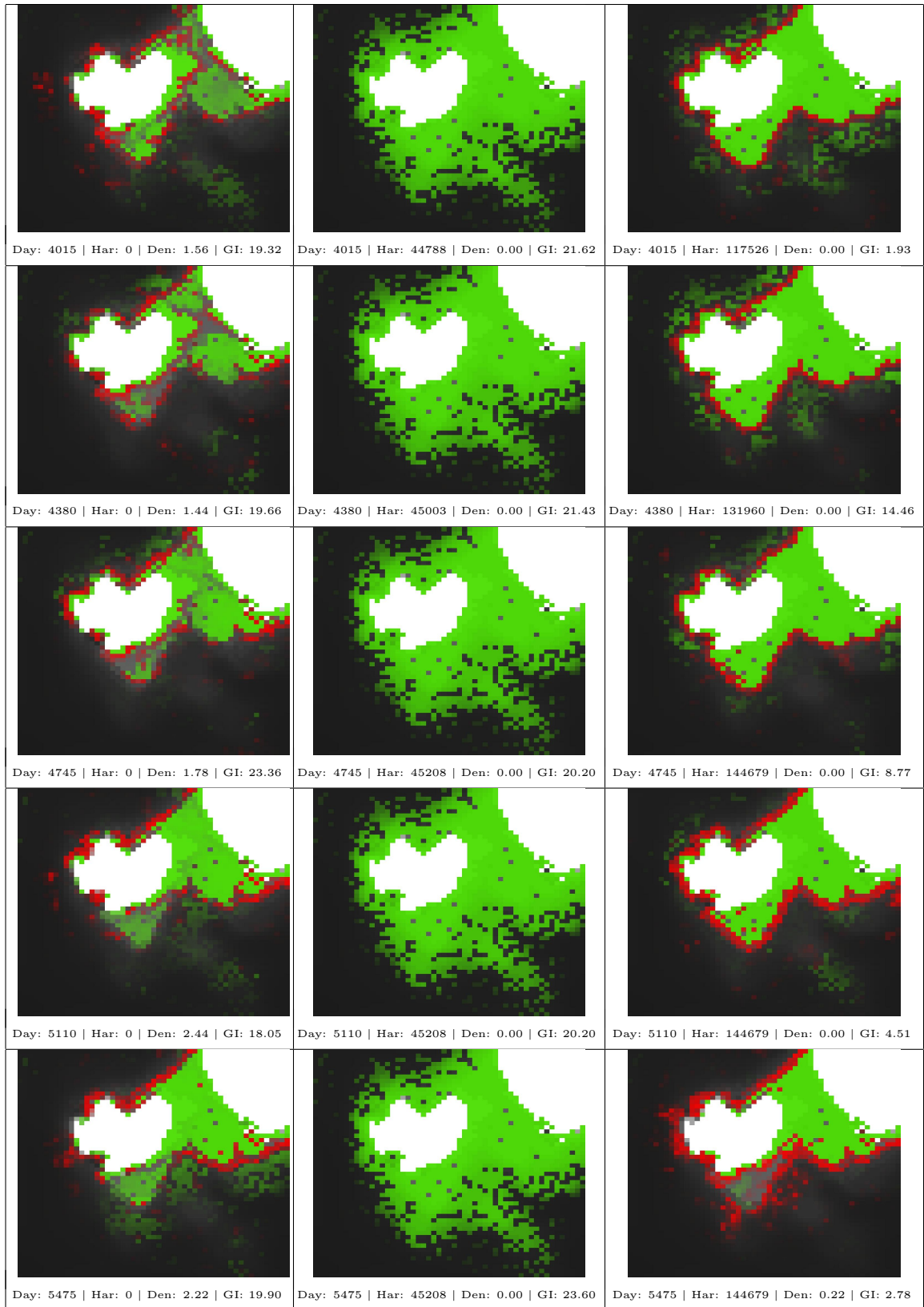


**Figure 14:** Big Nash:  $topGI$ . This graph shows the value of  $topGI$  over the course of the simulation. This metric is the other side of population health. Note that apparent oscillations here are not simple patterns. They can only be understood within the context of the whole simulation.

**Figure 15:** Big Nash: Snapshots. (Following pages) These snapshots are presented in triptych form as described above. They capture the state of the model, over a multi-year period as labeled in units of days, under each of the three modeled conditions: (1) no harvesting, (2) standard harvesting, and (3) circular harvesting.







## 6.5 BLACK LEDGE

The Black Ledge site is different from other simulated sites because it has no land, only two small regions of less depth. The site has no true shallows. Because of this lack of shallows, there is no fast-growing seaweed like all other sites. This feature is expected to alter the population dynamics.

As with all sites, all harvesting occurs after day 1,095. The third snapshot trio (third row of snapshots) refers to day 1,095 for all three Black Ledge simulations. As with other simulated locations, this is the last point at which all three simulations are in completely equivalent states.

At day 1,460 the divergence between the simulations is already apparent. At this point the no-harvesting situation is by far the healthiest and most robust urchin population. It's *topDensity* remains higher during most of the simulation, but its *topGI* drops low.

Two years later, at day 2,190, half of the urchin habitat is gone. They overconsumed a slowly replenishing food source until they were forced to move because of starvation. The seaweed didn't grow back until they had been gone for a much of a year, enabling the southern shallow region to become fully covered by seaweed without any significant urchin presence.

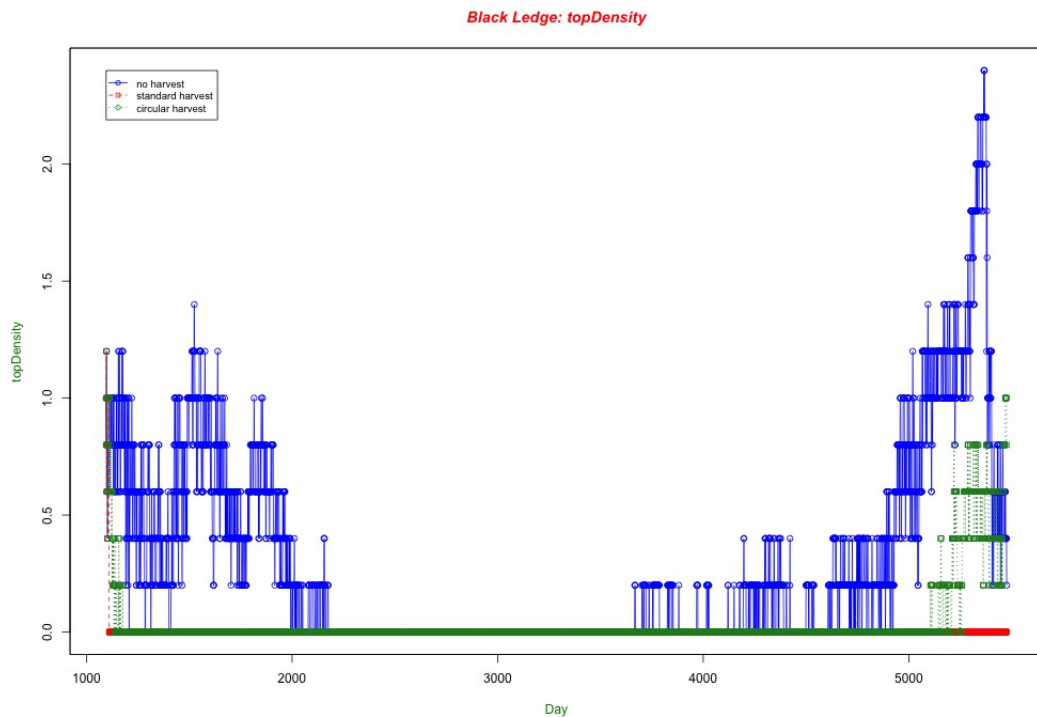
At this same point in time, under the standard-harvesting condition, the urchin habitat has completely flipped to the kelp-dominated state. It never recovers, even after two years of no harvesting at all, between days 4,745 - 5,475.

The circular-harvesting condition has the healthiest urchin population at this point as can be seen by looking at three factors: (1) Visually it looks viable – urchin feedlines are consuming a renewable resource, (2) *topGI* is high, and (3) *topDensity* is competitive with the other conditions. Under circular harvesting we see two solid feedlines that remain throughout the whole simulation. It has an extremely high GI of 22.99, and it has yielded more urchins than the standard-harvesting condition. While the

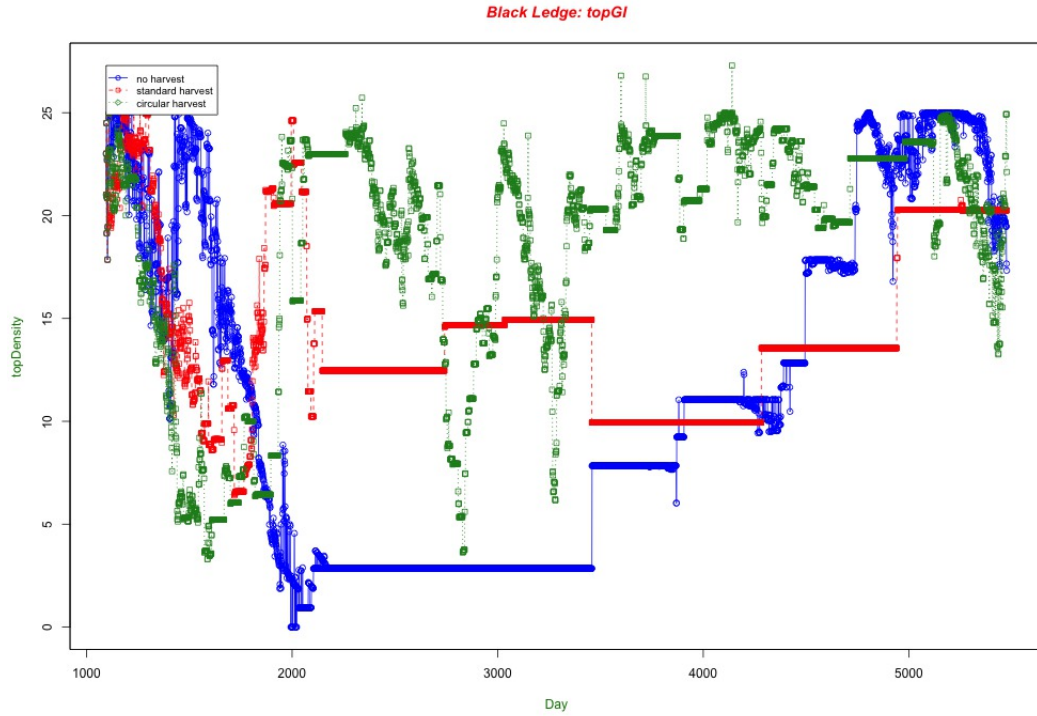
no-harvesting condition can compete on the values of its metrics, the southern population has overconsumed their resource and the northern population isn't significant enough to be visible.

Throughout the rest of the simulation the circular-harvesting condition encourages a healthy and robust urchin population. Not only does it continually foster urchin numbers, those urchins have consistently high GI. The no-harvesting condition makes a comeback near the end of the simulation, but it was in the kelp-dominated state during most of the 15-year simulation. At most sites, urchins are not so capable of recovering a kelp-dominated site. In this case it appears that a number of sparsely-dispersed urchins in the deeper regions converged on the southern knoll and were able to turn it to urchin barren rather rapidly due to the slow-growth of seaweed at that depth.

### 6.5.1 METRICS *TOPDENSITY* AND *TOPGI*

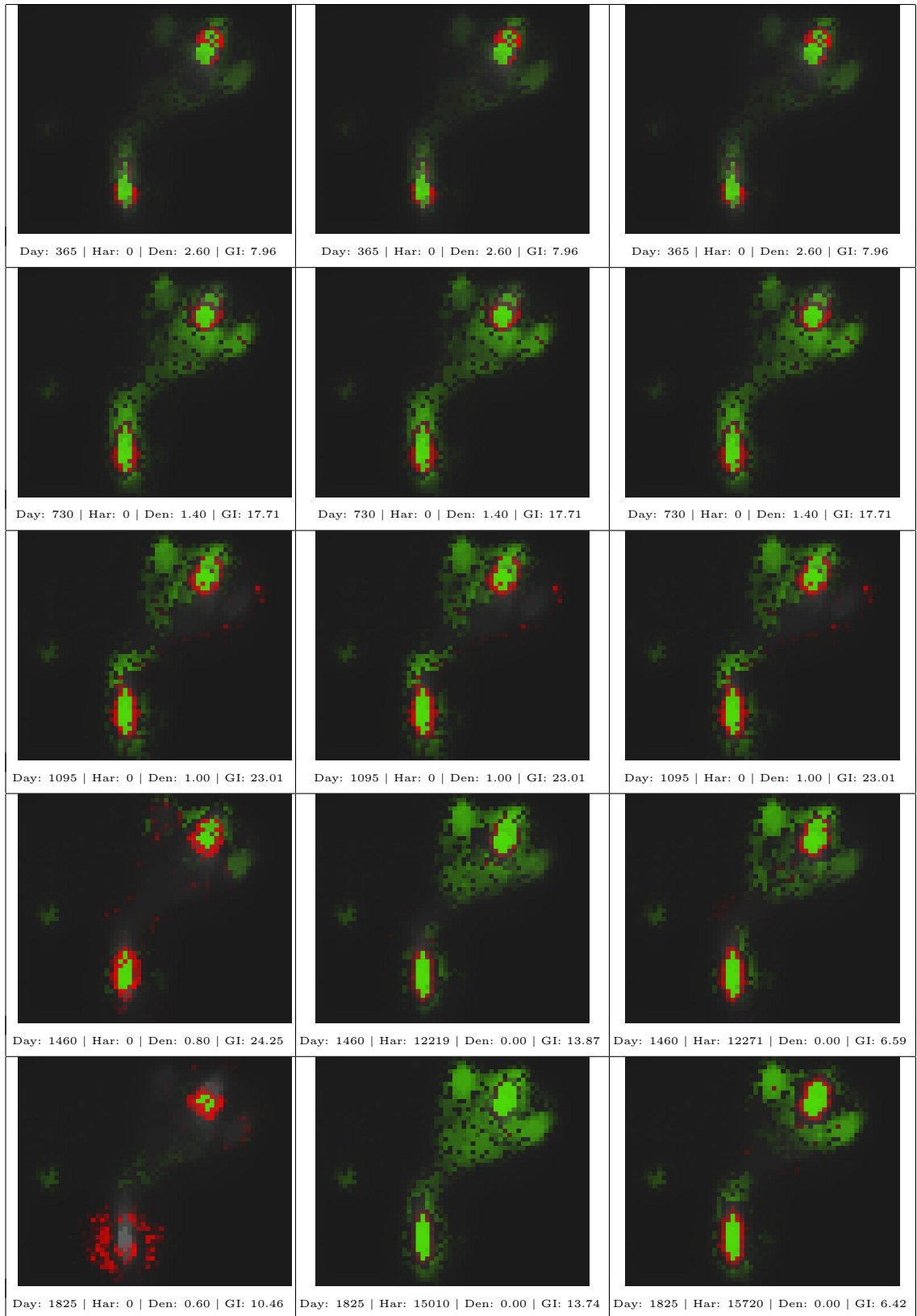


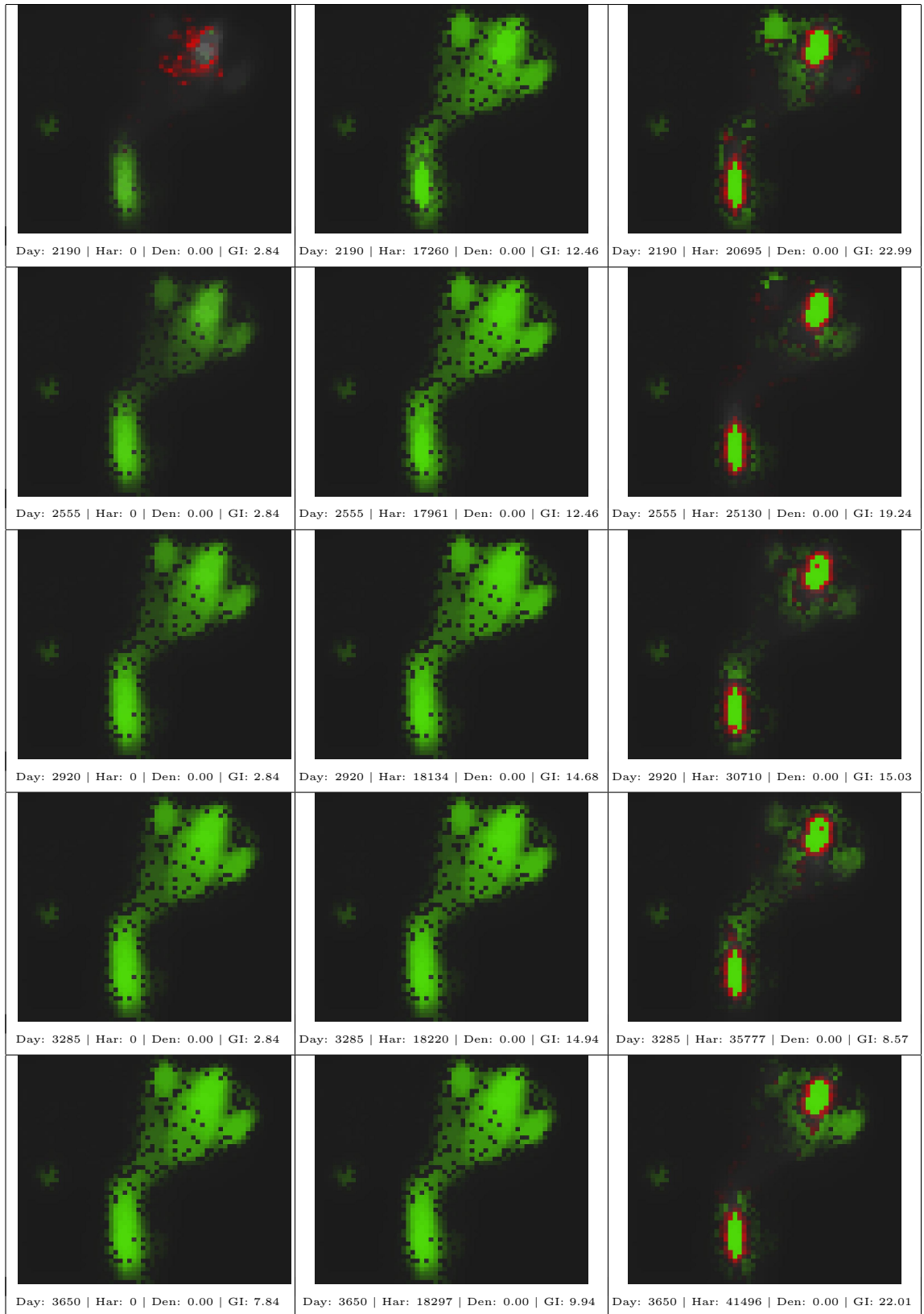
**Figure 16:** Black Ledge: This graphs shows the modulations of *topDensity* during the course of the simulation. More explanation in the section above.

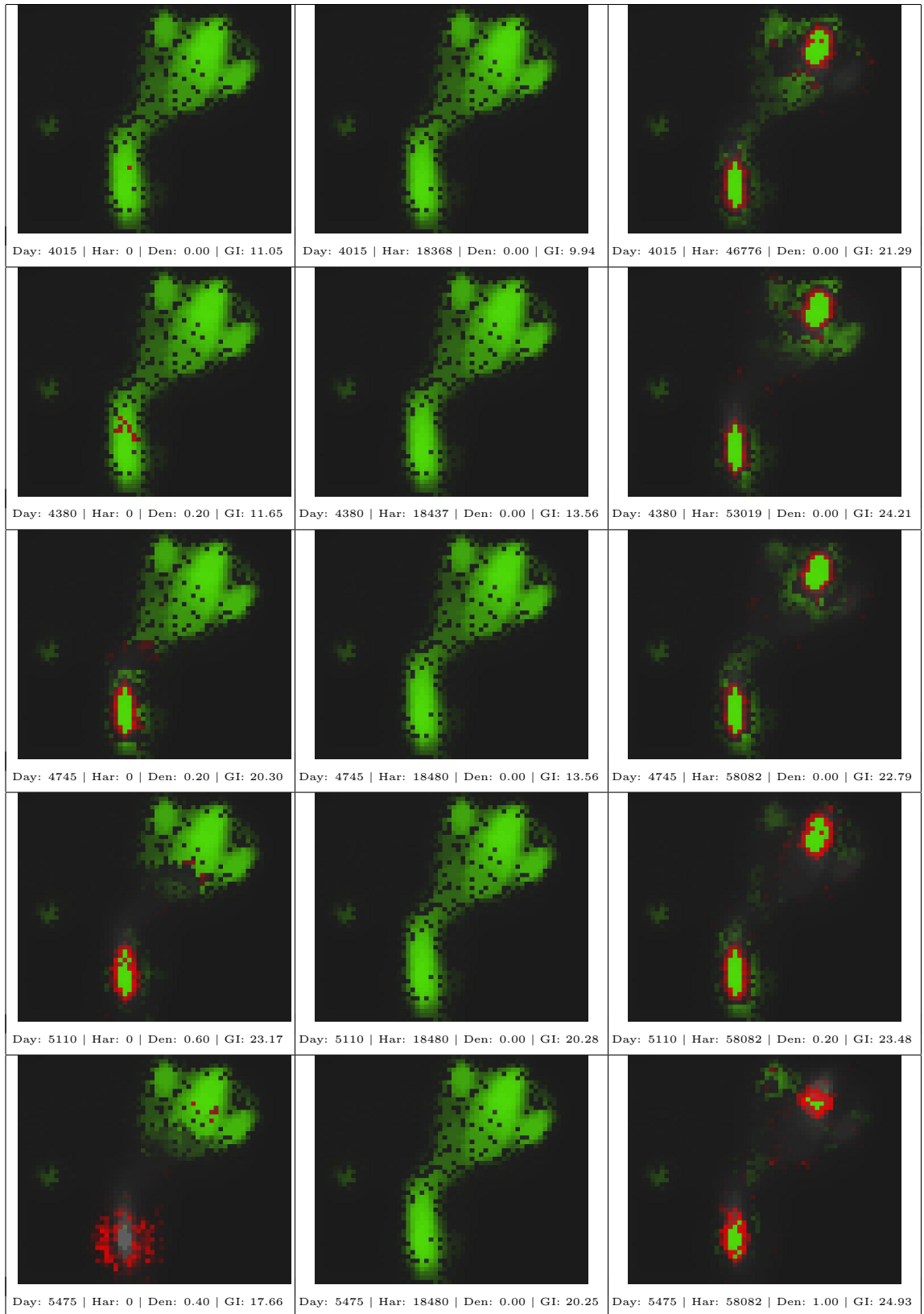


**Figure 17:** Black Ledge: This graphs shows the modulations of *topGI* during the course of the simulation. More explanation in the section above.

**Figure 18:** Black Ledge: Snapshots. (Following pages) These snapshots are presented in triptych form as described above. They capture the state of the model, over a multi-year period as labeled in units of days, under each of the three modeled conditions: (1) no harvesting, (2) standard harvesting, and (3) circular harvesting.







## 6.6 EASTERN BAY

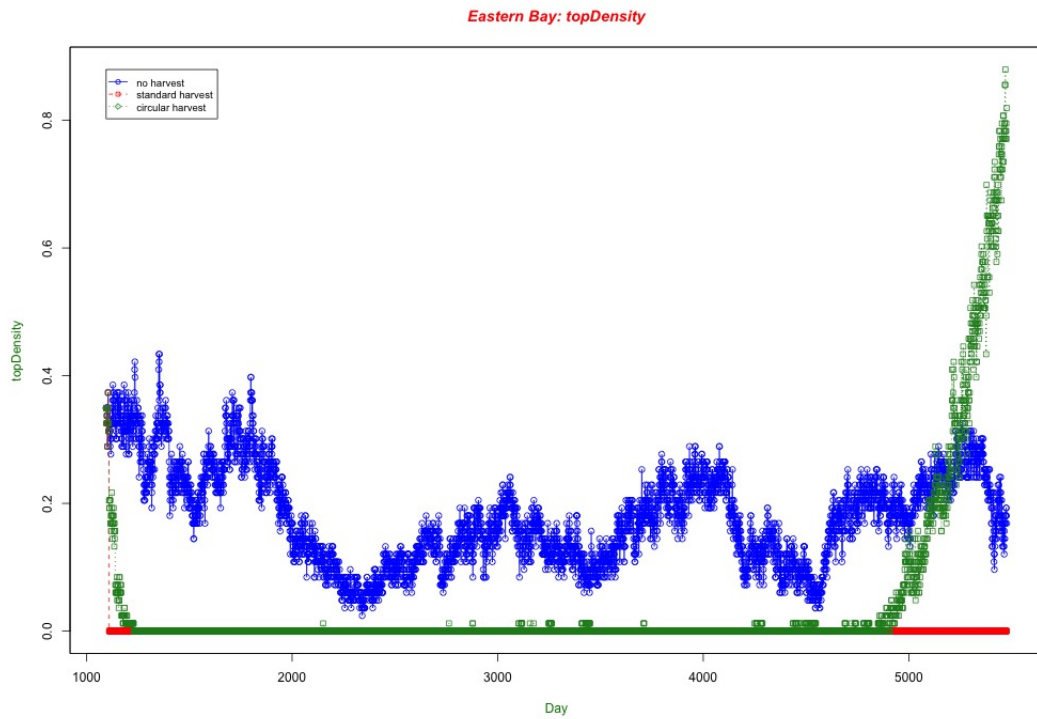
The Eastern Bay site is a larger site and has more varied topological features than the previous two. Specific details on the location may be found in the appendices. The large area of this site implies more datapoints. These contribute to smoothing of simulation-wide trends.

One year after harvesting begins, day 1,460, the three conditions already exemplify the expectations described earlier in this section. No-harvesting allows urchins to be most dominant. Standard harvesting has depleted most of the urchins and the site is already starting to flip to the kelp-dominated state. Circular harvesting has yielded many urchins as well, but several stable feedlines exist and remain stable throughout the rest of the simulation.

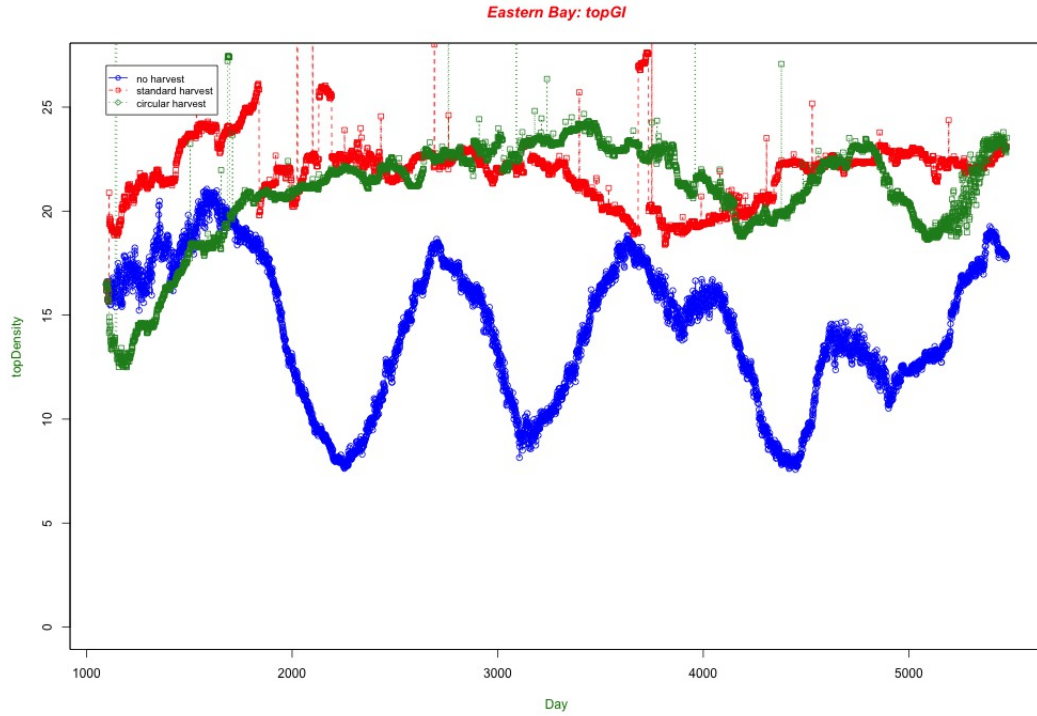
Through to the end (the 15-year mark) it can be seen that the no-harvesting condition generated populations that were expansive and moderately healthy. Values for *topGI* wandered up and down between 8 and 18. The standard-harvesting condition killed off its urchin population by day 1,460 and it never recovered. The circular-harvesting condition afforded several thriving urchin populations that remained healthy and in the same place throughout the first 13 years. Once harvesting ceased at the 13-year mark, this population expanded rapidly. At day 5,475, the size of its barrens rivaled those of the no-harvesting condition, and its population was much healthier. Urchins under the circular-harvesting condition maintained a *topGI* near or above 20 throughout the whole simulation.

The most surprising statistic is the rapid response of the population under circular harvesting to the cessation of that harvesting. As seen in the graph of *topDensity*, the density of urchins in the densest clusters shoots rapidly above even that of the no-harvesting condition. This metric attempts to measure the density of the urchins in precisely the cells where divers would harvest. Tandem to this positive assessment, the value of *topGI* is highest among the three conditions.

### 6.6.1 METRICS *TOPDENSITY* AND *TOPGI*

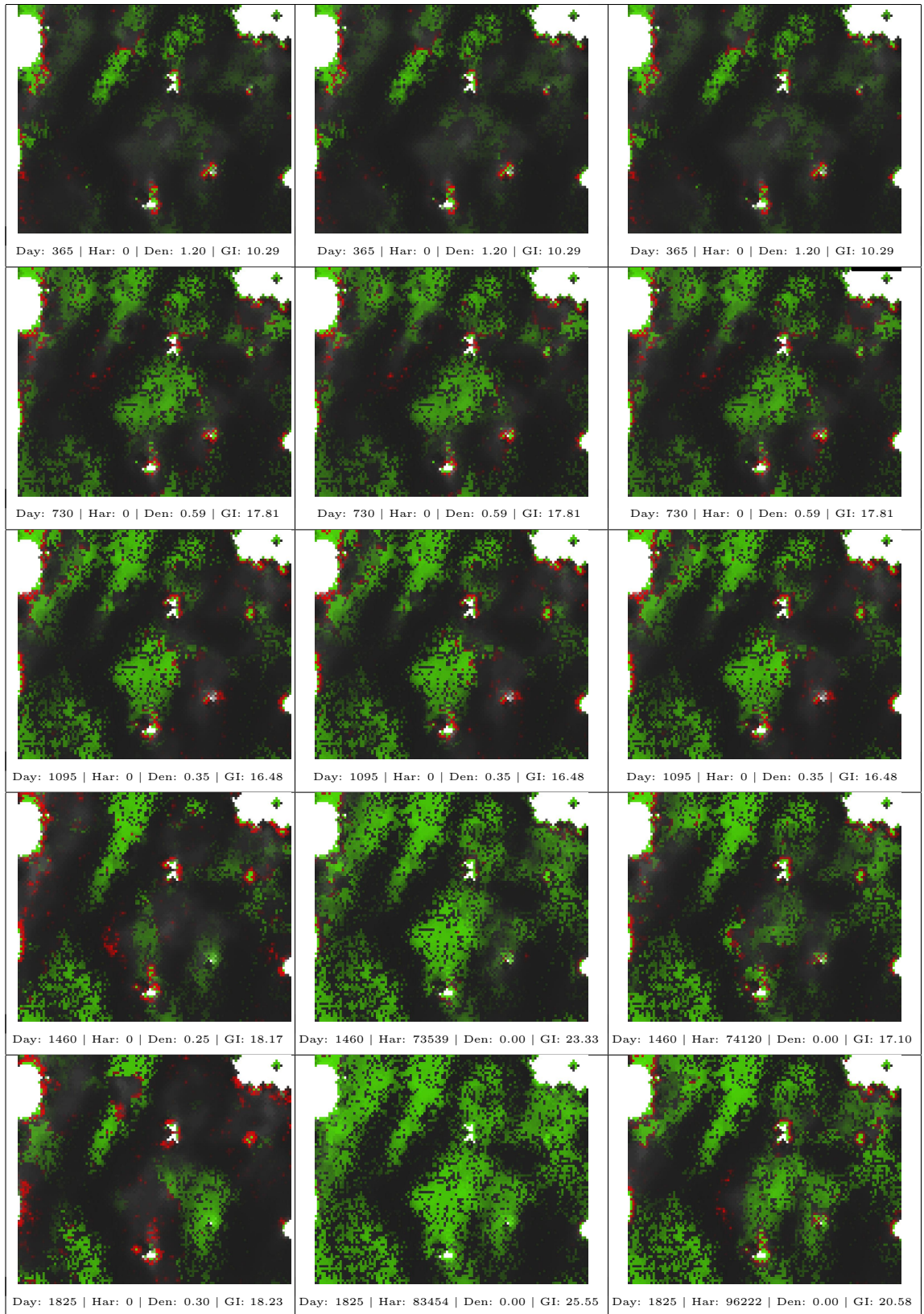


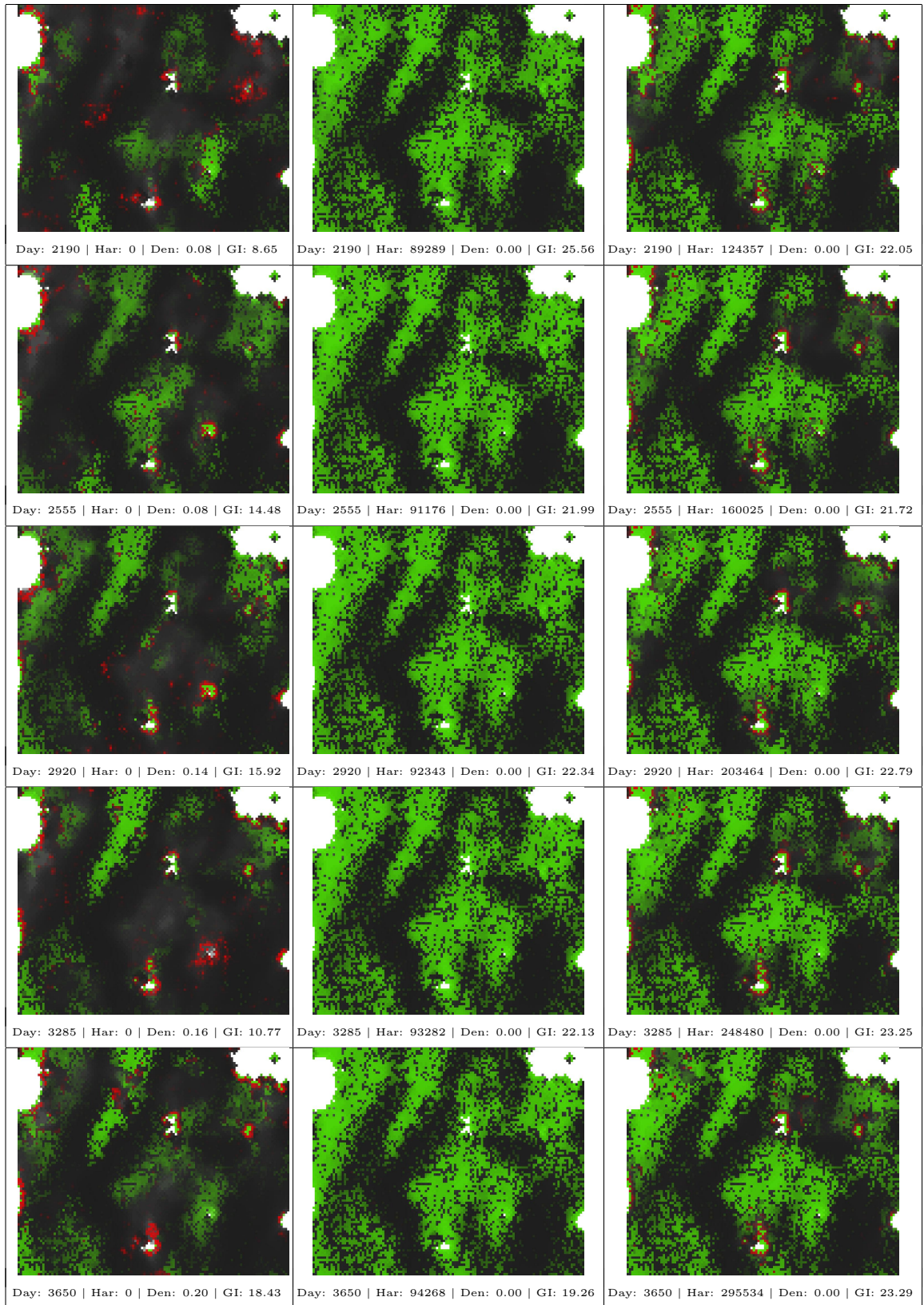
**Figure 19:** Eastern Bay: This graphs shows the modulations of *topDensity* during the course of the simulation. More explanation in the section above.

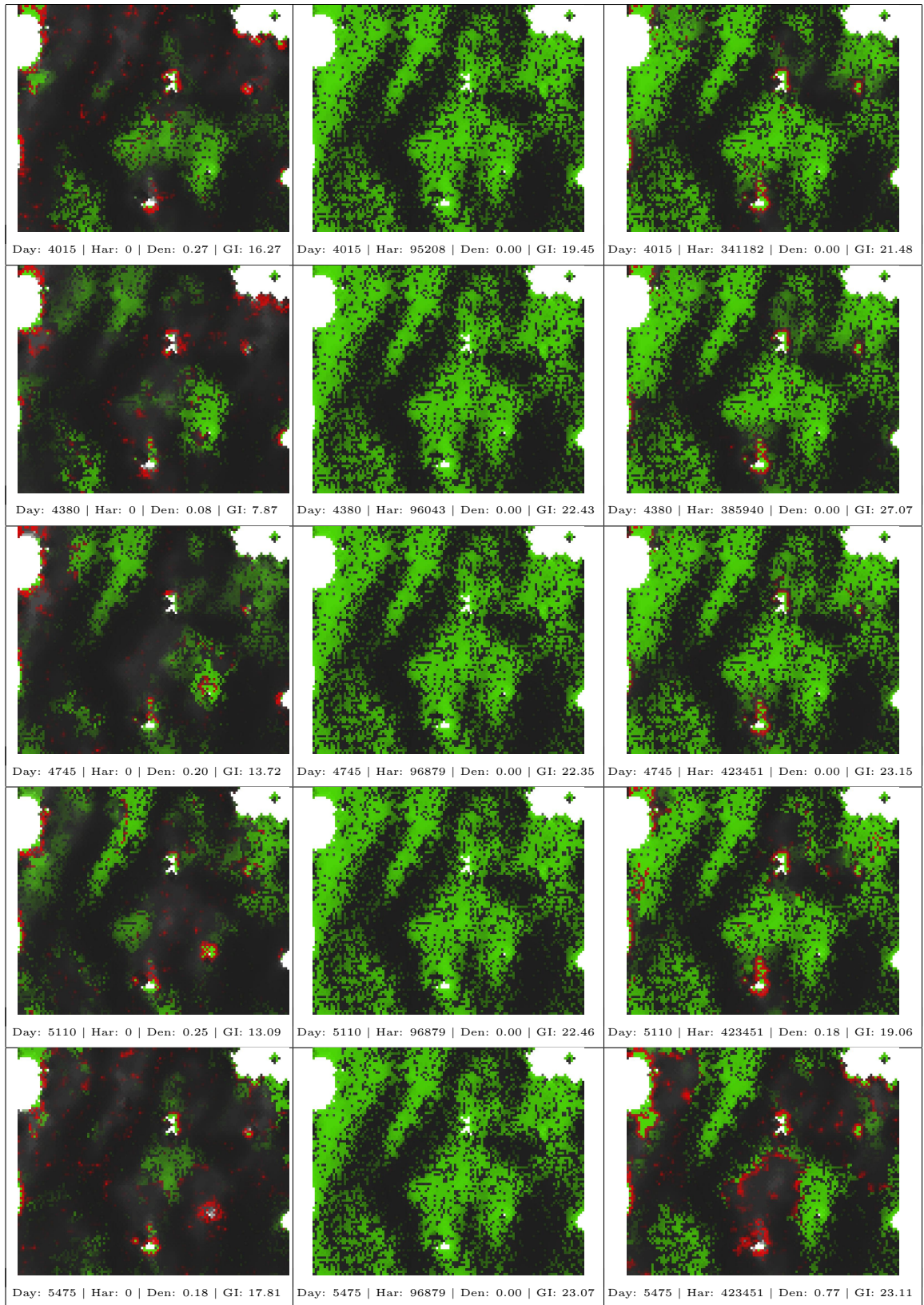


**Figure 20:** Eastern Bay: This graphs shows the modulations of  $topGI$  during the course of the simulation. More explanation in the section above.

**Figure 21:** Eastern Bay: Snapshots. (Following pages) These snapshots are presented in triptych form as described above. They capture the state of the model, over a multi-year period as labeled in units of days, under each of the three modeled conditions: (1) no harvesting, (2) standard harvesting, and (3) circular harvesting.





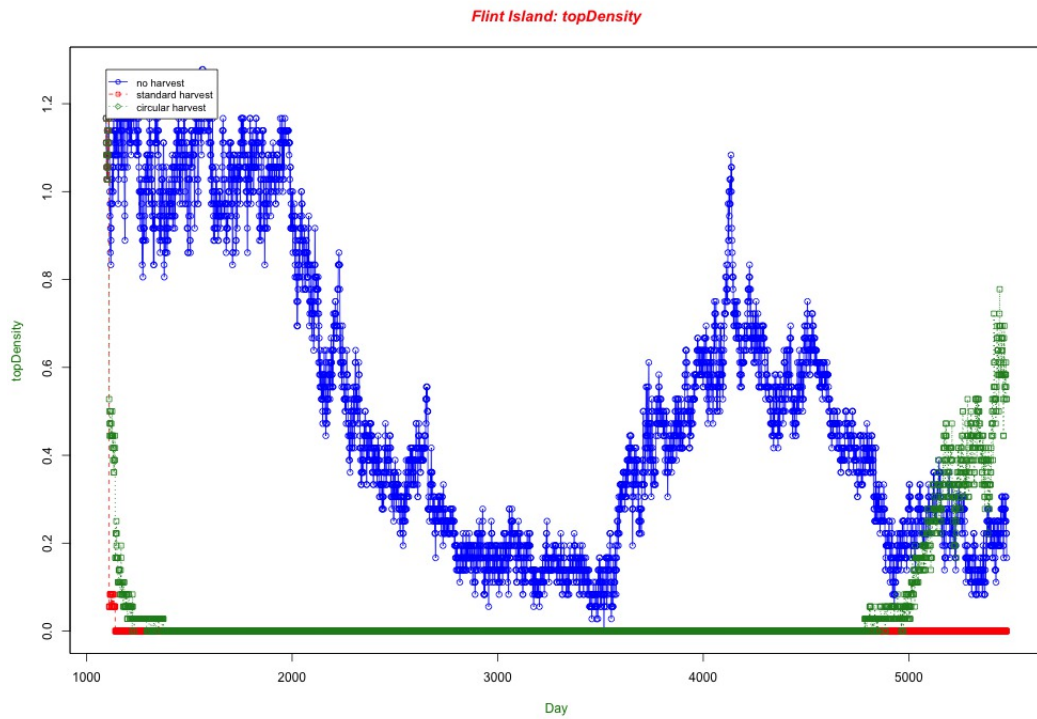


## 6.7 FLINT ISLAND

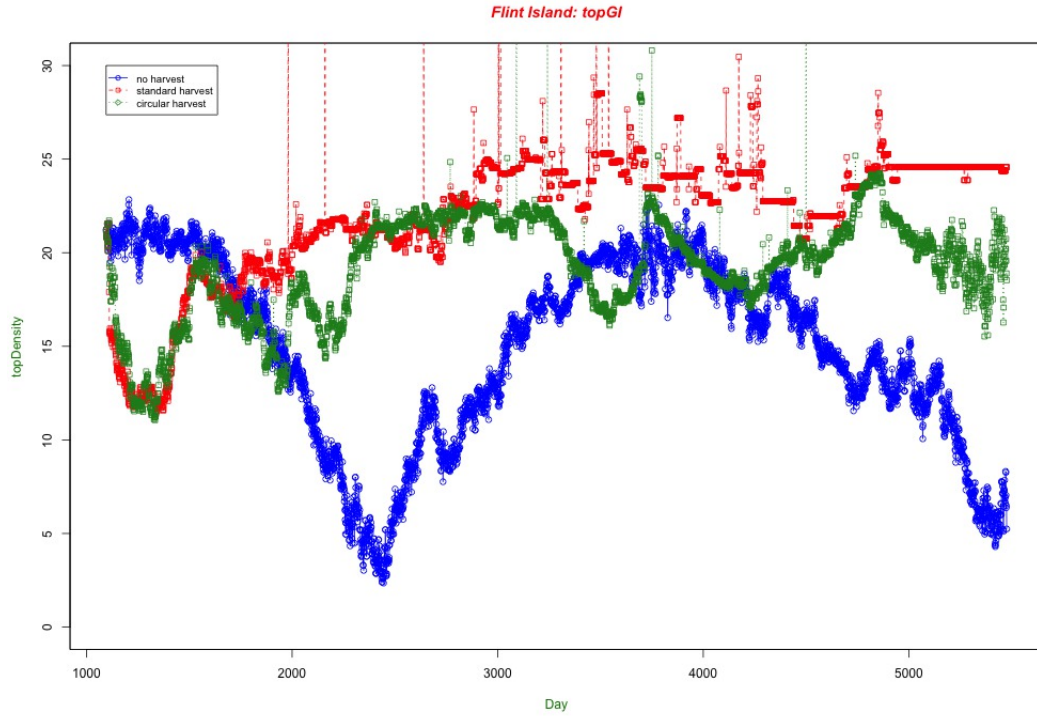
Flint Island is similar to Eastern Bay in its size and varied topology. Flint Island has more land and deeper depths where seaweed growth will be negligible. The islands at this site can act as separators which inhibit urchin movement throughout the site. This topology can sometimes prevent one pocket of urchins from repopulating depleted areas.

As with other sites, divergence can be seen in the snapshots within one year of the start of harvesting (Day 1,460). The trends exhibited at this site are similar to other sites and congruent with expectations. The standard-harvesting condition extirpates the urchin population. No harvesting causes a large urchin barren with starving urchins. The circular-harvesting condition causes strong urchin feedlines that look healthier than the no-harvesting condition and have a consistently strong *topGI*. Its *topDensity* is quite low during the harvesting period, but rises dramatically immediately after the cessation of harvesting. This quick recovery is a solid signal of population health. This kind of health is not seen under standard harvesting, which ceases at the same time, but doesn't recover, as can be seen in the graph of *topDensity* for this site.

### 6.7.1 METRICS *TOPDENSITY* AND *TOPGI*

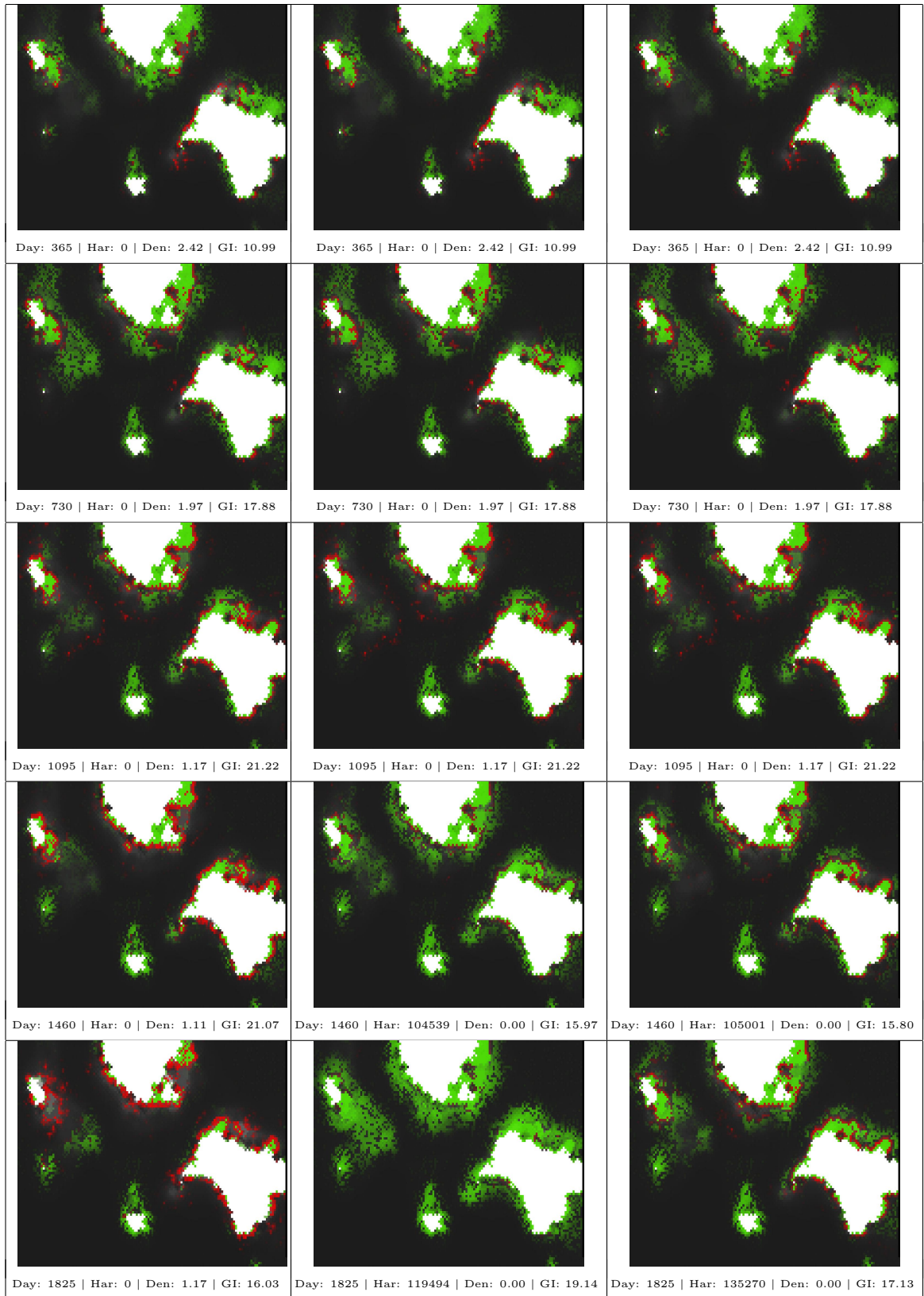


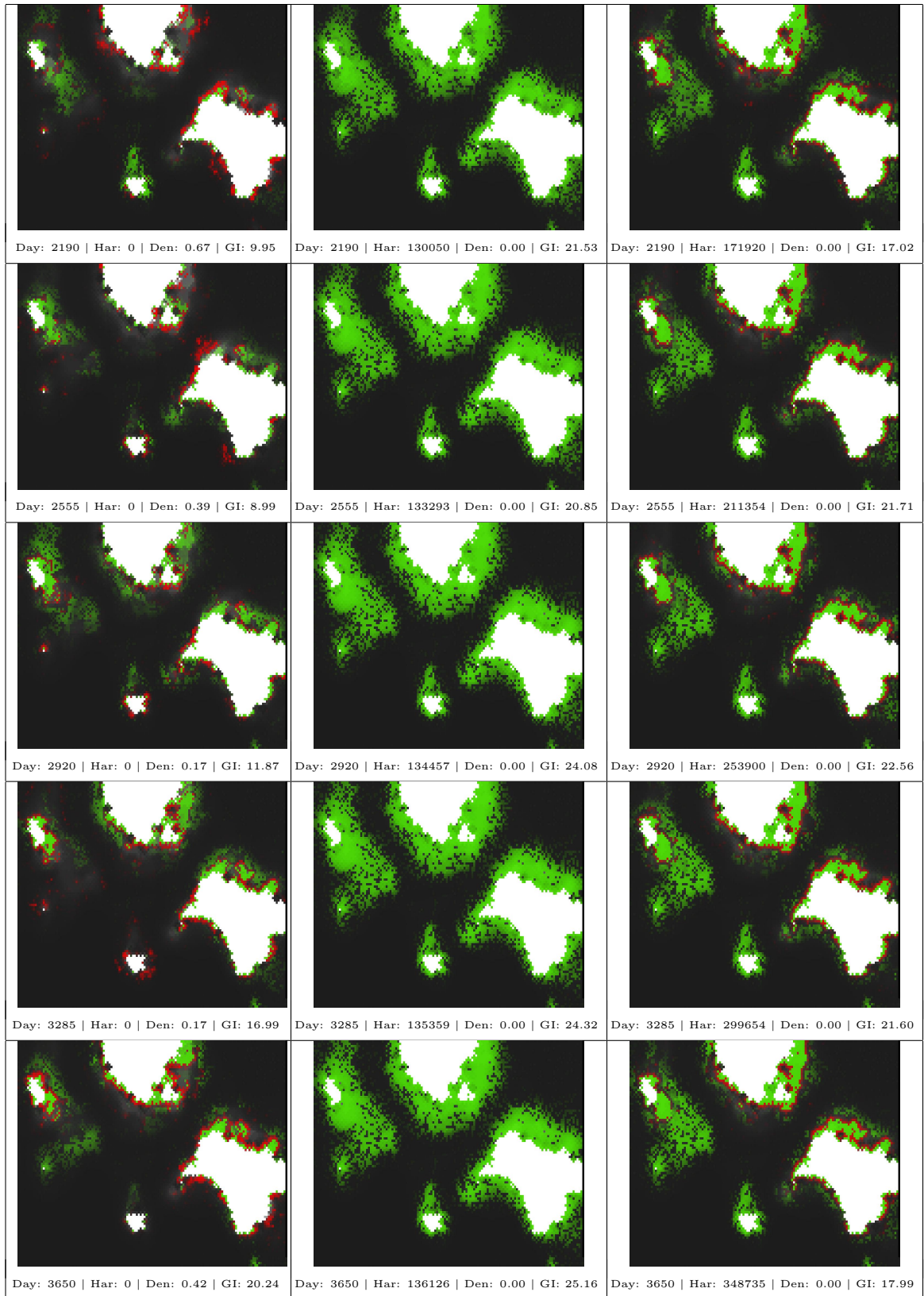
**Figure 22:** Flint Island: This graphs shows the modulations of *topDensity* during the course of the simulation. More explanation in the section above.

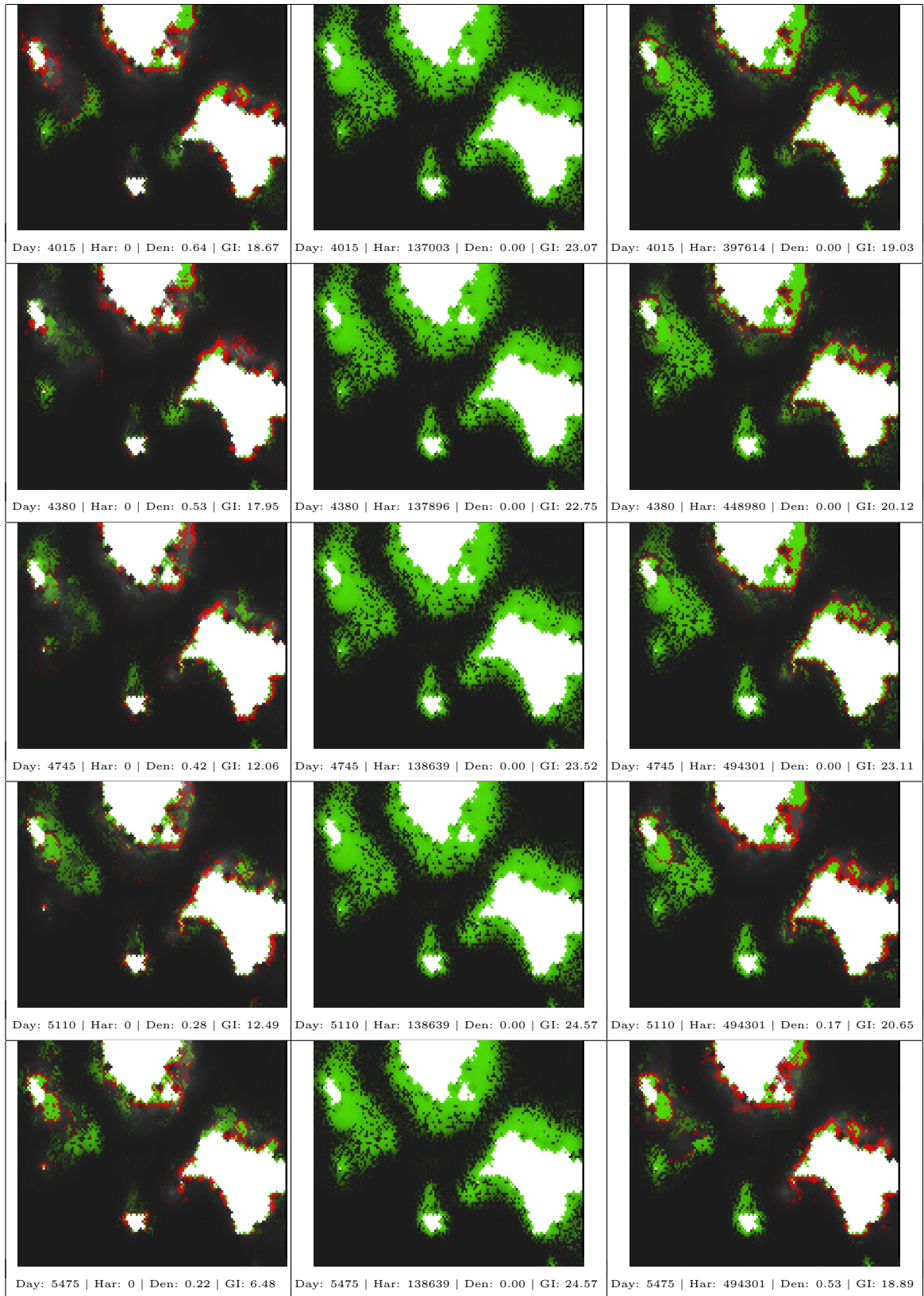


**Figure 23:** Flint Island: This graphs shows the modulations of  $topGI$  during the course of the simulation. More explanation in the section above.

**Figure 24:** Flint Island: Snapshots. (Following pages) These snapshots are presented in triptych form as described above. They capture the state of the model, over a multi-year period as labeled in units of days, under each of the three modeled conditions: (1) no harvesting, (2) standard harvesting, and (3) circular harvesting.





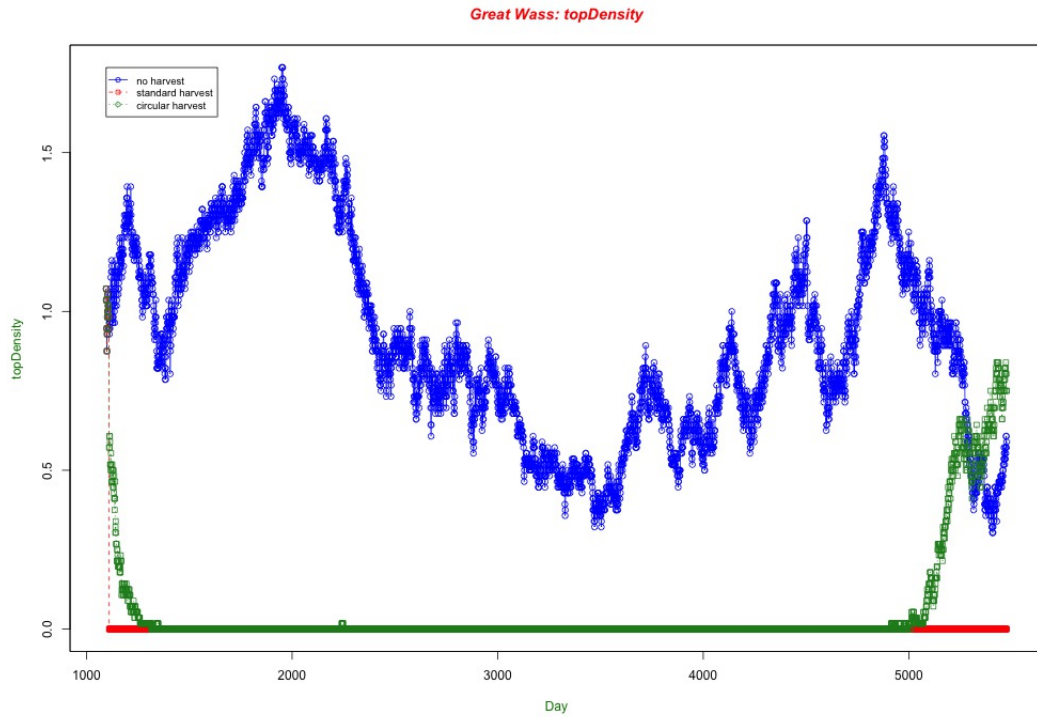


## 6.8 GREAT WASS

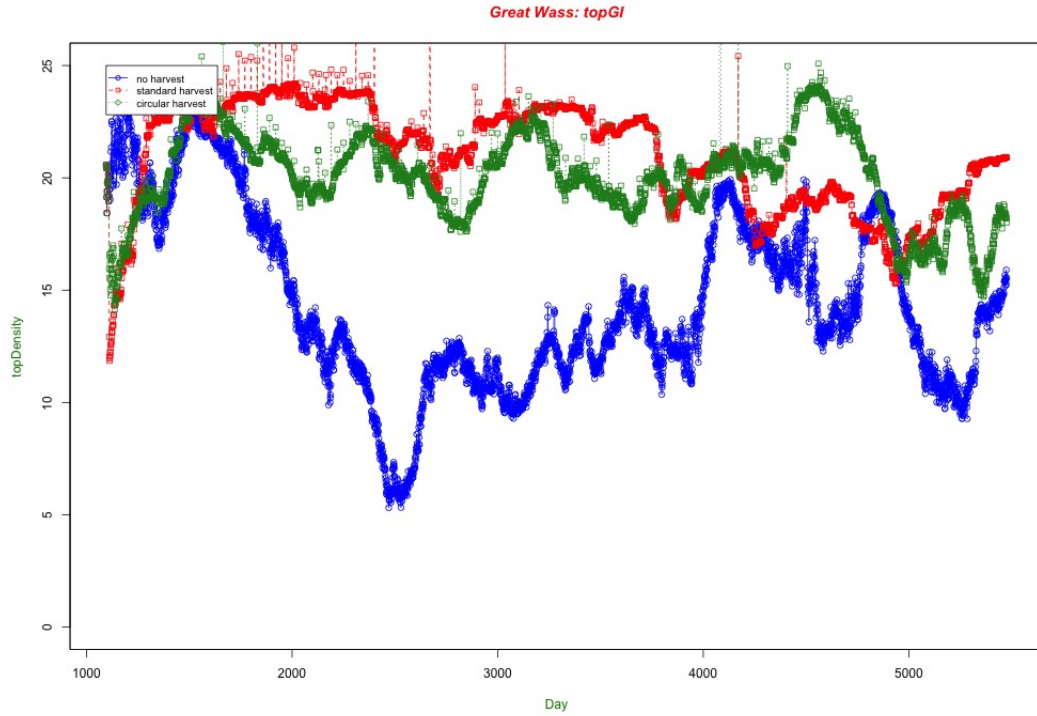
Great Wass is another large site with varied topology. This site is unique that although it has lots of land, all urchins are corralled in the middle. No sections are blocked by topological obstructions. The site is homogeneous enough that urchins in the deeper regions, normally drawn toward food sources, are slow in choosing a direction because they sense food equally in all directions.

Despite these unique features, this site exhibits all the expected trends seen in other simulations. Standard harvesting kills off the urchin population. Its *topDensity* drops immediately and never recovers. No-harvesting engenders a large and relatively healthy urchin barren, but not quite as healthy, as measured in terms of *topGI*. Circular harvesting engenders a strong, stable, and healthy urchin population while yielding more than 400% more urchins (over the standard harvesting yields) over a decade of monthly harvesting.

### 6.8.1 METRICS *TOPDENSITY* AND *TOPGI*

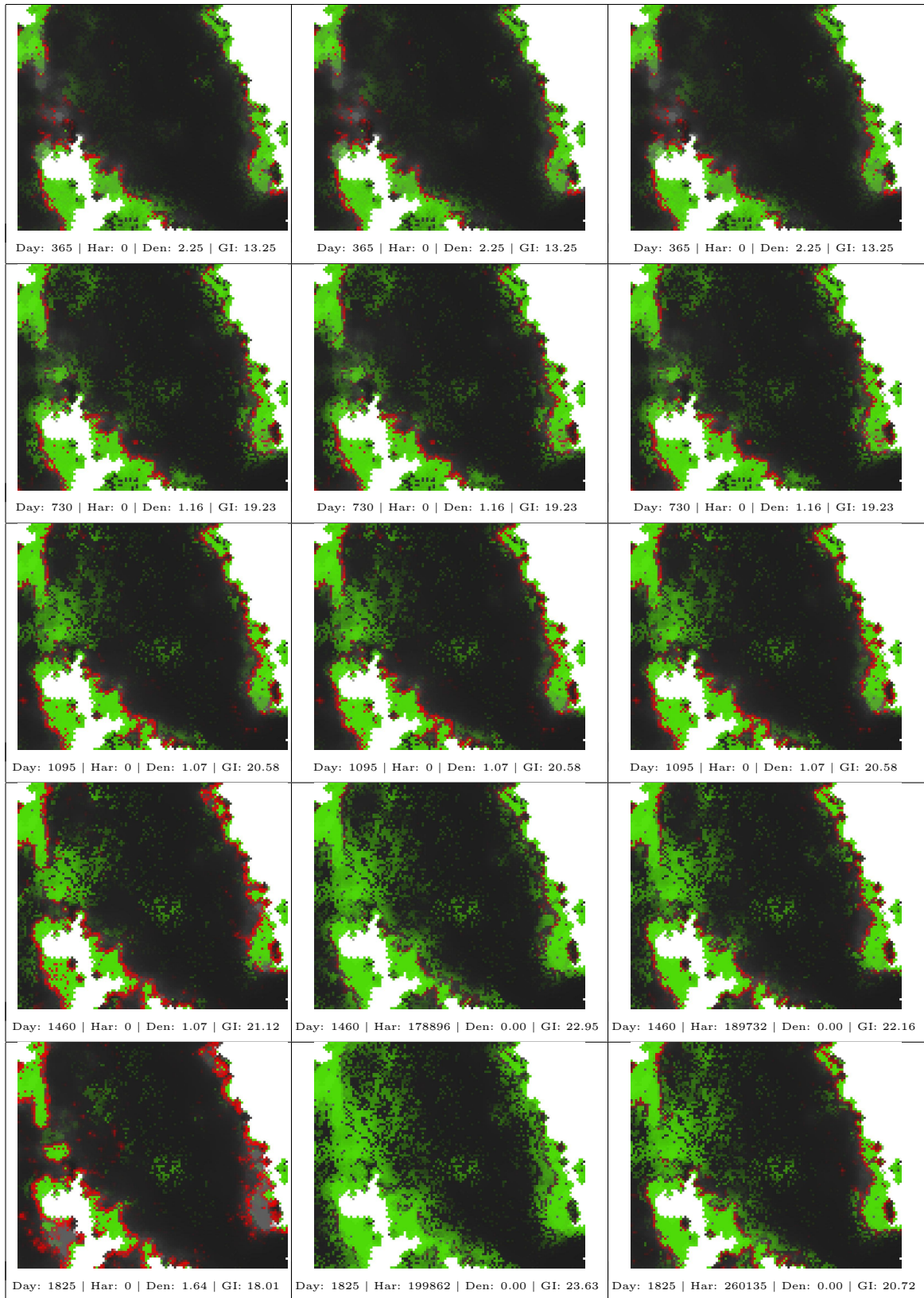


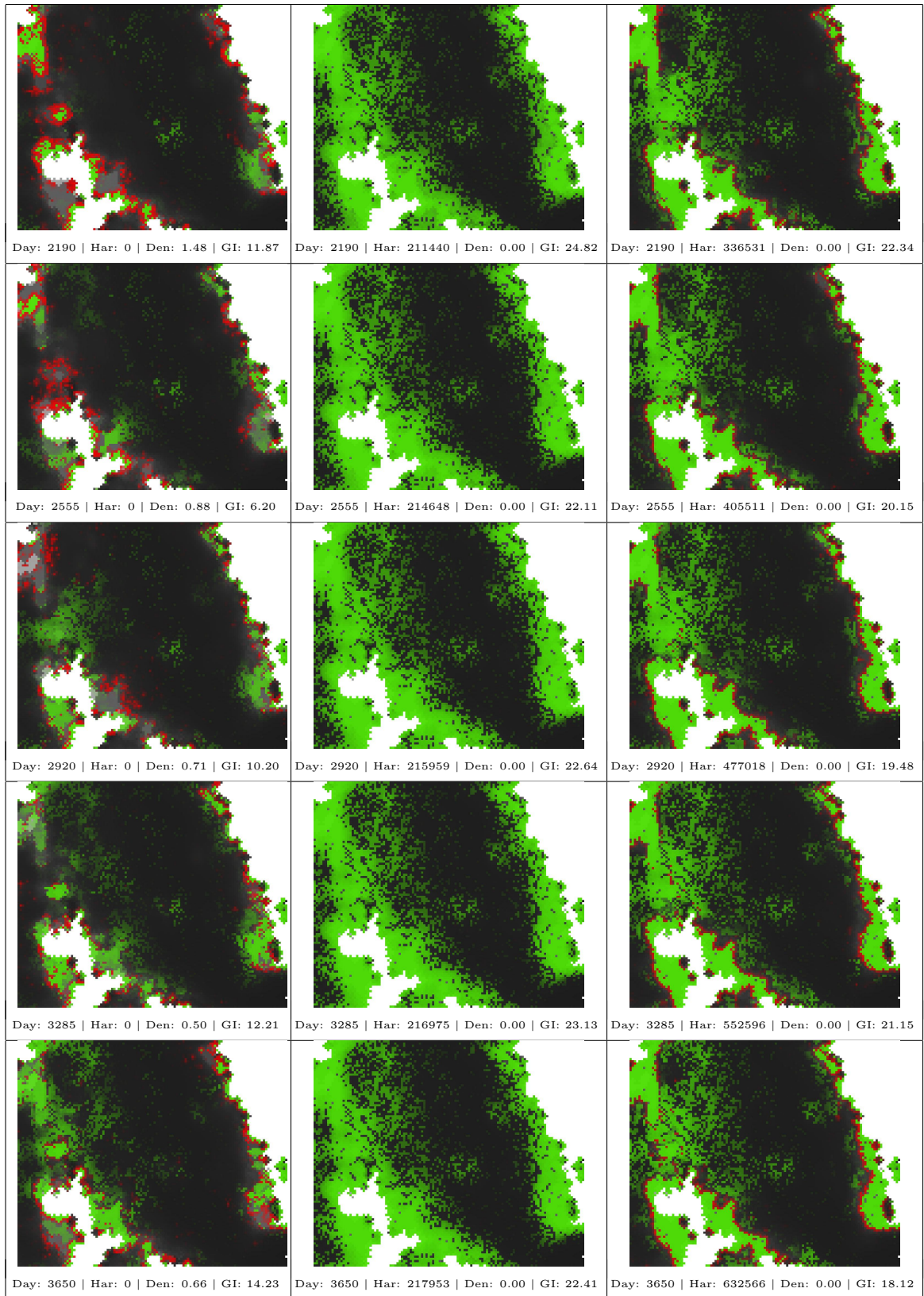
**Figure 25:** Great Wass: This graphs shows the modulations of *topDensity* during the course of the simulation. More explanation in the section above.

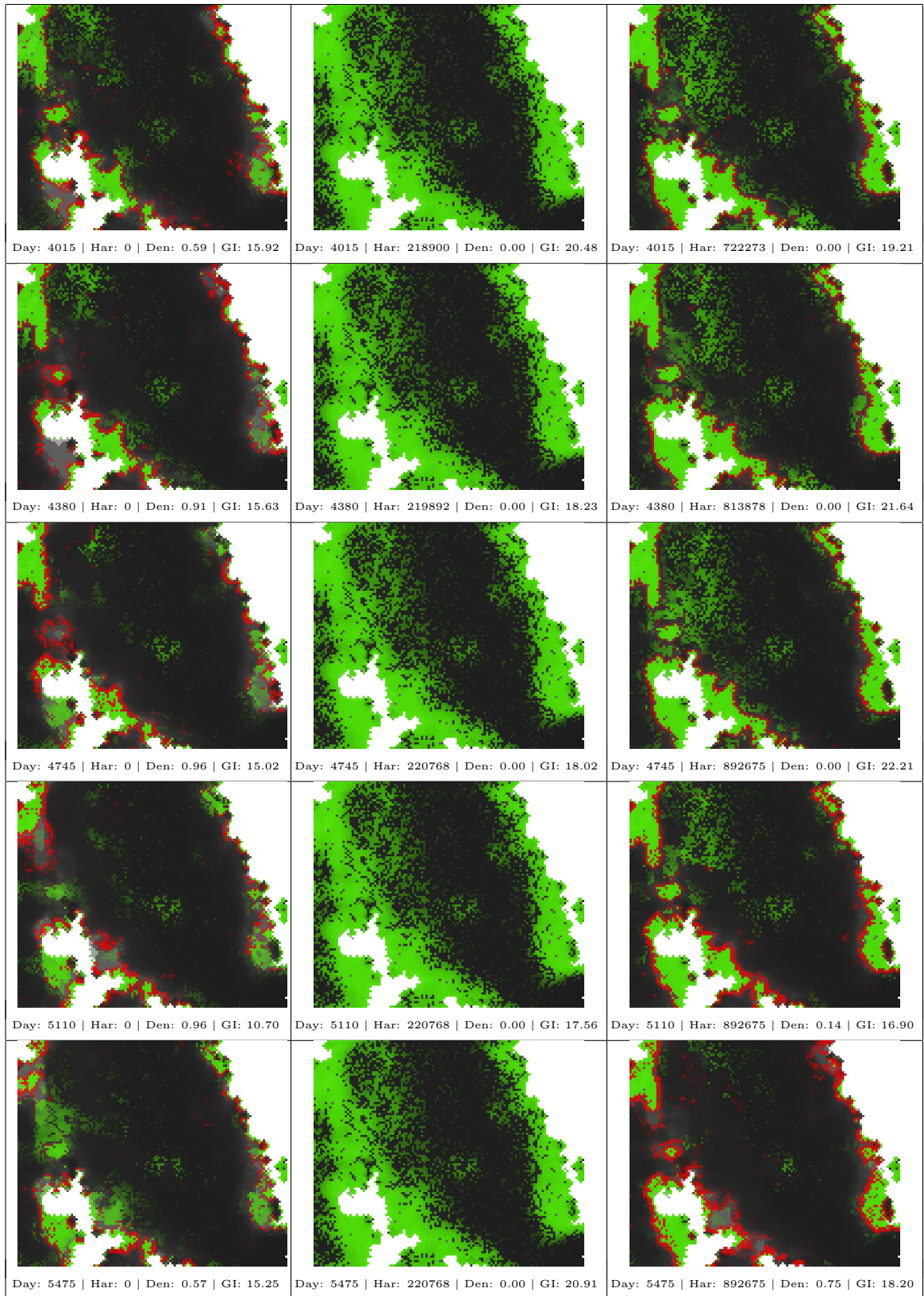


**Figure 26:** Great Wass: This graphs shows the modulations of  $topGI$  during the course of the simulation. More explanation in the section above.

**Figure 27:** Great Wass: Snapshots. (Following pages) These snapshots are presented in triptych form as described above. They capture the state of the model, over a multi-year period as labeled in units of days, under each of the three modeled conditions: (1) no harvesting, (2) standard harvesting, and (3) circular harvesting.





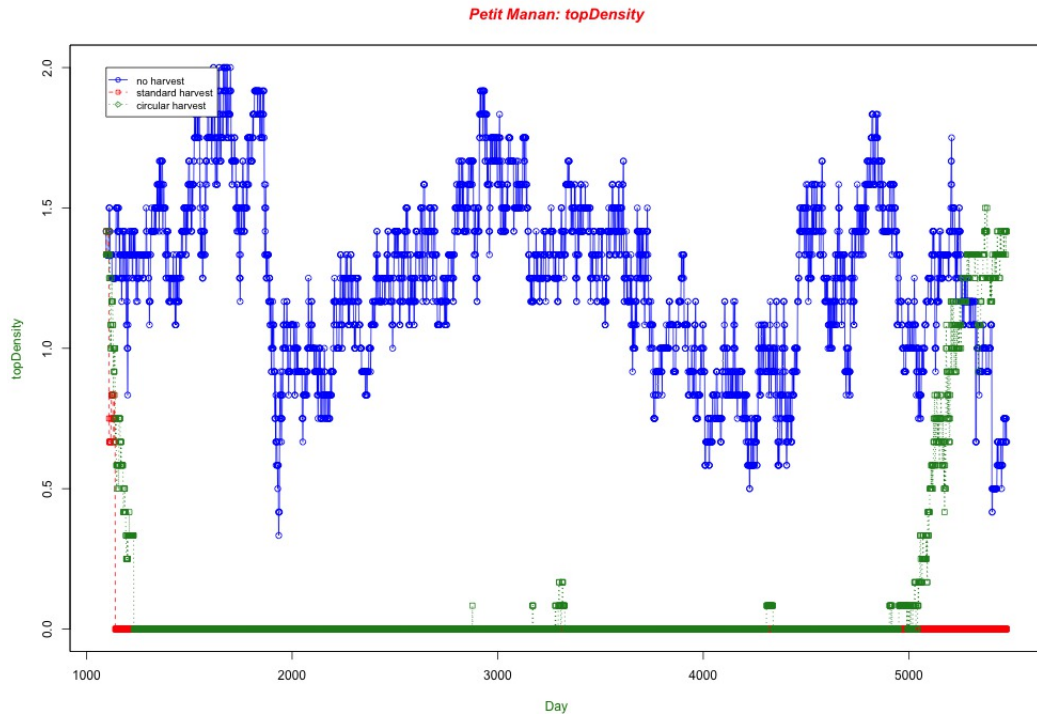


## 6.9 PETIT MANAN

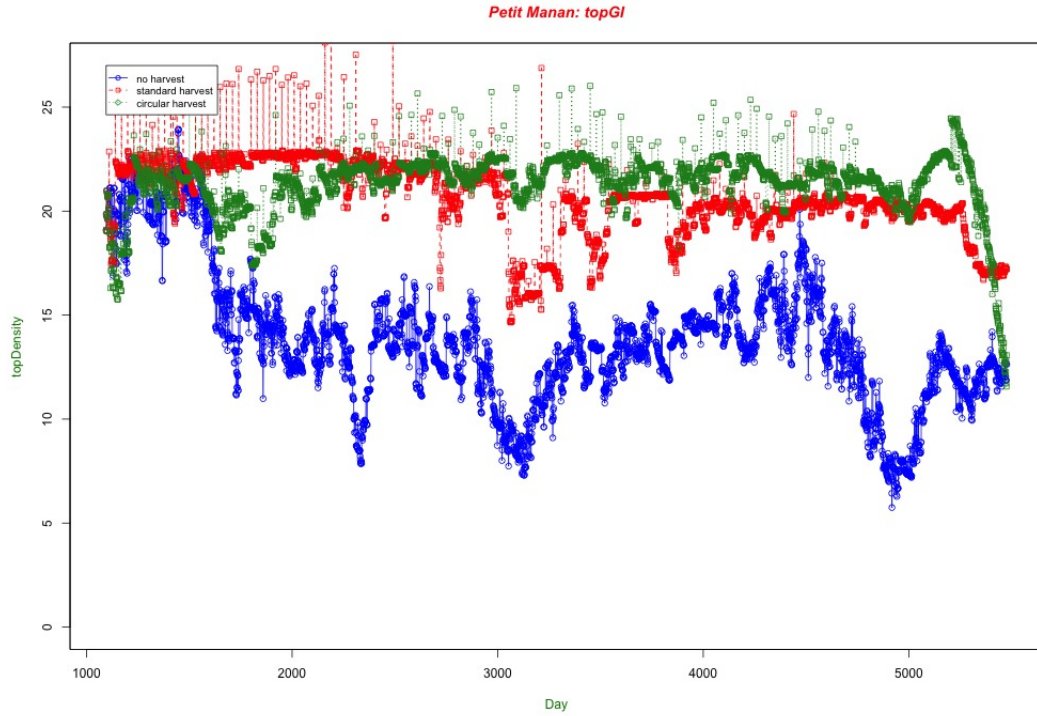
The Petit Manan site has a unique set of "bumps" which engender feedlines at varying depths. This site is smaller than the previous three sites. The relative size of a site can be intuited by the resolution of the cells. The cell size is consistent across all simulations: approximately  $20m^2$ .

All the same expected trends are exhibited at this site. The circular-harvesting condition affords the healthiest urchin population by far, as can be seen in the values of  $topGI$ . Once all harvesting ceases (Day 4745), the simulation shows that the site which underwent ten years of circular harvesting is well poised to quickly dominate the site. It dominates in terms of urchin barren area and  $topDensity$

### 6.9.1 METRICS $TOPDENSITY$ AND $TOPGI$

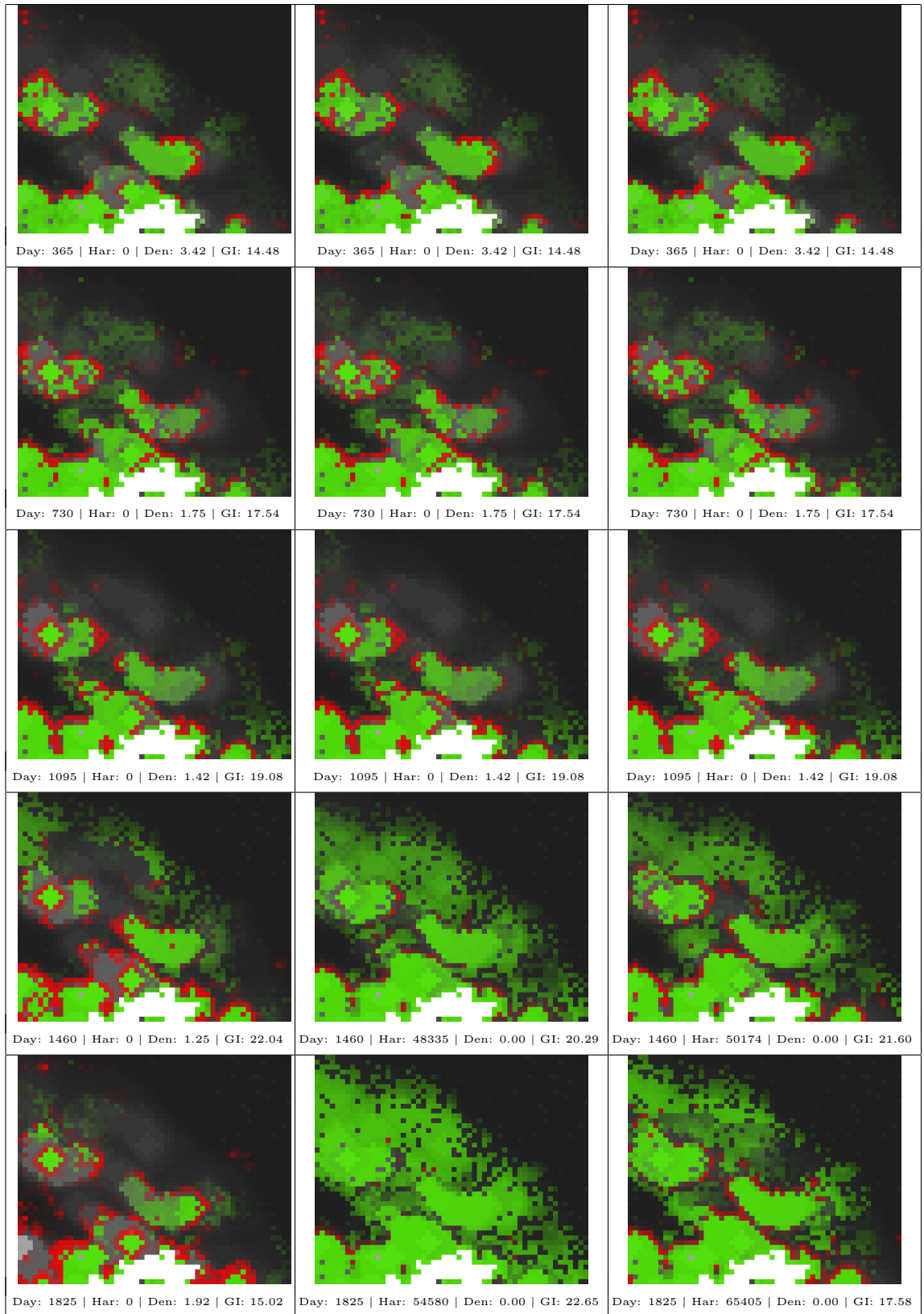


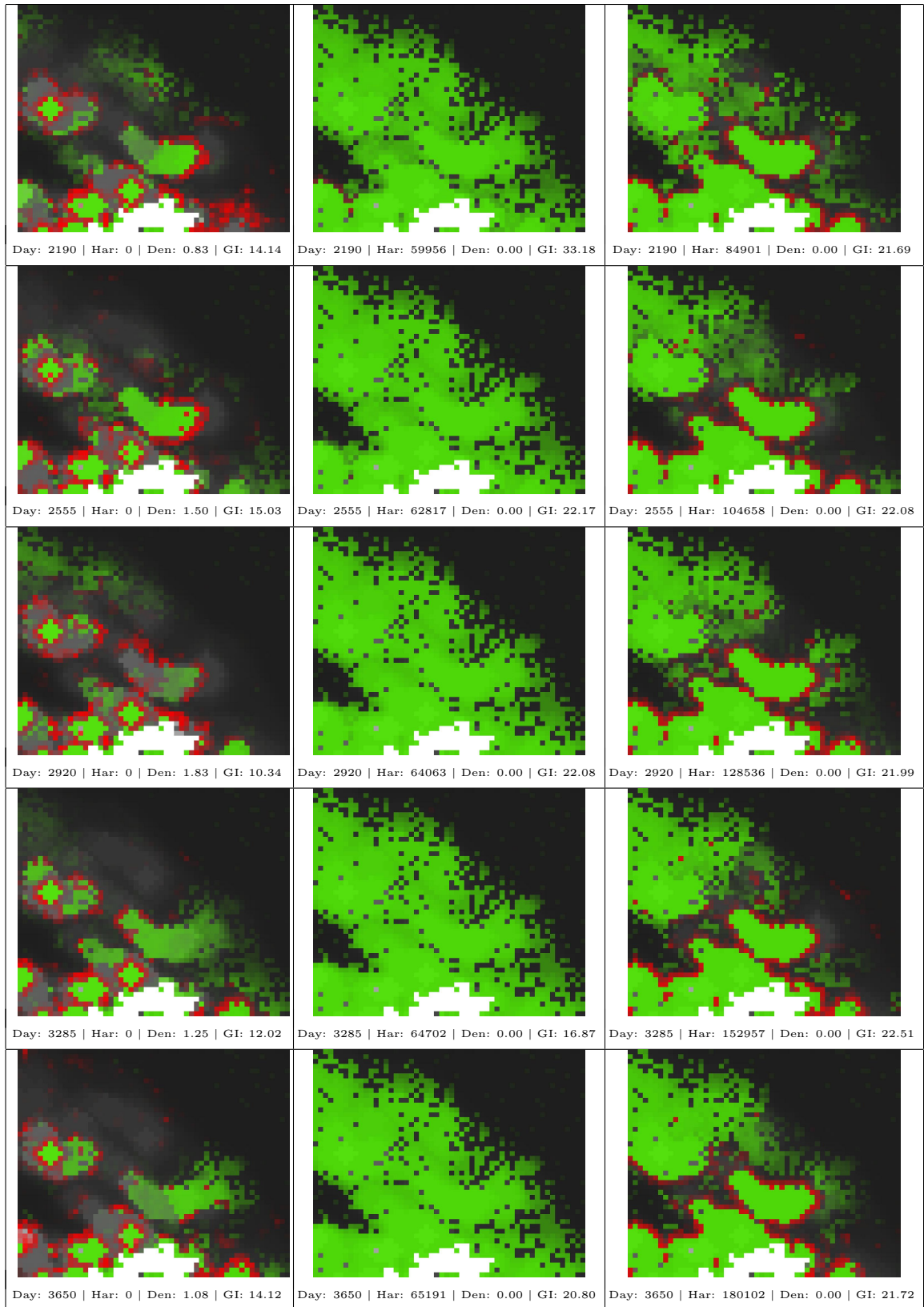
**Figure 28:** Petit Manan: This graphs shows the modulations of  $topDensity$  during the course of the simulation. More explanation in the section above.

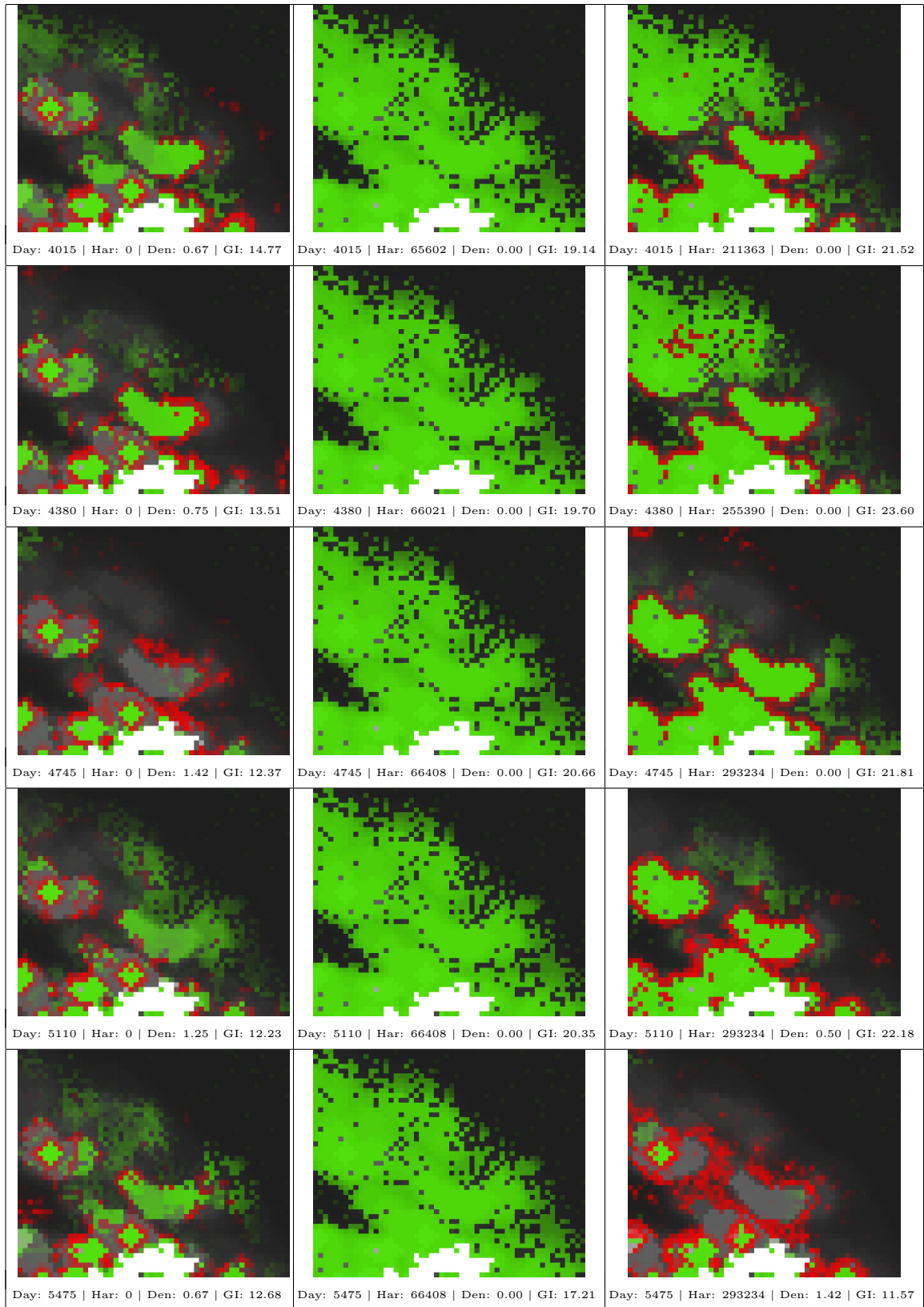


**Figure 29:** Petit Manan: This graphs shows the modulations of  $topGI$  during the course of the simulation. More explanation in the section above.

**Figure 30:** Petit Manan: Snapshots. (Following pages) These snapshots are presented in triptych form as described above. They capture the state of the model, over a multi-year period as labeled in units of days, under each of the three modeled conditions: (1) no harvesting, (2) standard harvesting, and (3) circular harvesting.





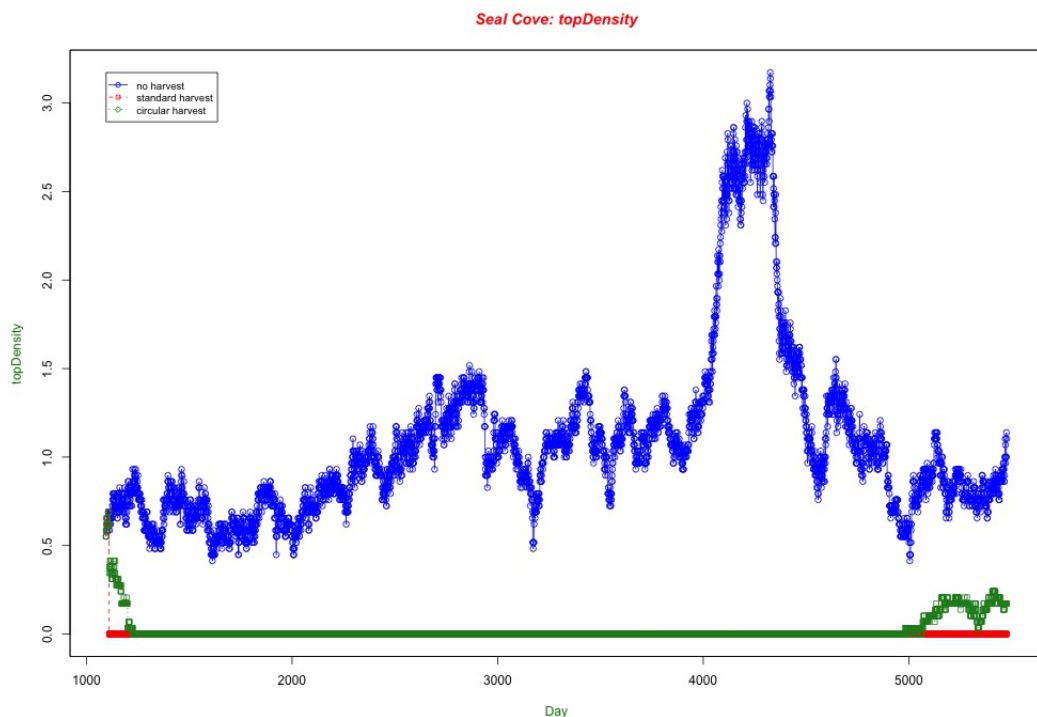


## 6.10 SEAL COVE

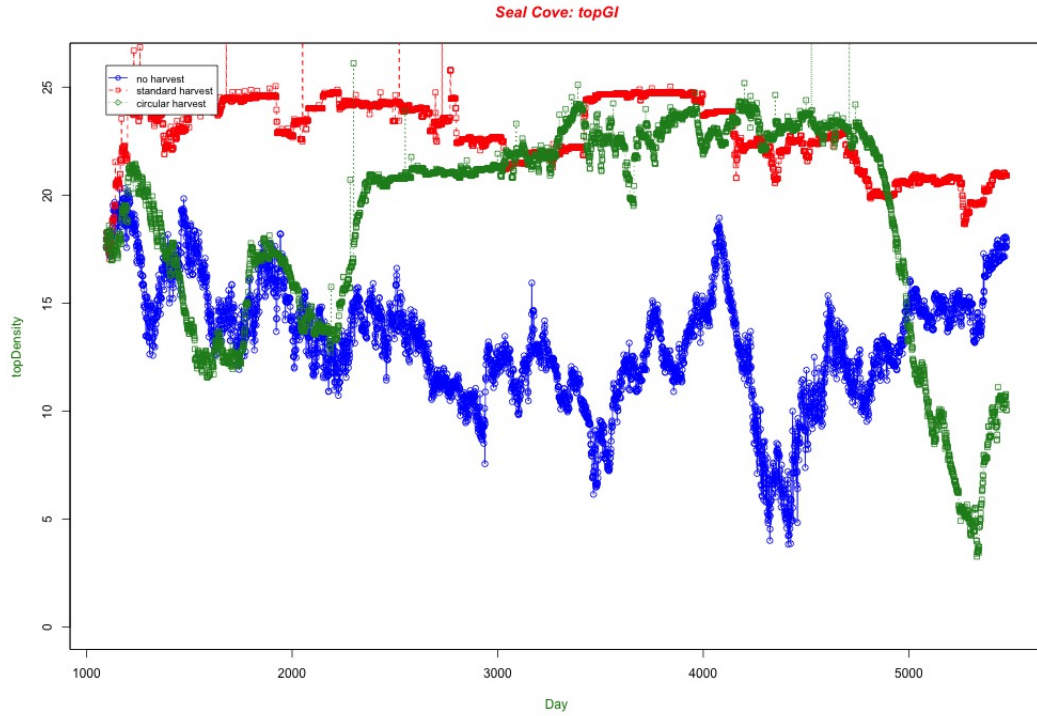
Seal Cove is a relatively small site with only a few topological features. It is unique in that it has lots of very shallow area where urchins have difficulty holding on and the seaweed grows very fast. The urchins tend to gather at its edge where a more propitious balance exists between having a thriving food source, and a food source that grows too quickly.

For the most part this site exhibits all the same expected trends as other sites. While circular harvesting was occurring, this condition fostered the healthiest (in terms of  $topGI$ ) and most robust urchin population, where its robustness is qualified by the persistence of feedlines under the circular-harvesting condition.

### 6.10.1 METRICS $TOPDENSITY$ AND $TOPGI$

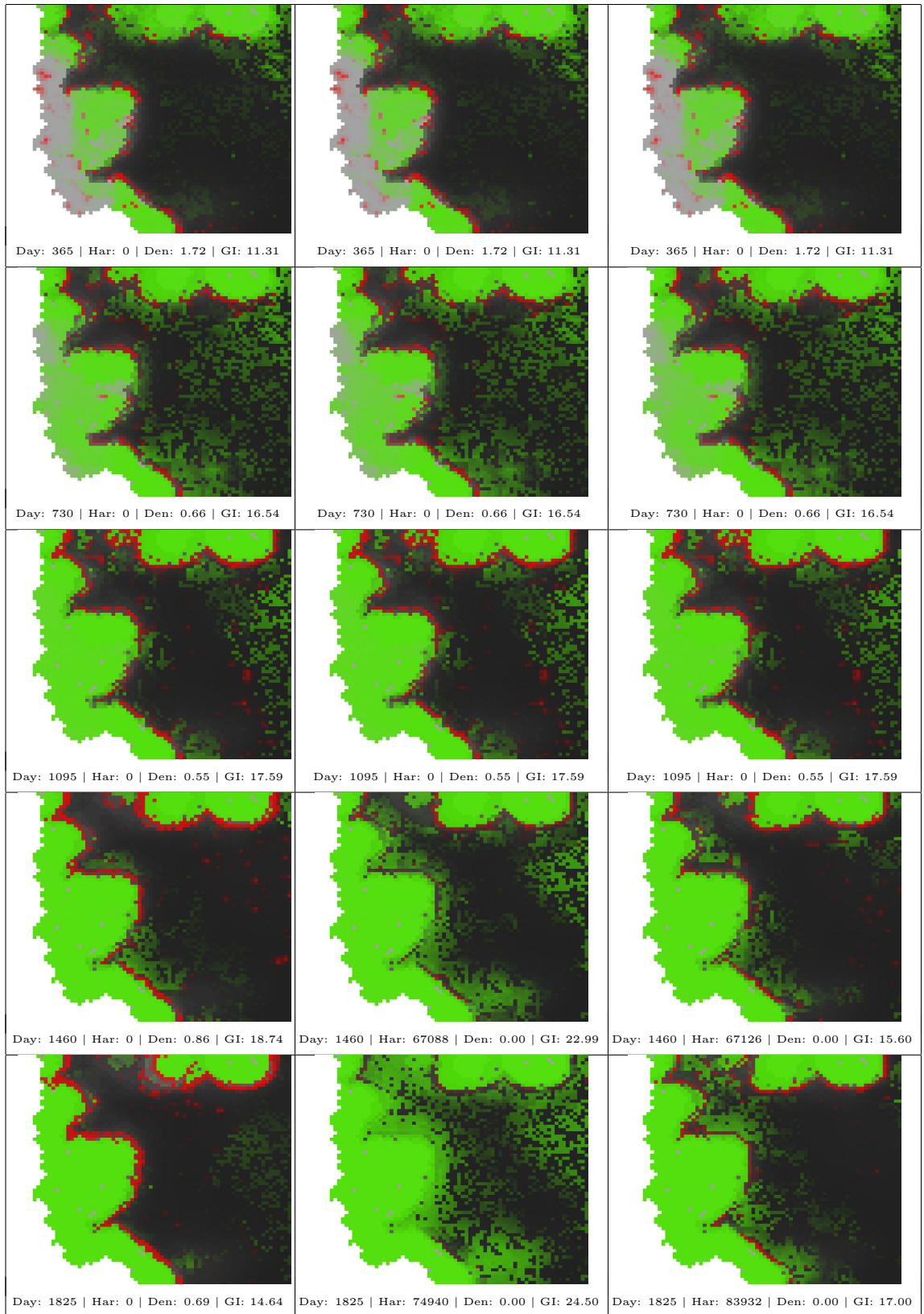


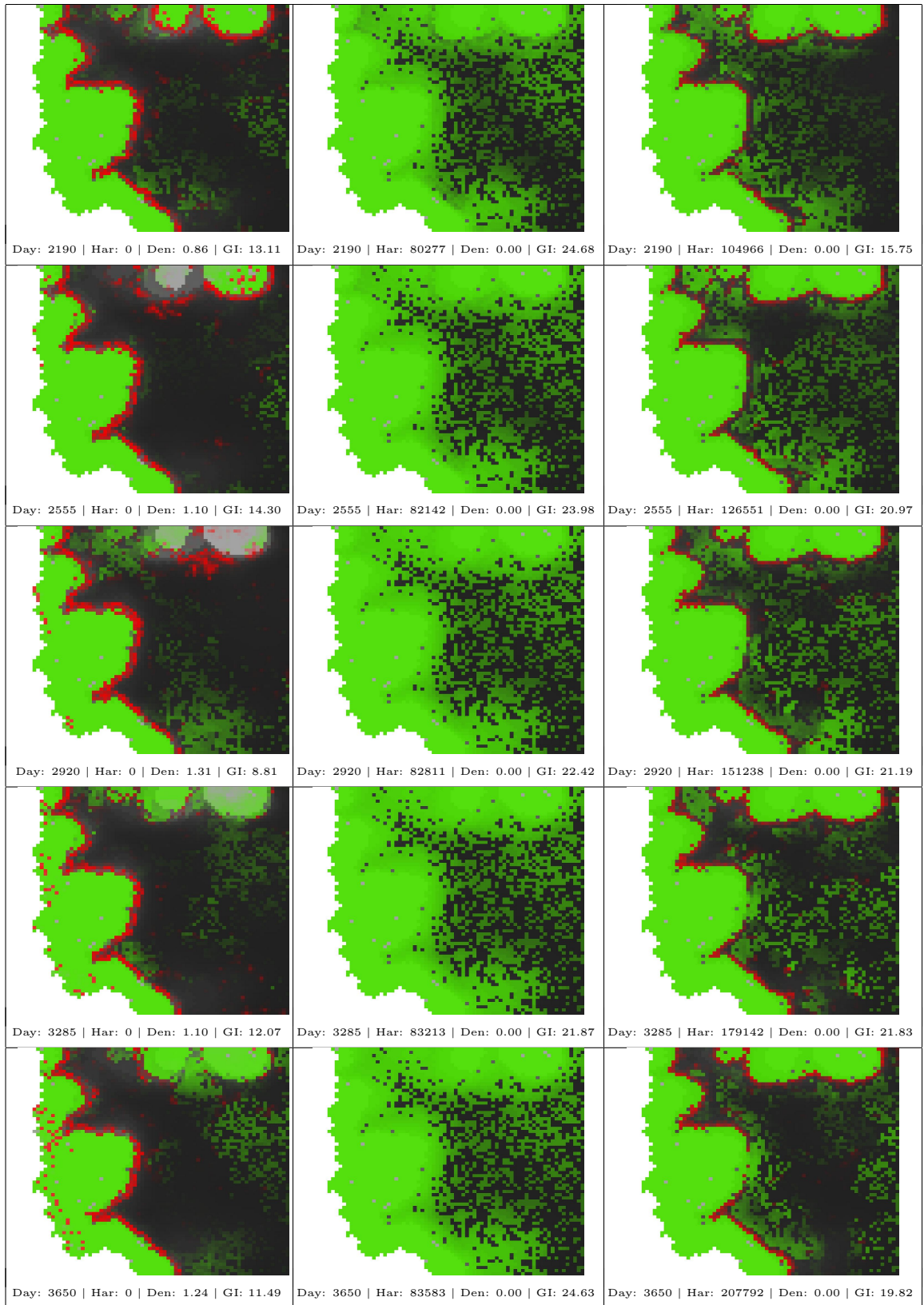
**Figure 31:** Seal Cove: This graphs shows the modulations of  $topDensity$  during the course of the simulation. More explanation in the section above.

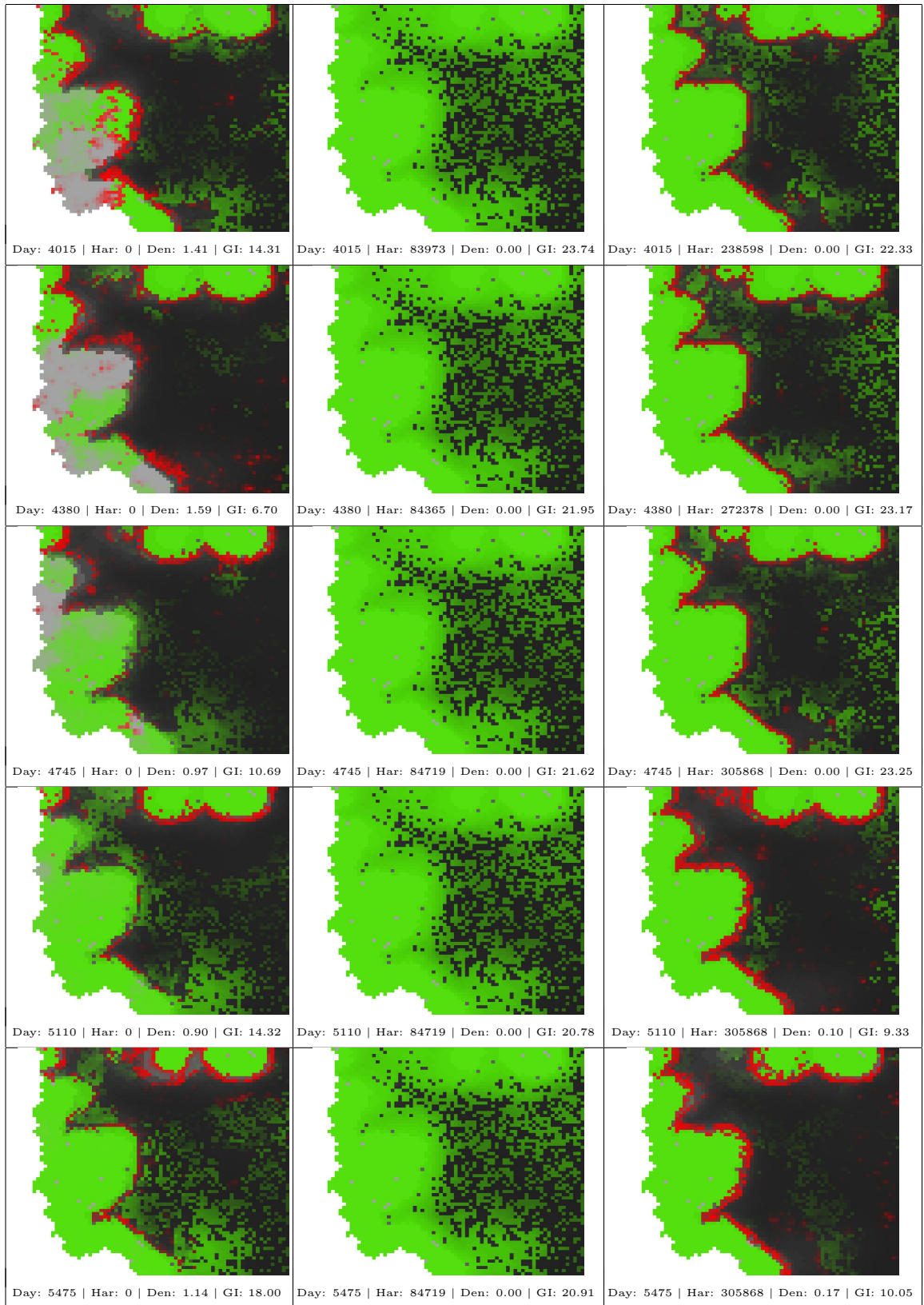


**Figure 32:** Seal Cove: This graphs shows the modulations of *topGI* during the course of the simulation. More explanation in the section above.

**Figure 33:** Seal Cove: Snapshots. (Following pages) These snapshots are presented in triptych form as described above. They capture the state of the model, over a multi-year period as labeled in units of days, under each of the three modeled conditions: (1) no harvesting, (2) standard harvesting, and (3) circular harvesting.







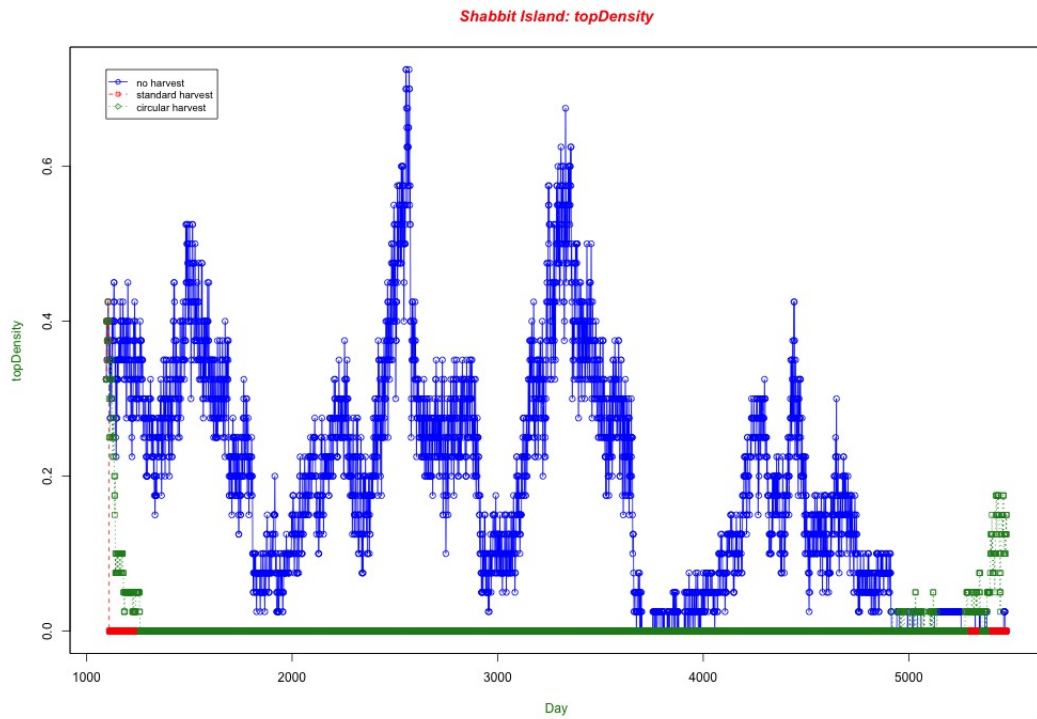
## 6.11 SHABBIT ISLAND

The Shabbit Island site combines some features of Black Ledge and Seal Cove, such as the areas of less depth at Black Ledge, and the large varied shallow regions of Seal Cove.

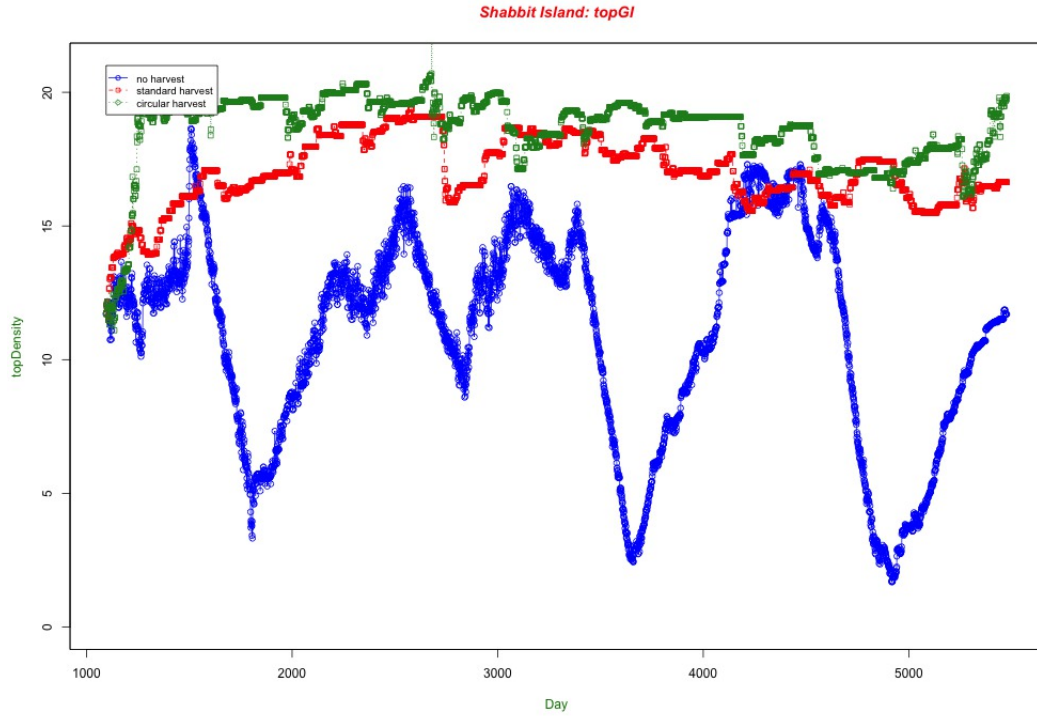
This site exhibits the same expected trends as other sites. The circular-harvesting condition creates a situation where there is always some small region with a stable and healthy urchin population. Neither of the other two conditions allowed for healthy urchin populations, where "healthy" indicates both a consistently favorable *topGI* (perhaps above 15) and some visually identifiable feedlines or urchin concentrations. As with other sites, this site yielded more than 400% more urchins under circular harvesting than standard harvesting over the same ten-year period.

Each of these comparisons between the two fishing methods are made stronger by the fact harvesters performing circular harvesting are modeled as "perfect fishermen," not leaving any behind. Even though the standard harvesters randomly leave many urchins untouched, their sites become rapidly devoid of urchin life. The value of *topDensity* never recovers for the standard-harvesting condition, but it recovers well for the circular-harvesting condition.

### 6.11.1 METRICS *TOPDENSITY* AND *TOPGI*

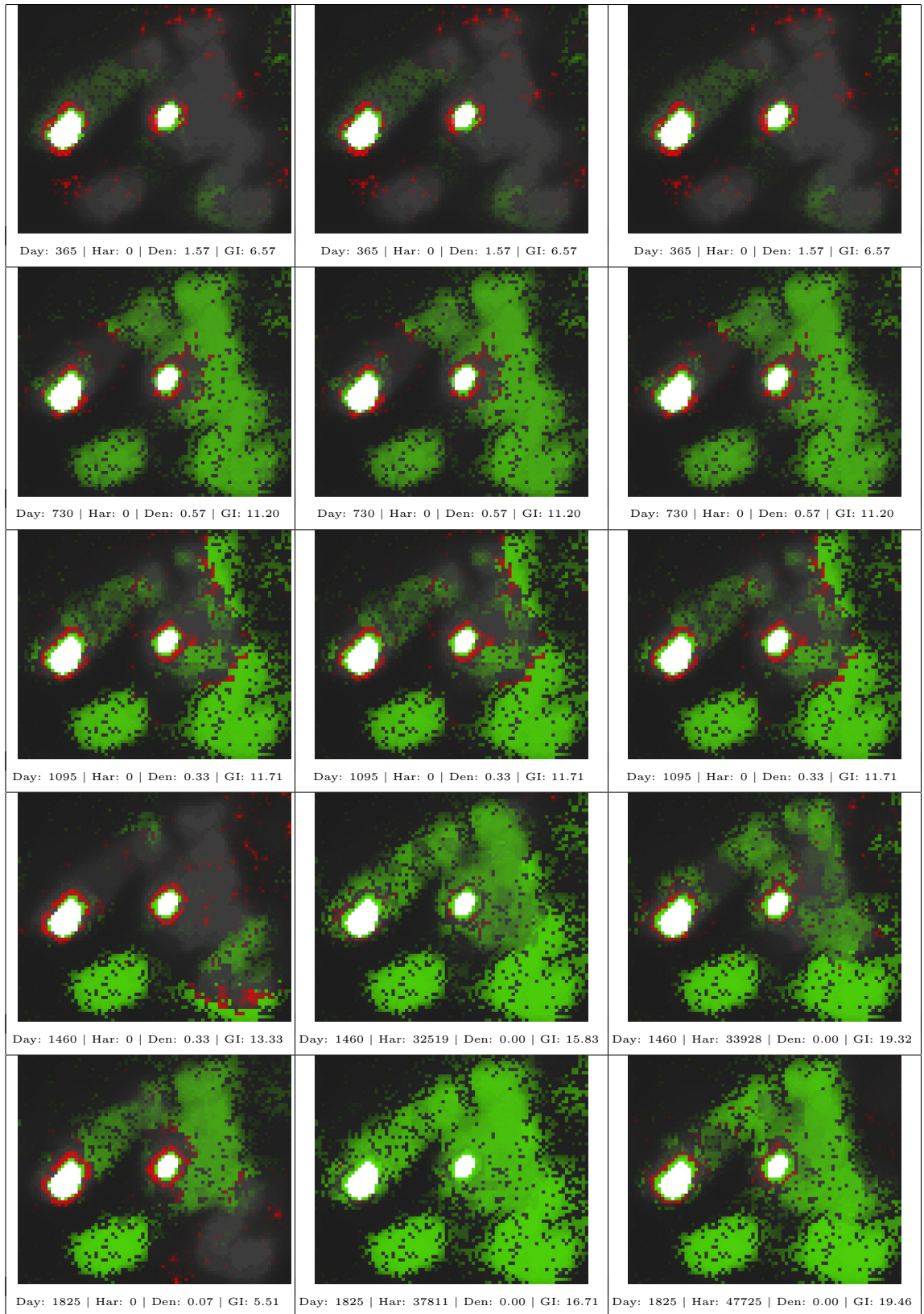


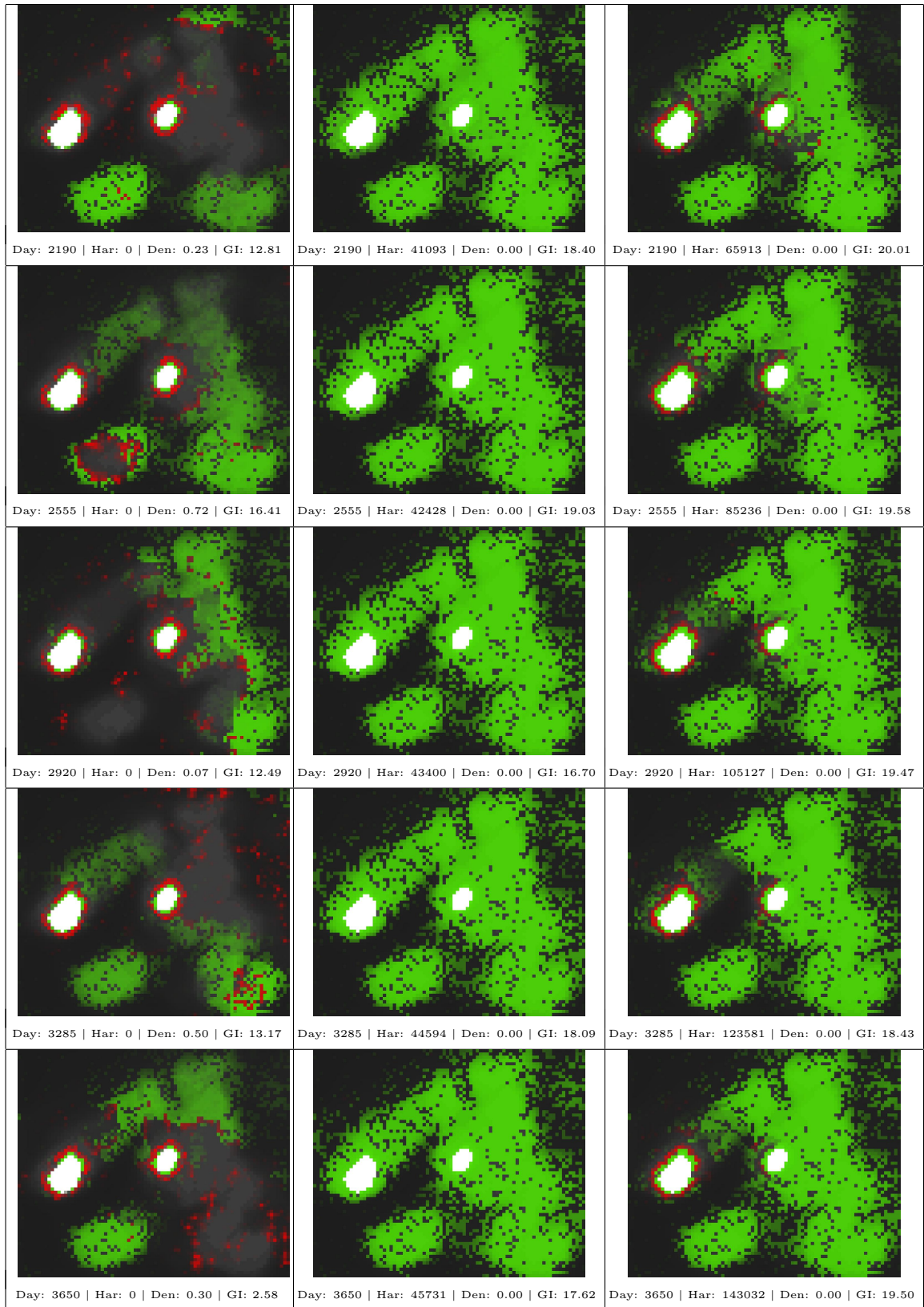
**Figure 34:** Shabbit Island: This graphs shows the modulations of *topDensity* during the course of the simulation. More explanation in the section above.

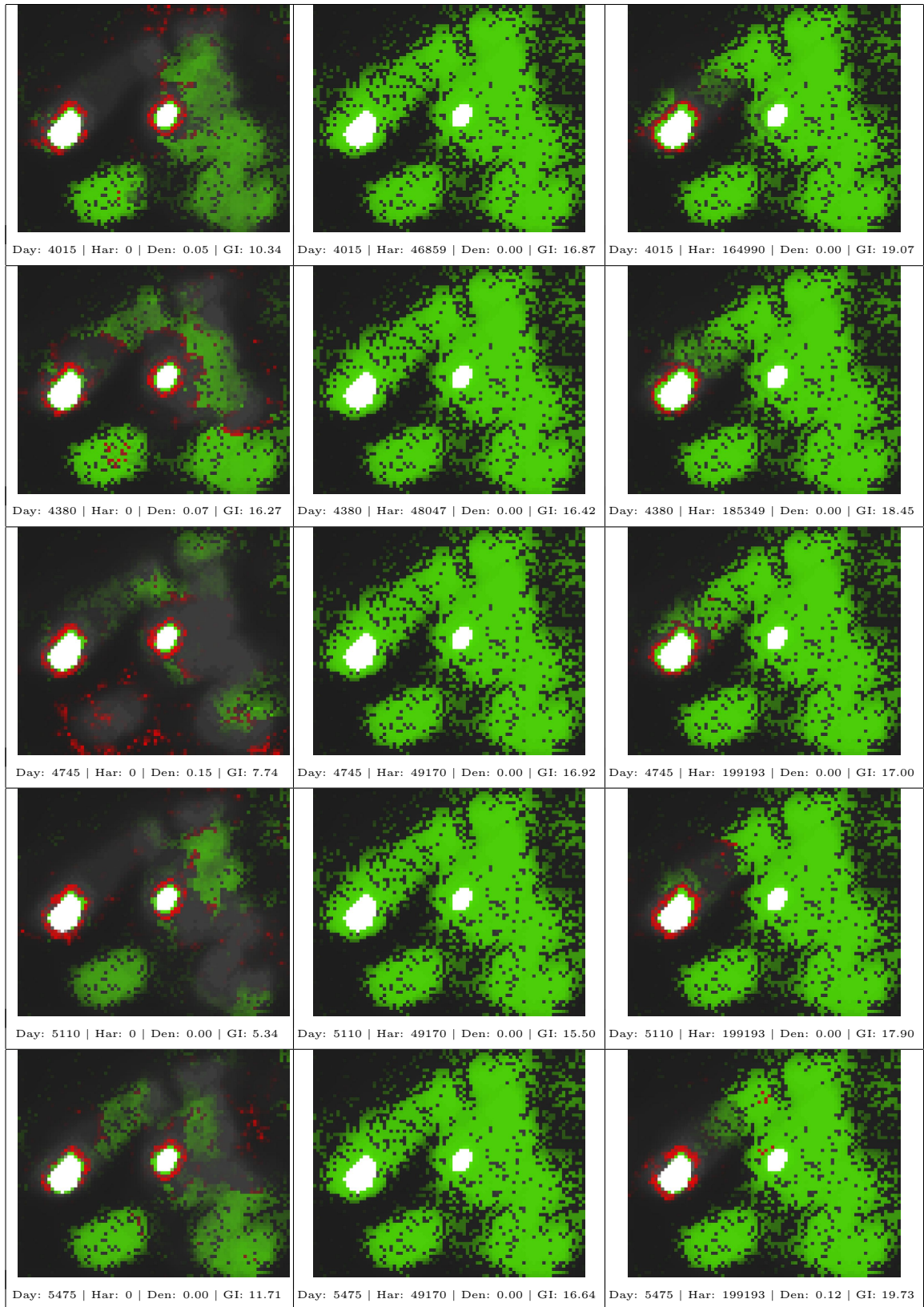


**Figure 35:** Shabbit Island: This graphs shows the modulations of  $topGI$  during the course of the simulation. More explanation in the section above.

**Figure 36:** Shabbit Island: Snapshots. (Following pages) These snapshots are presented in triptych form as described above. They capture the state of the model, over a multi-year period as labeled in units of days, under each of the three modeled conditions: (1) no harvesting, (2) standard harvesting, and (3) circular harvesting.







## 6.12 CONCLUSION

A clear set of trends was expected and then observed at each site. These trends were understood only via the simultaneous consideration of three forms of output:

1. *topDensity*
2. *topGI*
3. Snapshots of the model state in triptych form

The no-harvesting condition was revealed to be incongruent with a healthy and robust urchin population. While such populations will create large urchin barrens, they will live in a state of constant low-level starvation.

The standard-harvesting condition appears to be a guaranteed way to flip any site to the kelp dominated state. The few urchins left behind will have high gonad indices, but will be dispersed and difficult to find. This condition is wholly incompatible with any strategy for fishery sustainability.

The circular-harvesting condition afforded a healthy, robust, stable urchin population in almost all cases. This harvesting method appears to be sustainable and produces a healthier outcome for the urchins than even the no-harvesting condition. It is hoped that a more realistic harvesting solution can be found – one that shares two key features of circular harvesting:

1. Multiple quick-succession harvesting events leave numerous well-distributed spots untouched
2. Harvested zones are always in close proximity to some untouched region

If found, such a harvesting method could be tested in this model.

## 7. SENSITIVITY ANALYSIS

The purpose of sensitivity analysis is to study output variation as a function of input variation, i.e. if the inputs are altered by some small amount, are the outputs altered by a small, or by a large amount? The larger the output delta, the more *sensitive* the model is deemed to be. A highly sensitive model could be considered chaotic, which may cast doubt on any results garnered from its use.

The model was subjected to sensitivity analysis by executing numerous runs on different sets of inputs. The outputs from these runs were collected and analyzed. Relationships between the inputs and output variables were shown in the analysis. This analysis was performed for the non-fishing condition because this condition is most relevant to the validity of the biophysics of the model.

### 7.1 INPUT PARAMETERS

The inputs in this case are the parameters that govern model dynamics. These model parameters, the input variables  $X$ , are (see parameter descriptions in the appendices):

1. Seaweed\_maxBiomassDensity
2. Seaweed\_probRecoverPerMin
3. Seaweed\_timeToMaxBiomass
4. Urchins\_K
5. Urchins\_herbivoryRate
6. Urchins\_lowGonadIndex
7. Urchins\_maxGonadChangePerMin
8. Urchins\_maxGonadIndex
9. Urchins\_maxPredationPerMin
10. Urchins\_maxPredationPerMin\_juv
11. Urchins\_maxSize
12. Urchins\_maxTotalNumDensity
13. Urchins\_minGonadIndex

14. Urchins\_mortalityRatePerMin
15. Urchins\_predationRatePerMin
16. Urchins\_predationRatePerMin\_juv
17. Urchins\_recruitmentRate
18. World\_byCatchLoss"

This large set of inputs presents a problem known as "The curse of dimensionality." Exploring the model's sensitivity to these values implies searching a 18-dimensional space. A Monte-Carlo approach was taken. Numerous runs of the model were performed, each with a different value from 18-dimensional parameter space. The parameter space was covered by thousands of simulations. This coverage was deemed sufficiently dense because of the low incidence of local minima/maxima.

## 7.2 OUTPUT VARIABLES

The output of the model is studied in terms of four metrics, or response variables ( $Y$ ):

1. Urchins\_biomass (total urchin biomass)
2. Seaweed\_biomass (total seaweed biomass)
3. topDensity (urchin density in top 1% of cells)
4. topGI (GI in top 1% of cells)

Each of the above variables is measured in the model at each timestep. In order to ensure that this analysis would study the overall operation of the model and not be at the whim of the stochastic processes which underly some features, each of these was measured by recording the values and averaging them over a hundred-day period at the end of operation.

The possible values of these outputs represent a 4-dimensional output space. This fact will be referenced later.

### 7.3 PERTURBATION THEN SIMULATION

Each parameter in the model has both an assigned "best" value and a reasonable range, all of which come from the literature. There details are in the appendices on each of these parameters. For instance:

PARAMETER	ESTIMATE	RANGE
herbivoryRate	$0.00005 \text{ min}^{-1}$	$2.3 \times 10^{-6} - 7.7 \times 10^{-5}$

**herbivoryRate** : The maximum amount of seaweed, in kilograms, that one kilogram of urchins are able to consume per min. As this number represents a maximum, the actual herbivory will be lessened as needed (e.g. on a yearly cycle, peaking in warmer months).

Larson, Vadas, and Keser studied urchins between 25 and 30 mm in diameter. The urchins exhibited the highest preference for *S. longicruris* and the lowest for *A. cribrosum*. Presented with only *S. longicruris* the urchins consumed 52.9 mg per urchin per hour. Presented with only *A. cribrosum* they consumed 16.3 mg per urchin per hour.

When multiple species are available the urchins consume considerably less: 19.0 mg per urchin per hour for *S. longicruris* and only 1.6 mg per urchin per hour for *A. cribrosum*.

For an urchin radius of 0.014 m, under the spherical approximation, urchin mass  $m_u$  can be found from diameter and its density. The mass being considered here is the mass of an urchin in its environment, including the water contained within its body. The density used to find this number is approximately  $1000 \frac{\text{kg}}{\text{m}^3}$  [Vadas (pers. com.), 2012]:

$$m_u = \text{density} \cdot \text{volume} = 1000 \frac{kg}{m^3} \cdot \frac{4}{3} \pi (.014m)^3 \approx 0.0115 \frac{kg}{urchin}$$

or alternatively:  $87 \frac{urchins}{kg}$

The high and low estimates for per urchin per hour values found by Larson et al. are converted to  $\frac{kg}{kg \cdot min} \rightarrow \frac{1}{min}$ :

$$52.9 \frac{mg}{urchin \cdot hr} \times .000001 \frac{kg}{mg} \times 87 \frac{urchins}{kg} \times \frac{1}{60} \frac{hr}{min} \approx 7.7 \times 10^{-5} min^{-1}$$

$$1.6 \frac{mg}{urchin \cdot hr} \approx 2.3 \times 10^{-6} min^{-1}$$

This sensitivity analysis required numerous runs of the model under different sets of reasonable parameter values. These runs were performed by first perturbing each input parameter within its reasonable range, and then running the model for a fifteen year period, as was done for the Results section. The same random seed (as for the Results section) was used so that differences between the runs would not be purely from the semi-random functions used to model stochastic processes.

The perturbation of each parameter entailed drawing from a normal distribution, within the reasonable range as derived from the literature. The mean of each distribution is equal to the theoretical "best" value, and the variance is set such that the reasonable range covers a region equal to double the full width at half maximum, i.e.  $FWHM = 2.355 * sd$ .

Once the parameter values are set, a fifteen-year simulation is performed. For each of the eight sites, approximately 1300 simulations were executed, for a total of 10,575 simulations in all. In all, 158,625 years were simulated, under 10,575 different sets of conditions, at eight locations in Maine, for the purpose of testing model sensitivity.

## 7.4 SENSITIVITY: PARAMETER DELTA VS. OUTPUT DELTA

The results of the sensitivity analysis were scaled and then plotted. The scaling of each input and output distribution was done such that each has a mean of 0 and a standard deviation of 1. This was necessary because of the arbitrary and unrelated nature of the units involved. Input units included measures such as *days*, and *individual urchins/m<sup>2</sup>*, while the output units included *kg* and *G.I.*

### 7.4.1 DISTANCE IN PARAMETER / OUTPUT SPACE

Taking inspiration from Lyapunov Analysis [Cencini et al., 2010], the model's sensitivity can be seen as the relationship between how much the average perturbed model differs from the unperturbed one. The input and output values for a typical (non-perturbed) simulation were recorded for each site. The set of "best" values for the parameters represents an origin in 18-dimensional parameter space. Any perturbed point in that space can be found to have some distance to the origin. Similarly, the outputs for that typical run are considered to be an origin in 4-dimensional output space. The output of any run can be plotted in this space and a distance to the "output" origin may be calculated.

The task then becomes one of comparison between the distance in output space (*how big the effect was*) and the distance in parameter space (intuitively *how much the model was perturbed*). The average ratio between output effect and input distance was .45205, which implies that the output change was on average less than the input change. That alone is an indicator that the model is non-chaotic in parameter space. These comparisons did not yield clean linear relationships, but visualizations do indicate stability. Below is a figure for each site representing approximately 1,300 runs each. The X-axis charts the input distance (in 18-dimensional parameter space), and the Y-axis charts the output distance (in 4-dimensional output space). If the model were chaotic, the points would be distributed randomly all over the modeled region, i.e. there would be no relationship between input distance and output distance. These

figures show that the model is not chaotic. Small perturbations result in small output effects, and large perturbations result in large effects.

## Big Nash: Parameter Delta vs. Output Delta

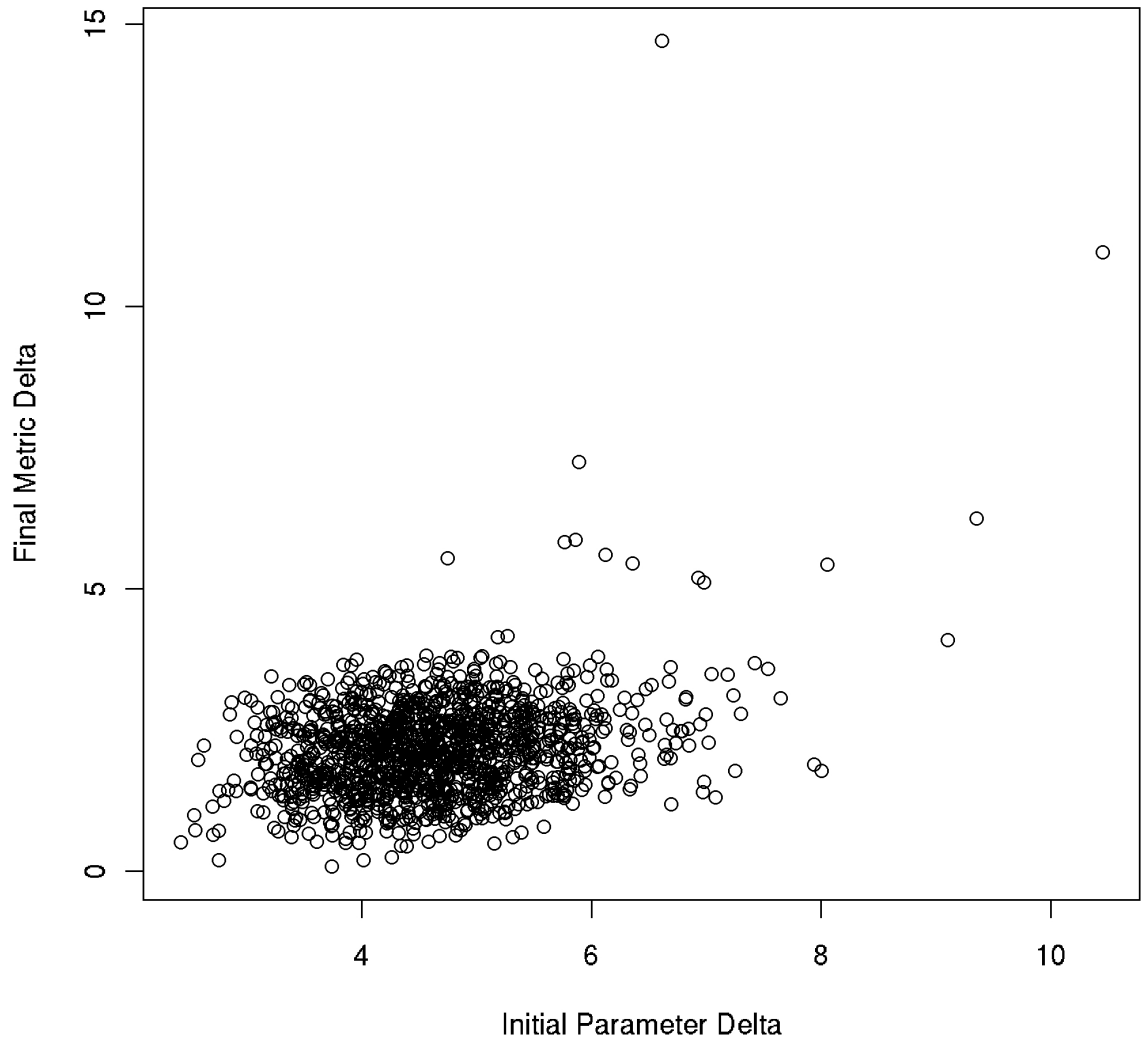


**Figure 37:** Big Nash: Parameter Delta vs. Output Delta

## Black Ledge: Parameter Delta vs. Output Delta

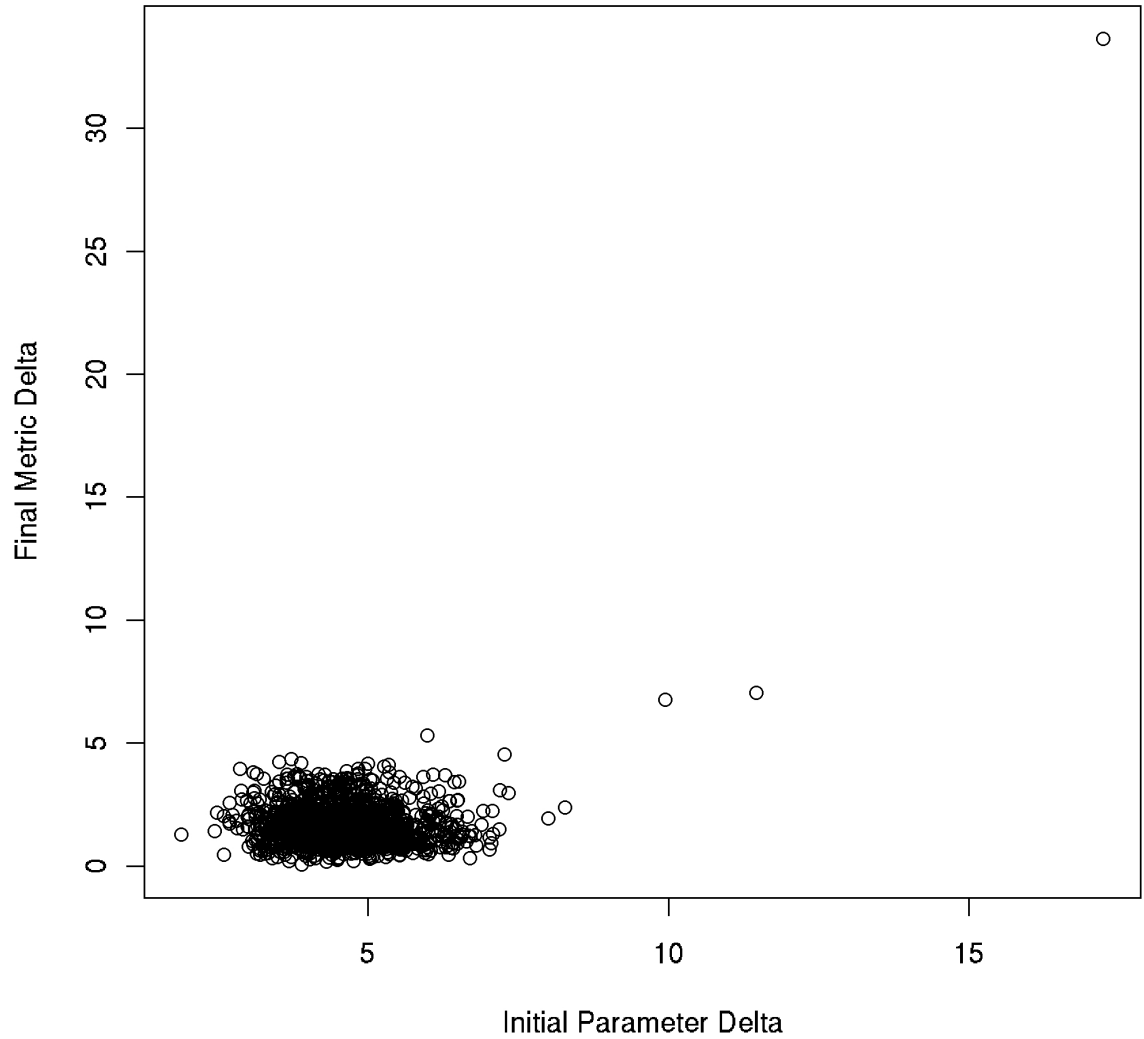


**Figure 38:** Black Ledge: Parameter Delta vs. Output Delta

## Eastern Bay: Parameter Delta vs. Output Delta

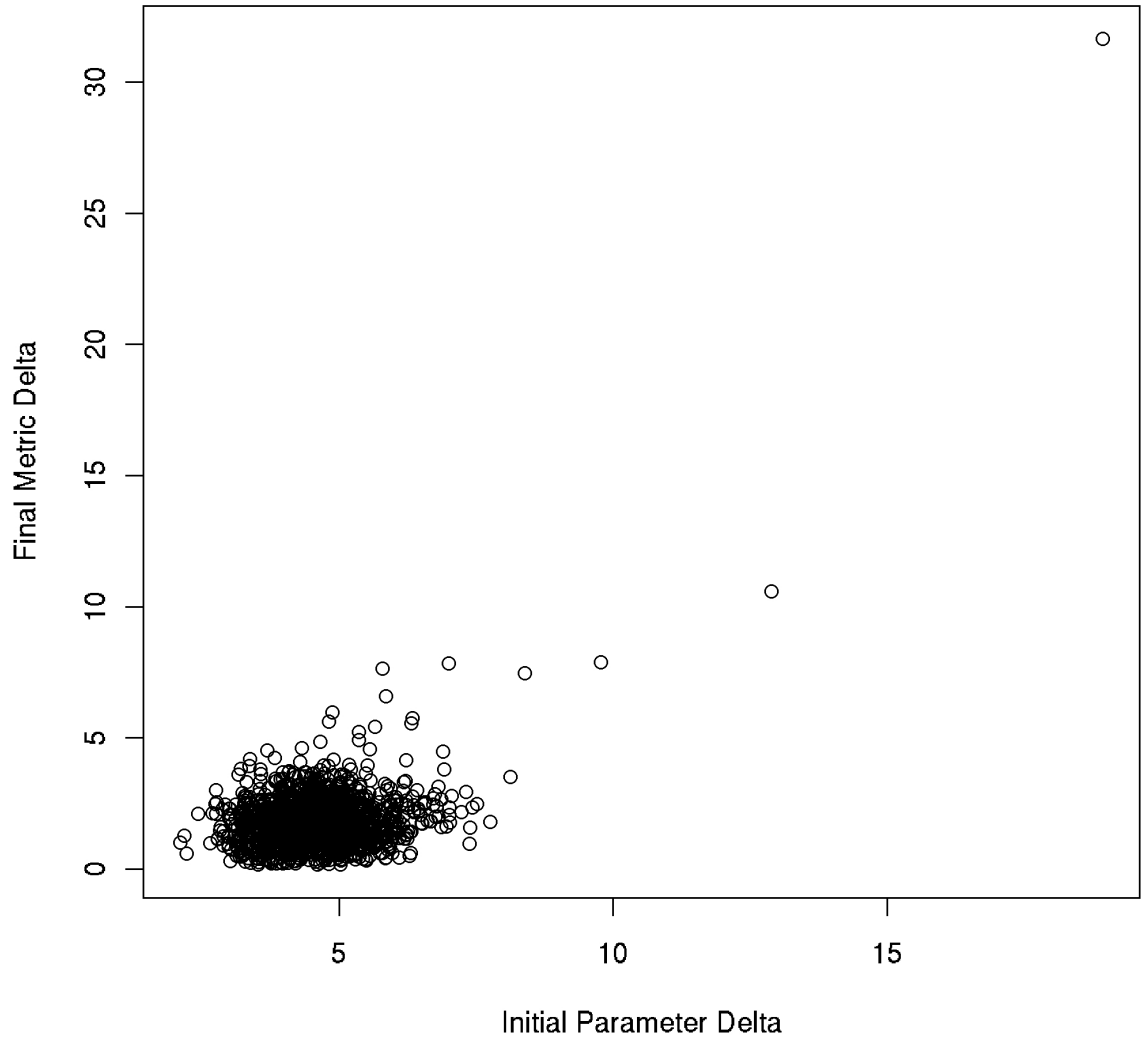
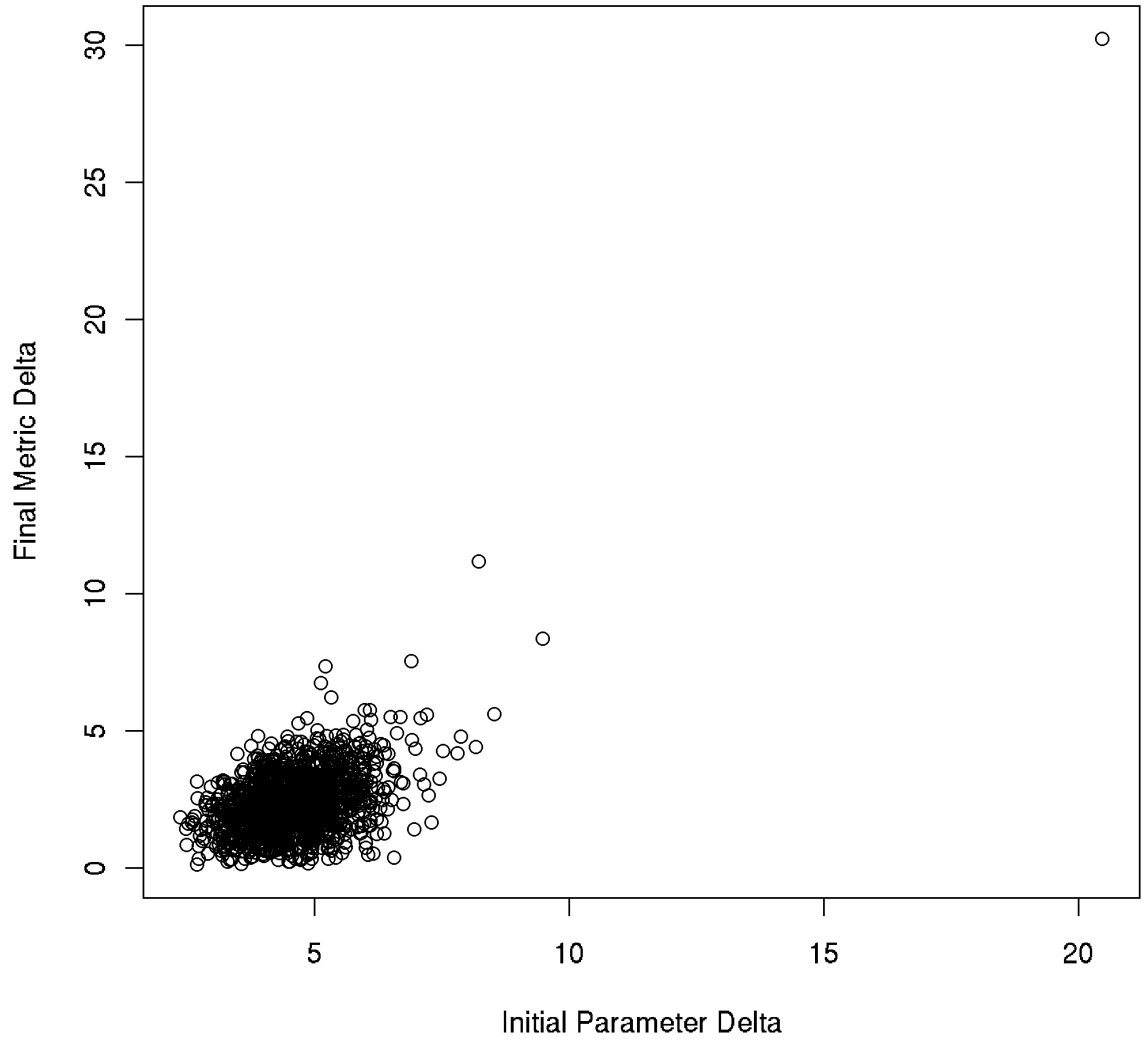


**Figure 39:** Eastern Bay: Parameter Delta vs. Output Delta

## Flint Island: Parameter Delta vs. Output Delta



## Great Wass: Parameter Delta vs. Output Delta

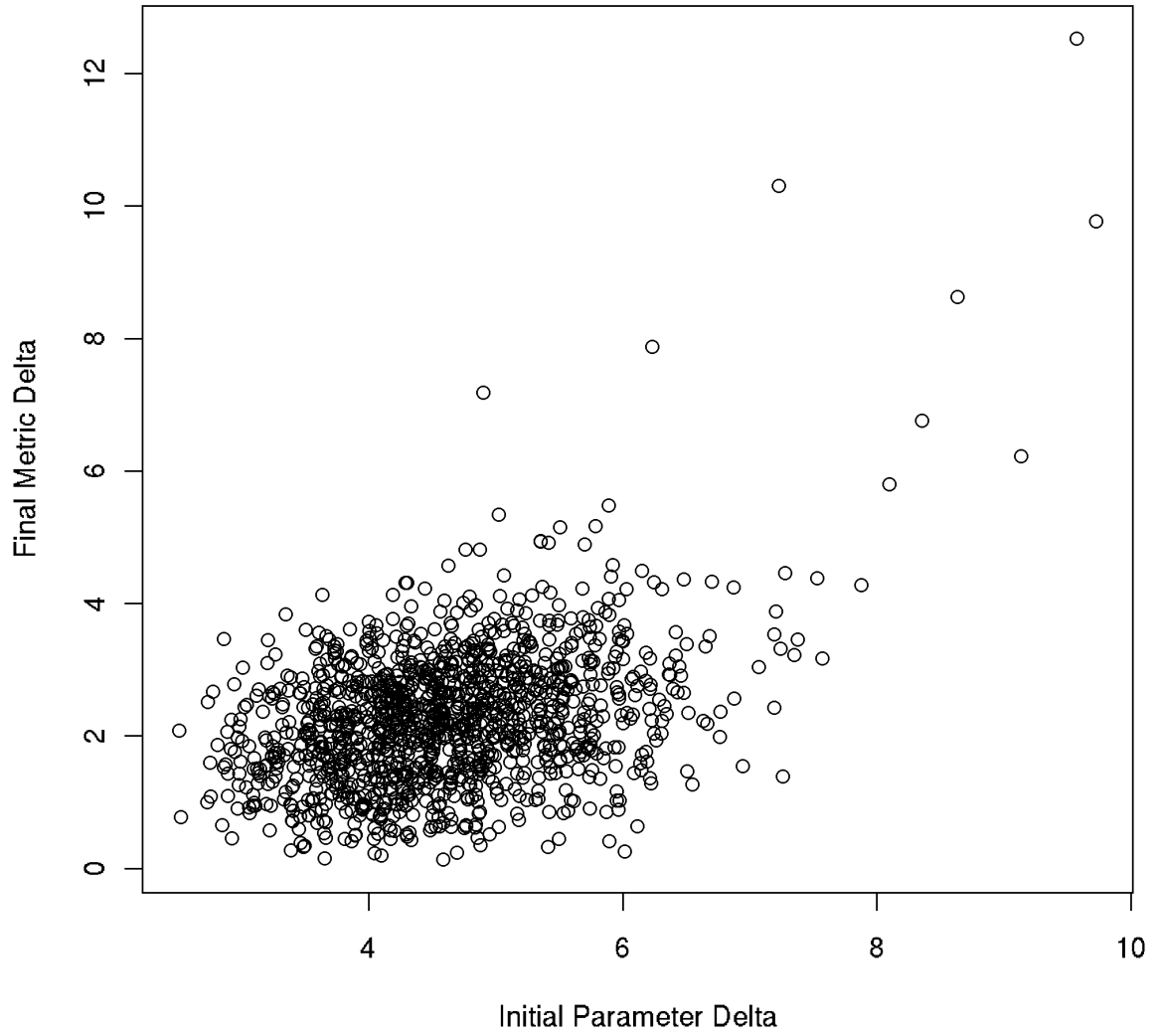


**Figure 41:** Great Wass: Parameter Delta vs. Output Delta

## Petit Manan: Parameter Delta vs. Output Delta

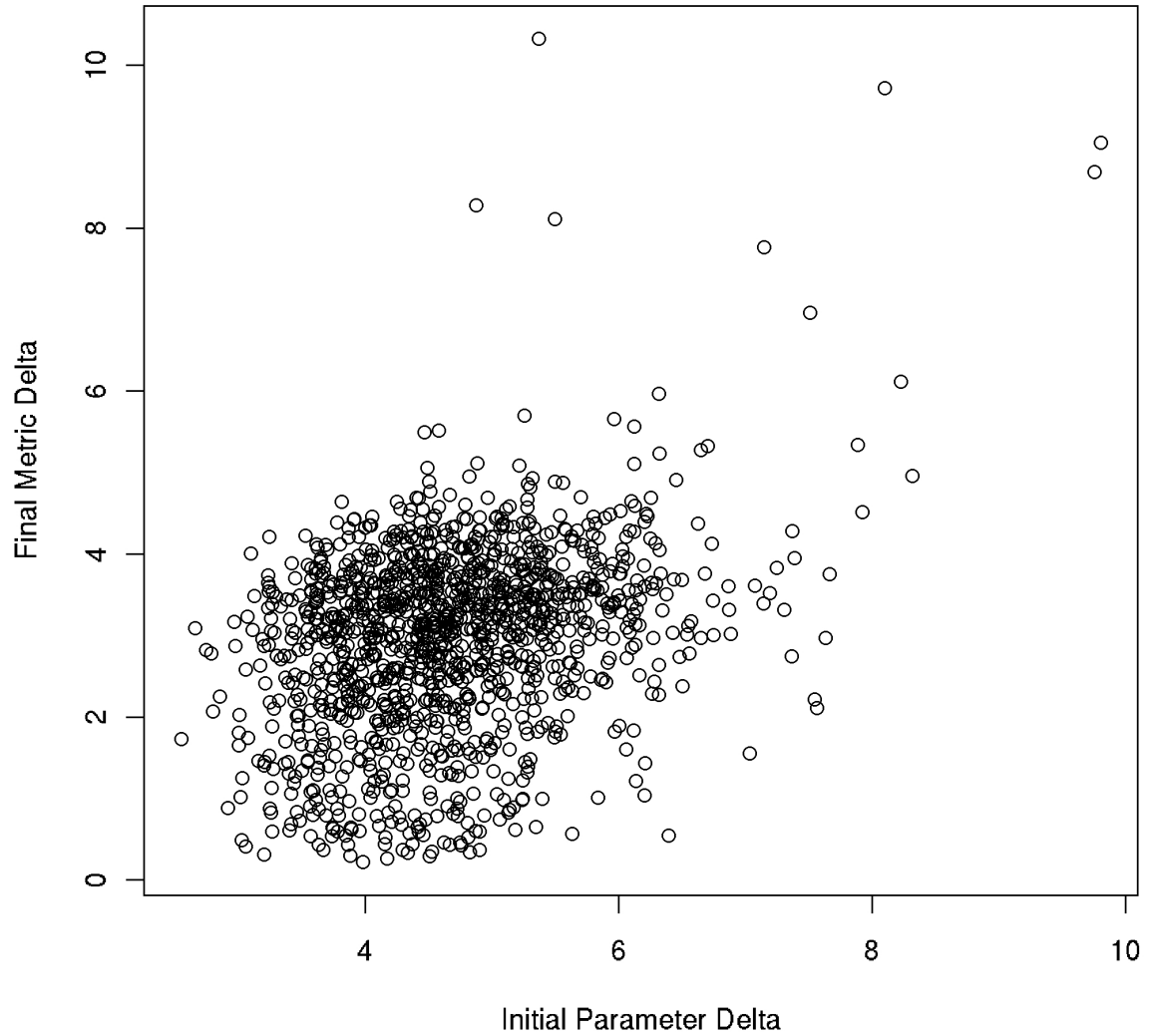


**Figure 42:** Petit Manan: Parameter Delta vs. Output Delta

### Seal Cove: Parameter Delta vs. Output Delta

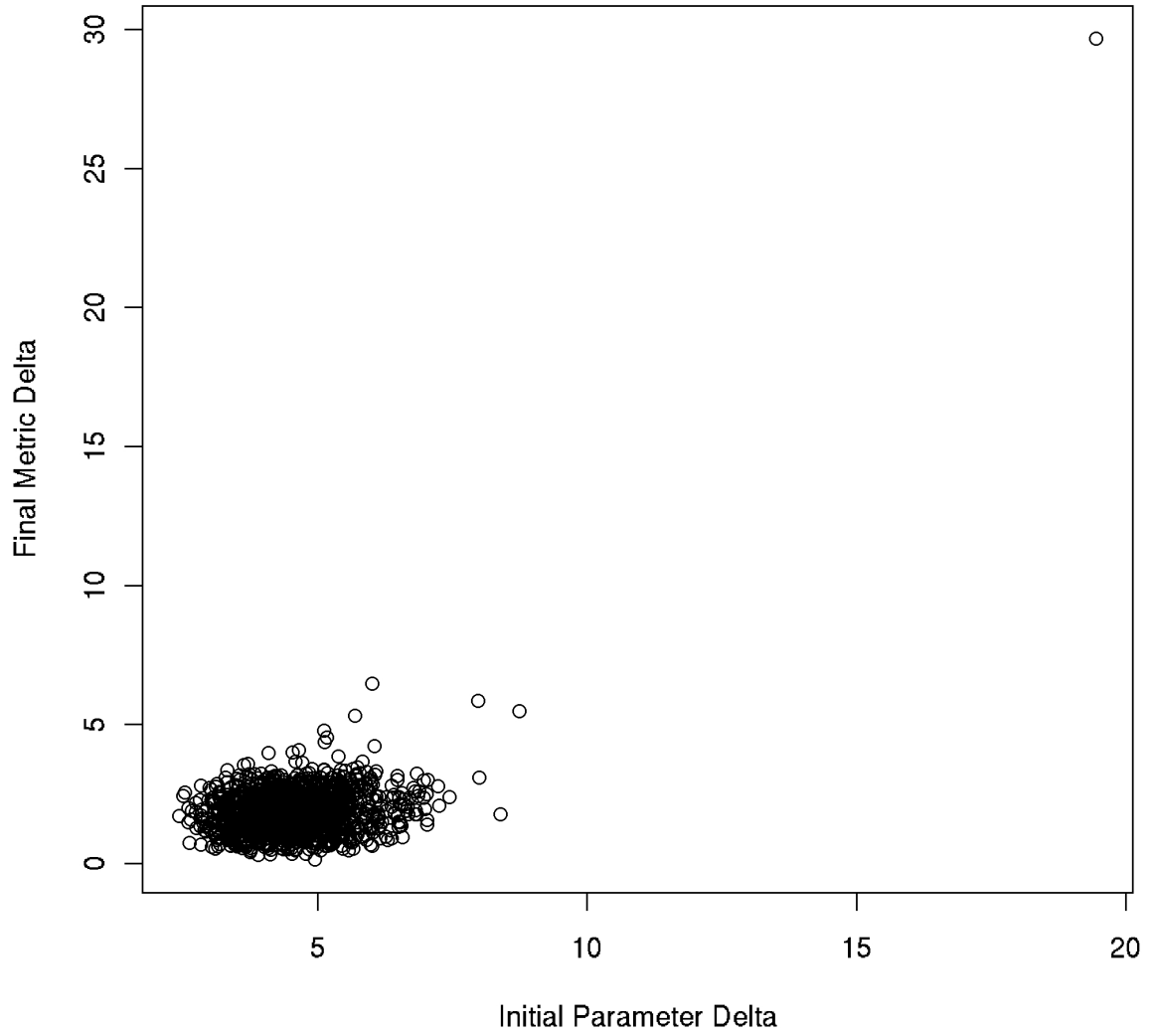


**Figure 43:** Seal Cove: Parameter Delta vs. Output Delta

## Shabbit Island: Parameter Delta vs. Output Delta

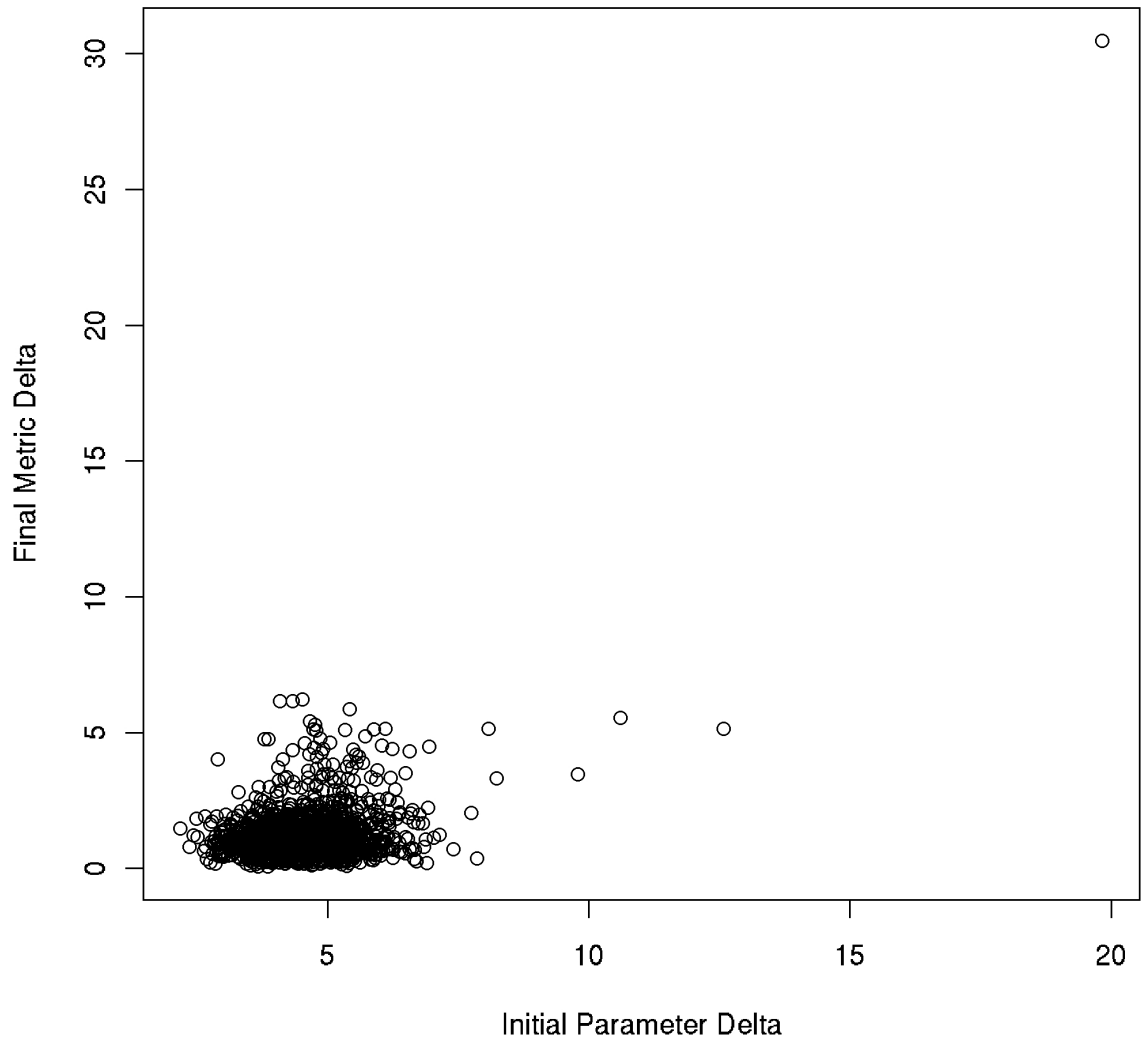


**Figure 44:** Shabbit Island: Parameter Delta vs. Output Delta

## 7.5 CORRELATION

Another way to analyze the effects of parameter perturbations is via the correlations between them. Each of the 10,757 runs represents a separate datapoint. These were used to find average correlations between the inputs and outputs.

PARAMETER	Urchins_biomass	Seaweed_biomass	topDensity	topGI
Urchins_maxPredationPerMin	-0.0078	-0.0050	-0.0056	0.0234
Urchins_maxGonadChangePerMin	-0.0093	0.0159	0.0037	0.0596
Urchins_lowGonadIndex	-0.0075	0.0044	-0.0046	0.0075
Seaweed_probRecoverPerMin	0.0460	-0.0049	0.0284	-0.0123
Urchins_maxGonadIndex	-0.0030	0.0006	-0.0185	0.1104
Urchins_mortalityRatePerMin	-0.0326	0.4096	-0.1628	0.0867
Urchins_predationRatePerMin	-0.0154	-0.0051	-0.0107	0.0115
Urchins_K	0.0626	-0.1490	0.0684	-0.0814
Urchins_maxPredationPerMin_juv	0.0048	0.0154	-0.0030	0.0024
Seaweed_timeToMaxBiomass	-0.2144	-0.1751	-0.0554	0.0865
Urchins_herbivoryRate	-0.5309	-0.0118	-0.2775	-0.2236
World_byCatchLoss	-0.0035	-0.0054	-0.0091	-0.0013
Urchins_maxTotalNumDensity	0.0466	-0.0657	-0.0033	-0.1433
Urchins_maxSize	0.0347	-0.0788	0.0505	-0.0185
Urchins_recruitmentRate	0.0312	-0.1297	-0.0876	-0.1854
Urchins_minGonadIndex	0.0058	-0.0055	0.0101	0.0030
Urchins_predationRatePerMin_juv	0.0104	0.0124	0.0067	0.0178
Seaweed_maxBiomassDensity	0.1914	0.3279	0.0594	0.0323

**Table 1:** Correlations Between Inputs and Outputs. Note: although the selected "best" values for many of these parameters are indicated in the appendices with only one or two significant digits, all of the values actually used in these trials were set with at least 8 significant digits.

While most of these correlations make intuitive sense, such as the fact that predation rates are negatively correlated with final urchin biomass at a given site, some correlations are harder to understand, such as the negative correlation between herbivory

rate and final urchin biomass. In this case, faster herbivory may lead to overconsumption that then leads to lower overall biomass.

## 7.6 CONCLUSION

Despite the high dimensionality of the model and the numerous complex interactions between model parameters, the output states are remarkably stable with respect to perturbations of parameter values. The model is considered non-chaotic in this sense only. Development of a single simulation may over time act chaotically, but the model is not overly sensitive to slightly misestimated parameter values.

## 8. DISCUSSION

The Results chapter displayed a very clear fact: The urchin-ecology simulator constructed for this thesis (AKA The Simulator) can model complexities that go far beyond any numerical population function. No matter how accurate, a single number to represent an urchin population will never have as much predictive or explanatory power as the Simulator.

In the opinion of marine biologists and fishermen, the Simulator successfully models the evolution of urchin populations and kelp distributions under various conditions and several known locations. The most salient phenomenon affecting the state of the urchin fishery is the state-flip from urchin barren to kelp bed. The Simulator is able to faithfully model this phenomon, and more importantly provide insight into prevention strategies.

The Simulator was used to model a period of time that corresponds to the first 15 years of the urchin fishery. Eight sites were selected after many interviews with fishermen. A clear set of trends was expected and then observed at each site. These trends were understood only via the simultaneous consideration of three forms of output:

1. *topDensity*
2. *topGI*
3. Snapshots of the model state in triptych form

The no-harvesting condition was revealed to be incongruent with a healthy and robust urchin population. While such populations will create large urchin barrens, they will live in a state of constant low-level starvation.

The standard-harvesting condition appears to be a guaranteed way to flip any site to the kelp dominated state. The few urchins left behind will have high gonad indices, but will be dispersed and difficult to find. This condition is wholly incompatible with any strategy for fishery sustainability.

The circular-harvesting condition afforded a healthy, robust, stable urchin population in almost all cases. This harvesting method appears to be sustainable and produces a healthier outcome for the urchins than even the no-harvesting condition. It is hoped that a more realistic harvesting solution can be found – one that shares two key features of circular harvesting:

1. Multiple quick-succession harvesting events leave numerous well-distributed spots untouched
2. Harvested zones are always in close proximity to some untouched region

If found, such a harvesting method could be tested in this model.

## 8.1 IMPLICATIONS FOR REGULATION

One implication of the assertions made in previous chapters is that fishery regulation should be sensitive to local conditions. It may be that a model similar to the one described in this thesis could be a sufficient basis on which to construct a new regulatory framework.

Regulations that remain unchanged under alterations to fine-scale conditions are incapable of addressing differences at that scale. Current urchin fishing restrictions are no different for a homogeneously dispersed urchin population than for a patchy one [State Legislature, Maine, 2012]. It is important because urchin populations of insufficient density cannot maintain enough herbivory to maintain their habitats. Since density at the fine scale can be a good predictor of a population's survival or demise, regulations should be sensitive to it.

A regulatory scheme that is sensitive to local density must straddle two conflicting requirements. It must recognize that fishermen need to harvest from dense aggregations in order to be profitable without ignoring the fact that urchins must maintain some minimum density or their populations won't remain viable. Harvesting from

dense populations always presents the possibility of a state flip to the kelp-dominated state when the urchins in a barren fall below some threshold of herbivory.

## 8.2 IMPLICATIONS FOR COOPERATIVE ACTION

The "straw-man" harvesting method referred to as "circular fishing" performs well in the simulator but is not considered to be realistic for actual divers to employ. Some other method must be devised which simply and easily leaves untouched zones next to harvested ones in such a way that urchins can redisperse between harvesting events. Whatever this method is, it is not likely to be something that the Maine DMR could police. Divers would have to buy into the strategy and self-regulate. The lobster fishery presents a positive example of local fishermen engaging in semi-altruistic self-regulated behavior while consistently accepting suboptimal short-term yields: v-notching. This and other cooperative behaviors are described below.

### 8.2.1 A MODEL FISHERY

The lobster fishery is one example of a fishery that works better than the urchin fishery [Wilson (pers. com.), 2012, Acheson (pers. com.), 2012]. The lobster population in the Gulf of Maine is not in the same kind of danger as the urchins. The relative stability of this fishery is the result of a self-regulatory scheme that exists among the lobstermen. This scheme was not mandated by law, but is instead an aspect of culture. Maine's lobstermen have their own regulatory system which operates outside the law. Officials are aware of it and allow it to exist as long as its function does not come to public attention [Acheson and Brewer, 2003].

Each individual lobsterman uses a unique paint pattern on the buoys that hold the lines to their traps. The typical lobsterman obtained his license from his father and has been fishing in the same places for many years. The lobstermen know each other. They have a strong sense of community and they actively protect it. Any

lobsterman who attempts to break into a new area has a serious uphill battle to fight [Acheson, 1988].

A typical such scenario begins with a local lobsterman finding a buoy with an unfamiliar pattern. After such a sighting, some lobsterman cut the line extending from the buoy. The buoy then floats free leaving the trap useless on the bottom. Others place half hitches on the buoy, cut out the nylon mesh "heads," or even leave a note in a bottle inside the trap. Each of these is meant as a message to the offending fisherman. Each cut trap represents an escalation. A number of cases included violence and/or destruction of property [Acheson, 1988, Acheson and Brewer, 2003].

Such activity occurs with sufficient regularity as to be considered one of the driving regulatory forces in the lobster fishery [Acheson and Brewer, 2003]. Since none of this behavior is mandated by law, but against the law, it is not top-down. The bottom-up nature of this behavior makes it a self-regulating system. In the absence of this behavior, a lobsterman would not face effective regulation. The Maine Department of Marine Resources (DMR) employs approximately 46 people in their enforcement division [Morris, 2008]. It is difficult to conceive how so few employees could effectively regulate all harvesting activity for any type of fishing along Maine's entire coast. With no effective oversight, a greater density of lobsterman in a given area would increase the likelihood of overfishing at that site. Intimidation by other fishermen is a recognized limit on fisherman density.

In addition to lobsterman density, the lobster fishery self-regulates with respect to its treatment of individual lobsters. Not all lobsters are treated equally. Upon catching a pregnant female, the typical lobsterman puts a triangular notch in the tail and returns it live. This action helps maintain the fishery by allowing the females to propagate the species. This practice began as an official policy. Fishermen were paid for these female lobsters, a notch would be cut in their tails and then they would be thrown back in. The notch was intended to prevent repeated sales of the same individual. Eventually, Maine's lobstermen stopped bringing these lobsters in for sale. They started to notch the lobsters themselves and toss them back immediately

[Wilson (pers. com.), 2012, Acheson (pers. com.), 2012]. A possible purpose of this behavior is to have pregnant lobsters give birth near their own fishing sites.

## 8.2.2 A DIFFERENT URCHIN REGULATORY SCHEME

It is the contention of the author that an appropriate model would indicate greater population stability under sparse harvesting than focused harvesting.

Consider an extreme example of sparse harvesting. After the removal of 10,000 urchins, where exactly 1 was taken from each of 10,000 distinct sites within a single zone, an appropriate model would show no observable change. In the other extreme, 10,000 urchins are removed from a single site. An appropriate model would show dramatic immediate change. The current regulatory scheme is unable to differentiate between these two scenarios, but the Simulator is able. The Simulator is an appropriate model.

An appropriate regulatory scheme for the sea urchin fishery should be sensitive to local conditions. It could also employ self-regulation. Such a scheme should be designed to prevent state flips from urchin barren to the kelp-dominated state, and would be sensitive to differences among individual urchins based on size or gonad mass.

This regulation could be applied through the creation of incentives instead of top-down enforcement. It should create incentives to leave some of the mature urchins found at any given fishing site. It should also incentivize fishermen to selectively hunt the urchins, either by supporting best husbandry practices or harvesting only at locations where research indicates that a conveyor-belt is in effect.<sup>18</sup>

---

<sup>18</sup>**conveyor-belt effect** : state in which urchins from a deeper population are continually replacing those harvested in a shallow zone

Typical mechanisms for regulating a fishery include:

1. Upper and lower limits on animal size
2. Limits on a fisherman's catch
3. Limits on the days a fisherman can harvest

These tools might be sufficient if the urchin ecology behaved like a classical population model. However, none of them address local conditions or population density.

Regardless of whether urchins are present at a given location, that location's topology can be inserted into the model described in this thesis. An estimate can be made for the minimum urchin density required at that site for viability. It is left up to the fishermen to find the subset of sites which currently have densities in excess of their respective minimum.

Fishermen could be asked to provide estimates for current density at each location they visit. Before and after densities would be submitted in the case that they harvest at that location.

The data provided by fishermen would be used for two purposes: modeling and soft-enforcement. The data would first be used by scientists to maintain a reasonable estimate of current urchin stocks. It could next be used to incentivize fishermen not to fish below minimum densities.

If such a level of cooperation could be achieved, experimentation can be done to discover viable alternatives to the circular harvesting condition. Cooperation is required for a positive outcome, as almost any strategy could be sabotaged by the dishonesty of a few.

The urchin fishery could learn from the lobster fishery by including social aspects of the lobster fishery. One reason the lobster fishery functions well is that lobstermen know where other lobstermen are fishing. This feature could be included in the urchin fishery through GPS transponders. A record could be kept of each fishing event, recording the coordinates automatically. The fisherman could enter estimated

densities on a smartphone, for instance. Technology exists to make this process relatively effortless, but their current culture would make acceptance of such an idea quite challenging.

There will always be incentives to lie about density and other features. Social pressures can be brought to bear on each fisherman. In the same way that lobstermen put pressure on each other (social and otherwise), urchin fishermen could put pressure on fishermen that do not cooperate. Pressure is not a guarantee of altered behavior, and social science is outside the scope of this thesis, but it is understood that without cooperation and honesty, there are no easy answers.

Relative cooperation could be judged through trends spotted in the density data. A designated institution (e.g. DMR), could maintain an official model of the state of all urchin populations. Incoming data supplied by fishermen would be used to update the model but also to highlight unexpected population drops. For example, fisherman B arrives at site X to find that it is well below its minimum density. After reporting this density, the official model highlights the fact that this density is significantly lower than expected. GPS records can then be mined to find the last fisherman who visited X. If fisherman B was the last one at that site, and B reported a satisfactory density, then the model and past data can be mined to scrutinize other sites visited by B. If a trend can be found showing that B consistently fishes below the minimum suggested density, this information can be made public. Pressure from other fishermen might be sufficient. Stronger pressure might take the form of a voting panel which has the power to deny license renewal to a bad actor.

Such a program would require significant buy-in. The fisherman involved must be convinced that their financial fates are linked, and that cooperation and openness (in terms of site data) will help them. It would obviously be necessary to limit the number of fishing licenses so that everybody has a reasonable expectation of harvesting enough to be profitable.

The above description comprises several of the author's ideas for a "parametric" or systems-based management scheme [Wilson et al., 1996]. It is contrasted with

classical management methods by utilizing parameters (e.g. urchin density) and social cooperation instead of size, catch, and time limits on monolithic fishing zones.

## 9. FUTURE WORK

### 9.1 MULTIPLE SIMULTANEOUS SIMULATIONS

Future work will include the concurrent parallel execution of multiple simulations. Each simulation will cover a separate fishing site. A method will be devised to initiate multiple sites and keep them synchronized. Experiments have already been performed with two such methods. Simulated fishermen will have to travel to each site to harvest their prey.

### 9.2 AGENT INTEGRATION

The code described in this thesis was written as a part of a large NSF-funded project managed by James Wilson.<sup>19</sup> The project intends to study human-ecological coupled systems as *complex adaptive systems* (CAS). Salient considerations of CAS research, such as scale-correctness and feedback loops, were discussed at length during the design and implementation of the simulator described in this thesis. Future work includes integration of the urchin simulator with other parts of the project already being worked on.

To simulate the urchin fishery as a human-coupled system, a master process will generate a number of agents acting as fishermen (written separately). The master process will also select a set of fishing sites, initiating an urchin simulation on each one. Through the master process, these agents will interact with the fishing sites, executing harvesting events. Each individual fishing site will be modeled by a simulation like the one described in this thesis.

Some knowledge of the fishing sites will be commonly held. This information will include things such as topology, and anything which might be ascertained from a map.

---

<sup>19</sup>Project Title: "Fine-scale Dynamics of Human Adaptation in Coupled Natural and Social Systems: An Integrated Computational Approach Applied to Three Fisheries"

Other knowledge will be specific to each agent. When an agent executes a harvesting event, that agent receives some information about the current state of that site, such as seaweed and urchin biomass density in the diveable zone.

Each agent will "learn" how to make profitable choices. A type of learning classifier system (LCS) [Holland et al., 2000], called an XCS [Wilson et al., 1998], will be used to record the payoff from previous decisions along with inputs (general and site-specific data). Each agent then uses their own XCS object at the beginning of each timestep to generate acts and predict associated payoffs.

The project intends to look for patterns in the behavior of the agents in this CAS. These patterns may be similar to those observed in the fishing community. If so, the model developed by the author may inform future regulation or provide explanatory power over the current state of the urchin fishery.

### 9.2.1 APPLICATION PROGRAMMER INTERFACE (API)

In future work, an API will be written to specify a set of hooks into the urchin simulation. These represent hooks that will allow an external process to initiate multiple urchin simulations and interact with them programmatically.

### 9.2.2 WORLDSIM

The *WorldSim* process will be the main process that initiates all agents and the urchin simulations, which in this context are referred to as the "biophysical" simulations. The WorldSim reads configuration files, spawns an individual biophysical simulation for each site described in the configuration files, and generates a number of fisherman agents. During simulation, the WorldSim acts as arbitrator of all harvesting events and functions as the repository of all publicly available knowledge. See Figure 64 for a pseudocode description.

As described in the main body of this thesis, each fishing site considers itself to be a separate entity, having its own world object. The WorldSim object has a list of these world objects and a list of agent objects. The basic timestep operation of an agent can be seen in Figure 65.

### 9.3 MID-LEVELS IN THE K-ARY TREE

In the current model, the simulated area is represented in multiple *Layer* objects, but only one of these layers is used – the bottom layer. Each layer is fundamentally the same, but has coarser or finer cells. The layers are related to each other by being "above" (at a coarser scale) or "below" (at a finer scale). The bottom layer is the one discussed in the body of this thesis. It is populated by urchin and seaweed, which operate at the finest scale. Other layers will be utilized in future work.

Real fishermen operate at a coarser level than urchins. So should simulated fishermen, if not for any other reason than so that fisherman logic may be simplified. Scale-appropriate representations allow for greater simplification. These simulated fishermen would perform recursive harvesting events, i.e. the fisherman harvests at the scale appropriate to the way they think. The coarse cell in which the harvesting occurs will propagate the harvesting event down through children cells, but only those which are actually populated with the target prey. The current state of children cells will be updated up the hierarchy whenever a change occurs.

Nothing in the model currently operates at any of the scales between the top (coarsest) and the bottom (finest). For this reason the in-between levels have been left out of the discussion for this thesis. These levels were included in the design to handle other species in the future. Lobsters, for example, would operate at a scale slightly coarser than that of the urchins because they move faster. When a lobster interacts with urchins, it could in theory interact with urchins in any cells that are children of its cell.

In the current model, each "parent cell" has no more than nine child cells. Nine was chosen as the degree of a k-ary tree to represent all cells. Therefore, each cell in this second layer has at most nine children cells in the next layer down. The same is true for each cell in each layer until the bottom layer. The purpose of building a k-ary tree is to allow each element in the CAS to operate in at an appropriate spatial scale.

The choice of  $k = 9$  for the degree of this k-ary tree was not totally arbitrary. Assume the bottom layer is generated first. Consider a cell in this layer along with its eight neighbors (counting diagonals). Each cell is linked to the one in the center, making a neighborhood of nine cells. Let these cells be considered the children cells of a cell in the layer above. A parent cell is generated having the average coordinates of its children cells. Coding this nine-to-one construction method was relatively simple.

After a parent cell is generated and properly linked, it is imbued with the accumulative or averaged attributes of its children. For instance, the area of the parent cell is the sum of the areas of each child cell. The depth is an average. The end result is a 9-ary tree of cell objects, each of which contain all necessary information for intra-cell operation. In future work, such attributes will define the simulated zone simultaneously at different scales.

Other cell-shapes and configurations may be considered if a compelling case can be made. Hexagonal models work better for cellular-automata models of gases because they more naturally allow the emergence of a physically-realistic Reynolds number [Frisch et al., 1986]. It is not known that such a case could be made for an animal ecology.

#### 9.4 AN ACCURATE DISTANCE MEASURE

A better geographic model will eventually be needed. Currently-used distance measures are not accurate enough for future work, which will include travel between arbitrary points in the Gulf of Maine. This is a concern of future work only, but when the research was started, this distinction had not yet been made.

The current system's inaccuracy was revealed in a simple test. Two points were selected at either end Maine's coastline. The distance was computed using this model's spherical model and using modern GIS software. The distances differed by approximately 100 km [Kaim (pers. com.), 2011].

The codebase developed for this model will be integrated into the larger project managed by James Wilson. Despite the fact that each individual simulation is on a small scale, multiple instances of the simulation will eventually be run concurrently for fishing sites throughout the entire Gulf of Maine. There will be a need to accurately compute the distance between any two fishing sites. Otherwise, distance-related incentives will not be realistic.

One commonly-used accurate measure of distance uses the Universal Transverse Mercator coordinate system (UTM). Any two points are first converted to UTM and then the cartesian distance is computed. UTM represents a projection of a small portion of the surface of the earth on to a plane. It is therefore distorted at the edges, but the distortion is small enough that it does not disrupt navigation. UTM divides the world up into numerous overlapping zones, each of which is projected separately. Finding the distance between two points in separate zones is not simple.

A simpler next approximation would be to represent the world as a oblate spheroid. Sufficiently accurate distances can be measured via a computational method known as Vincenty's Formulae. These formulae comprise a set of iterative methods to numerically calculate the shortest distance between two points on the surface of a oblate spheroid [Vincenty, 1975].

Consider again the two points at either end of Maine's coast (mentioned above). These points represent a worst-case scenario within our region of interest. Whereas the spherical model might differ from UTM-derived by 100 km, the output of Vincenty's formulas as computed by the author were within 0.04% of the measurements made by modern methods [Kaim (pers. com.), 2011]. Such methods are negligibly better within the context of a single fishing site. The higher computation requirements make them undesirable except when moving a significant distance.

When this simulation is eventually scaled up there will be elements operating at different scales. The urchins and kelp in this model both operate at the smallest scale (approx.  $20m \times 20m$ ), but fishermen will operate at the scale of whole fishing sites, approximately  $2km \times 2km$ . The distances they travel (between sites) need to be accurate. Considerations for scaling up do not directly affect the work of this thesis but were required for eventual integration into the larger research project already under development.

## 9.5 ARBITRARY SITE SELECTION

Eight fishing sites have been modeled thus far. A bathymetry for each of these sites was painstakingly prepared and input in a format understood by the model. Long after these sites had been prepared, another dataset became available. Work could be done to prepare that dataset in such a way that the model will be able to call up the bathymetry of any arbitrary zone within the Gulf of Maine. Future work will include the incorporation of this data.

## 9.6 MODULAR FORM

A future version of the simulator code should conform to the format of a standard Python module. As when downloading other python modules, the package should include standard installation instructions and scripts. These measures could help increase acceptance from and usage by other marine ecology researchers.

Given sufficient resources, the alterations and extra efforts described above will be done in the future.

---

---

# Pepper ... And Salt

THE WALL STREET JOURNAL



*"To keep the fish sustainable,  
only one of you may order it."*

## REFERENCES

- [Acheson, 1988] Acheson, J. (1988). *The Lobster Gangs of Maine*. UPNE.
- [Acheson and Brewer, 2003] Acheson, J. and Brewer, J. (2003). *Changes in the Territorial System of the Maine Lobster Industry*, pages 37–59. MIT Press.
- [Acheson (pers. com.), 2012] Acheson (pers. com.) (2011-2012). Unpublished personal communication. James Acheson.
- [AlgaeBase, 2012] AlgaeBase (2012). Database of information on algae that includes terrestrial, marine and freshwater organisms.
- [Allesina and Bondavalli, 2003] Allesina, S. and Bondavalli, C. (2003). Steady state of ecosystem flow networks: a comparison between balancing procedures. *Ecological Modelling*, 165(2-3):221–229.
- [Amaral and Uzzi, 2007] Amaral, L. A. N. and Uzzi, B. (2007). Complex systems - a new paradigm for the integrative study of management, physical, and technological systems. *Management Science*, 53(7):1033–1035.
- [Barinaga, 1995] Barinaga, M. (1995). New study provides some good news for fisheries. *Science*, 269:1043.
- [Brady and Scheibling, 2005] Brady, S. and Scheibling, R. (2005). Repopulation of the shallow subtidal zone by green sea urchins (*strongylocentrotus droebachiensis*) following mass mortality in nova scotia. *Journal of the Marine Biological Association of the United Kingdom*, 85:1511–1517.
- [Brawley (pers. com.), 2011] Brawley (pers. com.) (2011). Unpublished personal communication. Susan Brawley.
- [Breen et al., 2000] Breen, P., Andrew, N., and Kendrick, T. (2000). Stock assessment of pau 5b for 1998-99. new zealand fisheries assessment report 2000.
- [Breen and Mann, 1976] Breen, P. and Mann, K. (1976). Destructive grazing of kelp by sea urchins in eastern canada.
- [Cencini et al., 2010] Cencini, M., Cecconi, F., and Vulpiani, A. (2010). *Chaos: From Simple Models to Complex Systems*. World Scientific Publishing Co. Pte. Ltd.

- [Chen et al., 2000] Chen, Y., Breen, P. A., and Andrew, N. L. (2000). Impacts of outliers and mis-specification of priors on bayesian fisheries-stock assessment. *Canadian Journal of Fisheries and Aquatic Sciences*, 57(11):2293–2305.
- [Chen and Hunter, 2003] Chen, Y. and Hunter, M. (2003). Assessing the green sea urchin (*strongylocentrotus droebachiensis*) stock in maine, usa. *Fisheries Research*, 60:527–537.
- [Chen et al., 2003] Chen, Y., Hunter, M., Vadas, R., and Beal, B. (2003). Developing a growth-transition matrix for the stock assessment of the green sea urchin (*strongylocentrotus droebachiensis*) off maine. *Fishery Bulletin*, 101(4):737–744.
- [Chen (pers. com.), 2012] Chen (pers. com.) (2010-2012). Unpublished personal communication. Yong Chen.
- [Cleaver (pers. com.), 2012] Cleaver (pers. com.) (2010,2012). Unpublished interviews with various urchin divers. Caitlin Cleaver.
- [Dornhaus, 2008] Dornhaus, A. (2008). Specialization does not predict individual efficiency in an ant. *PLoS Biology*, 6(11): e285. doi:10.1371/journal.pbio.0060285.
- [Dumont et al., 2004] Dumont, C., Himmelman, J., and Russel, M. (2004). Size-specific movement of green sea urchins *strongylocentrotus droebachiensis* on urchin barrens in eastern canada. *Marine Ecology Progress Series*, 276:93–101.
- [Ebert and Southon, 2003] Ebert, T. and Southon, J. (2003). Red sea urchins can live over 100 years: confirmation with a-bomb [14.sup]carbon - *strongylocentrotus franciscanus*. *Fishery Bulletin*, 101(4):915–922.
- [Egan and Yarish, 1990] Egan, B. and Yarish, C. (1990). Productivity and life history of laminaria longicuris at its southern limit in the western atlantic ocean. *Marine Ecology Progress Series*, 67:263–273.
- [Epstein, 1999] Epstein, J. M. (1999). Agent-based computational models and generative social science. *Complexity*, 4(5).
- [FishBase, 2012] FishBase (2012). Database of information on fish that includes marine and freshwater organisms.
- [Fogarty, 1995] Fogarty, M. (1995). Rejoinder: Chaos, complexity and community management of fisheries. *Marine Policy*, 19(5):437–444.

- [Frisch et al., 1986] Frisch, Hasslacher, and Pomeau (1986). Lattice-gas automata for the navier-stokes equation. *Physical Review Letters*, 56.
- [Gaylord et al., 2004] Gaylord, B., Reed, D., Washburn, L., and Raimondi, P. (2004). Physical-biological coupling in spore dispersal of kelp forest macroalgae. *Journal of Marine Systems*, 49:19–39.
- [Grabowski et al., 2005] Grabowski, R., Russell, R., Chen, Y., and Hunter, M. (2005). Estimating the maine green sea urchin stock biomass using a spatial statistics approach. Funding from grants #: G601240, G701363.
- [Hancock, 1979] Hancock, D. A. (1979). *Population dynamics and management of shellfish stocks*, pages 8–19.
- [Hilborn and Gunderson, 1996] Hilborn, R. and Gunderson, D. (1996). Rejoinder: Chaos, and paradigms for fisheries management. *Marine Policy*, 20(1):87–89.
- [Holland et al., 2000] Holland, J., Booker, L., Colombetti, M., Dorigo, M., Goldberg, D., Forrest, S., Riolo, R., Smith, R., Lanzi, P., Stolzmann, W., and Wilson, S. (2000). What is a learning classifier system? In Lanzi, P., Stolzmann, W., and Wilson, S., editors, *Learning Classifier Systems*, volume 1813 of *Lecture Notes in Computer Science*, pages 3–32. Springer Berlin Heidelberg.
- [Hunter et al., 2010] Hunter, M., Lyons, K., and Russell, R. (2010). Monitoring and assessment of maine’s sea urchin resource. values used in thesis were computed from table values in this report.
- [Jackson and Ratnieks, 2006] Jackson, D. E. and Ratnieks, F. L. W. (2006). Communication in ants. *Current Biology*, 16(15):R570–R574.
- [Jackson et al., 2001] Jackson, J. B. C., Kirby, M. X., Berger, W. H., Bjorndal, K. A., Botsford, L. W., Bourque, B. J., Bradbury, R. H., Cooke, R., Erlandson, J., Estes, J. A., Hughes, T. P., Kidwell, S., Lange, C. B., Lenihan, H. S., Pandolfi, J. M., Peterson, C. H., Steneck, R. S., Tegner, M. J., and Warner, R. R. (2001). Historical overfishing and the recent collapse of coastal ecosystems. *Science*, 293(5530):629–637.
- [Jones, 1985] Jones, G. M. (1985). *Paramoeba invadens* n. sp. (amoebida, paramoebidae), a pathogenic amoeba from the sea urchin, *strongylocentrotus droebachiensis*, in eastern canada1. *Journal of Eukaryotic Microbiology*, 32(4):564–569.

- [Kaim (pers. com.), 2011] Kaim (pers. com.) (2011). Unpublished personal communication. Lucas Kaim.
- [Kawamura et al., 1999] Kawamura, H., Yamamoto, M., Suzuki, K., and Ohuchi, A. (1999). Ants war with evolutive pheromone style communication. *Lecture Notes in Computer Science*, 1674/1999:639–643.
- [Keats, 1991] Keats, D. (1991). Refugial *laminaria* abundance and reduction in urchin grazing in communities in the north-west atlantic. *Journal of the Marine Biological Association of the United Kingdom*, 71:867–876.
- [Kling, 2006] Kling, A. L. (2006). Effects of formulated feeds and saccharina latissima on growth, gonadal-somatic index, and gonad color in grow-out stage green sea urchins, *strongylocentrotus droebachiensis*, in land-based echiniculture. Master’s thesis.
- [Lauzon-Guay, 2009] Lauzon-Guay, J.-S. (2009). Modelling phase shifts in a rocky subtidal ecosystem. *Marine Ecology Progress Series*.
- [Lavigne, 1997] Lavigne, G. R. (1997). White-tailed deer assessment and strategic plan.
- [Maine DMR, 2004a] Maine DMR (2004a). Maine sea urchin landings and harvester participation data.
- [Maine DMR, 2004b] Maine DMR (2004b). Maine’s sea urchin fishery.
- [Maine DMR, 2012] Maine DMR (2012). 2012 - 2013 sea urchin season for maine.
- [Maine IFW, 2013] Maine IFW (2013). 2013 maine hunting seasons.
- [Manly, 2005] Manly, B. F. J. (2005). *Multivariate Statistical Methods: A Primer*. Chapman & Hall /CRC, third edition.
- [Mathieson, 1976] Mathieson, A. C. (1976). *Journal of Experimental Marine Biology and Ecology*, 25(3):273–284.
- [May, 1976] May, R. M. (1976). Simple mathematical models with very complicated dynamics. *Nature*, 261:459 – 467

- [McNaught, 1999] McNaught, D. C. (1999). *The indirect effects of macroalgae and micropredation on the post-settlement success of the green sea urchin in Maine*. PhD thesis.
- [Miller and Page, 2009] Miller, J. H. and Page, S. E. (2009). *Complex Adaptive Systems: An Introduction to Computational Models of Social Life*. Princeton University Press.
- [Miller, 1984] Miller, R. J. (1984). Succession in sea urchin and seaweed abundance in nova scotia, canada. *Marine Biology*, 1985:275–286.
- [Miller, 1985] Miller, R. J. (1985). Seaweeds, sea urchins, and lobsters: A reappraisal.
- [Miller, 2008] Miller, R. J. (2008). A sea urchin dive fishery managed by exclusive fishing areas. *FAO FISHERIES TECHNICAL PAPER*, 504.
- [Miller and Nolan, 2000] Miller, R. J. and Nolan, S. (2000). Management of the nova scotia sea urchin fishery: a nearly successful habitat based mangement regime.
- [Mitchell, 2009] Mitchell, M. (2009). *Complexity: a guided tour*. Oxford University Press.
- [Morris, 2008] Morris, L. D. (2008). The history of marine patrol.
- [Nishiura, 1999] Nishiura, Y. (1999). *Far-from-Equilibrium Dynamics*. The American Mathematical Society.
- [Norris, 2012] Norris, D. (2012-2012). unpublished personal communication. Sea Urchin Fisherman.
- [Peacock, 2011] Peacock, C. B. (2011). Sea Urchin Fisherman.
- [Perry et al., 2002] Perry, R. I., Zhang, Z., and Harbo, R. (2002). Development of the green sea urchin (*strongylocentrotus droebachiensis*) fishery in british columbia, canada - back from the brink using a precautionary framework. *Fisheries Research*, 55:253–266

- [Pham et al., 2006] Pham, D., Ghanbarzadeh, A., Koc, E., Otri, S., Rahim, S., and Zaidi, M. (2006). The bees algorithm – a novel tool for complex optimization problems. *Intelligent Production Machines and Systems*, pages 454–459.
- [Piaget, 1977] Piaget, J. (1977). *The essential Piaget*. Routledge and K. Paul.
- [Russell et al., 1998] Russell, M., Ebert, T., and Petraitis, P. (1998). Field estimates of growth and mortality of the green sea urchin. *Ophelia*, 48:137–153.
- [Santa-Fe-Inst., 2012] Santa-Fe-Inst. (2012). Santa fe institute mission and vision.
- [Scheibling and Hamm, 1991] Scheibling, R. and Hamm, J. (1991). Interactions between sea urchins (*strongylocentrotus drobachiensis*) and their predators in field and laboratory experiments. *Marine Biology*, 110:105–116.
- [Scheibling et al., 1999] Scheibling, R., Hennigar, A., and Balch, T. (1999). Destructive grazing, epiphytism, and disease. *Canadian Journal of Fisheries and Aquatic Sciences*, 56:2300–2314.
- [Sea Urchin Genome Sequencing Consortium, 2006] Sea Urchin Genome Sequencing Consortium (2006). The genome of the sea urchin *strongylocentrotus purpuratus*. *Science*, 314(5801):pp. 941–952.
- [Sheibling (pers. com.), 2011] Sheibling (pers. com.) (2011). unpublished personal communication. Robert Sheibling.
- [Smith (pers. com.), 2010] Smith (pers. com.) (2010). Unpublished personal communication with caitlin cleaver and james wilson. William 'Killer' Smith.
- [Sonu, 1995] Sonu, S. C. (1995). Noaa technical memorandum nmfs.
- [State Legislature, Maine, 2012] State Legislature, Maine (2012). *X SHELLFISH, SCALLOPS, WORMS AND MISCELLANEOUS LICENSES*, chapter 623.
- [Steneck, 1997] Steneck, R. (1997). *Fisheries-induced biological changes to the structure and function of the Gulf of Maine ecosystem*, pages 151–165.
- [Steneck (pers. com.), 2012] Steneck (pers. com.) (2011,2012). unpublished personal communication. Robert Steneck

- [Strathmann, 1978] Strathmann, R. (1978). Length of pelagic period in echinoderms with feeding larvae from the northwest pacific. *Journal of Experimental Marine Biology and Ecology*, 34:23–27.
- [Sturgis and Gordon, 2012] Sturgis, S. J. and Gordon, D. M. (2012). Nestmate recognition in ants (hymenoptera: Formicidae): a review. *Myrmecological News*, 16:101–110.
- [Sullivan, 1995] Sullivan, K. (1995). *North American Sea Urchin Fishery Management Strategies: Their Applicability to the Maine Green Sea Urchin Fishery*. PhD thesis.
- [Taylor, 2004] Taylor, P. H. (2004). Green gold, scientific findings for management of maine’s sea urchin fishery.
- [Tseng, 1987] Tseng, C. K. (1987). pages 311+.
- [Turchin, 2003] Turchin, P. (2003). *Complex population dynamics: a theoretical/empirical synthesis*. Princeton University Press.
- [Uhrmacher and Weyns, 2009] Uhrmacher, A. and Weyns, D. (2009). Multi-agent systems: Simulation and applications.
- [Vadas and Elner, 1992] Vadas, R. and Elner, R. (1992). *Plant-animal interactions in the north-west Atlantic*, volume 46, pages 33–60. Clarendon Press, Oxford.
- [Vadas, 1977] Vadas, R. L. (1977). Preferential feeding: An optimization strategy in sea urchins. *Ecological Monographs*, 47:337–371.
- [Vadas et al., 04b] Vadas, R. L., Beal, B. F., and Wright, W. A. (04b). Biomass and productivity of intertidal rockweeds (*ascophyllum nodosum*) lejolii in cobscook bay. *Northeastern Naturalist*, 11:123–142. Special Issue 2.
- [Vadas et al., 04c] Vadas, R. L., Beal, B. F., Wright, W. A., Nickl, S., and Emerson, S. (04c). Biomass and productivity of red and green algae in cobscook bay, maine. *Northeastern Naturalist*, 11:163–196. Special Issue 2.
- [Vadas et al., 2004] Vadas, R. L., Beal, B. F., Wright, W. A., Nickl, S., and Emerson, S. (2004). Growth and productivity of sublittoral fringe kelps (*laminaria longicruris*) bach. pyl. in cobscook bay, maine. *Northeastern Naturalist*, 11:143–162. Special Issue 2.

- [Vadas et al., 1980] Vadas, R. L., Larson, and Keser (1980). Feeding and nutritional ecology of the sea urchin *strongylocentrotus drobachiensis* in maine. *Marine Biology*, 59:49.
- [Vadas and Steneck, 1988] Vadas, R. L. and Steneck, R. S. (1988). Zonation of deep water benthic algae in the gulf of maine. *J. Phycol*, 24:338–346.
- [Vadas and Steneck, 1995] Vadas, R. L. and Steneck, R. S. (1995). Overfishing and inferences in kelp-sea urchin interactions. *Ecology of Fjords and Coastal Waters*, pages 509–524.
- [Vadas (pers. com.), 2012] Vadas (pers. com.) (2010-2012). unpublished personal communication. Robert Vadas.
- [Verhulst, 1838] Verhulst, P.-F. (1838). *Correspondance mathématique et physique*, 10:115.
- [Vincenty, 1975] Vincenty, T. (1975). Direct and inverse solutions of geodesics on the ellipsoid with application of nested equations. *Survey Review*, XXIII (originally misprinted as XXII)(176):88–93.
- [Weisstein, 2012] Weisstein, E. (2012).
- [Wilson, 1962] Wilson, E. O. (1962). Chemical communication among workers of the fire ant, *solenopsis saevissima*, the organization of mass-foraging. *Animal Behaviour*, 10(1-2):134–138.
- [Wilson, 1990] Wilson, J. (1990). Fishing for knowledge. *Land Economics*, 66(1):12–29.
- [Wilson, 2002] Wilson, J. (2002). *Scientific Uncertainty, Complex Systems, and the Design of Common-Pool Institutions*. National Academies Press.
- [Wilson and Acheson, 1996] Wilson, J. and Acheson, J. (1996). Order out of chaos: The case for parametric fisheries. *American Anthropologist*, 98(3):579–594.
- [Wilson et al., 1996] Wilson, J., Acheson, J., and Kleban, P. (1996). Chaos and parametric management. *Marine Policy*, 20(5):429–438.
- [Wilson et al., 2007] Wilson, J., Yan, L., and Wilson, C. (2007). The precursors of governance in the maine lobster fishery. *PNAS*, 104(39).

- [Wilson et al., 1998] Wilson, S. W., Wilson, S. W., Xcs, G., and System, C. (1998). Generalization in the xcs classifier system.
- [Wilson (pers. com.), 2012] Wilson (pers. com.) (2010-2012). unpublished personal communication. James Wilson.
- [Zhang et al., 2008] Zhang, Z., Campbell, A., and Bureau, D. (2008). Growth and natural mortality rates of red sea urchin (*strongylocentrotus franciscanus*) in british columbia. *Journal of Shellfish Research*, 27(5):1291–1299.

## APPENDIX A : GLOSSARY

**autopoiesis** : from Greek "auto" (meaning "self"), and "poiesis", meaning "creation, production". Describes the replacement of and creation of cellular matter within a living organism. First introduced by Humberto Maturana and Francisco Varela.

**bathymetry** : topology of the ocean floor

**biomass (wet)** : the tested mass of a living thing immediately after extrication from the water and mild shaking

**biomass (dry)** : the tested mass of a living thing after significant drying

**benthic** : on or near the ocean floor

**by-catch** : animals unintendedly caught in the process of fishing

**complex system** : a system of numerous elements, interacting with each other according to prescribed rules, whose aggregate behavior exhibits interesting regularities

**complex adaptive system** : complex systems containing learning agents

**conveyor-belt effect** : state in which urchins from a deeper population are continually replacing those harvested in a shallow zone

**far-from-equilibrium** : describes a system consistently far enough from equilibrium that traditional mathematical assumptions do not hold (e.g. Efficient Market Hypothesis)

**generative model** : A model which employs bottom-up processes to allow larger structures or phenomena to emerge

**gonad index (GI)** : percentage of an urchin (by weight) comprised of roe

**herbivory** : consumption of plants

**human-natural coupled system** : complex system comprising a set of humans interacting with a set of other animals or plants

**kelp-dominated** : describes a patch of sea floor covered by a relatively dense distribution of kelp

**numerosity** : a single scalar representing the number of individuals in a population

**parametric management** : regulatory framework that can utilize parameters (e.g.: urchin density) and is not limited to size catch and time limits

**pelagic** : free-floating in the open water

**photic** : relating or related to light

**photic zone** : the shallower depths where the amount of solar energy reaching the sea floor is sufficient for kelp growth

**recruitment** : introduction of new juvenile animals into an environment

**settlement** : deposition of a pelagic creature onto a substrate

**simulation** : representation in computer memory of the state of an idealized version of something in reality, where this state is a function of virtual time

**simulator** : computer program able to run a simulation

**state-flip** : relatively rapid transition from one stable state to another

**tritych** : three contemporaneous snapshots presented together

**urchin barren** : shallow patch of sea floor with sufficiently dense urchin population to maintain very low kelp levels through herbivory

**visualization** : graphical representation of the state of a simulation

**visualizer** : computer program able to run a visualization

## APPENDIX B : PARAMETERS

Below is a table containing values and reasonable ranges for parameters used in the model. Explanations of how these values were derived are on the pages following the table.

PARAMETER	ESTIMATE	RANGE
byCatchLoss	0.2	0.1 - 0.3
herbivoryRate	$0.00005 \text{ min}^{-1}$	$2.3 \times 10^{-6} - 7.7 \times 10^{-5}$
K (Brody Growth Parameter)	$4.5 \times 10^{-7} \text{ min}^{-1}$	$2.2 \times 10^{-7} - 6.2 \times 10^{-7}$
lowGonadIndex	1	0.5 - 2
maxBiomassDensity (Seaweed)	$0.8 \frac{\text{kg (dry)}}{\text{m}^2}$	0.32 - 1.0
maxGonadChangePerMin	$4.75 \times 10^{-7} \text{ min}^{-1}$	$3.87 \times 10^{-7} - 5.39 \times 10^{-7}$
maxGonadIndex	25	18 - 27
maxPredationPerMin	$4 \times 10^{-7}$	$3.0 \times 10^{-7} - 5.0 \times 10^{-7}$
maxPredationPerMin-juv	0.106	0.08 - 0.12
maxTotalNumDensity	$500 \frac{\text{urchins}}{\text{m}^2}$	100 - 1000
maxSize	85 mm	63.1 - 95.2
minGonadIndex	$1.0 \times 10^{-12}$	$0.0 - 1.0 \times 10^{-5}$
mortalityRatePerMin	$1 \times 10^{-8} \text{ min}^{-7}$	$4.05 \times 10^{-9} - 4.05 \times 10^{-7}$
photic function	$e^{7.05-0.17d}$	$e^{7.0-0.13d} - e^{7.1-0.27d}$
predationRatePerMin	$1.5 \times 10^{-7} \frac{\text{urchins}}{\text{m}^2 \text{min}}$	$7 \times 10^{-8} - 4 \times 10^{-7}$
predationRatePerMin-juv	$0.05 \frac{\text{urchins}}{\text{m}^2 \text{min}}$	0.0193 - 0.106
probRecoverPerMin	$7.0 \times 10^{-6} \text{ min}^{-1}$	$3.4 \times 10^{-6} - 1.4 \times 10^{-5}$
recruitmentRate	$0.04 \frac{\text{urchins}}{\text{m}^2 \text{min}}$	0.0057 - 0.086
timeToMaxBiomass (Seaweed)	600 days	55 - 5075
turbulentZone	2 m	1 - 3

**Table 2:** Values & ranges for parameters in the model.

The model utilizes a number of input parameters. Values for these parameters are set at the beginning of each simulation.

The true values of these parameters are unknown. Where possible, a range of reasonable values have been determined from the literature and from discussions with experts. Most settings are identical for all runs of the model (except during sensitivity analysis). The chosen values and reasonable ranges are delineated below, each with an explanation.

PARAMETER	ESTIMATE	RANGE
byCatchLoss	0.2	0.1 - 0.3

**byCatchLoss** : The proportion (unitless) of non-legal sized urchins that are lost during a fishing event. This only applies to urchins within a cell that experiences a harvesting event. In the 1980's this number was closer to 0.3 (30%). Currently, with fewer but more-skilled harvesters, this number is down to 0.1 (10%) [Vadas (pers. com.), 2012].

PARAMETER	ESTIMATE	RANGE
herbivoryRate	$0.00005 \text{ min}^{-1}$	$2.3 \times 10^{-6} - 7.7 \times 10^{-5}$

**herbivoryRate** : The maximum amount of seaweed, in kilograms, that one kilogram of urchins are able to consume per min. As this number represents a maximum, the actual herbivory will be lessened as needed (e.g. on a yearly cycle, peaking in warmer months).

Larson, Vadas, and Keser studied urchins between 25 and 30 mm in diameter. The urchins exhibited the highest preference for *S. longicruris* and the lowest for *A. cribrorum*. Presented with only *S. longicruris* the urchins consumed 52.9 mg per urchin per hour. Presented with only *A. cribrorum* they consumed 16.3 mg per urchin per hour.

When multiple species are available the urchins consume considerably less: 19.0 mg per urchin per hour for *S. longicruris* and only 1.6 mg per urchin per hour for *A. cribrosum*.

For an urchin radius of 0.014 m, under the spherical approximation, urchin mass  $m_u$  can be found from diameter and its density. The mass being considered here is the mass of an urchin in its environment, including the water contained within its body. The density used to find this number is approx.  $1000 \frac{kg}{m^3}$  [Vadas (pers. com.), 2012]:

$$m_u = \text{density} \cdot \text{volume} = 1000 \frac{kg}{m^3} \cdot \frac{4}{3} \pi (.014m)^3 \approx 0.0115 \frac{kg}{urchin}$$

or alternatively:  $87 \frac{urchins}{kg}$

The high and low estimates for per urchin per hour values found by Larson et al. are converted to  $\frac{kg}{kg \cdot min} \rightarrow \frac{1}{min}$ :

$$52.9 \frac{mg}{urchin \cdot hr} \times .000001 \frac{kg}{mg} \times 87 \frac{urchins}{kg} \times \frac{1}{60} \frac{hr}{min} \approx 7.7 \times 10^{-5} min^{-1}$$

$$1.6 \frac{mg}{urchin \cdot hr} \approx 2.3 \times 10^{-6} min^{-1}$$

PARAMETER	ESTIMATE	RANGE
K (Brody Growth Parameter)	$4.5 \times 10^{-7} min^{-1}$	$2.2 \times 10^{-7} - 6.2 \times 10^{-7}$

**K** : The Brody Growth Parameter is a constant used in the Von Bertalanffy Growth Function (VBGF), the function typically used to approximate urchin growth (see Equation (2)) [Chen et al., 2003].  $K$  is in units of  $\frac{1}{time}$ .

After researching habitats along the coast of Maine, the observations of Chen et al. yielded values for  $K$  that ranged from  $0.1181 \text{ year}^{-1}$  in the south to  $0.3268 \text{ year}^{-1}$  along the mid-coast. For the model these were converted:

$$0.1181 \frac{1}{\text{yr}} \times \frac{1}{525960} \frac{\text{yr}}{\text{min}} \approx 2.2 \times 10^{-7} \text{min}^{-1}$$

$$0.3268 \frac{1}{\text{yr}} \approx 6.2 \times 10^{-7} \text{min}^{-1}$$

PARAMETER	ESTIMATE	RANGE
lowGonadIndex	1	0.5 - 2

**lowGonadIndex** : GI below which mortality increases (see discussion below under *maxGonadIndex*). An urchin consuming its own gonads will reach a point where its mortality rate increases. Data is not available on this topic. Robert Vadas and Robert Steneck described the mechanisms involved. This threshold is an attempt to quantitatively capture this qualitative discussion [Vadas (pers. com.), 2012, Steneck (pers. com.), 2012].

PARAMETER	ESTIMATE	RANGE
maxBiomassDensity (Seaweed)	$0.8 \frac{\text{kg}(\text{dry})}{\text{m}^2}$	0.32 - 1.0

**maxBiomassDensity (Seaweed)** : The maximum seaweed biomass per  $m^2$ .

Since urchin growth and health depend on the amount of consumed seaweed biomass [Vadas et al., 1980], biomass is the operative quantity to model for seaweed. The biomass density of *Ascophyllum nodosum* has been observed as high as  $28.94 \frac{\text{kg}(\text{wet})}{\text{m}^2}$  and with a 95% CI in the range 20.78 -37.11 [Vadas et al., 04b]. For *Ulva lactuca* and *Enteromorpha spp.*, the mean biomass has been observed at  $321.1 \frac{\text{g}(\text{dry})}{\text{m}^2}$ , with a 95% CI range from: 115.8 - 608.4 [Vadas et al., 04c]. Biomass densities of *S. longicuris*, the species most eaten by urchins, have been observed as high as  $500 \frac{\text{g}(\text{dry})}{\text{m}^2}$  at Mahar

Point, and  $1000 \frac{g(dry)}{m^2}$  at Bar Island [Vadas et al., 2004]. Much further south it has been observed at  $47 \frac{kg(wet)}{m^2}$  [Egan and Yarish, 1990] (wet/dry weight ratios for *Laminaria* / *Saccharina* species can be as low as 5:1 [Tseng, 1987] and as high as 30:1 [Egan and Yarish, 1990]).

Wet weight numbers are used less often [Vadas (pers. com.), 2012], and their conversion is not precise, so only dry numbers were used here. Considering only the dry-weight data, the modeled seaweed is a functional substitute for the limited data we have: the range of  $0.32 - 1.0 \frac{kg(dry)}{m^2}$  for maximum biomass density was considered by the author to be not inconsistent with the above results.

PARAMETER	ESTIMATE	RANGE
maxGonadChangePerMin	$4.75 \times 10^{-7} \text{ min}^{-1}$	$3.87 \times 10^{-7} - 5.39 \times 10^{-7}$

**maxGonadChangePerMin** : The maximum relative per minute change allowed for gonad mass.

Gonad Index (GI) is used externally and in most discussions about the model, but gonad mass is the underlying value used for computation in the model. For the purpose of data output, the gonad mass is converted to GI, the metric generally accepted by biologists. The practice of discussing GI instead of gonad mass is maintained in this thesis, except where gonad mass is more appropriate.

This parameter has no mass units because it is a proportion. This proportion, multiplied by total biomass, represents the maximum amount of change in gonad mass the urchins in a given cell may experience.

It is known that GI is generally high for urchins found feeding on a copious food source, and low for urchins found at low-food location, but no data exists on how fast an urchin can go from having low GI to high and then back to low. Existing GI data collection only allows for one datapoint per urchin. Such data is garnered from urchins that were opened, or "sacrificed" [Vadas et al., 1980]. Robert Vadas, an expert on

*S. droebachiensis*, reported that a medium-sized urchin with high GI can most likely survive without sustenance for up to about a year [Vadas (pers. com.), 2012]. During that time the urchin is living purely by consuming its own gonads. Assuming such urchins begin with a high GI of 25 (.25 × mass), we can estimate the maximum amount gonad mass that can be lost or gained per min. In the model this parameter is called the *maxGonadChangePerMin*:

$$\text{maxGonadChangePerMin} \times \text{mass} = \frac{.25 \times \text{mass}}{525960 \text{ min}} \approx 4.75 \times 10^{-7} \text{ min}^{-1} \times \text{mass}$$

By adding or subtracting one month (measured in minutes below), and altering the starting GI (in the range 22-26), there are lower and higher bounds which were not inconsistent with our discussion:

$$\text{maxGonadChangePerMin (low)} = \frac{.26}{482760 \text{ min}} \approx 5.39 \times 10^{-7} \text{ min}^{-1}$$

$$\text{maxGonadChangePerMin (high)} = \frac{.22}{569160 \text{ min}} \approx 3.87 \times 10^{-7} \text{ min}^{-1}$$

The term "mass" applies to a single urchin. In the model, this parameter will be a ratio applied to biomass. Gonad change is applied simultaenously to all urchins within a given cell.

PARAMETER	ESTIMATE	RANGE
maxGonadIndex	25	18 - 27

**maxGonadIndex** : The Gonad Index (GI) is a quantity used by biologists to measure how much of an urchin's body the roe represents (by weight). The maximum for a mature urchin is about 25%, which corresponds to a GI of 25 [Vadas (pers. com.), 2012]. Some observations support this estimate. After extended feeding on preferred foods, *S. droebachiensis* have been observed having a GI of  $22.50 \pm 3.99$  [Vadas et al., 1980]. When well-fed, urchin GI will grow toward its maximum and maintain it until spawning. When not receiving enough nutrition, urchin GI will slowly decrease because the urchin is consuming its own gonads to stay alive [Vadas (pers. com.), 2012]. Urchin

GI is typically lower for smaller urchins but this has been overlooked as an approximation for the sake of simplicity.

PARAMETER	ESTIMATE	RANGE
maxPredationPerMin	$4.0 \times 10^{-7}$	$3.0 \times 10^{-7} - 5.0 \times 10^{-7}$

**maxPredationPerMin** : The maximum number of urchins eaten  $m^{-2}min^{-1}$ . Stochasticity in the model draws from distributions that sometimes produce unrealistically large numbers of urchins eaten. This parameter effectively truncates the long tail, limiting the number of urchins that could be eaten in one cell per unit time. Intuitively this models the limitation of a predator’s capacity for eating. This parameter and its range are arbitrary. Its value comes from intuition and discussions with biologists. See more discussion of **predationRatePerMin** below.

PARAMETER	ESTIMATE	RANGE
maxPredationPerMin-juv	0.106	0.08 - 0.12

**maxPredationPerMin-juv** : The maximum number of *juvenile* urchins eaten  $m^{-2}min^{-1}$ . Stochasticity in the model draws from distributions that sometimes produce unrealistically large numbers. This parameter effectively truncates the long tail, limiting the number of urchins that could be eaten in one cell per unit time. Intuitively this models the limits of a predator’s capacity for eating. This value was selected in a similar fashion to **maxPredationPerMin** (above).

PARAMETER	ESTIMATE	RANGE
maxTotalNumDensity	$500 \frac{urchins}{m^2}$	100 - 1000

**maxTotalNumDensity** : The maximum number of urchins that might be found on a given square meter of sea floor. Urchins can achieve extreme densities by piling on top of each other. Sometimes they even accumulate in several layers where the lower

layers eat the small pieces of food produced by the mastication of urchins in higher layers [Norris, 2012, Vadas (pers. com.), 2012].

PARAMETER	ESTIMATE	RANGE
maxSize	85 mm	63.1 - 95.2

**maxSize** : The maximum diameter an urchin can reach. Urchins will grow asymptotically toward this value,  $L_\infty$  from the VBGF (see Equation (2)) [Chen et al., 2003]. The observations of Chen et al. yielded values for  $L_\infty$  that ranged from 63.1 mm in the northeast to 95.2 mm in the south. These numbers were not computed by averaging measurements of naturally deceased urchins. Such data is extremely difficult to obtain. These numbers come from fitting the VBGF to size data. Characteristics of the VBGF aside, maximum urchin diameter may be as large as 90 to 100 mm [Vadas (pers. com.), 2012].

PARAMETER	ESTIMATE	RANGE
minGonadIndex	$1.0 \times 10^{-12}$	0.0 - $1.0 \times 10^{-5}$

**minGonadIndex** : GI below which an urchin dies from starvation.

An urchin consuming its own gonads will reach a point where no longer has anything left to consume. Data is not available on this topic. Robert Vadas and Robert Steneck described the mechanisms involved. This threshold is an attempt to quantitatively capture this qualitative discussion [Vadas (pers. com.), 2012] [Steneck (pers. com.), 2012]. It measures when the GI is effectively zero. Intuitively, this value should be between zero and some extremely low GI.

PARAMETER	ESTIMATE	RANGE
mortalityRatePerMin	$1 \times 10^{-8} \text{ min}^{-7}$	$4.05 \times 10^{-9} - 4.05 \times 10^{-7}$

**mortalityRatePerMin** : The mean number of urchins dying from natural causes *per m<sup>2</sup> per min.*

Some red urchins may be able to live in excess of 100 years [Ebert and Southon, 2003], but for *S. droebachiensis* there is no reliable data on mean and variance of lifespan. Estimates for mortality rates were not found for *Strongylocentrotus droebachiensis*, but mortality research was found for *Strongylocentrotus franciscanus*. Mean estimates for this mortality rate range from  $0.077 \text{ yr}^{-1}$  to  $0.213 \text{ yr}^{-1}$  [Zhang et al., 2008]. Field studies are difficult to interpret because of the need to disambiguate death by predation from death by "natural causes," but these estimates are not inconsistent with other studies [Russell et al., 1998, Chen and Hunter, 2003]. Zhang's estimates will be used to estimate an upper bound on the mortality rate.

An estimate of the lower bound on the mortality rate can be set by considering the optimistic case where only the most mature urchins (e.g. diameter  $\geq 70\text{mm}$ ) die of natural causes. To temper the optimism of this assumption, let all such mature urchins die within a year of reaching this advanced size. There were 26 censuses taken in Chebucto Head over a three-year period recording urchins up to a diameter of  $76\text{mm}$ . These mature urchins comprised a very small segment of the population. Pooling all samples together, only 9 out of 4,222 urchins were in this segment [Brady and Scheibling, 2005]. By this scheme,  $9/4222$  urchins would die per year of natural causes, or  $.00213\text{yr}^{-1}$ .

Converting the lower and upper bounds to the units used in the model:

$$0.00213 \text{ yr}^{-1} \times 1.9013 \times 10^{-6} \frac{\text{yr}}{\text{min}} = 4.05 \times 10^{-9} \text{ min}^{-1}$$

$$0.213 \text{ yr}^{-1} \times 1.9013 \times 10^{-6} \frac{\text{yr}}{\text{min}} = 4.05 \times 10^{-7} \text{ min}^{-1}$$

Note: It is purely coincidental that both the upper and lower bound contain the same digits.

PARAMETER	ESTIMATE	RANGE
photic function	$e^{7.05-0.17d}$	$e^{7.0-0.13d} - e^{7.1-0.27d}$

**photic function** : The function used to compute the exponential diminishing of solar energy per unit depth.

The available solar energy at a given depth  $d$  is given by  $e^{7.1-.17d}$ . The values 7.05 and 0.17 are averaged from regressions to two separate sets of measurements: one made at Pemaquid Point and the other at Ammen Rock Pinnacle (see the range listed above) [Vadas and Steneck, 1988]. Solar energy diminishes exponentially with depth. This energy is used to limit the maximum seaweed biomass that a given square meter of sea floor can support.

PARAMETER	ESTIMATE	RANGE
predationRatePerMin	$1.5 \times 10^{-7} \frac{urchins}{m^2min}$	$7 \times 10^{-8} - 4 \times 10^{-7}$

**predationRatePerMin** : The mean number of urchins eaten *per m<sup>2</sup> per min.*

One investigation looked at small, medium, and large urchins. Tethered to lines, a number of urchins were spread out over an area of about 1000  $m^2$ . Predation of these urchins was closely monitored. This experiment was performed in multiple locations and multiple depths for a cumulative time period of 46 days. Larger urchins were eaten in deeper waters, but were mostly immune closer to shore, where urchins smaller than 40 mm were the most common fare [Vadas and Steneck, 1995]. Rates varied with depth and predator abundance. Within a 95% confidence interval, the predation rate of small to medium urchins can range from 0.1 to 0.7  $\frac{urchins}{day \cdot 1000 m^2}$ .

$$0.1 \frac{\text{urchins}}{\text{day} \cdot 1000 \text{ m}^2} \times \frac{\text{day}}{1440 \text{ min}} \approx 7 \times 10^{-8} \frac{\text{urchins}}{\text{m}^2 \cdot \text{min}}$$

$$0.7 \frac{\text{urchins}}{\text{day} \cdot 1000 \text{ m}^2} \approx 4 \times 10^{-7} \frac{\text{urchins}}{\text{m}^2 \cdot \text{min}}$$

PARAMETER	ESTIMATE	RANGE
predationRatePerMin-juv	0.05 $\frac{\text{urchins}}{\text{m}^2 \text{min}}$	0.0193 - 0.106

**predationRatePerMin-juv** : The mean number of *juvenile* urchins eaten per  $m^2$  per *min*.

One investigation into urchin predation used astroturf collectors each with an area of  $20 \times 9 \text{ cm}$  ( $0.018 \text{ m}^2$ ), or  $55.6 \frac{\text{collectors}}{\text{m}^2}$ . These collectors were placed in various locations with 20 settled juvenile urchins on each ( $600\text{-}900 \mu\text{m}$ ). These urchins were marked with a dye so that researchers could determine how many of the original urchins remained at the end of each four-day study. Predation rates in this study were between 2 and 11 per collector [McNaught, 1999].

$$2 \frac{\text{urchins}}{\text{collector} \cdot \text{four days}} \times 55.6 \frac{\text{collectors}}{\text{m}^2} \times \frac{\text{four days}}{5760 \text{ min}} \approx 0.0193 \frac{\text{urchins}}{\text{m}^2 \text{min}}$$

$$11 \frac{\text{urchins}}{\text{collector} \cdot \text{four days}} \approx 0.106 \frac{\text{urchins}}{\text{m}^2 \text{min}}$$

PARAMETER	ESTIMATE	RANGE
probRecoverPerMin	$7.0 \times 10^{-6} \text{ min}^{-1}$	$3.4 \times 10^{-6} - 1.4 \times 10^{-5}$

**probRecoverPerMin** : Mean of stochastic process used to repopulated uncovered kelp habitat. A an area is not fully covered by seaweed, the portion of the uncovered

area is multiplied by *probRecoverPerMin* and the result is the mean of a stochastic process drawing from an exponential distribution. The real number output (always < 1.0) is the proportion of the uncovered portion of this cell which becomes newly covered in the current timestep.

The rate at which seaweed can recover unclaimed area can be estimated from the turnover rate among dense populations of kelp plants. If a unit area can be replaced by new plants within a given amount of time, then that time may be an estimate of the rate at which unclaimed areas can be repopulated (assuming no herbivory). Turnover times have been estimated around Bar Island, Mahar Point, and Garnet Point, in a range from 50 to 205 days [Vadas et al., 2004].

A reasonable range of values for this parameter can be calculated from these estimates by taking the inverse. Taking the quicker estimate, a cell's coverage can go from a coverage of 0.0 (representing zero coverage) to 1.0 (representing total coverage) in 50 days, or 72,000 minutes.

$$1/(50 \text{ days}) = (1)/(72000 \text{ min}) \approx 1.4 \times 10^{-5} \text{ min}^{-1}$$

$$1/(205 \text{ days}) \approx 3.4 \times 10^{-6} \text{ min}^{-1}$$

PARAMETER	ESTIMATE	RANGE
recruitmentRate	0.04 $\frac{\text{urchins}}{m^2 \text{ min}}$	0.0057 - 0.086

**recruitmentRate** : The rate (urchins per  $m^2$  per minute) at which urchins successfully settle on the bottom. This rate is used as the mean of a stochastic process. It only applies during two months: May and June. During the rest of the year this value is zero.

The rate of successful settlement for *S. droebachiensis* varies greatly from site to site. A reasonable range of values can be determined from data collected at four sites: Damariscove Is., Fisherman Is., Thrumcap Is., and Pemmaquid Pt. W. Astroturf

collectors were positioned at each site just before settlement began and left for two months after settlement began. Between 1995 and 1998 settlement rates ranged from 500 to 7500 per  $m^2$  with some sites hovering around 4000 per  $m^2$  [McNaught, 1999, p.21].

Assuming a typical settlement season of about two months, this range can be specified with the desired time units. 4000 per  $m^2$  over two months translates to about 0.046 per  $m^2$  per minute during the settlement season. McNaught reported that these numbers may be low due to predation. Of concern to the model is a good estimate of the number of urchins reaching median size within the smallest size bin. McNaught's data can therefore be used without any inflation to account for such predation.

PARAMETER	ESTIMATE	RANGE
timeToMaxBiomass (Seaweed)	600 days	55 - 5075

**timeToMaxBiomass (Seaweed)** : Time from zero to maximum biomass for seaweed.

As described in the chapter on model representation, seaweed is often modeled with a single number representing biomass. We chose to go further, modeling seaweed distributions with height and area (called *coverage*), where biomass becomes a computed value. Seaweed mass per unit volume is assumed constant. This representation was chosen because it revealed necessary differentiation. Marine biologists to whom this was explained raised no objection [Vadas (pers. com.), 2012, Steneck (pers. com.), 2012].

Seaweed abundance is greatest near the surface and diminishes with depth at some function that differs for each species. The modeled seaweed is considered to have a maximum biomass (assuming 100% coverage) at depth 0 (for more, see the description of maxBiomassDensity (Seaweed)). This maximum biomass diminishes as an exponential function of depth using light attenuation measurements made at Ammen Rock

Pinnacle and Pemaquid Point [Vadas and Steneck, 1988]. This second approximation was also presented to biologists without objection.

Optimal seaweed growth occurs in the low intertidal [Vadas et al., 04c]. Considering a relatively optimal case in the model (depth  $\leq 2 m$  , 100% coverage), time-ToMaxBiomass can be computed using maxBiomassDensity (see description above) and known growth rates (dry). In Cobscook Bay, low-intertidal Foliose and Filamentous Green Algae show maximum growth rates in the range  $43.2 - 988.2 \frac{g(dry)}{m^2 yr}$  [Vadas et al., 04c]. Productivity for *S. longicruris* at Bar Island has been estimated as high as  $8.61 \pm 2.37 \frac{g(dry)}{m^2 day}$ , or equivalently, in the range  $6.2 - 11.0 \frac{g(dry)}{m^2 day}$  [Vadas et al., 2004]. Converting these ranges to identical units:

$$\begin{aligned} \text{from: } 43.2 \text{ to: } 988.2 \frac{g(dry)}{m^2 yr} &= \text{from: } 8.21 \times 10^{-5} \text{ to: } .00188 \frac{g(dry)}{m^2 min} \\ \text{from: } 6.2 \text{ to: } 11.0 \frac{g(dry)}{m^2 day} &= \text{from: } .00431 \text{ to: } .00764 \frac{g(dry)}{m^2 min} \end{aligned}$$

The modeled seaweed should therefore have a growth rate in the range  $8.21 \times 10^{-5} - .00764 \frac{g(dry)}{m^2 min}$ . Using a maxBiomassDensity of  $0.6 \frac{kg(dry)}{m^2}$ , we can calculate the amount of time required for seaweed to go from zero to maximum biomass:

$$\begin{aligned} \text{Low Est.: } &\left( 600 \frac{g(dry)}{m^2} \right) / \left( .00764 \frac{g(dry)}{m^2 min} \right) \approx 78534 \text{ min} \approx 55 \text{ days} \\ \text{High Est.: } &\left( 600 \frac{g(dry)}{m^2} \right) / \left( 8.21 \times 10^{-5} \frac{g(dry)}{m^2 min} \right) \approx 7308160 \text{ min} \approx 5075 \text{ days} \end{aligned}$$

PARAMETER	ESTIMATE	RANGE
turbulentZone	2 m	1 - 3

**turbulentZone** : Urchins are observed in fewer numbers in shallow turbulent areas. Wave action interrupts their movement, allowing for more stable kelp growth [Keats, 1991]. There may also be a higher mortality in this zone [Vadas (pers. com.), 2012].

## APPENDIX C : PSEUDOCODE

```
01  c <- current cell
02  if c has enough food:
03      don't move
04  if deep(c):
05      will move with some probability
06  T <- select targets
07  for s in sizes:
08      t <- random select from T
09      if turbulent(t) and depth(t) < depth(c):
10          might not move
11          n <- random num less/equal to urchins of size s
12          move n urchins to t
```

**Figure 45:** Pseudocode: Urchin Movement. If food sources are plentiful in the local cell (line 02), these urchins don't move. If the local cell is very deep (04), observations show that some urchins don't move [Vadas (pers. com.), 2012]. A stochastic conditional (05) determines if these urchins move. Targets are selected (06). Iterating over all size bins (07), a random target is selected from those already chosen (08). If the target is too shallow (09), movement might not occur [Vadas (pers. com.), 2012]. Finally, move a random number of urchins to the target(11-12).

```

01   T <- (select top n/2 targets by food content)
02   if best has insufficient food:
03       if scent present:
04           T <- (select top n/2 targets by scent)
05       else:
06           T <- (select top n/2 by urchin density)
07   return T

```

**Figure 46:** Pseudocode: Target Selection (select a target cell for moving to). Taking an array of cells including the local cell and all adjacent cells, this algorithm begins by sorting them on food content and selecting the top  $n/2$  (01), where  $n$ =(number of adjacent cells). If the best has insufficient food content (02), and the scent of seaweed is present (03), then the three targets with greatest scent are selected (04). Otherwise the top two by urchin density are selected (06) modeling the tendency of urchins to aggregate even in deep low-food zones [Vadas (pers. com.), 2012]

```

01  func Urchins_grow():
02      org_capac <- capacPerBiomass * biomass - seasonal fluct.
03      capac <- orig_capac - detritus
04      capac <- capac - fresh seaweed
05      eaten <- orig_capac - capac
06      nutrition <- eaten / orig_capac
07      for s from penultimate size to lowest:
08          p <- promote(s, nutrition)
09          num[s] -= p
10          num[s+1] += p
11
12  func Urchins_promote(s, nutrition):
13      expect_n <- relativeGrowth[s] * num[s] * nutrition
14      return random(expect_n)

```

**Figure 47:** Pseudocode: Urchin Growth. (Note: "capac"=capacity for consumption). First find the total potential consumption, of all urchins in a cell, assuming infinite food (02). Next, some capacity is used up by eating detritus (03). Next (assuming  $capac > 0$ ), some capacity is used up eating living seaweed (04). Next, find the total amount eaten (05). The ratio between the amount eaten and the original capacity is a measure of nutritional intake (06). When food is plentiful this value will equal 1.0. Iterating over size bins from second-from-the-top to bottom (07), some number of urchins in each bin are promoted based on their size and the nutrition ratio (08-10).

The *promote* method is defined on lines 12-14. For a given  $s$  and *nutrition*, it computes the number of urchins to be promoted to bin  $s + 1$ . Line 13 represents Equation 9. The actual number of urchins promoted is drawn from a Poisson distribution (14).

```

01  for p in (input bathymetry):
02      for q in (cells closest to p):
03          if numRead(q) > 0:
04              depth(q) = (depth(q) * numRead(q)
                           + depth(p)) / (numRead(q) + 1)
05          else:
06              depth(q) = depth(p)
07          numRead(q)++

```

**Figure 48:** The Depth Interpolation Algorithm: The algorithm iterates over each element  $p$  in the input bathymetry as point data (01). Cells  $q$  in the model having coordinates within some  $\epsilon$  of  $p$  were iterated over (02). If  $q$  has already been assigned a depth (03), an iterative average depth was assigned to it (04), otherwise it was set to that of  $p$  (06). The number of input points  $p$  used to find a depth for each point  $q$  were tracked (07) to enable iterative averaging.

```

01  func closestCell(q, p):
02      q_c <- closest cell to p from neighbors(q)
03      if dist(p, q) < dist(p, q_c):
04          return q
05      else:
06          return closestCell(q_c, p)

```

**Figure 49:** The Point Selection Algorithm: This recursive algorithm operates on an input point  $p$  and a cell  $q$  (01). It first sorts  $q$ 's neighbors by their distance to  $p$  (02). If  $q$  is closest to  $p$  (03), it returns a pointer to itself (04). Otherwise the algorithm recurs on  $q_c$  (06)

```

01  func World_tick():
02      admin
03      BottomLayer.tick()
04      Display.update()

```

**Figure 50:** This is the central method of the *World* object. Everything that occurs during a timestep in the simulation is initiated by this method. After some administration (02) the *tick* function of the bottom layer object is called. Then the display database is updated (04)

```

01  func Layer_tick():
02      for c in activeCells:
03          c.compute()
04      admin
05      for c in activeCells:
06          c.tick()
07      for c in activeCells:
08          c.move()
09      for c in waterCells:
10          c.update()
11      for c in receivingCells:
12          c.activate()

```

**Figure 51:** The Layer's *tick* method is executed each timestep. It has five sub-steps. This method iterates over some subset of the cells during each substep. *activeCells* are those currently populated by animals or plants. *waterCells* are cells with  $\text{depth} > 0$ . *receivingCells* are cells with incoming urchins in their buffers (see section on urchin movement)

```
01 func Animals_compute():
02     for s in sizes:
03         totalNum += num[s]
04         biomass += mass[s] * num[s]
```

**Figure 52:** This method recomputes *totalNum* (03) and *biomass* (04), which may have changed during the previous timestep.

```
01 func Plants_tick():
02     grow()
03     if biomass == 0:
04         deactivate(self.cell)
05     stats.update(self)
```

**Figure 53:** This method first executes plant growth (02). If the biomass is exactly zero, remove from active list (04). Finally update the *Stats* object.

```
01  func Animals_tick():
02      mortality()
03      cull()
04      compute()
05      grow()
06      compute()
07      recruit()
08      stats.update(self)
```

**Figure 54:** This method executes the majority of the urchin activity during a timestep. *mortality* manages the removal of urchin by predation and natural causes (02). *cull* manages harvesting (if timestep is in a harvesting event). *grow* includes herbivory, gonad growth, and promotions (05). *recruit* handles the in-flux of new urchins in the smallest size class (07). Finally, the stats object is updated with data on this animals object (08).

```

01  func Urchins_mortality():
02      if gonad mass zero:
03          all die
04      if gonad mass low:
05          increase mortality rate
06      if in turbulent zone:
07          increase mortality rate
08      for s in sizes:
09          if large(s):
10              increase mortality rate
11              apply mortality rate
12              predation rate = default p. rate * seaweed biomass
13              if juvenile(s):
14                  predation rate increases
15              apply predation rate
16      stats.update(self)

```

**Figure 55:** Urchins *mortality* Method: Several factors determine the rate of death by natural causes (mortality). These include gonad mass (02,04), turbulence (06), and age (09). Predation depends on the local seaweed biomass (12) and being in the juvenile state (03) Finally, the stats object is updated with mortality data (16).

```

01  if harvestEvent == True:
02      generate blindspots
03      for c in activeCells:
04          might miss c
05          if ( density(c) > critical density
06              and depth(c) < 21 m ):
07              for s in sizes:
08                  if legal(s):
09                      harvest
10                  else:
11                      maybe bycatch

```

**Figure 56:** Each harvesting event lasts for an entire timestep. The World object generates blindspots (02), to model the patchiness of a fisherman’s activity [Wilson (pers. com.), 2012]. Iterating over all active cells (03), there is some further probability (modeled with another random number) that a fisherman might miss this cell (04), thus adding patchiness to the non-blindspot zone. Since fishermen don’t dive deeper than 20 m (06), and they focus on zones with a higher than average density of urchins (05) [Wilson (pers. com.), 2012], harvesting only occurs if both these conditionals are met. The algorithm iterates over the size classes. Legal-sized urchins are harvested (09), and some of the non-legal-sized urchins are killed as bycatch (11). See parameter *byCatchLoss*.

```

01  func Urchins_recruit():
02      if recruitmentSeason:
03          if favorability > 0:
04              mu <- favorability * recruitmentRate
05              return random(mu)

```

**Figure 57:** If during recruitment season (May and June), and if the cell is favorable to urchin life (03), the value  $\mu$  is determined by multiplying the favorability by the recruitment rate (04). In order to model the patchiness of urchin distributions [Wilson (pers. com.), 2012], the actual number of recruits is drawn from a random distribution having  $\mu$  for an expected value (05).

```

01  func Cell_update():
02      plants.update()
03      animals.update()
04      manage deactivation
05      update favorability
06      compute dispersal of seaweed scent
07      compute dispersal of detritus

```

**Figure 58:** After this method calls the *update* method of its animals and plants (02-03), it may deactivate this cell (04). Next it updates the cell's favorability (05) in terms of food quality, urchin density, and depth. Finally it computes the flux of seaweed scent (06) and detritus in the water (07).

```

01  func visualizer(dbFile):
02      m <- Map(dbFile)
03      configure glut
04      glut.callback <- m.display
05      glut.mainLoop()

```

**Figure 59:** Visualizer Overview. A *Map* object is initialized (02), which reads simulation-specific information from the database file specified as input (01). *glut* is configured (03). The map object's *display* method is set as the callback function (04). Finally, the glut main loop is started (05). This loop runs until externally stopped.

```

01  func display():
02      sleep(.2)
03      for row in database.getRows():
04          parse row -> depth, urchinMass, seaweedMass, etc
05          colors <- getColors(depth, urchinMass, seaweedMass, etc)
06          setSectors(colors)

```

**Figure 60:** Map Object's *display* Method: The visualizer pauses briefly in each loop (02). Then iterates over all rows (03), which corresponds to one row per cell. Information about each cell is parsed from the row (04). This information is used to determine the appropriate color for the cell (05), then the color is set via the frame object (06).

```

01  colors <- getColors(cell)
02  (x, y) <- getCoords(cell)
03  frame.setSectors(colors, x, y)
04  for s in frame.sectors:
05      i <- indexOf(s)
06      s.setPoint(x, y, colors[i])

```

**Figure 61:** *Sector* Object Usage for the 4-quadrant Display. The *colors* list holds four color vectors (01), one for each quadrant (topology, urchins, seaweed, favorability).  $(x, y)$  hold the column and row of a cell in the bottom layer (02). These function as relative coordinates for the cells. The *setSectors* method takes this data (03) and applies each datum and color vector to the correct sector (04-06).

```

01  func setPoint(x, y, color):
02      xOffset <- self.xOffset + (x * self.pixelWidth)
03      yOffset <- self.yOffset + (y * self.pixelHeight)
04      drawRectangle(color, self.pixelWidth, self.pixelHeight, xOffset,
                    yOffset)

```

**Figure 62:** The Sector *setPoint* Method. The relative coordinates (column& row), and the color vector for a cell are specified (01). Offsets are computed for the x and y dimensions using data already contained in the sector object (02-03). A rectangle representing a single cell is added to the OpenGL buffer through the frame object's *drawRectangle* method (04).

```
01  func drawRectangle(color, width, height, xOffset, yOffset)
02      (R, G, B) <- color
03      glColor3f (R, G, B)
04      glBegin(GL_QUADS)
05      glVertex3f (xOffset, yOffset, 0.0)
06      glVertex3f (xOffset+width, yOffset, 0.0)
07      glVertex3f (xOffset+width, yOffset+height, 0.0)
08      glVertex3f (xOffset, yOffset+height, 0.0)
09      glEnd()
```

**Figure 63:** The Frame *drawRectangle* Method hides the complexity of interacting with glut. First the color of a new QUADS object is specified (02). Then the vertices are specified by pixel coordinates relative to the window in which they are drawn (04-09). These commands submit this rectangle to the glut buffer.

```

01  func WorldSim_run(config):
02      for site in config:
03          site.initiate()
04      for agent in config:
05          agent.initiate()
06      loop indefinitely:
07          for site in sites:
08              site.world.tick()
09          for agent in agents:
10              agent.tick()

```

**Figure 64:** The *WorldSim* Object. *WorldSim* represents the master process that initiates all urchin simulations (02-03) and fisherman agents (04-05). Then looping indefinitely (06), it allows each individual site's *World* object (as described earlier) to execute a timestep (07-08), and each agent as well (09-10).

```

01  func Agent_tick():
02      action <- selectXCS(inputs)
03      payoff <- WorldSim_harvest(agent, site)
04      updateXCS(inputs, action, payoff)

```

**Figure 65:** The Agent's *tick* Method. The agent (also called a "Diver"), selects an action using its XCS and all available inputs (02). The *WorldSim* object arbitrates and keeps its own records of a harvesting event, returning some payoff to the agent (03). The agent then updates their XCS with the latest payoff and associated inputs (04).

## APPENDIX D : BATHYMETRIES

The simulator was run on eight bathymetries. Each bathymetry was encoded as a set of depths, one for each approximately square cell in a grid. Each bathymetry corresponds to a location in the Gulf of Maine. Depth data was derived from NOAA ENC Charts.

Below are details about each bathymetry. An image of each bathymetry is included along with the corresponding coordinates. The coordinates are specified in decimal latitude and longitude. Since each bathymetry is an approximate rectangle, the latitude and longitudes are each supplied as a range, identifying a unique rectangular region on the Earth's surface.

# PETIT MANAN

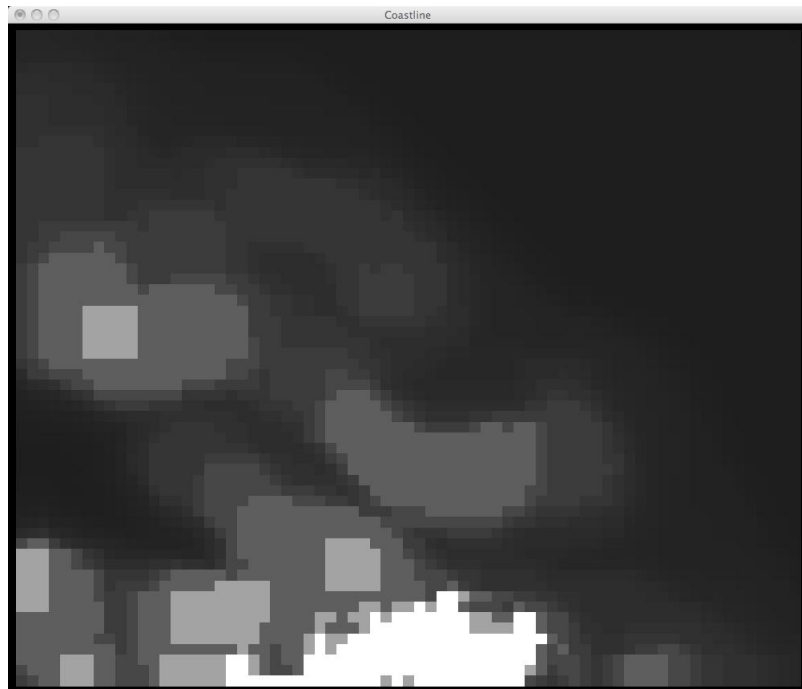


**Figure 66:** Bathymetry of the Petit Manan fishing site.

Latitudes	44.37405	44.38240
Longitudes	-67.87920	-67.86602

# SEAL COVE

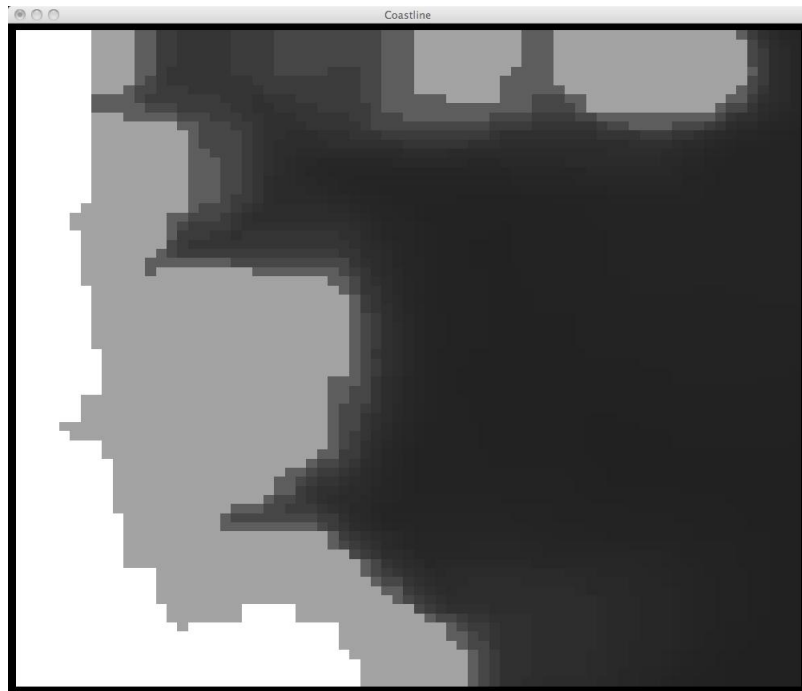
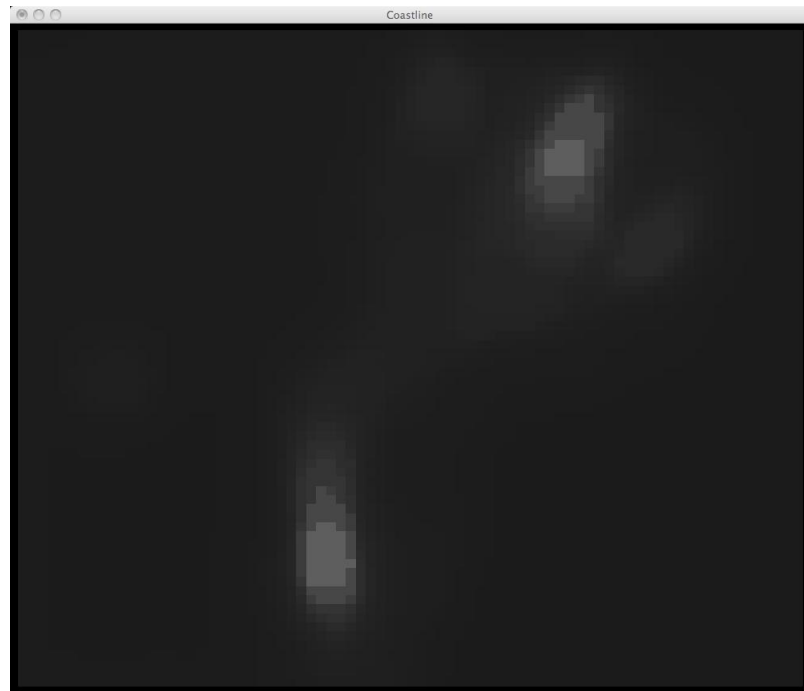


Figure 67: Bathymetry of the Seal Cove fishing site.

Latitudes	44.4370	44.4420
Longitudes	-67.9760	-67.8600

## BLACK LEDGE



**Figure 68:** Bathymetry of the Black Ledge fishing site.

Latitudes	44.437067	44.43815
Longitudes	-67.821100	-67.806467

# BIG NASH

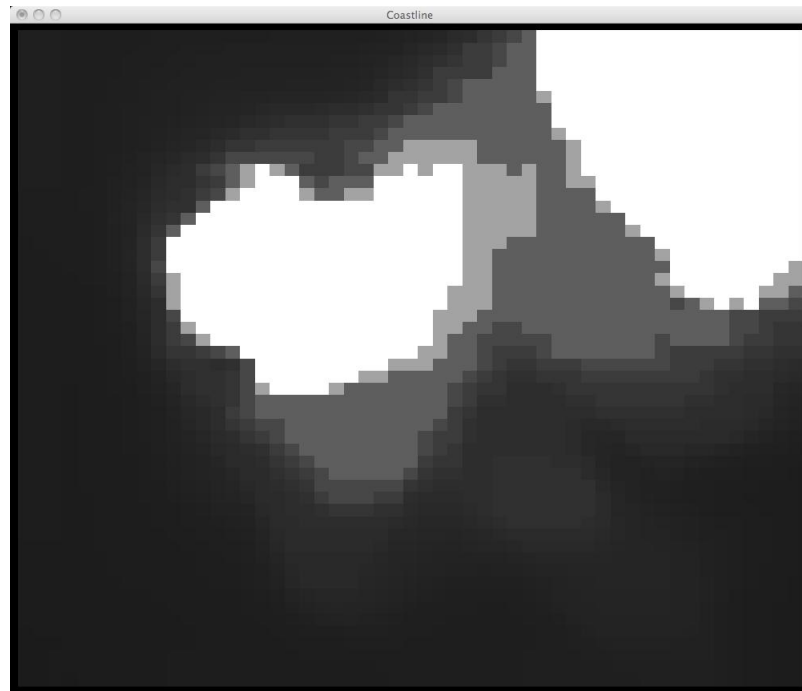


**Figure 69:** Bathymetry of the Big Nash fishing site.

Latitudes	44.45798	44.46752
Longitudes	-67.75042	-67.73732

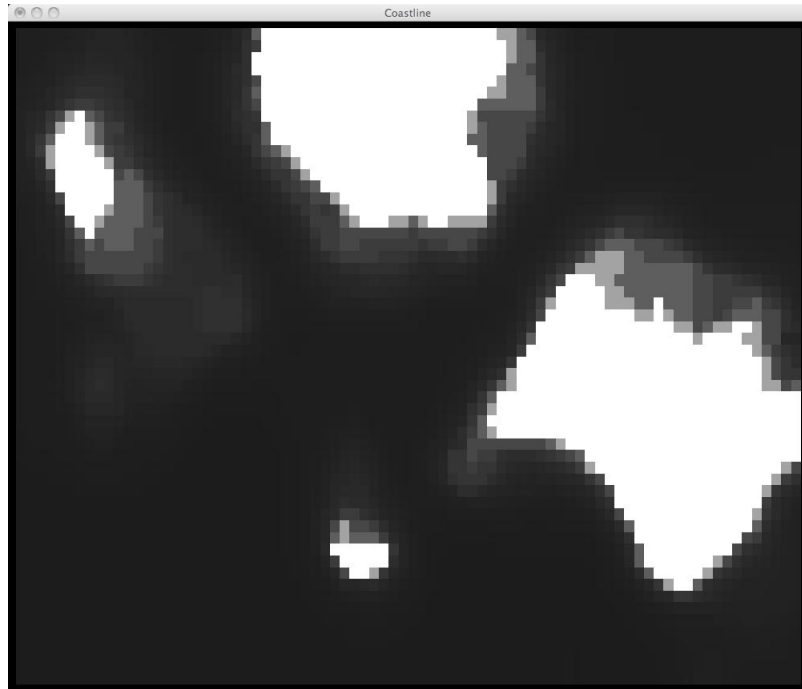
# SHABBIT ISLAND



Figure 70: Bathymetry of the Shabbit Island fishing site.

Latitudes	44.50085	44.51350
Longitudes	-67.68737	-67.66715

# FLINT ISLAND



**Figure 71:** Bathymetry of the Flint Island fishing site.

Latitudes	44.47012	44.48765
Longitudes	-67.81710	-67.78247

# GREAT WASS

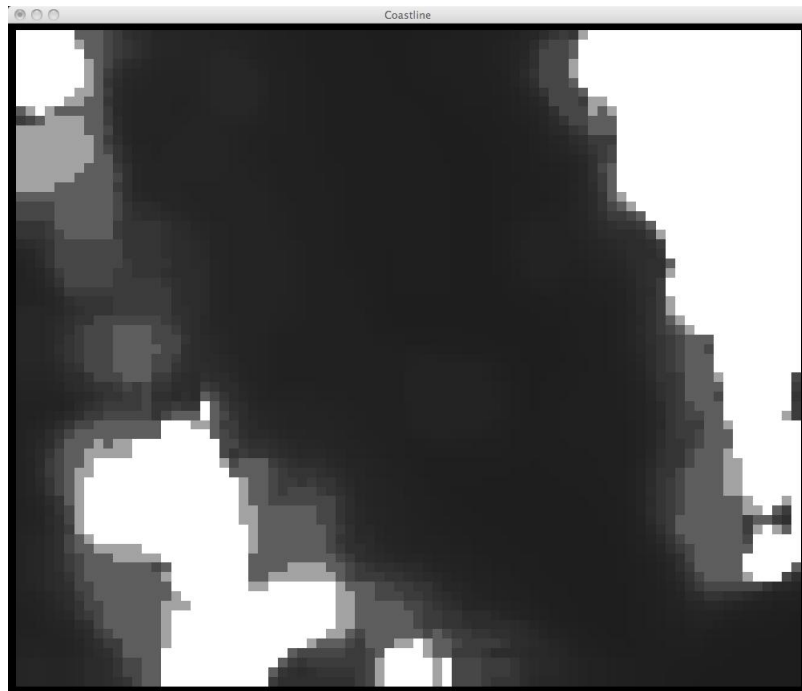


**Figure 72:** Bathymetry of the Great Wass fishing site.

Latitudes	44.44413	44.46262
Longitudes	-67.61720	-67.58708

## EASTERN BAY

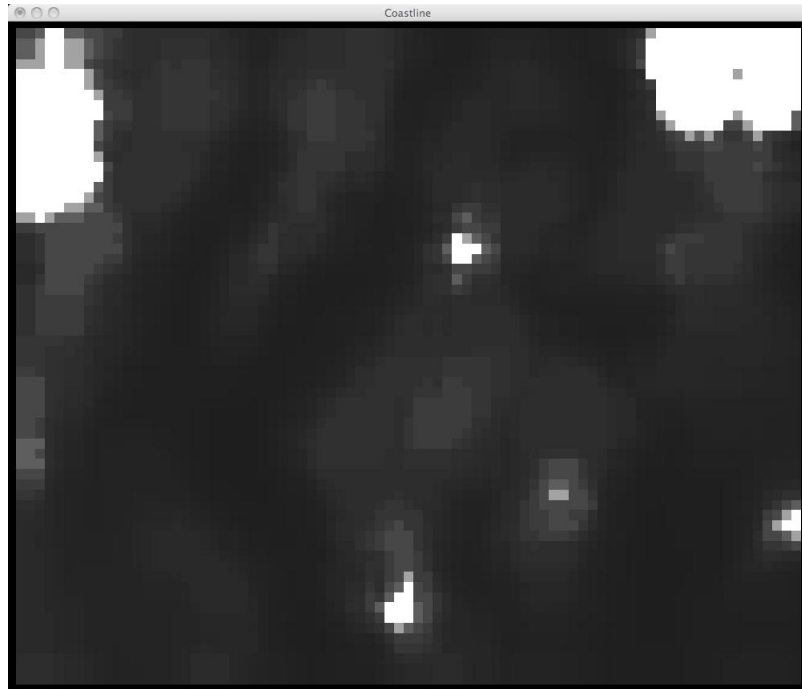


**Figure 73:** Bathymetry of the Eastern Bay fishing site.

Latitudes	44.49320	44.64376
Longitudes	-67.58703	-67.55708

## BIOGRAPHY OF THE AUTHOR

Graham Morehead was born in Boston. He graduated from Bedford High School in 1991. He graduated from Boston University in 1995 with a BA in Physics. He spent six years living overseas and has lived in Maine since early 2008.

He worked in various technology fields, including speech recognition, systems integration, app development, machine learning, statistical analysis, project management, and IT management. In 2010 he entered the University of Maine computer science program with a focus in natural language processing. This focus moved subsequently to complex systems and ecological modeling. Future goals include a sustained interest in complexity and its applications to language technologies.

He is a candidate for the Master of Science degree in Computer Science from The University of Maine in May 2014.